

Comparative morphology of part of the integumental fine structure of two Erythroneurine species: *Singapora shinshana* (Matsumura, 1932) and *Empoascanara sipra* Dworakowska, 1980 (Hemiptera, Cicadellidae, Typhlocybinae)

Jia Jiang¹, Christopher H. Dietrich², Can Li³, Yuehua Song¹

1 School of Karst Science, Guizhou Normal University / State Engineering Technology Institute for Karst Desertification Control, Guizhou, Guiyang, 550001, China **2** Illinois Natural History Survey, Prairie Research Institute, University of Illinois, 1816 S. Oak St., Champaign, IL 61820, USA **3** Guizhou Provincial Key Laboratory for Rare Animal and Economic Insect of the Mountainous Region, Guiyang University, Guiyang, Guizhou, 550005, China

Corresponding author: Yuehua Song (songyuehua@163.com)

Academic editor: Mick Webb | Received 19 January 2022 | Accepted 24 April 2022 | Published 26 May 2022

<http://zoobank.org/69A365B4-AD0B-4B1D-8FAB-4AFA8B5D2652>

Citation: Jiang J, Dietrich CH, Li C, Song Y (2022) Comparative morphology of part of the integumental fine structure of two Erythroneurine species: *Singapora shinshana* (Matsumura, 1932) and *Empoascanara sipra* Dworakowska, 1980 (Hemiptera, Cicadellidae, Typhlocybinae). ZooKeys 1103: 1–23. <https://doi.org/10.3897/zookeys.1103.80787>

Abstract

This study describes the fine structure of the mouthparts, antennae, forewings, and brochosomes of two leafhopper species belonging to the typhlocybinae tribe Erythroneurini collected from the Karst area of Guizhou Province, southern China: *Singapora shinshana*, which prefers woody dicot hosts, and *Empoascanara sipra*, which feeds on grasses. As in other leafhoppers, the piercing-sucking mouthparts consist of a conical labrum, a cylindrical three-segmented labium, and a slender stylet fascicle. The labrum of both species has no sensilla and the labium has several common types of sensilla, but the two species differ in the numbers, types, and distribution of sensilla and in other aspects of the surface sculpture of the mouthparts. The stylet fascicle has distinctive dentition on both the maxillary and mandibular stylets. The antennae of the two species differ in several respects, including the sensilla and sculpture of the scape, pedicel, and flagellum, as well as the degree of sub-segmentation of the flagellum. Except for the variable scaly structure and rounded protrusions on the surface of *S. shinshana*, the fine structure of the forewing surfaces of the two species are similar to those of other leafhoppers. Only small spherical brochosomes were found on the body surface of *S. shinshana* and *E. sipra*. Similar studies of additional erythroneurine species are needed to determine whether differences in mouthpart and antennal fine structure may reflect adaptation to different host plant.

Keywords

Antennae, brochosomes, fine structure, forewings, karst, mouthparts

Introduction

Leafhoppers, the Cicadellidae, are the largest family of Hemiptera and are widely distributed in six zoogeographic regions with more than 2,600 genera and 22,000 species (Oman et al. 1990; Dietrich 2005). Leafhopper nymphs and adults use piercing-sucking mouthparts to pierce the surface of the plant and suck either the phloem or xylem sap, or leaf parenchyma cell contents. The latter type of feeding is restricted to the sub-family Typhlocybinæ and causes characteristic white spots on the leaves, which may cause the leaves to wither and fall off (Backus and McLean 1982; Leopold et al. 2003). Some leafhoppers are vectors of viral or bacterial plant pathogens, which can cause plant diseases, such as the common maize chlorotic dwarf virus, rice waika virus, and the recently discovered wheat yellow striate virus (Hirao and Inoue 1979; Hunt and Nault 1990; Yan et al. 2018). The feeding strategies of leafhoppers and their potential for rapid reproduction, often make them difficult to control using conventional pest management strategies and their impacts on yield and quality of crops may be severe.

Over the course of their more than 400 million years of evolution, different insects have acquired a wide variety of integumental structures, including sensilla and sculpturing that enabled them to interact and adapt to various environmental conditions. Such structures play important roles in finding hosts, mating, and defense. Using light microscopy and scanning electron microscopy, Willis (1949), Moulins (1971), Rice (1973), and others successively studied the fine structure on body surfaces of insect and characterized various sensilla found on different body parts and regions. Within the order Hemiptera, the fine structure of aphids has been studied extensively, especially their feeding structure (Davidson 1914; Forbes 1977; Pointeau et al. 2012). Another economically important group of Hemiptera, the leafhoppers, also have a large variety of sensilla and epidermal structures, but their morphology, types, and quantity are quite different from those of other hemipterans (Backus and McLean 1982; Brozek et al. 2006; Zhang et al. 2016). Leafhoppers appear to be unique among insects in producing brochosomes, tiny proteinaceous particles produced in the Malpighian tubules and spread over the body as a hydrophobic coating (Rakitov and Carolina 2005; Rakitov 2009). Brochosomes are often deposited on a particular area of the forewing called the brochosome field prior to being spread over the rest of the body. The mouthparts of leafhoppers are very similar overall to those of other Hemiptera in having a modified, elongated labrum, labium, and stylet fascicle, but their shape, segmentation and fine structure differ from those of other hemipterans (Tavella and Arzone 1993; Hao et al. 2016a; Ge et al. 2016). Leafhoppers have three-segmented antennae, and the structural variation appears to be relatively low compared to other Hemiptera (Mazzoni et

al. 2009; Zhang et al. 2016). However, relatively few studies so far have focused on the fine structure of leafhoppers, and these mostly focused on representatives of a single subfamily, Deltocephalinae, that includes vectors of various plant pathogens (Backus and McLean 1982; Zhao et al. 2010; Liu et al. 2020; Zhang et al. 2020). Such studies have not been performed on Typhlocybinae, which mostly includes species that feed on leaf parenchyma cell contents and, therefore, occupy a different feeding niche from other leafhoppers.

To date, the fine structure of the integument of Typhlocybinae remains largely unstudied. Dong and Huang (2013) described the anointing behavior of *Singapura shinshana* (Matsuma, 1932) and mentioned the morphology of the brochosomes but did not study or illustrate the fine structure of brochosomes and other features of the integumental fine structure. This paper provides the first detailed SEM study of the integumental fine structure of species of Typhlocybinae, focusing on the mouthparts, antennae, forewings, and brochosomes of two species of Chinese Erythroneurini.

Materials and methods

The adult specimens of *S. shinshana* were collected on a peach tree on the Baoshan Campus of Guizhou Normal University, Guiyang City, Guizhou Province, China (26°35'30"N, 106°43'9"E) on 21 June 2020. The temperature at the time of collection was 27 °C, and the humidity was 91%. The adult specimens of *E. sipra* Dworakowska, 1980 were collected on *Festuca elata* Keng ex E. Alexeev, 1977 in Changpoling Forest Park, Guiyang City, Guizhou Province, China (26°38'45"N, 106°39'10"E) on 27 June 2020. The temperature was 20 °C and the humidity was 99% during collection. The overall appearance of the two leafhopper species is shown in Fig. 1. All specimens examined are deposited in the collection of the School of Karst Science, Guizhou Normal University, China (GZNU).

Newly captured adult specimens were placed in a -24 °C freezer for 20 min. Then ten frozen specimens (5 males and 5 females) were selected at random and dissected under a stereo microscope (Olympus SZX16, Japan), with the head and wings removed on dry filter paper, then placed in 2.5% glutaraldehyde fixative at 4 °C for 12 hours. Specimens were subsequently transferred to phosphate buffer saline (PBS, 0.1M, pH7.2) and rinsed five times, 5 min each time. Dissected parts (except wings) were then placed in an ultrasonic cleaner for 30 s, and then dehydrated in a graded series of 30%, 50%, 70%, 90%, 95%, and 100% acetonitrile for 20 min. Thereafter, the samples were mounted on aluminum stubs with double-sided sticky copper tape and sputtered with gold/palladium in a JEOL JFC-1600 high resolution sputter coater. The samples were subsequently examined with a JSM-6490LV SEM operated at 20 kV. The measurement data were obtained by scanning electron microscope.

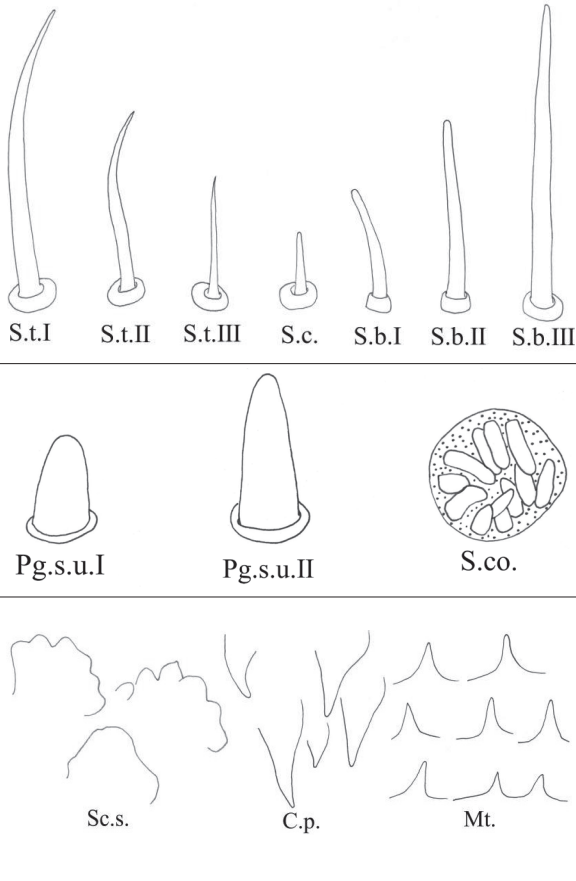
General terminology for the classification of sensilla follows Altner and Prillinger (1980) and Zacharuk (1980) with terminology more specific to leafhopper structures



Figure 1. **A** habitus of *Singapora shinshana*, dorsal view **B** habitus of *Emposcanara sipra*, dorsal view.

following more recent authors (Rakitov 2000; Zhao et al. 2010; Stacconi and Romani 2012; Brozek and Bourgoïn 2013; Ge et al. 2016; Hao et al. 2016a, b). Sensilla classification is summarized in Table 1.

Table 1. Classification of sensilla and cuticular processes.

Type		Features	Reference images
Sensilla trichodea	S.t. I	Hair-like, slender, slightly curved, length $\geq 20 \mu\text{m}$.	
	S.t. II	Relatively short.	
	S.t. III	Short and thin, length $\leq 10 \mu\text{m}$.	
Sensilla chaetica	S.c.	Shaped like short spines, erect or curved along the axis.	
sensilla basiconica	S.b. I	Upright or curved along the axis, the top is blunt, thick and short, length $\leq 10 \mu\text{m}$.	
	S.b. II	Relatively thick and long.	
	S.b. III	Thick and long, length $\geq 20 \mu\text{m}$.	
Peg sensilla	Pg.s.u. I	Peg-like, length 2.0-5.0 μm .	
	Pg.s.u. II	Peg-like, length 5.0-7.0 μm .	
Sensilla coeloconica	S.co.	A cluster of finger-like structures arranged in a round concavity, 6-16 finger-like protrusions.	
Scaly structures	Sc.s.	A scaly protrusion or a scaly structure composed of many small protrusions (non-sensilla).	
Cuticular processes	C.p.	Triangular protrusions with thin and pointed ends (non-sensilla).	
Microtrichia	Mt.	Small rigid projections occurring singly or in groups of two or three arranged together (non-sensilla).	

Results

The mouthparts of *S. shinshana* and *E. supra* are typical piercing-sucking mouthparts, consisting of a labrum (Lm), labium (Lb), two mandibular stylets (Md), and two maxillary stylets (Mx) comprising the stylet fascicle (Sf) (Figs 2, 5). The three-segmented labium has a deep longitudinal groove (Lg) on the anterior surface that houses and protects the stylet fascicle (Figs 3A, 5A). Except for the difference in size, the shape of the mouthparts and the distribution of sensilla are not different between male and female adults. Measurements are summarized in Table 2. The distribution and numbers of sensilla are summarized in Table 4.

The labrum is conical in shape and connected to the apical margin of the anteclypeus. The anteclypeus has many irregular protrusions on its surface, with some sensilla trichodea I and sensilla trichodea II symmetrically distributed on its surface (Figs 2, 5D). The labrum has a smooth surface, except for a few slight bumps (Figs 2, 5D).

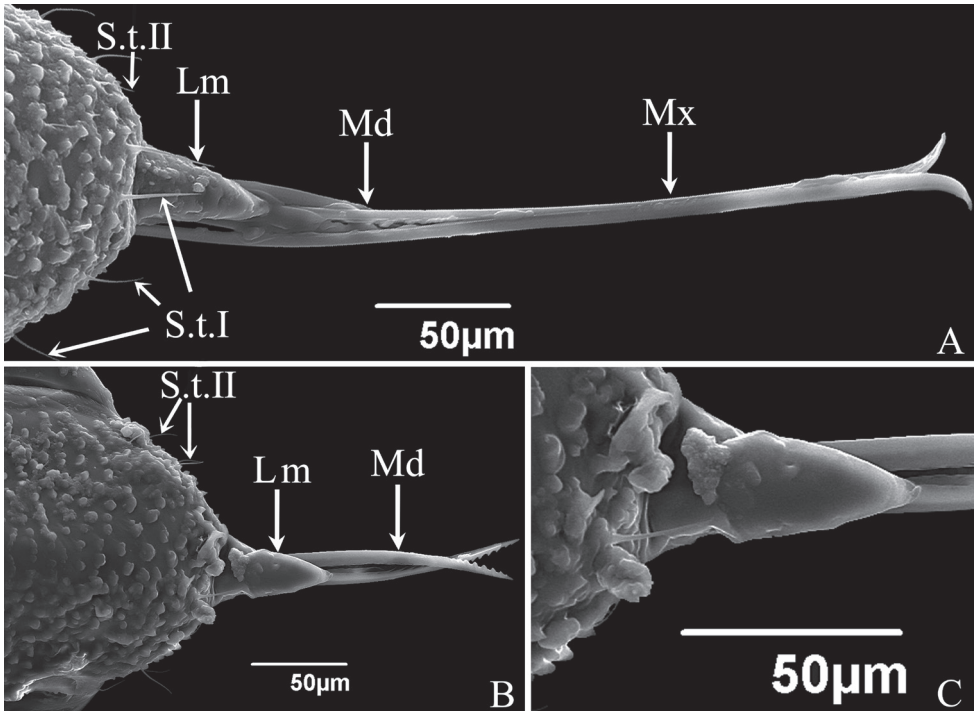


Figure 2. SEM of the mouthparts of *S. shinshana* **A** anterior view, showing labrum (Lm), mandibular stylets (Md), maxillary stylets (Mx), sensilla trichodea I (S.t. I) and sensilla trichodea II (S.t. II) **B** anterior view of anteclypeus and labrum (Lm), showing irregular protrusions on surface of anteclypeus, labrum, mandibular stylets (Md) and sensilla trichodea II (S.t. II) **C** cone-shaped labrum showing a smooth surface.

The labium consists of three cylindrical segments (Figs 3A, G, 5A); its length varies in proportion to the overall body size of individuals. The length relationship between the three labial segments is: $I < II < III$; the first and second segments are almost equal in length, the third segment is distinctly longer. The first labial segment is smooth on the surface without sensilla in dorsal view (Figs 3G, 5G). The anterior surface in *S. shinshana* has two sensilla coeloconica ($\sim 2.64 \mu\text{m}$ in diameter) and a sensilla basiconica II. Sensilla basiconica I are symmetrically distributed, sensilla basiconica II is distributed only at one side, a very rare occurrence (Fig. 3B, C). *Empoascanara sipra* has two sensilla basiconica I and two sensilla trichodea II symmetrically distributed in anterior view (Fig. 5K). Numerous transverse wrinkles are present on the anterior surface of the first labial segment of *S. shinshana*, and many small spinelike cuticular processes $< 8 \mu\text{m}$ in length are clearly visible (Fig. 3B). These cuticular processes all have the same distal orientation, and are scattered on the anterior surface of the first and second labial segments, but the second segment only has a few cuticular processes near the junction with the first segment (Fig. 3B, D). The first labial segment of *E. sipra* also has many transverse wrinkles but differs from *S. shinshana* in having groups of small microtrichia instead of larger spinelike processes (Fig. 5K).

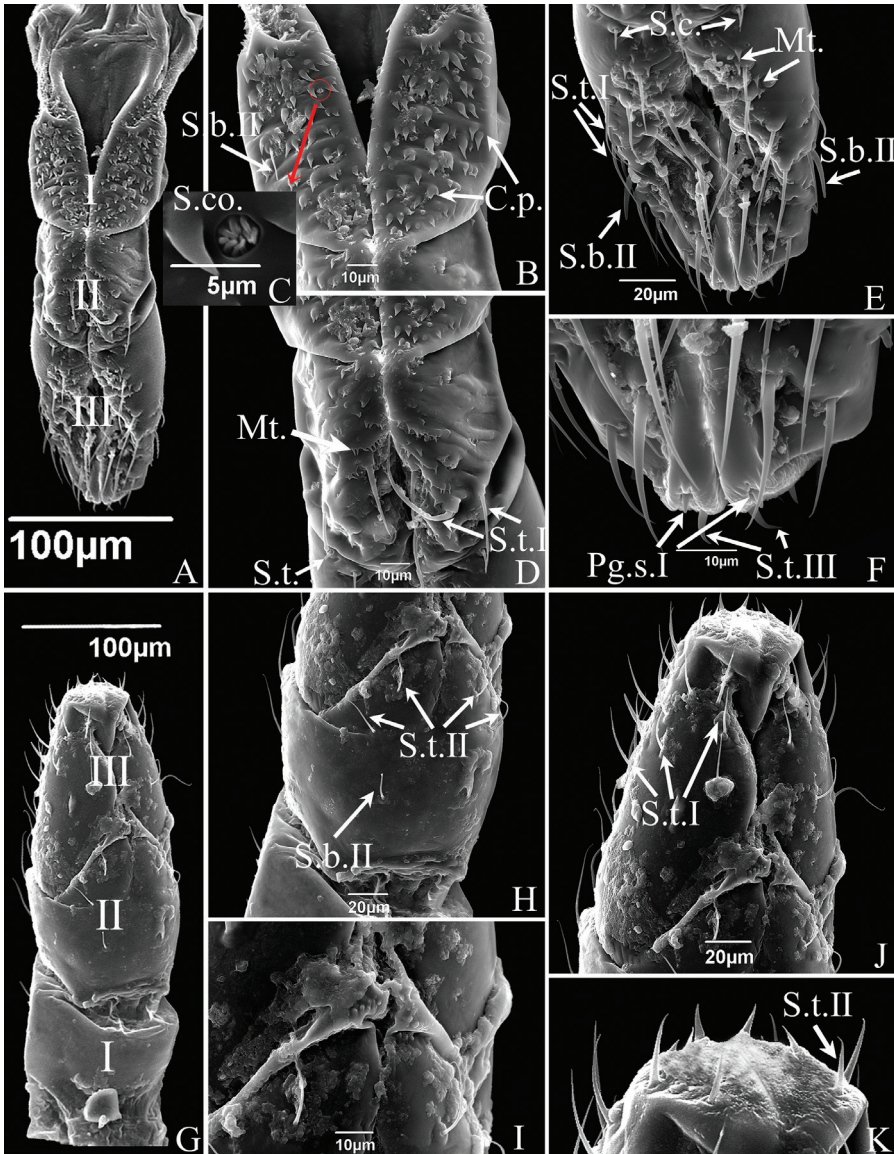


Figure 3. SEM of the labium of *S. shinshana* **A** anterior view of labium showing three-segmented labium (I-III), and sensilla symmetrically located on each side of the labial groove **B** anterior view of first segment of labium showing sensilla basiconica II (S.b.II) and cuticular processes (C.p.) **C** sensilla coeloconica (S.co.) **D** the anterior view of second segment of labium showing sensilla trichodea I (S.t.I) and microtrichia (Mt.) **E** anterior view of third segment of labium showing sensilla trichodea I (S.t.I), sensilla basiconica II (S.b.II), sensilla chaetica (S.c.) and microtrichia (Mt.) **F** anterior view of labial tip showing peg sensilla I (Pg.s.I) and sensilla trichodea III (S.t.III) **G** dorsal view of mouthparts showing three-segmented labium (I-III) and some sensilla **H** dorsal view of second segment of labium showing sensilla trichodea II (S.t.II) and sensilla basiconica II (S.b.II) **I** junction of second and third labial segments showing spherical protrusions **J** dorsal view of third segment of labium showing sensilla trichodea I (S.t.I) **K** tip of labium, showing distribution of sensilla.

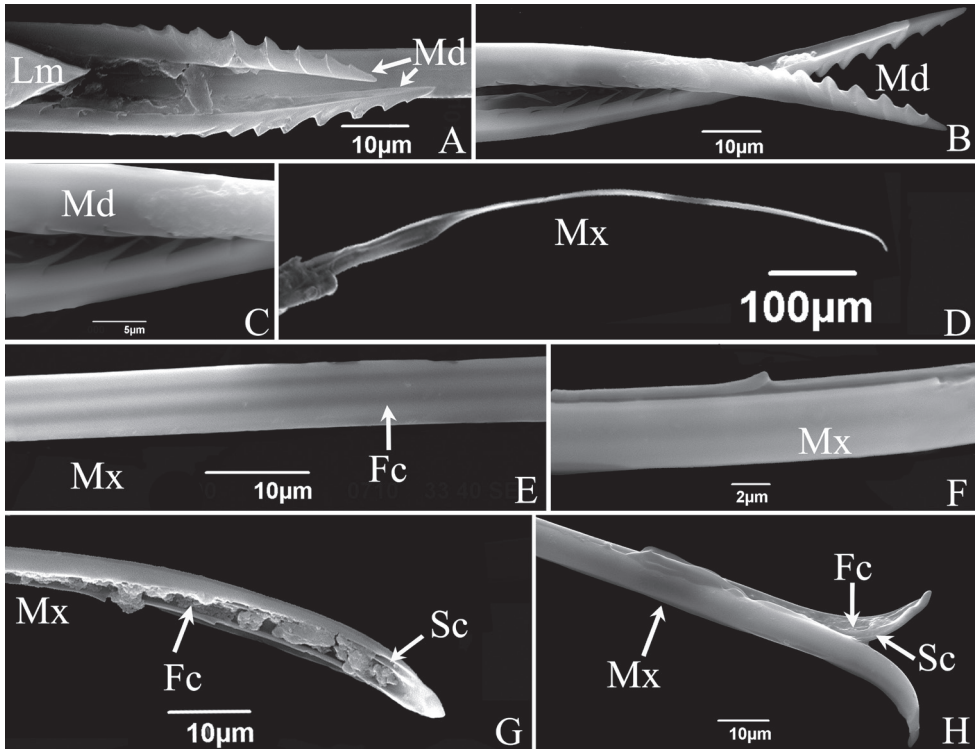


Figure 4. SEM of the stylet fascicle of *S. shinshana* **A** mandibular stylets (Md), showing relative position of mandibular stylets and labrum (Lm) **B** mandibular stylet (Md), showing serrate ridge on the convex external surface and zigzag structure on inner edge **C** enlarged middle of mandibular stylet (Md), showing zigzag structure on inner edge **D** maxillary stylets **E** dorsal view of middle section of maxillary stylets (Mx), showing lines indicating food canal (Fc) **F** lateral view of middle section of maxillary stylets (Mx), showing relatively blunt tooth-like protrusion **G** tip of maxillary stylet (Mx), showing salivary canal (Sc) and food canal (Fc) **H** tip of maxillary stylets (Mx), showing two stylets with different lengths.

A few microtrichia are concentrated on oblique ridges near the median longitudinal groove on the second labial segment of *S. shinshana*, while a larger number of microtrichia are distributed on the second and third labial segments of *E. sipra* (Figs 3D, E, 5H–M). Twelve sensilla trichodea I are distributed asymmetrically on both sides of the groove of *S. shinshana*. Four sensilla trichodea II are symmetrically distributed on the dorsal surface of the second labial segment, and one sensilla basiconica II is present on the left side (Fig. 3H, the sensillum on the opposite side may have fallen off). The junction of the second and third labial segments in dorsal view is heavily sclerotized, forming a raised ridge, and a round protrusion is present in middle of the ridge (Fig. 3I). The second labial segment of *E. sipra* has six sensilla trichodea II, which are symmetrically distributed on both sides of the groove, and eight sensilla trichodea I are symmetrically distributed on the second labial section and close to the third labial segment in anterior view; two sensilla trichodea I and four sensilla trichodea II are symmetrically distributed in dorsal view (Fig. 5H, L).

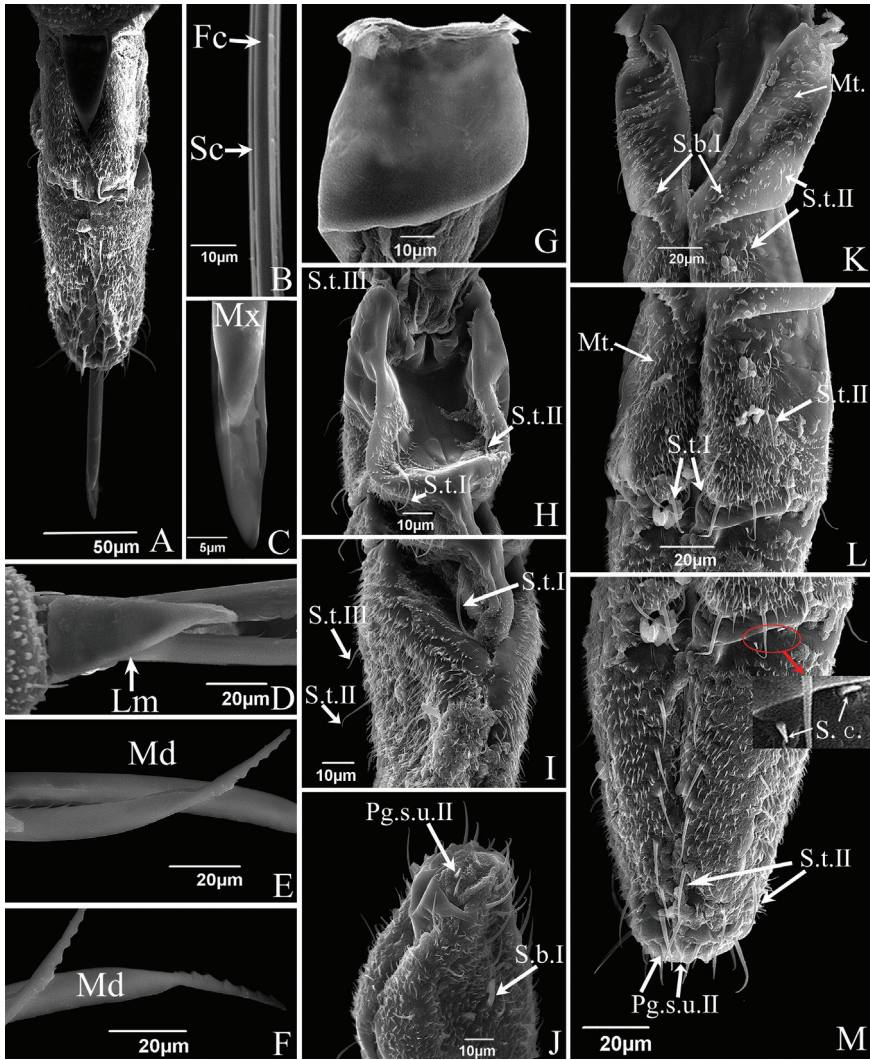


Figure 5. SEM of the mouthparts of *E. sipra* **A** the anterior view of labrum and labium showing sensilla symmetrically located on each side of the labial groove or around the tip of the labium **B** one of the maxillary stylets (Mx) showing food canal (Fc) and salivary canal (Sc) **C** the enlarged view of the tip of maxillary stylets (Mx) which are pointed and incurved **D** cone-shaped labrum showing a smooth surface **E** mandibular stylet (Md), showing serrate ridge on the convex external surface and zigzag structure on inner edge **F** mandibular stylet (Md), showing the depression on the side of the mandibular stylet **G** dorsal view of first segment of labium showing a smooth surface **H** dorsal view of second segment of labium showing sensilla trichodea I (S.t.I) and sensilla trichodea II (S.t.II) **I** dorsal view of third segment of labium showing sensilla trichodea I (S.t.I), sensilla trichodea II (S.t.II), sensilla trichodea III (S.t.III) **J** tip of labium, showing sensilla basiconica I (S.b.I) and peg sensilla II (Pg.s.u.II) **K** anterior view of first segment of labium showing sensilla basiconica, II (S.b.II) and cuticular processes (C.p) **L** anterior view of second segment of labium showing sensilla trichodea I (S.t.I), sensilla trichodea II (S.t.II) and microtrichia (Mt.) **M** anterior view of third segment of labium showing sensilla trichodea II (S.t.II), sensilla chaetica (S.c.) and peg sensilla II (Pg.s.u.II).

The third labial segment is longer than other two segments, gradually tapered towards the apex, and more densely covered with sensilla, mostly symmetrically distributed. Sensilla trichodea I–III, peg sensilla (*S. shinshana*: peg sensilla I, ~ 3.32 µm in length; *E. sipra*: peg sensilla II, ~ 5.57 µm in length) and sensilla basiconica (*S. shinshana*: sensilla basiconica II, ~ 18.05 µm in length; *E. sipra*: sensilla basiconica I, ~ 9.58 µm in length) are distributed on the third labial segment of the two species; and there is a pair of peg sensilla distributed on both sides of the longitudinal groove. The labial tip surface is uneven, with many small, rounded protrusions (Figs 3E, F, J, K, M, 5I, J). The majority of sensilla trichodea of *E. sipra* are arranged in an obvious order, while the sensilla trichodea of *S. shinshana* are scattered (Figs 3E, 5M). In addition, two sensilla chaetica are distributed on the right side of the third segment of *E. sipra*, adjacent to the second segment (Fig. 5M).

The stylet fascicle is composed of paired, elongated mandibular and interlocking maxillary stylets. The mandibular stylets partially sheathe the maxillary stylets laterally and are significantly shorter than the latter. They are crescent-shaped in cross-section, thus forming a deep groove enclosing the maxillary stylets. Each mandibular stylet has a row of slender tooth-like protrusions on its inner edge in the basal half, and the protrusions together form a zigzag structure (Figs 4B, C, 5E); the outer surfaces of the distal half have a serrate ridge consisting of eight or nine, more or less evenly spaced, teeth (Figs 4A, B, 5E, F). The mandibular stylets of *S. shinshana* have a wider base that gradually narrows toward the apex; the mandibular stylets of *E. sipra* suddenly narrow at the base of the serrate ridge, then slightly expand, and then gradually narrow toward the apex (Figs 4A, B, 5E, F).

The two maxillary stylets are semicircular in cross-section and tightly interlocked to form a salivary canal (Sc) and a food canal (Fc) (Figs 4G, H, 5B, C). The maxillary stylets are elongated, smooth on the outer surface, but longitudinal lines representing the food canal can be clearly seen (Fig. 4D–F); widely spaced, blunt, tooth-like protrusions are present on the two sides and prevent them from separating during feeding (Figs 4E, 5B). The two maxillary stylets are asymmetrical and differ in length; with sharp tips used to pierce plant tissues.

The antennae of the two studied species are of the typical arisoid type present in other Cicadellidae, composed of three parts: scape (Sc), pedicel (Pe) and flagellum (Fl) (Figs 6A, 7A). Their length relationship is: $Sc < Pe < Fl$, the flagellum is three times as long as the combined length of scape and pedicel. Measurements of each part of the antennae are summarized in Table 3. Except for the differences in length, there are no obvious differences in the morphology of the antennae of male and female adults and the distribution of sensilla. The distribution and numbers of sensilla are summarized in Table 4.

The scape is short, thick, approximately bell-shaped, with the base consisting of a flexible antennal membrane (Figs 6B, 7B). The scape of *E. sipra* has scalelike structures and microtrichia on the surface, while the scape of *S. shinshana* is relatively smooth without obvious surface sculpturing; the base in *E. sipra* has one sensilla chaetica and one sensilla trichodea III that are widely spaced, while the base in *S. shinshana* has two close-set sensilla chaetica (Figs 6B, 7B).

Table 2. Measurements of labrum and labium (mean \pm SE) obtained from scanning electron microscopy, $n = 5$. Lm: labrum; Lb: labium; Lb-1: first segment of labium; Lb-2: second segment of labium; Lb-3: third segment of labium.

Segment	Lm		Lb-1		Lb-2		Lb-3		Lb total length	
	<i>S. shinsbana</i>	<i>E. sipra</i>	<i>S. shinsbana</i>	<i>E. sipra</i>	<i>S. shinsbana</i>	<i>E. sipra</i>	<i>S. shinsbana</i>	<i>E. sipra</i>	<i>S. shinsbana</i>	<i>E. sipra</i>
Length (μm)	Male 62.7 \pm 12.0	52.37 \pm 3.2	81.3 \pm 8.7	73.1 \pm 7.9	90.8 \pm 10.3	73.7 \pm 5.6	108.3 \pm 5.4	96.0 \pm 15.1	280.4 \pm 24.4	242.8 \pm 28.6
	Female 72.7 \pm 9.8	69.4 \pm 10.1	96.1 \pm 16.1	78.6 \pm 5.2	99.7 \pm 9.2	84.6 \pm 3.5	122.1 \pm 6.4	114.4 \pm 7.9	317.9 \pm 31.7	275.6 \pm 16.6

Table 3. Measurements of antennae (mean \pm SE) obtained from scanning electron microscopy, $n = 5$. Sc: scape; Pe: pedicel; Fl: flagellum.

Segment		Sc		Pe		Fl		total length	
		<i>S. shinsbana</i>	<i>E. sipra</i>	<i>S. shinsbana</i>	<i>E. sipra</i>	<i>S. shinsbana</i>	<i>E. sipra</i>	<i>S. shinsbana</i>	<i>E. sipra</i>
Length (μm)	Male	58.7 \pm 3.9	52.7 \pm 9.6	78.3 \pm 6.8	72.9 \pm 6.1	518.5 \pm 14.1	496.9 \pm 13.5	655.5 \pm 25.9	622.5 \pm 29.2
	Female	59.1 \pm 2.8	56.4 \pm 8.1	80.6 \pm 9.2	75.6 \pm 10.4	548.7 \pm 25.1	513.3 \pm 12.3	688.4 \pm 37.1	645.3 \pm 30.8

Table 4. A statistical table of the sensilla and cuticular processes of the labium, antennae, and forewings. Lb-1: first segment of labium; Lb-2: second segment of labium; Lb-3: third segment of labium; Sc: scape; Pe: pedicel; Fl: flagellum; Fw: forewing. Note: The number of sensilla or cuticular processes is the average for the number of samples ($n = 10$); no entry indicates that the number of some sensors was not counted.

Sensilla type	Distribution (number)	
	<i>S. shinsbana</i>	<i>E. sipra</i>
S.t. I	Lb-2(12); Lb-3	Lb-2(10); Lb-3(2)
S.t. II	Lb-2(4); Lb-3(4)	Lb-1(2); Lb-2(10); Lb-3
S.t. III	Lb-3(2); Pe(4)	Lb-3; Sc(1); Pe(2)
S.c.	Lb-3(2); Sc(2); Fw	Sc(1); Lb-3(2); Fw
S.b. I		Lb-1(2); Lb-3(2)
S.b. II	Lb-1(1); Lb-3(2)	Fl(1)
S.b. III	Fl(1)	
Pg.s.u. I	Lb-3(2)	
Pg.s.u. II		Lb-3(2)
S.co.	Lb-1(2)	
Sc.s.	Pe	Sc; Pe
C.p.	Lb-1	
Mt.	Lb-2; Lb-3; Fl; Fw	Lb-1; Lb-2; Lb-3; Pe; Fl; Fw

The pedicel is connected to the recessed socket at the end of the scape (Figs 6C, 7B). It is cylindrical, with many scale-like structures on the surface that gradually become fragmented from base to apex. The pedicel of *S. shinsbana* has four sensilla trichodea III scattered on the surface, and the pedicel of *E. sipra* has two sensilla trichodea III and a large number of microtrichia (Figs 6C, D, 7B).

The flagellum is elongated and divided into numerous subsegments (Figs 6A, 7A). The flagellum of *S. shinsbana* is divided into three morphologically distinct regions, while the flagellum of *E. sipra* is divided into two regions. The first (basal) region of *S. shinsbana* is relatively thick and tapered, comprising the first nine subsegments, each with a large number of microtrichia (Fig. 6E, F, G, I). The first two subsegments are approximately bell-shaped and slightly swollen and widest distally, but the remaining subsegments of

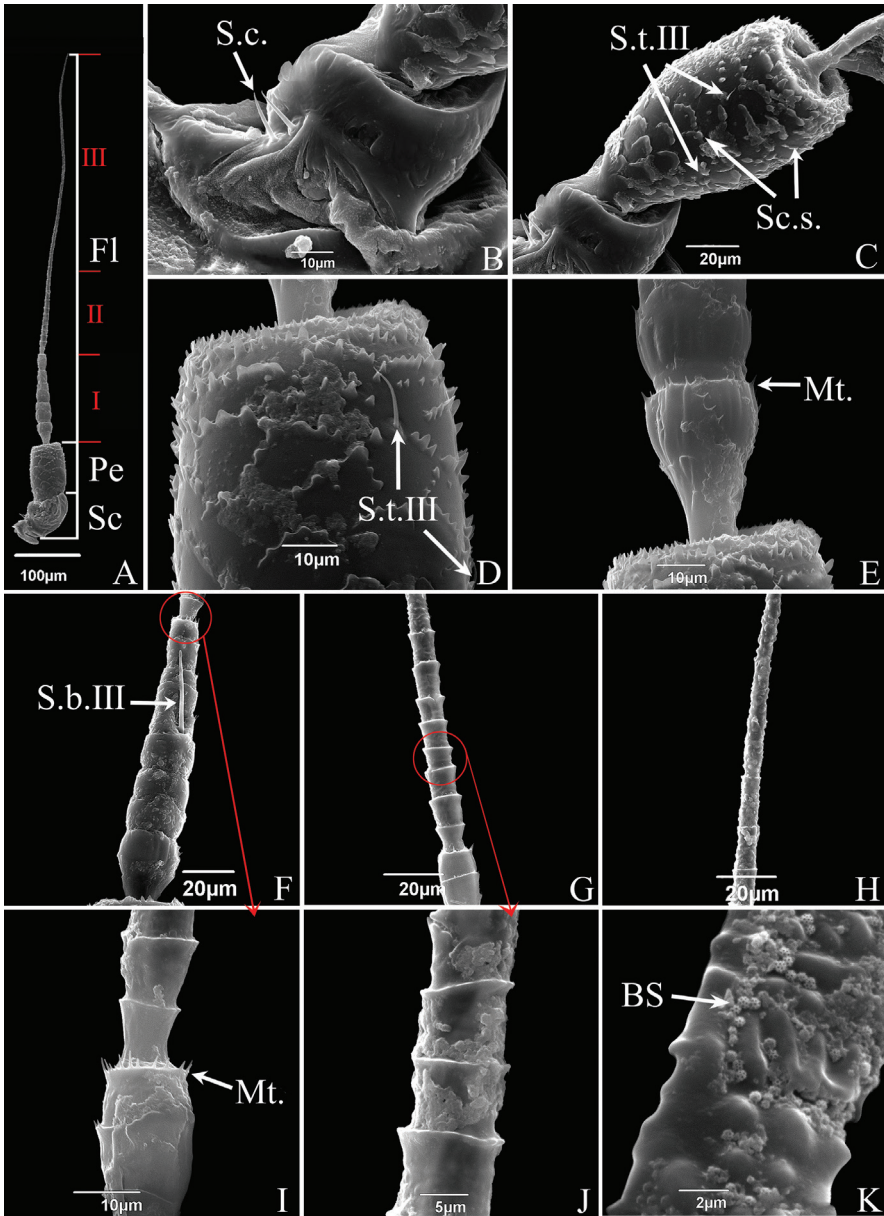


Figure 6. SEM of the antennae of *S. shinsbana* **A** antenna, composed of three parts: scape (Sc), pedicel (Pe) and three regions of flagellum (Fl) **B** scape, showing smooth surface, with two sensilla chaetica (S.c.) **C** pedicel, showing scale-like structures (Sc.s.) and sensilla trichodea III (S.t.III) **D** enlarged view of pedicel, showing scaly structures and sensilla trichodea III (S.t.III) **E** junction between pedicel and flagellum, showing microtrichia (Mt.) **F** first region of flagellum, showing sensilla basiconica III (S.b.III) **G** second region of the flagellum **H** junction between second and third regions of flagellum, showing change in surface protrusions **I** junction between first part and second regions of flagellum, showing microtrichia (Mt.) **J** enlarged view of second part of flagellum, showing cylindrical subsegments **K** enlarged view of third part of flagellum, showing brochosomes (BS).

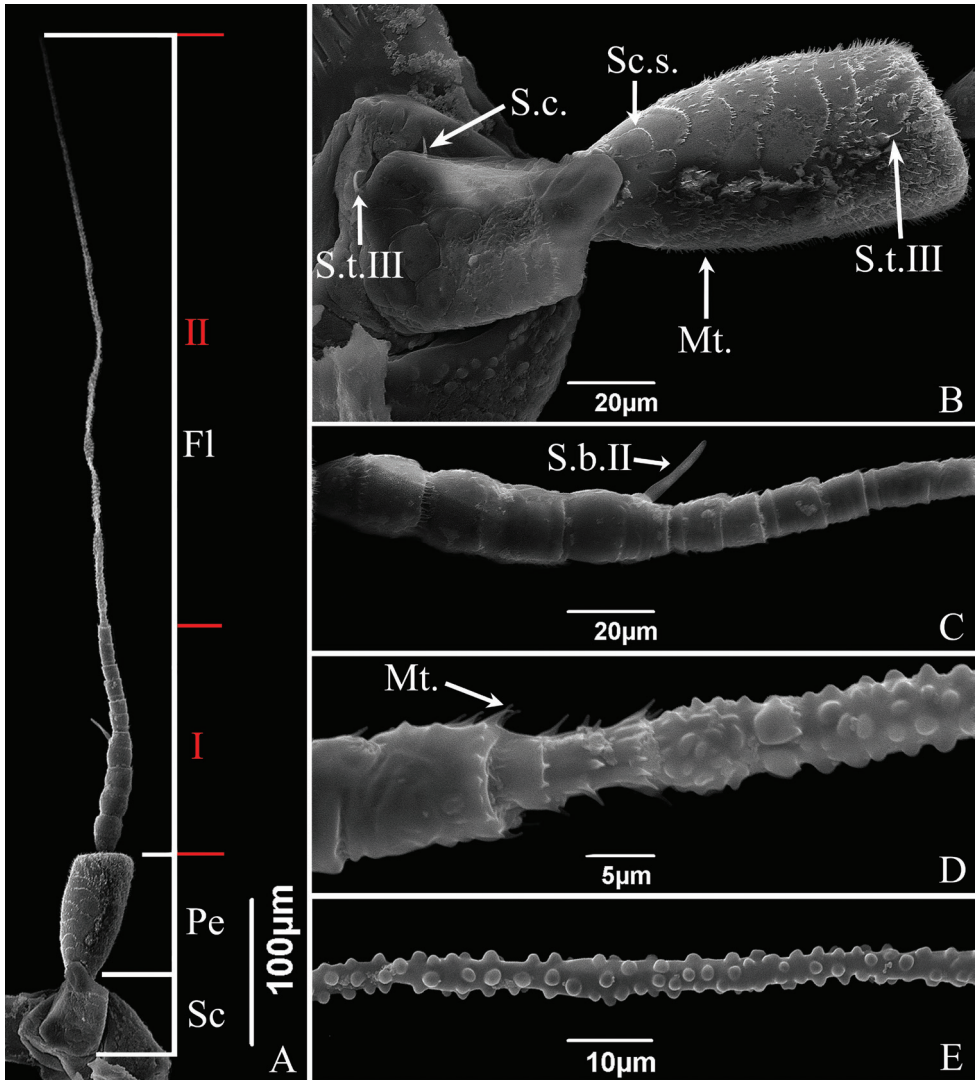


Figure 7. SEM of the antennae of *E. sipra* **A** antenna, composed of three parts: scape (Sc), pedicel (Pe) and three regions of flagellum (FI) **B** scape and pedicel, showing scale-like structures (Sc.s.), sensilla trichodea III (S.t.III), sensilla chaetica (S.c.), microtrichia (Mt.) **C** first region of flagellum, showing sensilla basiconica II (S.b.II) **D** junction between first and second regions of flagellum, showing change in surface protrusions and microtrichia (Mt.) **E** second region of the flagellum, showing spherical protrusions on the surface.

this section are more or less parallel sided (Fig. 6E, 6F). The second region starts from the tenth subsegment which is obviously narrowed compared to the previous subsegment; this region includes ten subsegments, each of which is cylindrical with no microtrichia at the apex but with the apex slightly flared (Fig. 6G–J). As in the first region, the first two subsegments of the second region are gradually expanded (Fig. 6G). The third region

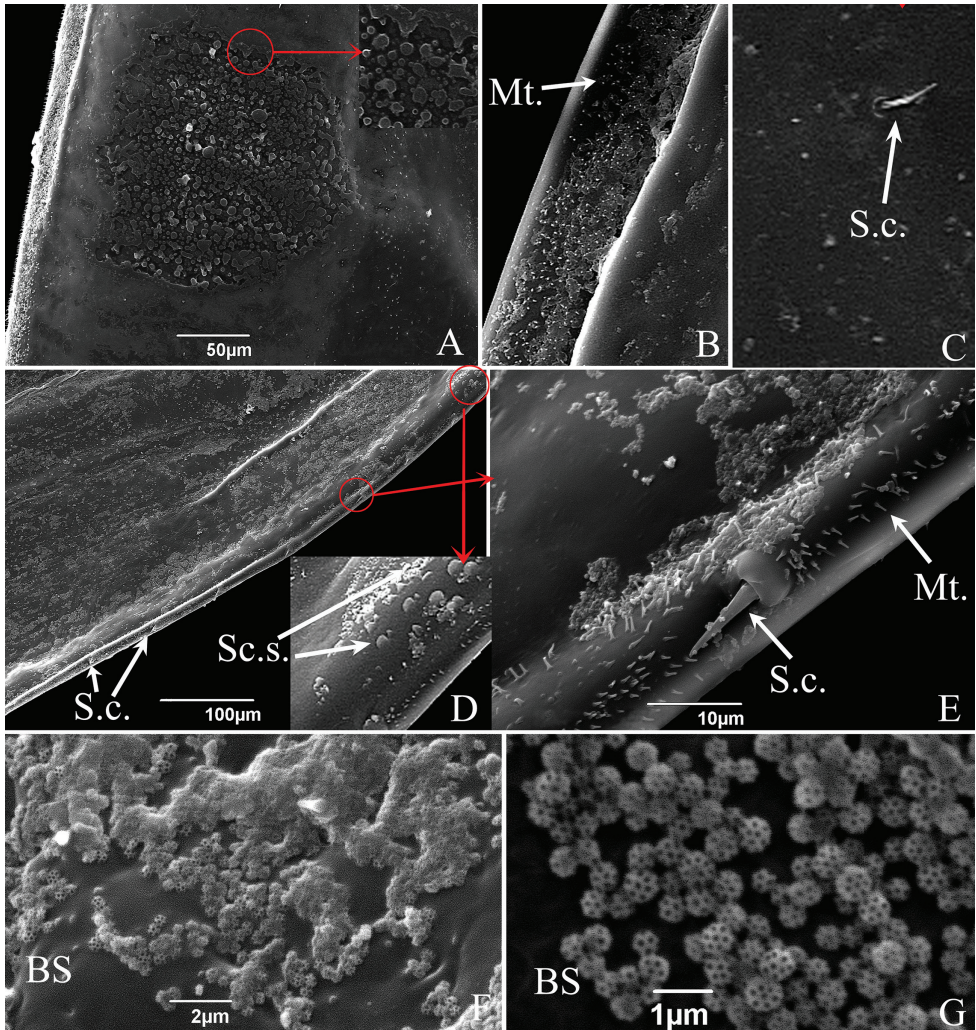


Figure 8. SEM of the brochosomes of *S. shinshana* **A** peculiar fine structure of brochosomal area **B** microtrichia (Mt.) on transparent membrane of brochosomal area **C** sensilla chaetica (S.c.) on front edge of forewing **D** posterior edge of forewing, showing surface folds, scaly structure (Sc.s.) and sensilla chaetica (S.c.) **E** posterior edge of forewing, showing sensilla chaetica (S.c.) and microtrichia (Mt.) **F** brochosomes (BS) on front edge of forewing **G** enlarged view of brochosomes (BS) on front edge of forewing.

lacks has the subsegments more elongated and less well delimited, and has many protrusions of different sizes on the surface, giving the surface a rough, uneven appearance (Fig. 6H). From base to apex these protrusions gradually decrease in density; they are nearly spherical near the base and ridgelike near the apex (Fig. 6K). The first (basal) region of *E. supra* consists of the eleven subsegments, with morphological characteristics similar to those of the basal region *S. shinshana* (Fig. 7A, C). The junction between the first region and the second region is significantly narrowed, and the second region lacks any indica-

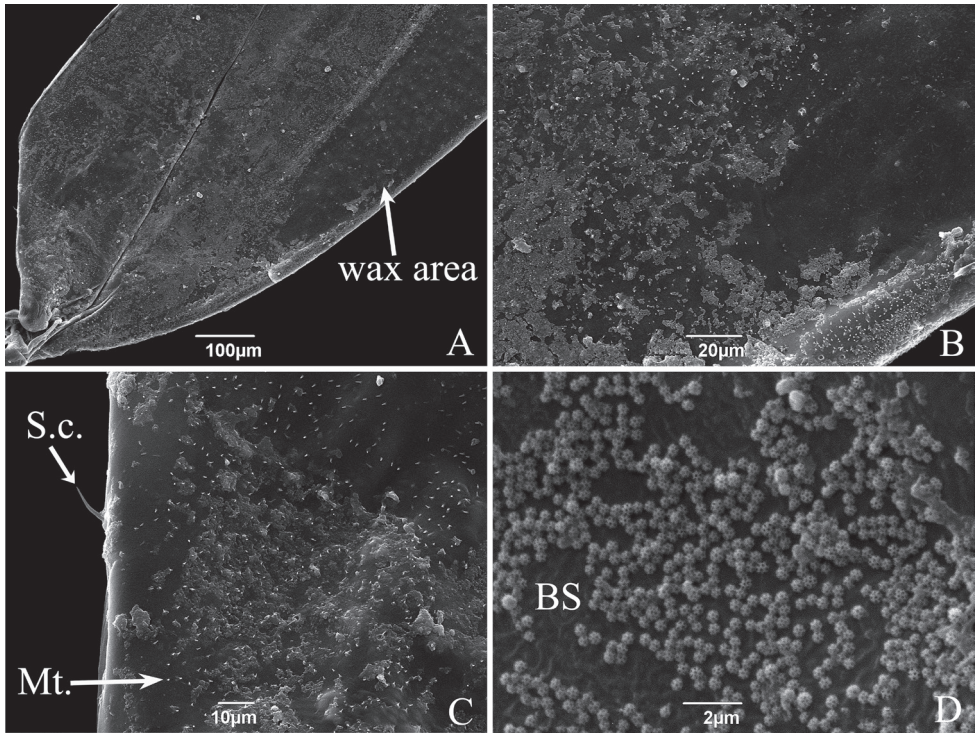


Figure 9. SEM of the brochosomes of *E. sipra* **A** forewing, showing the distribution of brochosomes **B** the enlarged forewing part shows brochosomes and microtrichia (Mt.) **C** posterior edge of forewing, showing sensilla chaetica (S.c.) and microtrichia (Mt.) **D** brochosomes (BS).

tion of sub-segmentation, with many spherical protrusions on the surface but without ridgelike protrusions (Fig. 7D, E). The flagellum has only one long sensilla basiconica III ($\sim 40.67 \mu\text{m}$ in length) near the middle of the basal region (Fig. 6F). Both leafhoppers have a sensilla basiconica on their flagellum respectively (*S. shinshana*: sensilla basiconica III; *E. sipra*: sensilla basiconica II) near the middle of the basal region (Figs 6F, 7C).

As in other Typhlocybae, the costal area has an elongated oval white area often referred to in previous literature as the “brochosomal area” or “wax field”, but actually consisting of a patch of brochosomes. There are numerous microtrichia and small sensilla chaetica scattered on upper forewing surface of the two erythroneurine species (Figs 8B–E, 9B, C); with a large number of microtrichia densely distributed on the transparent membrane of the front edge (costal margin) and a protruding ridge on the underside of the forewing (Figs 8A, B, 9B); relatively large sensilla chaetica are widely spaced along the edge of the forewing (Figs 8D, E, 9C). In addition, the forewing of *S. shinshana* has some small scalelike structures scattered around the hind edge (anal margin) near the base (Fig. 8D). Some samples have a unique microstructure near the forewing tip, which is composed of numerous rounded protrusions of various sizes and irregular shapes (Fig. 8A), and a few samples did not have

this structure. No obvious differences in forewing fine structure were noted between male and female adults.

Small spherical brochosomes (the white powder on the forewings) were found on body surfaces of both male and female adults, with diameters of 402.00–583.10 nm (Figs 8G, 9D). Each brochosome is composed of multiple regular pentagonal and hexagonal cells partitioned by walls, the number of cells depends on the size of the brochosomes; smaller brochosomes have significantly fewer cells (Figs 8E, G, 9D). The brochosomes of *S. shinshana* and *E. sipra* are mostly concentrated at the base of the forewing, but there are fewer brochosomes on the brochosomal area (Figs 8A–D, 9A, B). The distribution of brochosomes on various surfaces of the body probably depends on how recently that individual leafhopper anointed and groomed itself with brochosomes. Observed under a scanning electron microscope, brochosomes are widely distributed on body surfaces of *S. shinshana* and *E. sipra*, with the largest concentrations usually on the hind legs, which are used by the leafhoppers during grooming to spread brochosomes over other parts of the body. When dense, brochosomes tend to gather together to form clumps (Fig. 8E). On mouthparts, brochosomes are mostly distributed on both sides of the longitudinal groove of the labium and around some sensilla (Figs 3A, B, D–I, 5H–M); on antennae, brochosomes are mostly distributed in the recesses of folds, and such distribution is most obvious in the distal region of the flagellum (Figs 6, 7).

Discussion

Despite belonging to a single leafhopper tribe, the two studied species of Erythroneurini show remarkable differences in the fine structure of their mouthparts and antennae. The mouthparts of *S. shinshana* and *E. sipra* are generally similar to those of other Hemiptera in gross morphology (Tavella and Arzone 1993; Boyd 2003; Leopold et al. 2003; Wiesenborn 2004; Anderson et al. 2006; Zhao et al. 2010; Dai et al. 2014; Ge et al. 2016; Hao et al. 2016a, 2016b), but differ in many details including the fine structure of the labium and labrum, and the dentition of the stylets. Unlike most previously studied Hemiptera, which have protrusions on the labrum surface, some including sensilla (Leopold et al. 2003; Zhao et al. 2010; Dai et al. 2014; Hao et al. 2016a, 2016b), *S. shinshana* and *E. sipra* have the labrum surface with no sensilla. The labrum is similar to that of some aphids, e.g., *Eriosoma lanigerum* (Hausmann, 1802) and *Aphis citricola* Van der Goot, 1912, which have few labrum folds (Razaq et al. 2000; Ge et al. 2016). A few other studied leafhoppers, e.g., *Exitianus indicus* (Distant, 1908), *Laburris impictifrons* (Boheman, 1852) and *Aguriabana triangularis* (Matsumura 1932) also have a smooth labrum (Pan 2013). This structure has been largely neglected in taxonomy and phylogenetic studies, but further comparative study of the labrum may show that its traits are useful for inferring relationships and distinguishing taxa.

The number of labium segments of Hemiptera insects varies between 1–5, but most species have 3 or 4 (Emeljanov 1987). Most Auchenorrhyncha have a three-

segmented labium (*Lycorma delicatula* (White, 1845), with 5 segments, is an exception). The relative length of the segments can vary among species. The first segment of the labium of both *S. shinshana* and *E. sipra* are slightly shorter than the second. Although the cuticular processes on the first labium segment of the two species are different, such structures are common among leafhoppers (Zhao et al. 2010; Pan 2013; Hao et al. 2016b). Multiple sensilla are asymmetrically distributed along the longitudinal groove of the labium. Other sensilla present belong to more common types. We observed no clustered peg-structures on the tip of the labium as found in many other Auchenorrhyncha, only a pair of peg sensilla and a few sensilla trichodea are scattered on the surface, which is also seen in *Homalodisca vitripennis* (Germar, 1821), *Psammotettix striatus* (Linnaeus, 1758), *Taurotettix elegans* (Melichar, 1900) and other leafhoppers (Leopold et al. 2003; Zhao et al. 2010; Pan 2013). The structures at the tip of the labium are used to perceive the host plant surface. Some may also be used to rid the stylet fascicle of plant and salivary sheath debris during withdrawal of stylets from the plant tissue (Leopold et al. 2003). The specific roles of the various structures remain to be verified by further experiments.

The stylet fascicle is the main tool used for feeding, and it is also an important medium for spreading plant pathogens. *Singapora shinshana* and *E. sipra* have a ridge at the apex of the feeding stylet with a serrated structure in the middle. The ridges are not connected to the serrated structure, and their shape is very similar to that of *A. triangularis* (Pan 2013). Serrated structures were also found in other Hemipteran insects (Boyd 2003; Leopold et al. 2003; Anderson et al. 2006), but the numbers and shapes of teeth varies among species. These teeth cut channels into the plant tissues and help anchor the stylets during feeding. As in other Hemiptera, the interlocking part of the maxillary stylets of the two leafhoppers have a blunt and small toothed structure that facilitates tight coupling of the stylets during feeding. This is considered by Leopold et al. (2003) to be a ratchet device for positioning the stylets in apposition to each other.

Insect antennae are variously used in insect communication, foraging for food and courtship. Leafhopper antennae are relatively simple in structure and have relatively few sensory structures compared to those of some other Auchenorrhyncha (particularly Fulgoroidea); thus they have been little studied from a comparative perspective. The antennae of *S. shinshana* and *E. sipra* generally resemble those of other leafhoppers (Aljunid and Anderson 1983; Liang and Fletcher 2002; Romani et al. 2009; Stacconi and Romani 2012; Guo et al. 2018; Wang et al. 2018) but differ somewhat in fine structure. The scape of most previously studied leafhoppers has scale-like protrusions, as found in *E. sipra*, but the scape of *S. shinshana* has no protrusions and only has some shallow folds, which are similar to those found on the antennae of the lace bug (Tingidae) species *Stephanitis nashi* Esaki & Takeya, 1931 (Wang et al. 2020). This kind of scape is not common in Hemiptera, which usually have many projections on the surface, such as the papilla-like protrusions in *Sogatella furcifera* (Horváth, 1899) in Delphacidae (Zhang et al. 2016), or reticular protrusions in *Triatoma guazu* Lent & Wygodzinsky, 1979 and *T. jurbergi* Carcavallo, Galvão & Lent, 1998 in Reduviidae (Silva et al. 2002).

The cylindrical pedicel is slightly longer than the scape. *Singapora shinshana* and *E. supra* have scaly structures of different sizes scattered on the surface of the pedicel, but the cuticular processes that make up the scaly structure are different. The cuticular processes of *S. shinshana* are obviously wider than those of *E. supra*. The scaly structure of *E. supra* composed of micro-thorn-like cuticular processes is different from that of other leafhoppers (Mazzoni et al. 2009; Wang et al. 2018). This kind of microsculpture is similar to that found on the labium of this species and may represent the more generally distributed microsculpture pattern present on other external surfaces of this species.

The flagellum is the longest segment and has a large number of microtrichia at the end of each basal subsegment. Both *S. shinshana* and *E. supra* have only one very long sensilla basiconica that appears on the 5th subsegment of the flagellum. Previously studied leafhopper species, such as *Scaphoideus titanus* Ball, 1932, *Empoasca onukii* Matsuda, 1952, and *Chlorotettix nigromaculatus* (Dai, Chen & Li, 2006), have a longer sensillum between the 3rd and 6th subsegments of the flagellum (Mazzoni et al. 2009; Qiao et al. 2016; Guo et al. 2018). Although the antenna of leafhoppers remains little studied, perhaps because it does not appear to vary obviously among species when observed under light microscopy, the flagellum may be quite variable in fine structure among different leafhoppers. These differences are mainly manifested in the different numbers of segments, differences in the size and shape of the few sensilla present, and differences in the shapes of surface protrusions. For example, the flagella of *S. titanus* and *C. nigromaculatus* are sub-segmented from base to apex (Mazzoni et al. 2009; Guo et al. 2018), while the flagellum of *E. onukii* has only seven subsegments near the base (Qiao et al. 2016). The flagella of *S. shinshana* and *E. supra* have numerous irregular protrusions but these differ in structure and density. Further comparative studies are needed to elucidate the morphological differences of these protrusions between species and their possible functions.

Brochosomes are minute protein-lipid particles with a net-like surface produced intracellularly in specialized glandular segments of the Malpighian tubules of leafhoppers. Their protein content ranges from 45–70% (Rakitov 2009; Rakitov et al. 2018). According to the shape, they are divided into two different types: integumental brochosomes (IBS) and egg brochosomes (EBS) by Rakitov (2009). The latter apparently occur only in some species of Proconiini in which the females exhibit a unique “egg-powdering” behavior. Rakitov (2004) also found that females of the genus *Proconia* are covered with a coating composed of large and small brochosomes, while the brochosomes of males are uniform in size and different from those of the female. The brochosomes of *S. shinshana* and *E. supra* all appear to be the spherical type, similar to those found in other leafhoppers (Rakitov 1999, 2000, 2009; Humphrey and Dworakowska 2002). No differences in brochosome structure were observed between males and females.

After leafhoppers molt, brochosomes are secreted and anointed onto the body surface. Leafhopper species may differ in the amount of brochosomes secreted and in the time spent anointing. *Singapora shinshana* secretes 19 drops during each anointing episode on average, and the anointing behavior takes 2–4 h (Dong and Huang 2013). After leafhoppers secrete the liquid containing brochosomes, the liquid dries and gives rise to a visible pellet on the long oval “wax-area” of the front edge of the forewing. The

fine structure of this area shows obvious differences among different species (Rakitov 1999, 2000). In order to improve adherence of brochosomes, the brochosomal area has horizontal ridges on the surface.

Brochosomes form a hydrophobic coating of the integument that can protect leafhoppers from wetting in areas of high humidity or rainfall. The brochosome coating may also provide some protection against high temperature and solar radiation, may help prevent evaporation of body surface water, and may also help leafhoppers avoid natural enemies, diseases, and parasites (Humphrey and Dworakowska 2002; Rakitov and Carolina 2005; Dong and Huang 2013), but most of these additional proposed benefits have yet to be proven.

Conclusions

SEM comparisons of the integumental fine structure of two species of erythroneurine leafhoppers representing two different genera show that, although the overall structure of the mouthparts, antennae, and forewings are highly similar, many details differ between these species in integumental sculpturing, and the numbers, types, and distribution of sensilla. *Singapora shinshana* feeds on the leaves of peach and related Rosaceous trees while *E. supra* and other species of *Empoasca* feed on grasses. Thus, some of the observed differences may reflect adaptation to the very different chemical composition and structure of the host plants of these species. Further studies of other species in this tribe are needed to determine whether particular aspects of the mouthpart and antennal structures may be more broadly correlated to particular feeding preferences.

Acknowledgements

This study was partly funded by the World Top Discipline Program of Guizhou Province: Karst Ecoenvironment Sciences (No.125 2019 Qianjiao Keyan Fa), the Guizhou Provincial Science and Technology Foundation ([2018]1411), the Innovation Group Project of Education Department of Guizhou Province ([2021]013), the Guizhou Science and Technology Support Project ([2019]2855), the Science and Technology Project of Guiyang City ([2020]7-18), the Training Program for High-level Innovative Talents of Guizhou Province ([2016]4020) and the Project for Regional Top Discipline Construction of Guizhou Province: Ecology in Guiyang University [Qian Jiao Keyan Fa [2017]85].

References

- Aljunid SF, Anderson M (1983) Ultrastructure of sensilla on the antennal pedicel of the brown planthopper *Nilaparvata lugens* Stal (Insecta: Homoptera). Cell and Tissue Research 228(2): 313–322. <https://doi.org/10.1007/BF00204881>

- Altner H, Prillinger L (1980) Ultrastructure of invertebrate chemo-, thermo-, and hygroreceptors and its functional significance. *International Review of Cytology* 67: 69–139. [https://doi.org/10.1016/S0074-7696\(08\)62427-4](https://doi.org/10.1016/S0074-7696(08)62427-4)
- Anderson WG, Heng-Moss T, Baxendale FP, Baird LM, Sarath G, Higley L (2006) Chinch Bug (Hemiptera: Blissidae) mouthpart morphology, probing frequencies, and locations on resistant and susceptible germplasm. *Journal of Economic Entomology* 99(1): 212–221. <https://doi.org/10.1093/jee/99.1.212>
- Backus EA, McLean DL (1982) The sensory systems and feeding behavior of leafhoppers. I. The aster leafhopper, *Macrosteles fascifrons* Stål (Homoptera, Cicadellidae). *Journal of Morphology* 172(3): 361–379. <https://doi.org/10.1002/jmor.1051720310>
- Boyd DW (2003) Digestive enzymes and stylet morphology of *Deraeocoris nigriritulus* (Uhler) (Hemiptera: Miridae) reflect adaptations for predatory habits. *Annals of the Entomological Society of America* 96(5): 667–671. [https://doi.org/10.1603/0013-8746\(2003\)096\[0667:DEASMO\]2.0.CO;2](https://doi.org/10.1603/0013-8746(2003)096[0667:DEASMO]2.0.CO;2)
- Brozek J, Bourgoïn T (2013) Morphology and distribution of the external labial sensilla in Fulgoromorpha (Insecta: Hemiptera). *Zoomorphology* 135(1): 33–65. <https://doi.org/10.1007/s00435-012-0174-z>
- Brozek J, Bourgoïn T, Szwedó J (2006) The interlocking mechanism of maxillae and mandibles in Fulgoroidea (Insecta: Hemiptera: Fulgoromorpha). *Polskie Pismo Entomologiczne* 75: 239–253.
- Dai W, Pan LX, Lu YP, Jin L, Zhang CN (2014) External morphology of the mouthparts of the white-backed planthopper *Sogatella furcifera* (Hemiptera: Delphacidae), with special reference to the sensilla. *Micron (Oxford, England)* 56: 8–16. <https://doi.org/10.1016/j.micron.2013.09.005>
- Davidson J (1914) On the mouthparts and mechanism of suction in *Schizoneuru lanigera* Hausm. *Journal of the Linnean Society of London* 32(218): 307–330. <https://doi.org/10.1111/j.1096-3642.1914.tb01460.x>
- Dietrich CH (2005) Keys to the families of Cicadomorpha and subfamilies and tribes of Cicadellidae (Hemiptera: Auchenorrhyncha). *The Florida Entomologist* 88(4): 502–517. [https://doi.org/10.1653/0015-4040\(2005\)88\[502:KTTFOC\]2.0.CO;2](https://doi.org/10.1653/0015-4040(2005)88[502:KTTFOC]2.0.CO;2)
- Dong HY, Huang M (2013) Analysis of the anointing and grooming behavior of several adult insects in Typhlocybinæ (Hemiptera: Cicadellidae). *Journal of Insect Behavior* 26(4): 540–549. <https://doi.org/10.1007/s10905-012-9370-4>
- Emeljanov AF (1987) Phylogeny of Cicadina (Homoptera, Cicadina) according to data on comparative morphology. *Trudy Vsesoiuznogo Entomologicheskogo Obschestva* 69: 19–109.
- Forbes AR (1977) The mouthparts and feeding mechanism of aphids. *Aphids As Virus Vectors* 35(138): 83–103. <https://doi.org/10.1016/B978-0-12-327550-9.50008-2>
- Ge FR, Dietrich C, Dai W (2016) Mouthpart structure in the woolly apple aphid *Eriosoma lanigerum* (Hausmann) (Hemiptera: Aphidoidea: Pemphigidae). *Arthropod Structure & Development* 45(3): 230–241. <https://doi.org/10.1016/j.asd.2016.01.005>
- Guo FZ, Yuan SX, Wang HR, Guo KJ (2018) Observation of the antenna and antennal sensilla of adults of the leafhopper *Chlorotettix nigromaculatus* (Hemiptera: Cicadellidae) with scanning electron microscope. *Acta Entomologica Sinica* 61(10): 1192–1201. <https://doi.org/10.16380/j.kcxb.2018.10.009>

- Hao Y, Dietrich CH, Dai W (2016a) Development of mouthparts in the cicada *Meimuna mongolica* (Distant): Successive morphological patterning and sensilla differentiation from nymph to adult. *Scientific Reports* 6(1): e38151. <https://doi.org/10.1038/srep38151>
- Hao YN, Dietrich CH, Dai W (2016b) Structure and sensilla of the mouthparts of the spotted Lanternfly *Lycorma delicatula* (Hemiptera: Fulgoromorpha: Fulgoridae), a polyphagous invasive planthopper. *PLoS ONE* 11(6): e0156640. <https://doi.org/10.1371/journal.pone.0156640>
- Hirao J, Inoue H (1979) Transmission characteristics of rice waika virus by the green rice leafhopper, *Nephotettix cincticeps* Uhler (Hemiptera: Cicadellidae). *Applied Entomology and Zoology* 14(1): 44–50. <https://doi.org/10.1303/aez.14.44>
- Humphrey EC, Dworakowska I (2002) The natural history of brochosomes in *Yakuza gaunga* (Hemiptera, Auchenorrhyncha, Cicadellidae, Typhlocybinae, Erythroneurini). *Denisia* 4: 433–454.
- Hunt RE, Nault LR (1990) Influence of life history of grasses and maize chlorotic dwarf virus on the biotic potential of the leafhopper *Graminella nigrifrons* (Homoptera: Cicadellidae). *Environmental Entomology* 19(1): 76–84. <https://doi.org/10.1093/ee/19.1.76>
- Leopold RA, Freeman TP, Buckner JS, Dennis RN (2003) Mouthpart morphology and stylet penetration of host plants by the glassy-winged sharpshooter, *Homalodisca coagulata* (Homoptera: Cicadellidae). *Arthropod Structure & Development* 32(2–3): 189–199. [https://doi.org/10.1016/S1467-8039\(03\)00047-1](https://doi.org/10.1016/S1467-8039(03)00047-1)
- Liang AP, Fletcher MJ (2002) Morphology of the antennal sensilla in four Australian spittlebug species (Hemiptera: Cercopidae) with implications for phylogeny. *Australian Journal of Entomology* 41(1): 39–44. <https://doi.org/10.1046/j.1440-6055.2002.00266.x>
- Liu W, Zhang Y, Dietrich CH, Duan Y (2020) Comparative analysis of antennal fine structure of *Goniagnathus punctifer*, *Stirellus yeongnamensis* and *Stirellus indrus* (Hemiptera: Cicadellidae: Deltocephalinae). *Zoomorphology* 139(4): 461–469. <https://doi.org/10.1007/s00435-020-00501-5>
- Matsumura S (1932) A revision of the Palaearctic and Oriental Typhlocybid genera with descriptions of new species and new genera. *Insecta Matsumurana* 6(3): 93–120.
- Mazzoni V, Ioriatti C, Trona F, Lucchi A, De Cristofaro A, Anfora G (2009) Study on the role of olfaction in host plant detection of *Scaphoideus titanus* (Hemiptera: Cicadellidae) nymphs. *Journal of Economic Entomology* 102(3): 974–980. <https://doi.org/10.1603/029.102.0316>
- Moulins M (1971) Ultrastructure et physiologie des organes épipharyngiens et hypopharyngiens (chimiorécepteurs cibariaux) de *Blabera craniifer* Burm (Insecte, Dictyoptère). *Zeitschrift für Vergleichende Physiologie* 73(2): 139–166. <https://doi.org/10.1007/BF00304130>
- Oman PW, Knight WJ, Nielson MW (1990) Leafhoppers (Cicadellidae): A bibliography, generic check-list and index to the world literature 1956–1985. *Annals of the Entomological Society of America* 51(5): 53–89. [https://doi.org/10.1016/0022-0965\(91\)90077-6](https://doi.org/10.1016/0022-0965(91)90077-6)
- Pan LX (2013) Comparative morphology of the mouthparts in Auchenorrhyncha (Insecta: Hemiptera). *Northwest A & F University*, 26–37.
- Pointeau S, Ameline A, Laurans F, Sallé A, Rahbé Y, Bankhead-Dronnet S, Lieutier F (2012) Exceptional plant penetration and feeding upon cortical parenchyma cells by the woolly poplar aphid. *Journal of Insect Physiology* 58(6): 857–866. <https://doi.org/10.1016/j.jinphys.2012.03.008>

- Qiao L, Zhang L, Qin DZ, Li BL, Lu ZC, Li HL, Xia MC (2016) Ultramicro morphology of antennal sensilla and brochosome of adult *Empoasca onukii*. Xibei Nongye Xuebao 25(03): 471–476.
- Rakitov RA (1999) Secretory products of the Malpighian tubules of Cicadellidae (Hemiptera, Membracoidea): An ultrastructural study. International Journal of Insect Morphology & Embryology 28(3): 179–193. [https://doi.org/10.1016/S0020-7322\(99\)00023-9](https://doi.org/10.1016/S0020-7322(99)00023-9)
- Rakitov RA (2000) Secretion of brochosomes during the ontogenesis of a leafhopper, *Oncometopia orbona* (F.) (Insecta, Homoptera, Cicadellidae). Tissue & Cell 32(1): 28–39. <https://doi.org/10.1054/tice.1999.0084>
- Rakitov RA (2004) Powdering of egg nests with brochosomes and related sexual dimorphism in leafhoppers (Insecta, Hemiptera, Cicadellidae). Zoological Journal of the Linnean Society 140: 353–381. <https://doi.org/10.1111/j.1096-3642.2003.00103.x>
- Rakitov RA (2009) Brochosomal coatings of the integument of leafhoppers (Hemiptera, Cicadellidae). Functional Surfaces in Biology 1: 113–137. https://doi.org/10.1007/978-1-4020-6697-9_8
- Rakitov RA, Carolina G (2005) New egg-powdering sharpshooters (Hemiptera: Cicadellidae: Proconiini) from Costa Rica. Annals of the Entomological Society of America 98(4): 444–457. [https://doi.org/10.1603/0013-8746\(2005\)098\[0444:NESHCP\]2.0.CO;2](https://doi.org/10.1603/0013-8746(2005)098[0444:NESHCP]2.0.CO;2)
- Rakitov R, Moysa AA, Kopylov AT, Moshkovskii SA, Peters RS, Meusemann K, Misof B, Dietrich CH, Johnson CH, Podsiadlowski L, Walden KKO (2018) Brochosomins and other novel proteins from brochosomes of leafhoppers (Insecta, Hemiptera, Cicadellidae). Insect Biochemistry and Molecular Biology 94: 10–17. <https://doi.org/10.1016/j.ibmb.2018.01.001>
- Razaq A, Kashiwazaki T, Mohammad P, Shiraiishi M (2000) SEM observations on the citrus green aphid, *Aphis citricola* van der Goot (Homoptera: Aphididae). Pakistan Journal of Biological Sciences 3(6): 949–952. <https://doi.org/10.3923/pjbs.2000.949.952>
- Rice MJ (1973) Cibarial sense organs of the blowfly, *Calliphora erythrocephala* (Meigen) (Diptera: Calliphoridae). International Journal of Insect Morphology & Embryology 2(2): 109–116. [https://doi.org/10.1016/0020-7322\(73\)90012-3](https://doi.org/10.1016/0020-7322(73)90012-3)
- Romani R, Rossi Stacconi MV, Riolo P, Isidoro N (2009) The sensory structures of the antennal flagellum in *Hyalesthes obsoletus* (Hemiptera: Fulgoromorpha: Ciixidae): A functional reduction? Arthropod Structure & Development 38(6): 473–483. <https://doi.org/10.1016/j.asd.2009.08.002>
- Silva MBA, Barbosa HS, Jurberg J, Galvão C, Carcavallo RU (2002) Comparative ultrastructural analysis of the antennae of *Triatoma guazu* and *Triatoma jurbergi* (Hemiptera: Reduviidae) during the nymphal stage development. Journal of Medical Entomology 39(5): 705–715. <https://doi.org/10.1603/0022-2585-39.5.705>
- Stacconi MVR, Romani R (2012) Antennal sensory structures in *Scaphoideus titanus* ball (Hemiptera: Cicadellidae). Microscopy Research and Technique 75(4): 458–466. <https://doi.org/10.1002/jemt.21078>
- Tavella L, Arzone A (1993) Comparative morphology of mouth parts of *Zyginidia pullula*, *Empoasca vitis*, and *Graphocephala fennabi* (Homoptera, Auchenorrhyncha). Bollettino di Zoologia 60(1): 33–39. <https://doi.org/10.1080/11250009309355788>

- Wang X, Li QL, Wei C (2018) Comparative morphology of antennae in Cicadoidea (Insecta: Hemiptera), with respect to functional, taxonomic and phylogenetic implications. *Zoologischer Anzeiger* 276: 57–70. <https://doi.org/10.1016/j.jcz.2018.05.003>
- Wang Y, Brožek J, Dai W (2020) Functional morphology and sexual dimorphism of antennae of the pear lace bug *Stephanitis nashi* (Hemiptera: Tingidae). *Zoologischer Anzeiger* 286: 11–19. <https://doi.org/10.1016/j.jcz.2020.03.001>
- Wiesenborn WD (2004) Mouth parts and alimentary canal of *Opsius stactogalus* Fieber (Homoptera: Cicadellidae). *Journal of the Kansas Entomological Society* 77(2): 152–155. <https://doi.org/10.2317/0307.28.1>
- Willis D (1949) The anatomy and histology of the head, gut and associated structures of *Typhlocyba ulmi*. *Proceedings of the Zoological Society of London* 118(4): 984–1001. <https://doi.org/10.1111/j.1096-3642.1949.tb00416.x>
- Yan L, Du Z, Wang H, Zhang S, Cao M, Wang X (2018) Identification and characterization of wheat yellow striate virus, a novel leafhopper-transmitted nucleorhabdovirus infecting wheat. *Frontiers in Microbiology* 9: e468. <https://doi.org/10.3389/fmicb.2018.00468>
- Zacharuk RY (1980) Ultrastructure and function of insect chemosensilla. *Annual Review of Entomology* 25(1): 27–47. <https://doi.org/10.1146/annurev.en.25.010180.000331>
- Zhang CN, Pan LX, Lu YP, Dietrich C, Dai W (2016) Reinvestigation of the antennal morphology of the white-backed planthopper *Sogatella furcifera* (Horváth) (Hemiptera: Delphacidae). *Zoologischer Anzeiger* 262: 20–28. <https://doi.org/10.1016/j.jcz.2016.03.011>
- Zhang Y, Dietrich CH, Duan Y (2020) Structure and sensilla of the mouthparts of *Alobaldia tobae*, *Maiestas dorsalis* and *Stirellus indrus* (Hemiptera: Cicadellidae: Deltocephalinae). *Zoomorphology* 139(2): 189–198. <https://doi.org/10.1007/s00435-020-00478-1>
- Zhao LQ, Dai W, Zhang CN, Zhang YL (2010) Morphological characterization of the mouthparts of the vector leafhopper *Psammotettix striatus* (L.) (Hemiptera: Cicadellidae). *Micron* (Oxford, England) 41(7): 754–759. <https://doi.org/10.1016/j.micron.2010.06.001>

A new species of *Notacanthella* Jacobus & McCafferty, 2008 (Ephemeroptera, Ephemerellidae) from Yunnan, China

Xian-Fu Li^{1,3,4}, Ye-Kang Sun¹, Zi-Ye Liu¹, Luke M. Jacobus², Wen Xiao^{1,3,4}

1 Institute of Eastern-Himalaya Biodiversity Research, Dali University, Dali 671000, Yunnan, China
2 Division of Science, Indiana University Purdue University Columbus, Columbus 47203, IN, USA
3 Collaborative Innovation Center for Biodiversity and Conservation in the Tree Parallel Rivers Region of China, Dali University, Dali, Yunnan, China **4** Research Center of Ecology and Governance for Er'hai Lake Streams, Dali, Yunnan, China

Corresponding authors: Luke M. Jacobus (luke.jacobus@gmail.com), Wen Xiao (xiaow@eastern-himalaya.cn)

Academic editor: Eduardo Dominguez | Received 2 March 2022 | Accepted 28 April 2022 | Published 26 May 2022

<http://zoobank.org/4711CEFE-3F64-4C89-9667-37F78DCFF5B5>

Citation: Li X-F, Sun Y-K, Liu Z-Y, Jacobus LM, Xiao W (2022) A new species of *Notacanthella* Jacobus & McCafferty, 2008 (Ephemeroptera, Ephemerellidae) from Yunnan, China. ZooKeys 1103: 25–44. <https://doi.org/10.3897/zookeys.1103.82984>

Abstract

Notacanthella jinwu Li & Jacobus, **sp. nov.** is described based on egg, nymph, and winged stages from Dali Bai Autonomous Prefecture, Yunnan Province, China. The nymph of the new species is closely related to *N. commodema* (Allen, 1971), whose nymphs share a similar tuberculation of head, pronotum, and mesonotum. However, the nymph of our new species can be distinguished based on the structures of male sternum IX and abdominal tergal tubercles. In addition, the new species is distributed in subtropical high-altitude areas. The description of the male imago of the new species is the first certain one for the genus *Notacanthella*. Data associated with our new species allow for expanded discussion and diagnosis of *Notacanthella* and closely related genera. An identification key for nymphs of these groups is provided.

Keywords

Cangshan Mountain, Hengduan Mountains, Mayfly, Southwest China

Introduction

Jacobus and McCafferty (2008) were the last to revise the genera of the mayfly family Ephemerellidae (Ephemeroptera). Their “*nigra* group” (Jacobus and McCafferty 2008: fig. 94) included five eastern Palearctic and Indomalayan genera: *Adoranexa* Jacobus & McCafferty, 2008, *Cincticostella* Allen, 1971, *Ephacerella* Paclt, 1994, *Notacanthella* Jacobus & McCafferty, 2008, and *Spinorea* Jacobus & McCafferty, 2008. Subsequent studies have emphasized the relationships of these groups but have had limited taxon sampling (Ogden et al. 2009; Zhang et al. 2021). Considerable contributions have been made in the last few years to our knowledge of the genera *Cincticostella* and *Notacanthella* (Martynov et al. 2019, 2021; Auychinda et al. 2020a, b; Li et al. 2020; Zhang et al. 2020, 2021; Zheng and Zhou 2021).

Based on the work reviewed above, *Cincticostella* now contains 21 species, *Notacanthella* and *Spinorea* each contain three species, and *Adoranexa* and *Ephacerella* are monospecific.

The genus *Notacanthella* has been reported low altitude areas of China, Thailand, and Vietnam, and it currently is comprised of the following species: *Notacanthella commodema* (Allen, 1971), *N. perculata* (Allen, 1971), and *N. quadrata* (Kluge & Zhou in Kluge et al. 2004). Two other species attributed to this genus that were known only as male imagos were recently confirmed to be conspecific with a related species, *Cincticostella gosei* (Allen, 1975) (Zhang et al. 2021). At one time, *Notacanthella* species were divided into two subgenera. However, this classification was revised based on new observations of the lateral serration of the maxillary canines, which is prone to wear and is often difficult to examine. As a result, the subgenus *Samiocca* Jacobus & McCafferty, 2008 is considered to be a strict synonym of *Notacanthella* (Auychinda et al. 2020b). The imago stages of the three *Notacanthella* species remain unknown, and the egg is known only for *N. quadrata* (Auychinda et al. 2020b: fig. 7). Zhang et al. (2021) emphasized the need for research on this group and both Zhang et al. (2021) and Martynov et al. (2021) raised questions about the relationships of species within *Cincticostella* and among related genera.

During our recent survey of the mayfly fauna of Hengduan Mountain Area, southwest China, an undescribed species of *Notacanthella* was found only in high altitude areas. Here, we describe this new *Notacanthella* species based on imago, subimago, nymph, and egg stages. Our laboratory association of the male imago provides the basis for the first confident description of the male imago of *Notacanthella*.

Materials and methods

Notacanthella nymphs were collected with a D-frame net from moderately fast-flowing areas of streams in Dali Bai Autonomous Prefecture, western Yunnan, China. Habitat photographs were taken using a Huawei Nova 8 mobile phone equipped with a Kase 40–75 mm macro lens. Some specimens were dissected under the stereomicroscope

and were mounted on slides with Hoyer's solution for examination under the digital microscope. Slide-mounted specimens were examined and photographed under a Keyence VHX-S550E digital microscope. For scanning electron microscopy (SEM), eggs were dried, coated with gold, and observed with a VEGA3 SBU SEM (Tescan, Brno, Czech Republic). Measurements were taken using ImageJ image processing software. Final plates were prepared with Adobe Photoshop CC 2018.

All materials examined of the new species are deposited in the Museum of Biology, Institute of Eastern-Himalaya Biodiversity Research, Dali University, Dali, Yunnan, China (MBDU).

The map of the sampling sites was made in QGIS Standalone Installer v. 3.10 and the 30-m Digital Elevation Model (DEM) data is provided by Geospatial Data Cloud site, Computer Network Information Center, Chinese Academy of Sciences (<http://www.gscloud.cn>).

We utilized a combination of morphological and ecological species concepts when formulating species hypotheses.

Results

Notacanthella jinwu Li & Jacobus, sp. nov.

<http://zoobank.org/9C000D1-7B7E-4367-BC67-0548820E97DD>

Figs 1–10

Material examined. Holotype: male, with final nymphal instar exuvia (in ethanol, deposited in MBDU), China, Yunnan Province, Dali City, Mt. Cangshan, Mocan Stream, 25°39'22.2"N, 100°11'10.1"E, 2020 m a.s.l., 23.X.2021, coll. Xian-Fu Li. **Paratypes:** 10 nymphs, 6 imagos and 3 subimagos reared from nymphs with same data as holotype; 10 nymphs and 4 imagos reared from nymphs from same location as holotype, but 23.X.2021, coll. Xian-Fu Li; 20 nymphs and 5 imagos reared from nymphs from type locality, but 19.IX.2021, coll. Xian-Fu Li; 1 nymph, Dali City, Mount Cangshan, Qingbi Stream, 25°39'05.5"N, 100°9'08.4"E, 2316 m a.s.l., 14.V.2021, coll. Kun Yang; 3 nymphs, Qingbi Stream, 25°40'11.0"N, 100°11'02.7"E, 1974 m a.s.l., 3 nymphs, Qingbi Stream, 25°39'20.2"N, 100°9'44.1"E, 2098 m a.s.l., 16.VIII.2021, coll. Kun Yang; 3 nymphs, Qingbi Stream, 25°39'08.6"N, 100°9'27.3"E, 2221 m a.s.l., 21.VIII.2021, coll. Kun Yang; 2 nymphs, Yunnan, Bincuan City, Mount Jizushan, Shazhi River, 25°56'54.4"N, 100°21'40.0"E, 1947 m a.s.l., 21.VIII.2021, coll. Rong-Long Yang and Kun Yang. All the specimens are deposited in MBDU.

Diagnoses. The new species is similar to *N. commodema* because both have nymphs with two pairs of flattened tubercles on the head, genae that are not produced into sharp projections, seven prominent tubercles on the pronotum, seven tubercles on the mesonotum, claws of all legs with five or six basal denticles, and posterolateral projections of abdominal segment IX that are not elongate. The new species can be distinguished from *N. commodema* by the shape and orientation of its longer and sharper

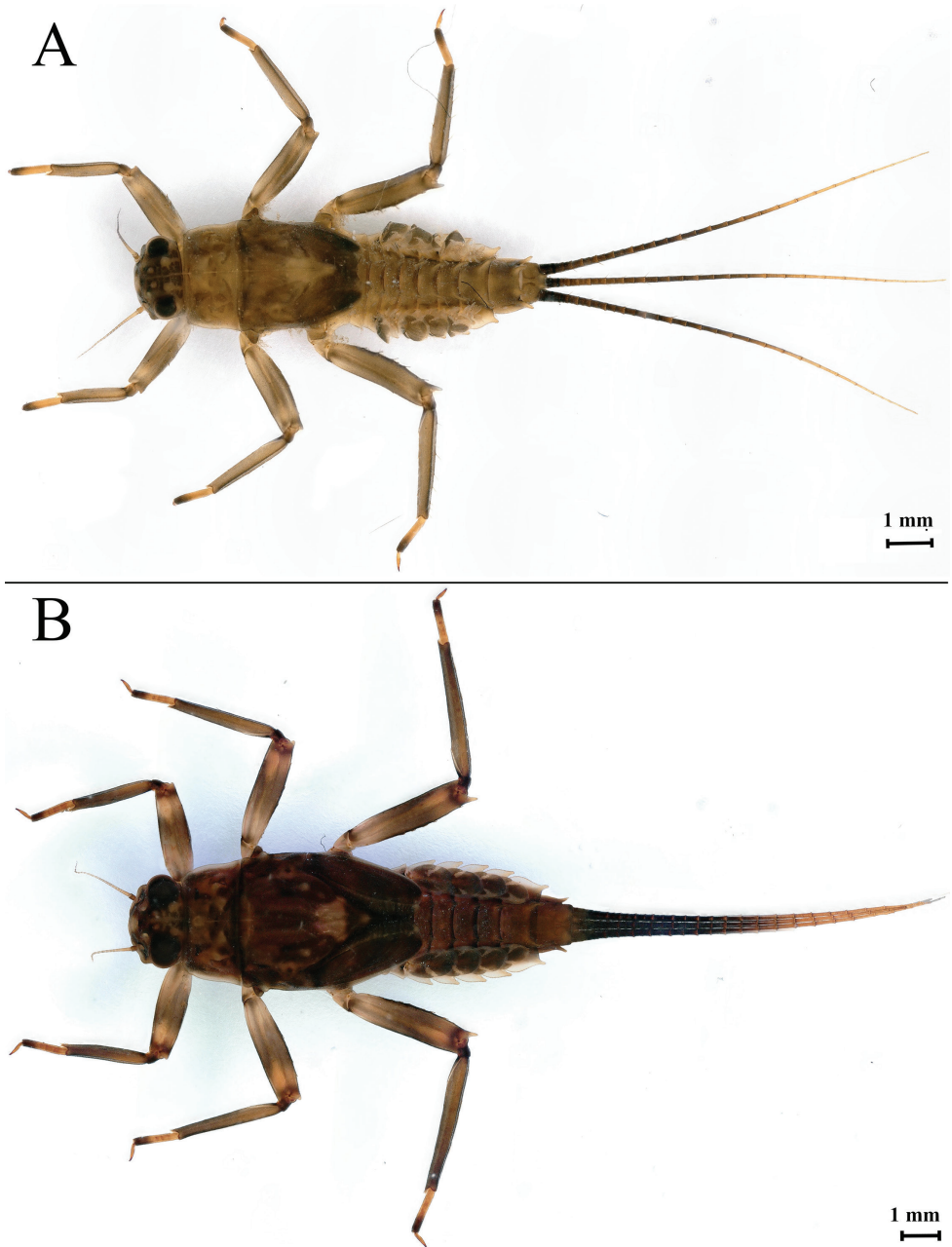


Figure 1. *Notacanthella jinwu* Li & Jacobus, sp. nov. **A** middle instar, dorsal habitus **B** last nymphal instar, dorsal habitus.

abdominal tergal tubercles and by the structure of abdominal sternum IX in males, which is subquadrate with rounded posterolateral projections (see identification key, below). The ecological distribution of our new species is in subtropical high-altitude

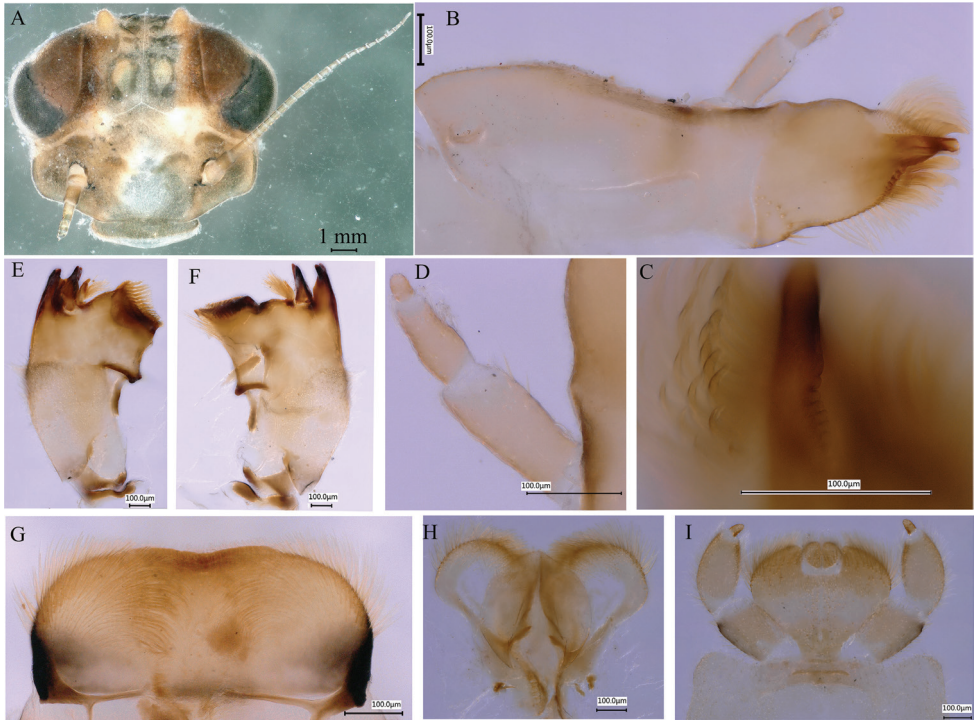


Figure 2. *Notacanthella jinwu* Li & Jacobus, sp. nov. **A** head, anterior view **B** maxilla **C** maxillary canines with lateral serration **D** maxillary palp **E** left mandible **F** right mandible **G** labrum **H** hypopharynx **I** labium.

areas, in contrast to *N. commodema*, which is found in areas below 1000 m elevation. The imagos of other *Notacanthella* species are not known, so a diagnosis is not possible. Likewise, a meaningful diagnosis of the egg stage is not possible, either. See discussion for further information and remarks.

Descriptions. Final nymphal instar (in ethanol). Body length 12.08–12.30 mm (excluding tails); head width 2.15–2.54 mm, cerci lengths 9.04–10.50 mm, median filament 9.57–10.60 mm. Body coloration brown with dark brown markings (Fig. 1A, B).

Head. Brown, with two pairs of tubercles; large occipital tubercles and small suboccipital tubercles (Fig. 2A). Maxillae with maxillary canine length greater than relative width (Fig. 2B), and with lateral serration (Fig. 2C); three-segmented maxillary palp covered with hair-like setae, segment length ratio from base to apex = 3.1: 2.4: 1 (Fig. 2D). Left mandible (Fig. 2E) and right mandible (Fig. 2F), with three outer incisors and two inner incisors, with tuft of short setae present in concavity close to molar area, and densely covered with irregularly ordered hair-like setae on dorsolateral surface. Labrum densely covered with setae, anterior margin somewhat concave medially (Fig. 2G). Hypopharynx: sublingua rounded with anterolateral hair-like setae, lingua oval with anterolateral, short setae (Fig. 2H). Labium densely covered with hair-like setae and with transverse stripes; glossae length greater than width; labial

palp three-segmented, first and second segments subequal in length, third segment smaller (Fig. 2I).

Thorax. Pronotum without anterolateral projections; lateral margins convex; dorsal surface with seven tubercles: one medially, two submedially, two laterally, and two sublaterally; lateral tubercles prominent, but sublateral tubercles inconspicuous (Fig. 3A, B). Mesonotum with paired small and rounded anterolateral projection; lateral margins convex; dorsal surface with seven tubercles: two anteromedially, two medially, and three posteromedially (Fig. 3A, B). Foreleg: femur brown with dark brown bands medially and distally; dorsal margin with chalazae, short fine setae, and a few stout, pinnate, and clavate setae; ventral and outer margins densely covered with short, fine setae and few stout pinnate and clavate setae; dorsal and ventral aspects of tibia and tarsi brown with short, fine setae, few short, stout, pinnate, and clavate setae; apex of tibia and inner margin of tarsi with set of acute setae; ratio of femur: tibia: tarsus = 2.0: 1.9: 1 (Fig. 3C). Middle leg similar to foreleg, but ratio of femur: tibia: tarsus = 2.3: 2.5: 1 (Fig. 3C). Hind leg similar to foreleg and middle leg, but ratio of femur: tibia: tarsus = 2.5: 3.0: 1 and outer margin of tibia with row of long, stout, pinnate, and clavate setae (Fig. 3F). Long hair-like setae densely distributed at base of outer margin of each femur. Various stout setae of different lengths, some pointed and some rounded, present at apex of each tarsus (Fig. 3G–I). All claws with one row of five or six denticles (Fig. 3G–I).

Abdomen. Abdominal terga brown, convex; terga III–VIII with prominent wing-like lateral projections (Fig. 4A); paired dorsal tubercles on segments I–X, tubercles short and tips parallel at base of segments I–IV, longer and tips progressively divergent on segments V–IX, long and divergent tubercles on segment IX, shorter and tips parallel on segment X; lateral projections of segment IX not extending beyond segment X (Fig. 4A, C). Lateral projections and apices of tubercles of each segment with stout, clavate setae (Fig. 4D, E). Posterior margin of sternum IX of male straight (Fig. 5A); posterior margin of sternum IX of female concave (Fig. 5B). Gills III–V with bifurcate and multifoliate ventral lamellae, gill VI ventral lamella integral and multifoliate, gill VII ventral lamella multifoliate; dorsal lamella of gill III rounded (Fig. 4F), dorsal lamellae of gills IV–VII paddle-shaped (Fig. 4G–J). Caudal filaments brown with whorls of small, almost rounded, scale-like setae and few long, unbranched setae at apex of each segment (Fig. 5C).

Character variability. We examined specimens of different instars and some characters may vary between earlier and later instars, similar to its close relative, *N. commodema* (Allen 1971; Auychinda et al. 2020b).

Male imago (in ethanol). Body length 11.73–13.17 mm (excluding tails), head width 2.13–2.36 mm, cerci lengths 11.31–13.98 mm, median filament length 11.07–14.52 mm, forewing length 14.12–17.31 mm, hindwing length 3.92–6.88 mm. Compound eyes contiguous, upper portion reddish brown and lower portion black. Body generally reddish brown to dark brown (Fig. 6). Prosternum dark brown, with slightly concave central longitudinal carina. Mesonotal scutellum with three projections at posterior margin, middle projection short (Fig. 7B). Forewings

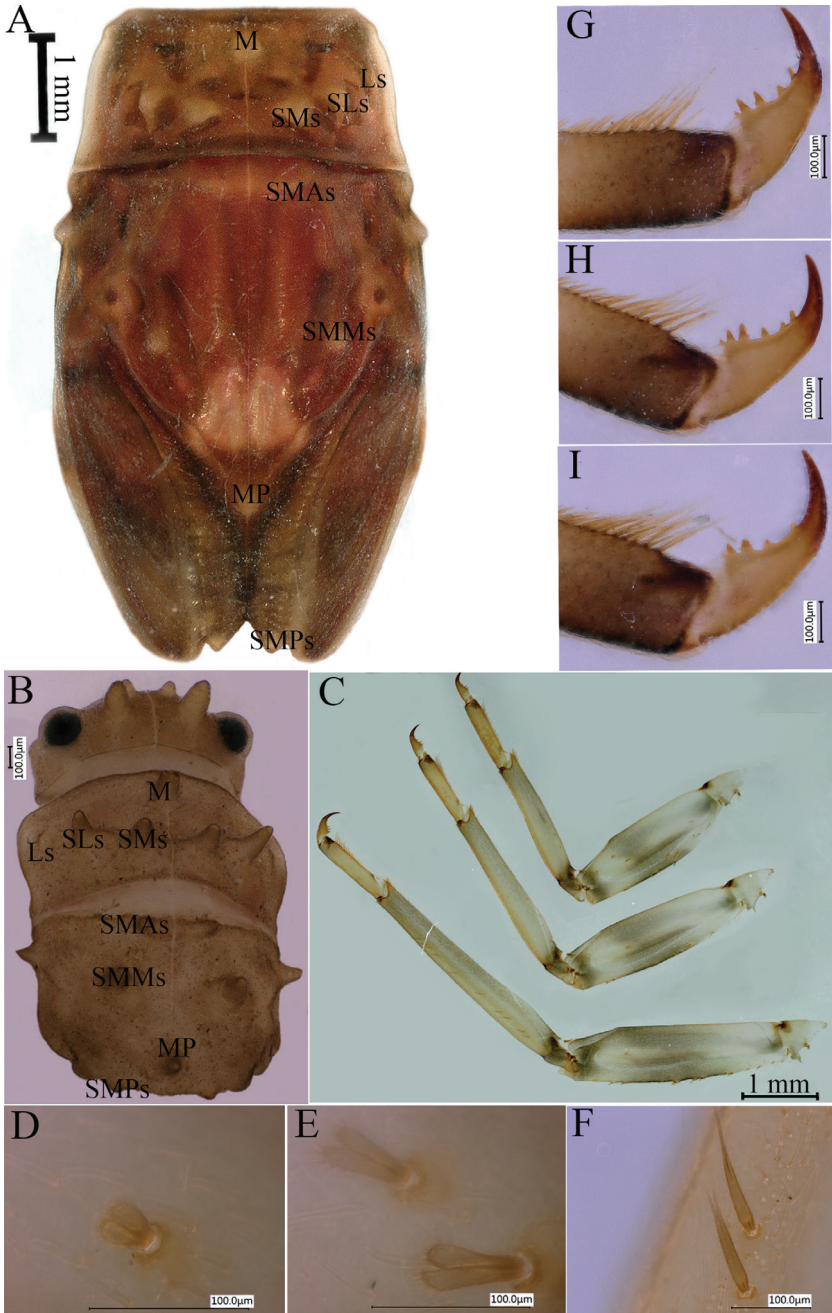


Figure 3. *Notacanthella jinwu* Li & Jacobus sp. nov. **A** thorax of last nymphal instar, dorsal view **B** thorax of early instar, dorsal view **C** legs, dorsal view, from top to bottom foreleg, midleg and hindleg **D** setae on femur **E** setae on femur **F** setae on tibia of hind leg **G** claw of foreleg **H** claw of midleg **I** claw of hindleg. (M=median tubercle; SMs = submedian tubercles; Ls = lateral tubercles; SLs = sublateral tubercles; SMAs = submedian anterior tubercles; SMMs = submedian tubercles at middle; MP = median posterior tubercle; SMPs = submedian posterior tubercles).

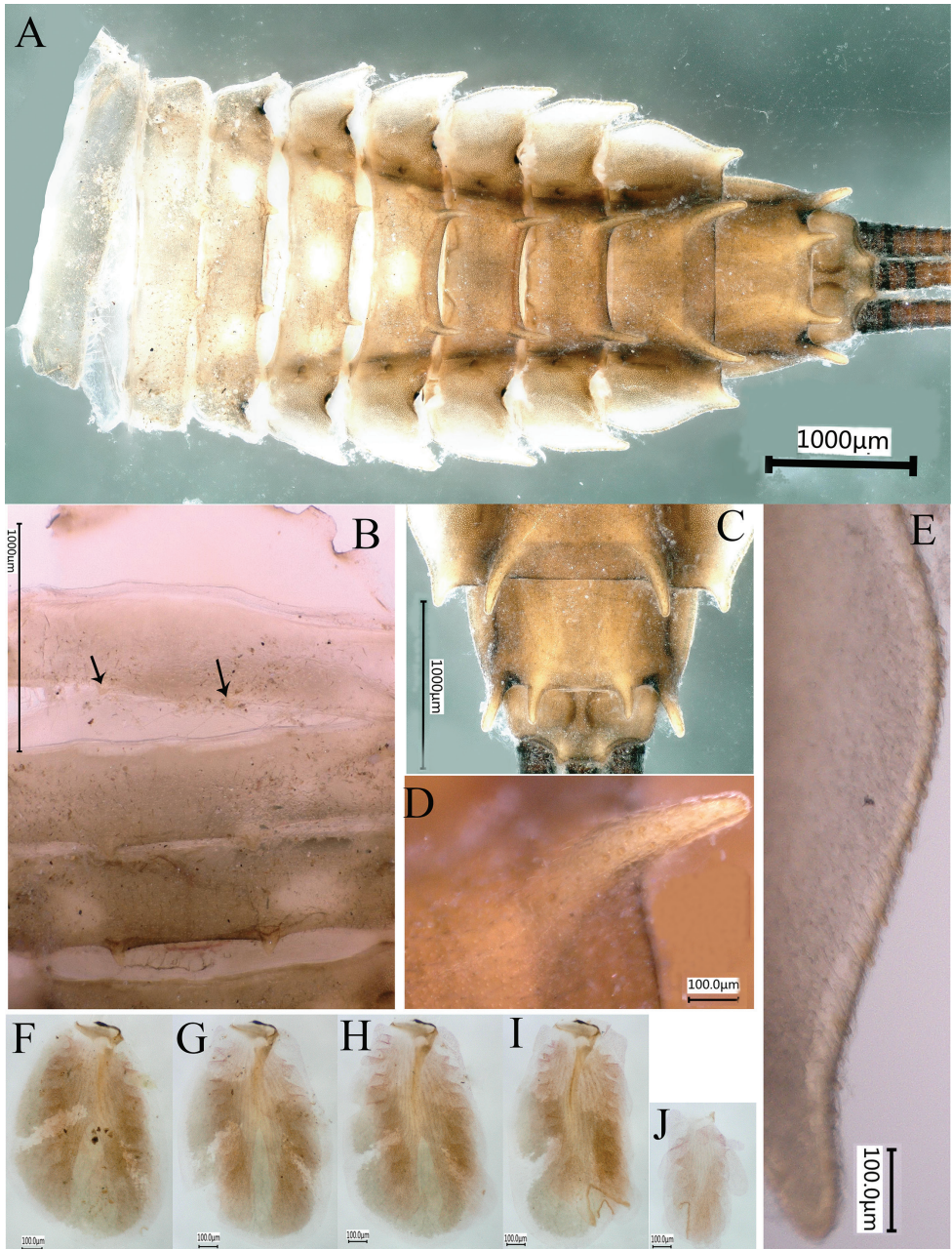


Figure 4. *Notacanthella jinwu* Li & Jacobus sp. nov. **A** abdomen, nymph, dorsal view **B** abdominal segments I–III of last nymphal instar **C** abdominal segments VII–X of last nymphal instar **D** tubercle of abdominal tergum VII of last nymphal instar **E** lateral margins of abdominal segment VII of last nymphal instar **F** gill III **G** gill IV **H** gill V **I** gill VI **J** gill VII.

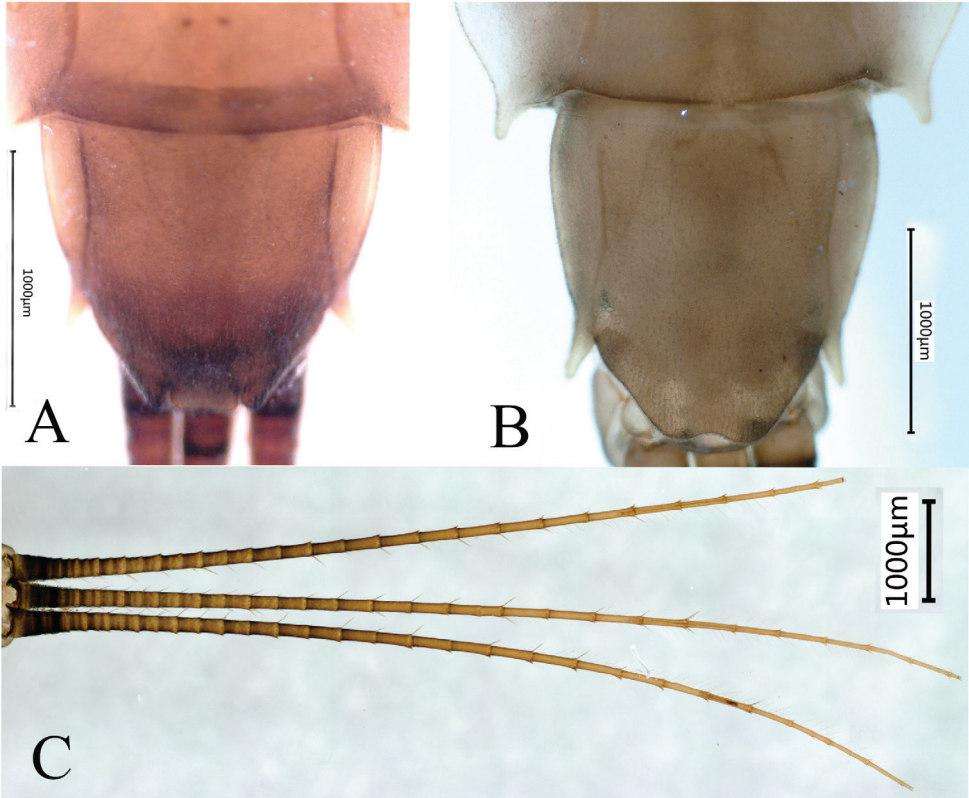


Figure 5. *Notacanthella jinwu* Li & Jacobus sp. nov. **A** structure of sternum IX of male nymph **B** structure of sternum IX of female nymph **C** nymphal caudal filaments.

generally hyaline, veins reddish brown; cells of costal and subcostal fields tinted with reddish brown; cross veins in stigmatic area slightly oblique, and those between costal and subcostal separated into two rows cells; MA forked 1/4 distance from base to margin; MP forked 2/3 distance from base to margin (Fig. 7C). Hindwings hyaline, veins reddish brown; leading margin slightly concave; MA single, MP margin forked symmetrically (Fig. 7D). Fore legs reddish brown to dark brown, middle and hind legs reddish brown (Fig. 7E). All legs without distinct markings. Femur: tibia: tarsus of foreleg = 1: 1.3: 1.2, tarsal segments from basal to apical = 1: 3.5: 3.1: 2.0: 1.4; femur: tibia: tarsus of midleg = 1.8: 2.1: 1.0, tarsal segments from basal to apical = 1: 1.9: 1.8: 1.4: 2.3; femur: tibia: tarsus of hindleg = 2.8: 3.6: 1, tarsal segments from basal to apical = 1: 1.9: 1.8: 1.4: 2.3. Claws of all legs similar, one blunt and one hooked. Abdomen reddish brown to dark brown, terga I–VII each with one or three longitudinal median pale stripes; terga VIII–IX each with large and irregular pale stripes, posterolateral projections of terga VIII–IX each extended into sharp spine-like structures.



Figure 6. Male imago of *Notacanthella jinwu* Li & Jacobus sp. nov. (living).

Genitalia. Forceps covered with stout setae (Fig. 8D, E); segment 3 globular; segment 2 angled inward distally and with slight subapical constriction (Fig. 8A, B). Penes lobes compact, with linear groove on ventral face; lobes separated by slight cleft; anteromedial, dorsomedial and lateral stout setae absent; dorsolateral projection absent (Fig. 8A–C).

Female imago. Colour pattern similar to male; body general reddish brown to dark brown (Fig. 9A). Body length 8.08–14.1 mm (excluding tails), head width 1.65–2.2 mm, cerci lengths 10.08–10.32 mm, median filament length 9.66–11.3 mm. Prosternum reddish brown, with slightly convex central longitudinal carina. Mesonotum dark brown; scutellum with three projections at posterior margin, middle projection short. Forewing 13.28–16.5 mm, hyaline, with veins reddish brown; cells C and SC tinted with reddish brown. Hindwing 3.45–4.8 mm, totally hyaline, with veins reddish brown. Each leg reddish brown to dark brown; length of femur: tibia: tarsus of foreleg = 2.0: 1.8: 1, tarsal segments from basal to apical = 1.4: 1.7: 1.7: 1: 2.4; femur: tibia: tarsus of midleg = 2.6: 2.7: 1.0, tarsal segments from basal to apical = 1: 1.1: 1.2: 1: 2.1; femur: tibia: tarsus of hindleg = 3.1: 3.7: 1.0, tarsal segments from basal to apical = 1.1: 1: 1.2: 1.2: 2.2. Abdomen reddish brown to dark brown; subgenital plate produced to 1/5 length of sternum VIII; posterior margin of subanal plate without obvious median cleft (Fig. 9B).

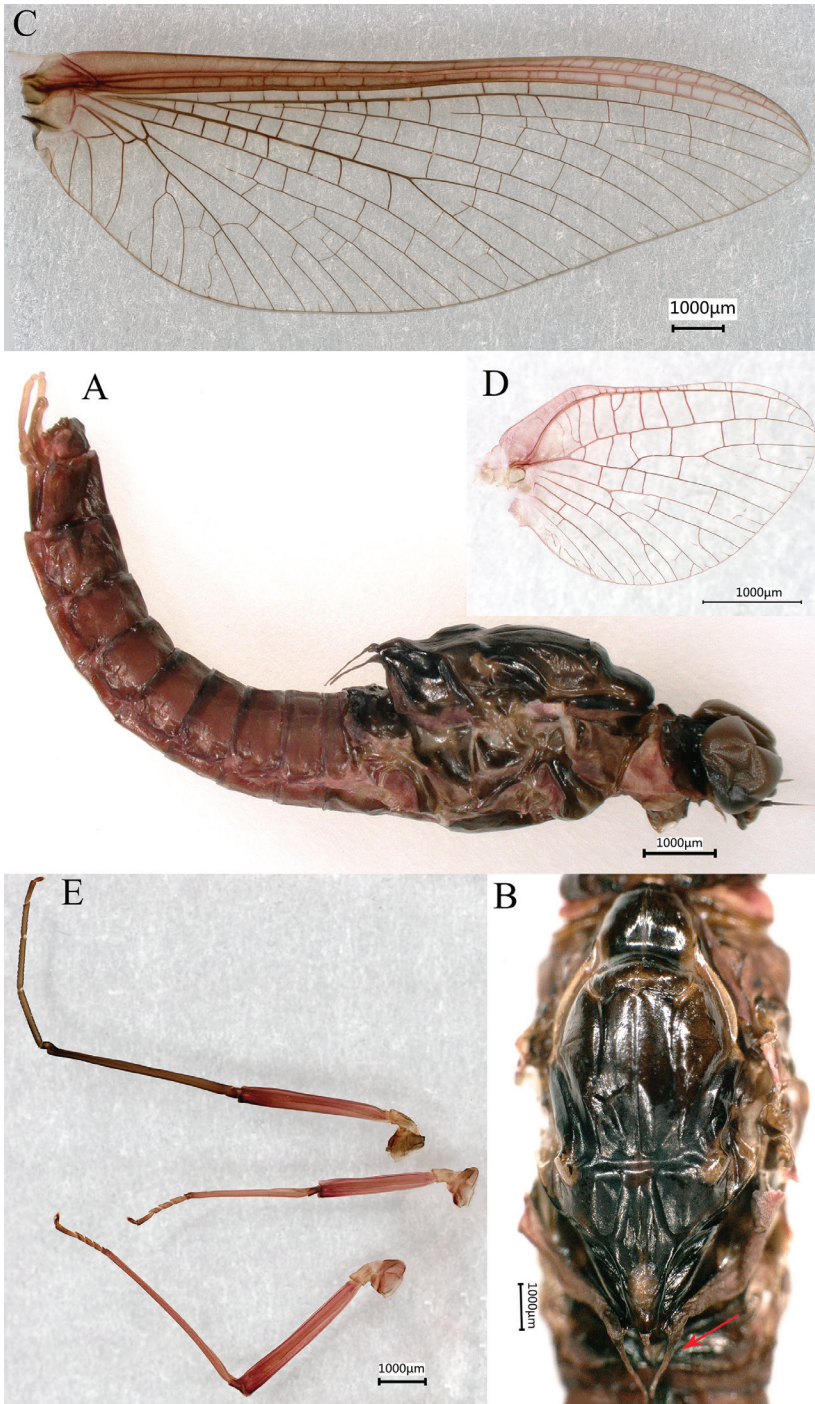


Figure 7. Male imago of *Notacanthella jinwu* Li & Jacobus sp. nov. **A** lateral view of body **B** dorsal view of thorax (lateral scutellar projection indicated by red arrow) **C** forewing **D** hindwing **E** legs, from top to bottom foreleg, midleg and hindleg.

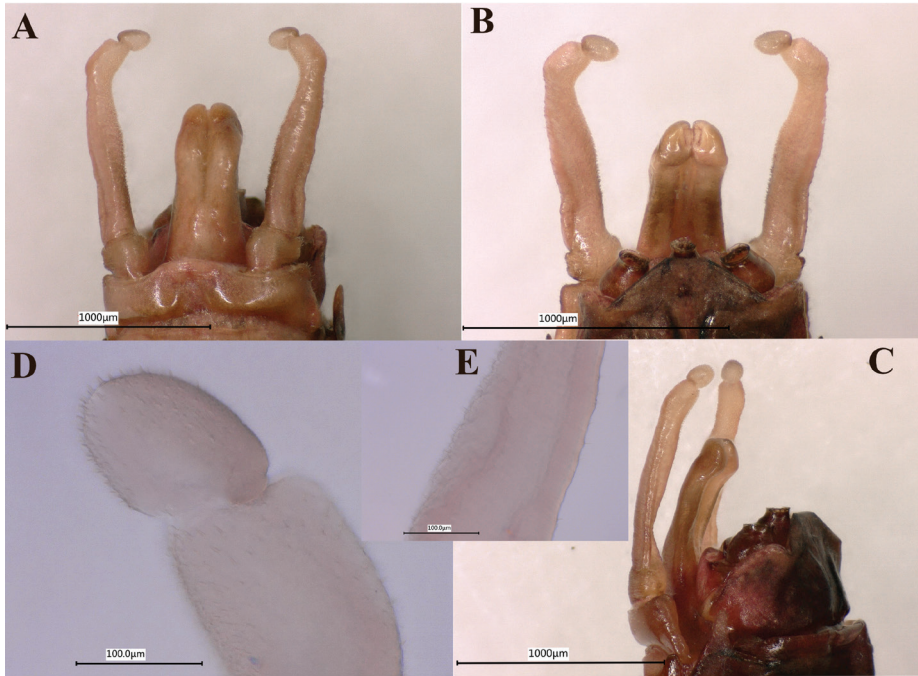


Figure 8. Male imago genitalia of *Notacanthella jinwu* Li & Jacobus sp. nov. **A** ventral view **B** dorsal view **C** lateral view **D** forceps segments 2 and 3 **E** bottom of forceps segment 2.

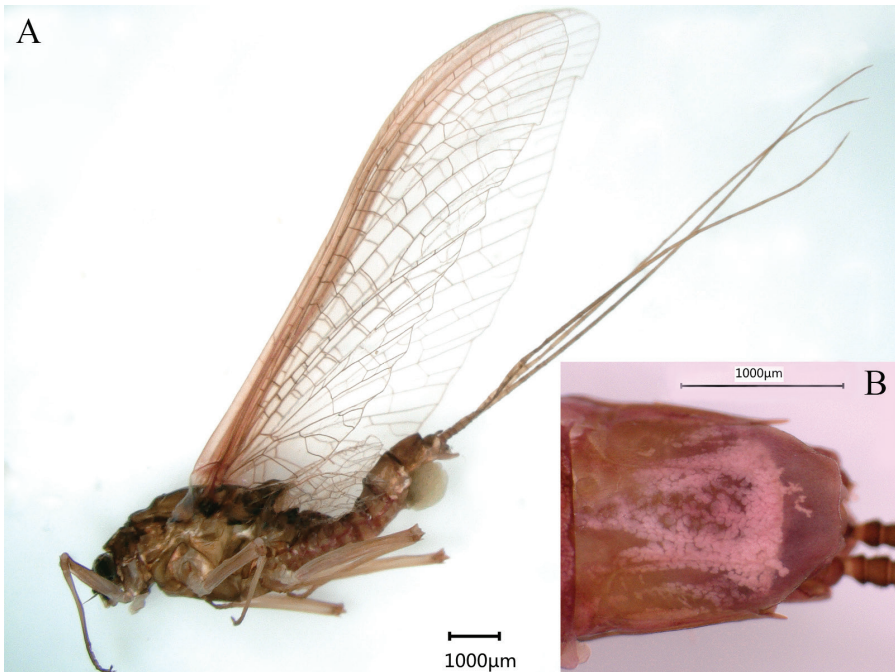


Figure 9. Female imago of *Notacanthella jinwu* Li & Jacobus sp. nov. **A** lateral view **B** terminal parts of abdomen, ventral view.

Male subimago. Body reddish brown (Fig. 10A); wings brown and subhyaline; scutellum with three long, pointed posterior prolongations (Fig. 10B); tarsus of foreleg shorter than femur, caudal filaments shorter than body length.

Female subimago. Body red brown; wings brown and subhyaline; scutellum with three long, pointed posterior prolongations; tarsus of foreleg shorter than femur, caudal filaments shorter than body length. Posterior margin of subanal plate without obvious median cleft, similar to female imago. Otherwise, similar to male subimago except for usual sexual differences.

Egg (dissected from female imago). Length 171–218 μm , width 134–158 μm . Ovoid with one small polar cap (Fig. 11A, B); chorion with reticulations, strands ridged; mesh with multiple central tubercles (Fig. 11A, C, D); several lateral attachment structures in subpolar areas (Fig. 11A, C); knob of attachment structure and micropyle (Fig. 11D) distributed near equator (Fig. 11A, C), micropyle round and micropylar rim absent.

Etymology. The name, *jinwu* (feminine), comes from Jin Wu, a Chinese mythical creature. In China, ancient people took “Jin Wu” as the alias of the sun. The reddish brown subimago is similar to the color of a rising sun. Given that the emergence of *N. jinwu* sp. nov. happened at sunrise, we can imagine *N. jinwu* as the body double of the sun. The common name of this species is the Jinwu spiny crawler mayfly.

Distribution. China (Yunnan).

Ecology. The stream in Dali City and Binchuan County where the nymphs of *N. jinwu* were collected is 1.2–5.0 m wide, with a natural water body depth 5–35 cm. It contains stones of various sizes, aquatic plants, and litter (Fig. 12A). During collecting, the nymphs were found hiding under stones or climbing on aquatic plants,



Figure 10. Male subimago of *Notacanthella jinwu* Li & Jacobus sp. nov. **A** living specimen **B** thorax, dorsal view.

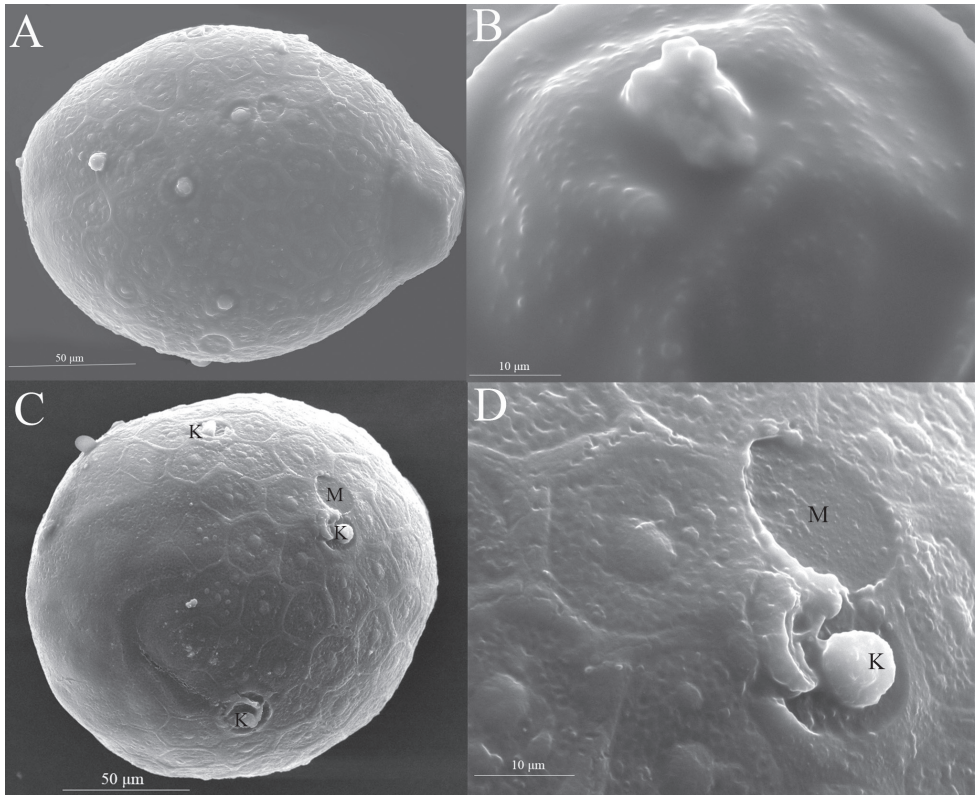


Figure 11. Egg of *Notacanthella jinwu* Li & Jacobus, sp. nov. **A** lateral view **B** polar cap **C** bottom view of the opposite pole **D** knob of attachment structure (K) and micropyle (M).

moving slowly and swimming weakly. The nymphs are only distributed between 1947 and 2316 m above sea level (Fig. 12C). In indoor conditions, nymphs generally hid under rocks (Fig. 12B), but they were more active when eating aquatic plants and litter. The last instar nymphs molted at sunrise and flew after a short rest. The subimago stage persisted for 2 days and molted during the daytime. The observed timespan of the imago stage was about 3 days. According to our monthly field survey, the nymphs of *N. jinwu* Li & Jacobus, sp. nov. are found from May to November.

Discussion

Morphological plasticity within species is well documented for insects (e.g., Moczek 2010) and has been widely documented and assumed for mayflies. In our study, however, the morphology was remarkably unchanged between the early emergence individuals and the later ones. However, we did observe the morphological differences between instars, such as relative development of body armature, that have been documented elsewhere for this genus (e.g., Allen 1971; Auychinda et al. 2020b).

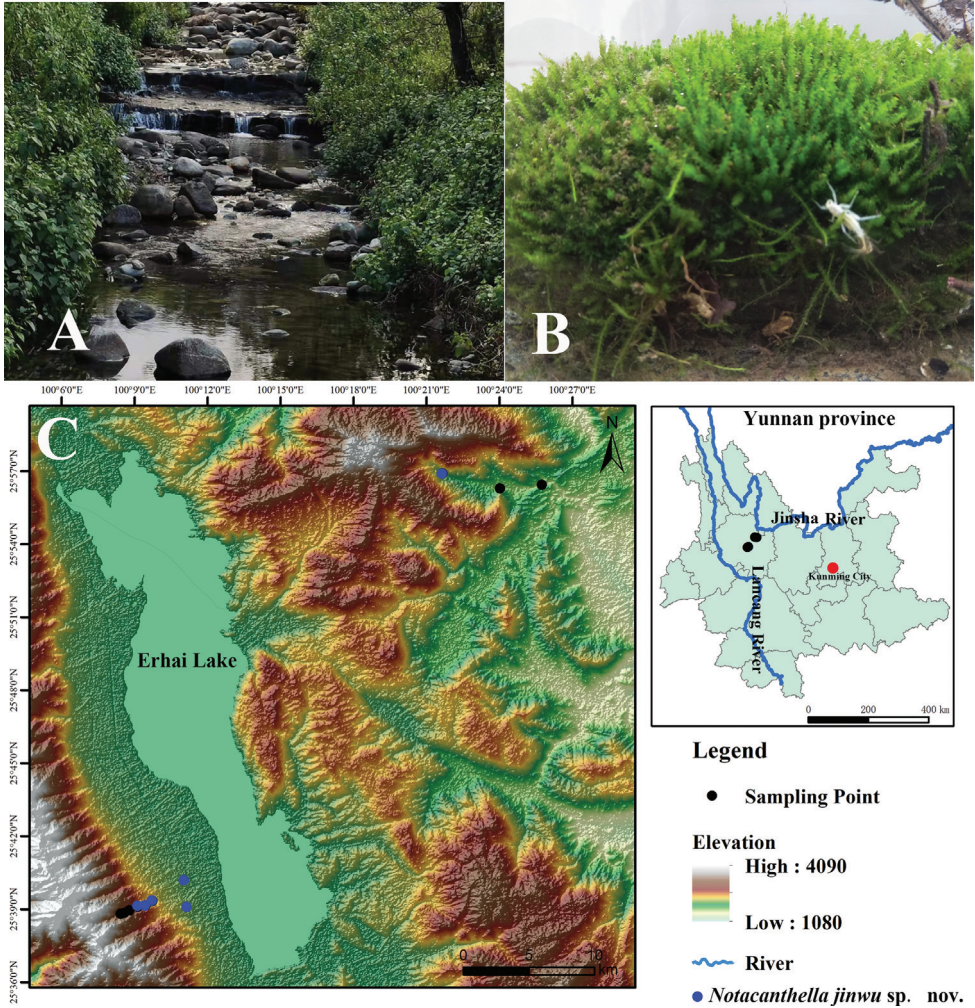


Figure 12. Habitat and distribution map of *Notacanthella jinwu* Li & Jacobus, sp. nov. **A, B** habitats in Dali City (note recently molted nymph in **B**) **C** distribution map of *N. jinwu* sp. nov. in Dali Bai Autonomous Prefecture.

The different ecological niches of aquatic organisms influence their altitudinal patterns of distribution, based on differences in adaptability to the environment (Liu et al. 2021). In addition to morphological differences between our new species and *N. commodema*, there are also important differences in the ecological niches of the two species. *Notacanthella commodema* is distributed in areas below 1000 m altitude in the tropics, but *N. jinwu* Li & Jacobus, sp. nov. is found in areas at altitudes around 2000 m in the subtropics.

A holistic approach is needed to address the systematics of *Notacanthella*, and so the related genera *Adoranexa*, *Cincticostella*, *Ephacerella*, and *Spinorea* are included in the discussion that follows, insofar as the state of knowledge allows.

The eggs of our new species (Fig. 11) have strands that are relatively smooth, in contrast to the strands of *N. quadrata* (Auychinda et al. 2020b: fig. 7) which are covered with excrescences and small papillae. The eggs of *N. commodema* and *N. perculta* are not known. The eggs of both *N. quadrata* and our new species differ from the egg of *Cincticostella gosei* (Zhang et al. 2021: fig. 6), which has a chorionic surface that lacks distinct strands; it is apparently roughened, with a variety of excrescences and a wrinkled appearance. *Spinorea montana* (Kang & Yang, 1995) (Kang and Yang 1995: figs 9, 10) and several other *Cincticostella* species (e.g., Kang and Yang 1995: figs 14–17; Jacobus and McCafferty 2008: fig. 3) have eggs generally similar to our new species, but the eggs of *Spinorea glebosa* (Kang & Yang, 1995) are different (Kang and Yang 1995: fig. 8). The eggs of *Spinorea gilliesi* (Allen & Edmunds, 1963) are not known. In *Ephacerella longicaudata* (Ueno, 1928) (Ishiwata and Nishino 2020: figs 19, 20) the eggs have smooth strands and a rough, pitted mesh, extremely similar to many *Cincticostella* species. The eggs of *Adoranexa soldani* (Allen, 1986) are unknown. Some other ephemereid genera that are not part of this group of genera also have similar eggs (e.g., Jacobus and McCafferty 2008: fig. 1; p. 245: key couplet 8), and thus this morphology may represent either a pleisiotypic or convergent condition.

The male genitalia of our new species (Figs 7A, 8) have a distal constriction on forceps segment 2. The forceps are constricted more distally than *Ephacerella* and some *Cincticostella* species (Jacobus and McCafferty 2008; Zhang et al. 2021), but other *Cincticostella* species have a similar position of this constriction (e.g., Jacobus and McCafferty 2008: fig. 86). Worth noting, too, is that yet other *Cincticostella* species (Zheng and Zhou 2021: figs 6, 7) have forceps extremely similar to some *Ephemerella* Walsh, 1862 species (e.g., Jacobus and McCafferty 2008: figs 74, 75). Unfortunately, the other *Notacanthella* species and most *Cincticostella* species are not known in the male imago stage, nor are the genera *Adoranexa* and *Spinorea*. Thus, meaningful and informative comparisons are not possible, and few conclusions can be made at this time. Anecdotally, the male genitalia and coloration of our new species are very similar to how LMJ remembers the genitalia and appearance of *Notacanthella* sp. A of Jacobus and McCafferty (2008) from Thailand (Phitsanulok Province, Phu Hin Rongkla National Park; altitude 1280 m).

Commonly, the structure of nymphal sternum IX reflects the morphology of mayfly male genitalia developing underneath. So, we speculate that there will be male genitalia differences between the new species and *N. commodema*. However, since the imago of *N. commodema* remains unknown, this hypothesis remains untested. We note that Auychinda et al. (2020b) reported differences in sternum IX of female nymphs identifiable as *N. commodema*, and they considered the possibility of a cryptic species complex. More work, using different kinds of data, clearly is needed to investigate species diversity of *Notacanthella*.

Despite our fragmentary knowledge of the egg and male imago stages of this group of ephemereid genera, all species are known in the nymphal stage. An updated key that would include all *Cincticostella* species is beyond the scope of this study. Eight *Cincticostella* species have been described since the last key was provided by Xie et al. (2009), and we are aware of several additional undescribed new species from western China alone. We do provide a key below, though, to all the species of *Adoranexa*,

Ephacerella, *Notacanthella*, and *Spinorea* in order to facilitate recognition and further detailed studies of these species that might be easily confused with one another. Such detailed studies will help to resolve the poorly supported systematics of this group (Jacobus and McCafferty 2008; Ogden et al. 2009) and lead to evolutionary hypotheses important for understanding aquatic life in the Indomalayan region.

Key to final nymphal instars of *Cincticostella*-complex genera and of species of *Adoranexa*, *Ephacerella*, *Notacanthella*, and *Spinorea*

- 1 Pronotum with prominent anterolateral projections...*Cincticostella* and *Notacanthella* (in part) **2**
- Pronotum with anterolateral projections very subtle or absent **3**
- 2 Maxillary canines reduced to short, denticulate blade *Cincticostella*
- Maxillary canines long and acute at apices **8** (*Notacanthella*)
- 3 Lateral margins of abdominal posterolateral projections bare or with only a few, inconspicuous setae (e.g., Fig. 4E); maxillary canines fused and distinctly spoonlike, with no notch at apex **8** (*Notacanthella*)
- Lateral margins of abdominal posterolateral projections with distinct setae; maxillary canines fused and either spoonlike with a single apical notch, or reduced to a wide blade..... **4**
- 4 Lateral margins of mesal plate with paired spines or ridges..... **5**
- Lateral margins of mesal plate unadorned *Ephacerella longicaudata*
- 5 Maxillary canine blade length much less than width *Adoranexa soldani*
- Maxillary canine blade length subequal to width **6** (*Spinorea*)
- 6 Maxillary palp long, tip nearly reaching apex of maxilla (Kang and Yang 1995: fig. 1E); abdominal tergal tubercles relatively short, not much longer than posterolateral projections of same abdominal segment (Kang and Yang 1995: fig. 1D)..... *Spinorea glebosa*
- Maxillary palp relatively short, extending only to middle of galea-lacinia (Allen and Edmunds 1963: fig. 32; Kang and Yang 1995: fig. 2E); most abdominal tergal tubercles distinctly longer than posterolateral projections of same abdominal segment (Allen and Edmunds 1963: fig. 36; Kang and Yang 1995: fig. 2D)..... **7**
- 7 Abdominal terga tubercles distinctly divergent (Kang and Yang 1995: fig. 2D); tarsal claw with 5–7 denticles (proximal denticle often tiny and easily overlooked) *Spinorea montana*
- Abdominal tergal tubercles subparallel (Allen and Edmunds 1963: fig. 36); tarsal claw with 2–4 denticles (proximal denticle often tiny and easily overlooked)..... *Spinorea gilliesi*
- 8 Head with strong and acute genal projections; pronotum with distinct anterior projections *Notacanthella quadrata*
- Head without strong genal projections; pronotum with anterior projections very subtle or absent **9**

- 9 Posterolateral projections on abdominal segment IX extend well beyond posterior margin of segment X (Allen 1971: fig. 28).....*Notacanthella perculata*
- Posterolateral projections on abdominal segment IX do not extend beyond posterior margin of segment X (Figs 1A–B, 4A; Allen 1971: fig. 27)..... **10**
- 10 Paired tubercles on terga VIII and IX short and blunt (Auychinda et al. 2020b: Fig. 4F); medial projection of male sternum IX short and rounded, with adjacent projections sharp at tips (see Auychinda et al. 2020b: fig. 5D)
-*Notacanthella commodema*
- Paired tubercles on terga VIII and IX long and sharp (Fig. 4A, C); medial projection of male sternum IX longer and subquadrate, with adjacent projections rounded at tips (Fig. 5A) *Notacanthella jinwu* sp. nov.

Acknowledgements

This work was supported by the National Natural Science Foundation of China (31960255) and the Second Tibetan Plateau Scientific Expedition and Research Program (2019QZKK0402). We thank Michel Sartori (Museum of Zoology, Palais de Rumine, Lausanne, Switzerland) and Chonlakran Auychinda (Kasetsart University, Bangkok, Thailand) for past discussion, examination of specimens of related species, and sharing of images and data. Thanks are due to Rong-Long Yang, Kun Yang, Zhen Tian, and Xin-Lei Hou (Dali University) for help with fieldwork. We are grateful to Xiao-Li Tong (South China Agricultural University), Michel Sartori (Musée cantonal de zoologie, Lausanne, Switzerland), and an anonymous reviewer for useful suggestions and corrections that improved the quality of the manuscript.

References

- Allen RK (1971) New Asian Ephemeroptera with notes (Ephemeroptera: Ephemerellidae). Canadian Entomologist 103(4): 512–528. <https://doi.org/10.4039/Ent103512-4>
- Allen RK (1975) *Ephemerella* (*Cincticostella*): A revision of the nymphal stages. The Pan-Pacific Entomologist 51(1): 16–22.
- Allen RK (1986) Mayflies of Vietnam: *Acerella* and *Drunella* (Ephemeroptera: Ephemerellidae). The Pan-Pacific Entomologist 62: 301–302.
- Allen RK, Edmunds GF (1963) New and little known Ephemerellidae from southern Asia, Africa and Madagascar (Ephemeroptera). Pacific Insects 5: 11–22.
- Auychinda C, Muranyi D, Li W, Sartori M, Gattolliat JL (2020a) A new species of *Cincticostella* (Ephemeroptera, Ephemerellidae) from China. Alpine Entomology 4: 129–138. <https://doi.org/10.3897/alpento.4.50597>
- Auychinda C, Sartori M, Boonsoong B (2020b) Review of *Notacanthella* Jacobus & McCafferty, 2008 (Ephemeroptera: Ephemerellidae) in Thailand, with the redescription

- of *Notacanthella commodema* (Allen, 1971). *Zootaxa* 4731(3): 414–424. <https://doi.org/10.11646/zootaxa.4731.3.9>
- Ishiwata SI, Nishino M (2020) Mayflies of Lake Biwa. In: Kawanabe H, Nishino M, Maehata M (Eds) *Lake Biwa: Interactions Between Nature and People*, 2nd edn. Springer, Cham, 175–182.
- Jacobus LM, McCafferty WP (2008) Revision of Ephemerellidae genera (Ephemeroptera). *Transactions of the American Entomological Society* 134(1): 185–274. [https://doi.org/10.3157/0002-8320\(2008\)134\[185:ROEGE\]2.0.CO;2](https://doi.org/10.3157/0002-8320(2008)134[185:ROEGE]2.0.CO;2)
- Kang SC, Yang CT (1995) Ephemerellidae of Taiwan (Insecta, Ephemeroptera). *Bulletin of National Museum of Natural Science* 5: 95–116.
- Kluge N, Zhou CF, Jacobus LM, McCafferty WP (2004) A new southeast Asian mayfly species (Ephemeroptera: Ephemerellidae: Ephemerellinae). *Journal of the New York Entomological Society* 112(2–3): 148–152. [https://doi.org/10.1664/0028-7199\(2004\)112\[0148:ANSA MS\]2.0.CO;2](https://doi.org/10.1664/0028-7199(2004)112[0148:ANSA MS]2.0.CO;2)
- Li R, Zhang W, Ma Z, Zhou C (2020) Novel gene rearrangement pattern in the mitochondrial genomes of *Torleya mikhaili* and *Cincticostella fusca* (Ephemeroptera: Ephemerellidae). *International Journal of Biological Macromolecules* 165: 3106–3114. <https://doi.org/10.1016/j.ijbiomac.2020.10.124>
- Liu S, Li X, Tan L, Fornacca D, Fang Y, Zhu L, Rao C, Cao Y, Huang J, Ren G, Cai H, Xiao W (2021) The ecological niche and terrestrial environment jointly influence the altitudinal pattern of aquatic biodiversity. *The Science of the Total Environment* 800: e149404. <https://doi.org/10.1016/j.scitotenv.2021.149404>
- Martynov AV, Selvakumar C, Subramanian KA, Sivaramakrishnan KG, Chandra K, Palatov DM, Sinha B, Jacobus LM (2019) Review of the *Cincticostella insolta* (Allen, 1971) complex (Ephemeroptera: Ephemerellidae), with description of three new species from northern India and Nepal. *Zootaxa* 4551(2): 147–179. <https://doi.org/10.11646/zootaxa.4551.2.2>
- Martynov AV, Selvakumar C, Palatov DM, Subramanian KA, Sivaramakrishnan KG, Vasanth M, Jacobus LM (2021) Overview of Indian and Nepali representatives of the *Cincticostella nigra* (Ueno, 1928) complex (Ephemeroptera, Ephemerellidae), with discussion about *Cincticostella* Allen, 1971 species complexes. *ZooKeys* 1040: 123–166. <https://doi.org/10.3897/zookeys.1040.64280>
- Moczek AP (2010) Phenotypic plasticity and diversity in insects. *Philosophical Transactions of the Royal Society of London* 365(1540): 593–603. <https://doi.org/10.1098/rstb.2009.0263>
- Ogden TH, Osborne JT, Jacobus LM, Whiting MF (2009) Combined molecular and morphological phylogeny of Ephemerellinae (Ephemeroptera), with remarks about classification. *Zootaxa* 1991(1): 28–42. <https://doi.org/10.11646/zootaxa.1991.1.2>
- Paclt J (1994) *Ephacerella*, a replacement name for *Acerella* Allen, 1971 (Ephemeroptera), nec Berlese, 1909 (Protura). *Entomological News* 105: 283–284.
- Ueno M (1928) Some Japanese mayfly nymphs. *Memoirs of the College of Science, Kyoto Imperial University, Series B* 4(1): 19–63. [pls 3–17]

- Walsh BD (1862) List of the Pseudoneuroptera of Illinois contained in the cabinet of the writer, with descriptions of over forty new species, and notes on their structural affinities. Proceedings. Academy of Natural Sciences of Philadelphia 1862: 361–402.
- Xie H, Jia Y-Y, Chen P, Jacobus LM, Zhou C-F (2009) Two new *Cincticostella* species from China with a larval key to species of the genus (Ephemeroptera: Ephemerellidae). Zootaxa 2299(1): 53–61. <https://doi.org/10.11646/zootaxa.2299.1.5>
- Zhang W, Han N, Zhang M, Wang Y-F, Zhou C-F (2020) The imaginal and detailed nymphal characters of *Cincticostella fusca* (Kang & Yang, 1995) (Ephemeroptera: Ephemerellidae). Zootaxa 4729(2): 277–285. <https://doi.org/10.11646/zootaxa.4729.2.8>
- Zhang M, Li WJ, Ying XL, Zhou CF (2021) The imaginal characters of *Cincticostella gosei* (Allen, 1975) linking the genus *Cincticostella* Allen, 1971 to *Ephacrerella* Paclt, 1994 (Ephemeroptera: Ephemerellidae). Zootaxa 5081(1): 131–140. <https://doi.org/10.11646/zootaxa.5081.1.5>
- Zheng X, Zhou C (2021) First detailed description of adults and nymph of *Cincticostella femorata* (Tshernova, 1972) (Ephemeroptera: Ephemerellidae). Aquatic Insects 42(1): 23–36. <https://doi.org/10.1080/01650424.2020.1871026>

Two new species of *Hemiptarsenus* Westwood (Hymenoptera, Eulophidae) from China, with a key to Chinese species

Jun-Jie Fan¹, Cheng-De Li¹

¹ School of Forestry, Northeast Forestry University, Harbin, 150040, China

Corresponding author: Cheng-De Li (lichengde0608@sina.com)

Academic editor: Miles Zhang | Received 13 April 2022 | Accepted 10 May 2022 | Published 26 May 2022

<http://zoobank.org/9AC886E7-D12E-42FC-9A3F-C3D45F9BE90F>

Citation: Fan J-J, Li C-D (2022) Two new species of *Hemiptarsenus* Westwood (Hymenoptera, Eulophidae) from China, with a key to Chinese species. ZooKeys 1103: 45–56. <https://doi.org/10.3897/zookeys.1103.85228>

Abstract

Two new species of *Hemiptarsenus* Westwood, *H. tianshuiensis* **sp. nov.** and *H. longjiangensis* **sp. nov.**, are described from China. New distributional data for *H. jilinus* Tao, 2021 are provided, and a key to Chinese species of the genus is given based on females.

Keywords

Chalcidoidea, Eulophinae, parasitoid, taxonomy

Introduction

The genus *Hemiptarsenus* (Hymenoptera, Eulophidae) was erected by Westwood (1833) with *Hemiptarsenus fulvicollis* Westwood as the type species. This genus is mainly distributed in the Palaearctic region, where 17 species were recorded. Currently the genus contains 34 valid species worldwide: 33 species were recorded in the Universal Chalcidoidea Database (Noyes 2019), and one species was described

recently by Tao et al. (2021). Eight species are known from China: *H. fulvicollis* Westwood, 1833, *H. jilinus* Tao, 2021, *H. ornatus* (Nees, 1834), *H. strigiscuta* Zhu, LaSalle & Huang, 2000, *H. tabulaeformisi* Yang, 2015, *H. unguicellus* (Zetterstedt, 1813), *H. varicornis* (Girault, 1913), and *H. zilahisebessi* Erdős, 1951 (Sheng et al. 1989; Lee 1990; Zhu et al. 2000; Xu et al. 2001; Zhu and Huang 2002; Yang et al. 2015; Tao et al. 2021). Members of this genus are mainly larval or nymphal parasitoids of Diptera (Agromyzidae, Ephydriidae), Hemiptera (Coccidae), Lepidoptera (Cosmopterigidae, Elachistidae, Gracillariidae, Lyonetiidae, Momphidae, Nepticulidae, Pyralidae, Yponomeutidae), Coleoptera (Curculionidae), and Hymenoptera (Tenthredinidae) (Yang et al. 2015).

Hemiptarsenus species can be recognized by the following combination of characteristics: funicle 4-segmented in females and with three branches in males; apex of scape extending above level of vertex; notauli incomplete; mesoscutellum without sublateral grooves; fore wing costal cell narrow, at least 10 times as long as wide.

This study describes two new species of the genus. New distributional data for *H. jilinus* Tao, 2021 and a key to females of all species of the genus are provided.

Material and methods

All specimens were collected by sweeping or yellow-pan trapping, and they were dissected and mounted in Canada balsam on slides following the method of Noyes (1982) or mounted on cards. Slide-mounted specimens were photographed with a digital CCD camera attached to an Olympus BX51 compound microscope. Specimens on card were photographed with an Aosvi AO-HK830-5870T microscope. Measurements were made using the built-in software of the Aosvi AO-HK830-5870T. The quality of these photos was improved by using Helicon Focus 7 and Adobe Photoshop 2020.

Terminology follows the Hymenoptera Anatomy Consortium (2022) for most body parts except the callus, which follows Gibson (1997). The following abbreviations are used:

- F1–4** flagellomeres 1–4;
- MV** marginal vein;
- OOL** minimum distance between a posterior ocellus and corresponding eye margin;
- PMV** postmarginal vein;
- POL** minimum distance between posterior ocelli;
- SMV** submarginal vein;
- STV** stigmal vein.

All type material is deposited in the insect collections at Northeast Forestry University (NEFU), Harbin, China.

Results

Key to Chinese species of *Hemiptarsenus* Westwood based on females

- 1 Mesoscutellum longitudinally sculptured (e.g. Fig. 20) 2
- Mesoscutellum reticulate (e.g. Figs 5, 15)..... 4
- 2 Propodeum, axillae and metascutellum smooth.....
..... *H. strigiscuta* Zhu, LaSalle & Huang
- Propodeum, axillae and metascutellum reticulate 3
- 3 Mesoscutellum orange-yellow or yellow; propodeum without median carina and plicae *H. ornatus* (Nees)
- Mesoscutellum dark metallic green; propodeum with complete median carina and plicae.....*H. jilinus* Tao
- 4 Metascutellum predominantly smooth..... 5
- Metascutellum predominantly reticulate 8
- 5 Clava dark brown basally and pale yellow or white apically*H. varicornis* (Girault)
- Clava completely dark brown..... 6
- 6 Mesoscutum metallic green with transverse yellow patch; length of propodeum at most half the length of mesoscutellum, plicae and median carina absent.....
..... *H. zilahisebessi* Erdős
- Mesoscutum completely metallic green; length of propodeum at least 0.7× as long as mesoscutellum, plicae and median carina present 7
- 7 Axillae mostly smooth; midlobe of mesoscutum with 3 pairs of setae (Fig. 5)
..... *H. tianshuiensis* sp. nov.
- Axillae reticulate; midlobe of mesoscutum with 2 pairs of setae.....
..... *H. unguicellus* (Zetterstedt)
- 8 PMV shorter than or at most as long as STV; disc of fore wing slightly clouded .
..... *H. fulvicollis* Westwood
- PMV at least 1.9× as long as STV; fore wing hyaline..... 9
- 9 Gaster with a large median longitudinal black patch from base to apex, margins of tergites 1–5 yellow; plicae complete (Fig. 10).....*H. longjiangensis* sp. nov.
- Gaster predominantly dark brown; plicae short and incomplete, only present in posterior 1/5 *H. tabulaeformisi* Yang

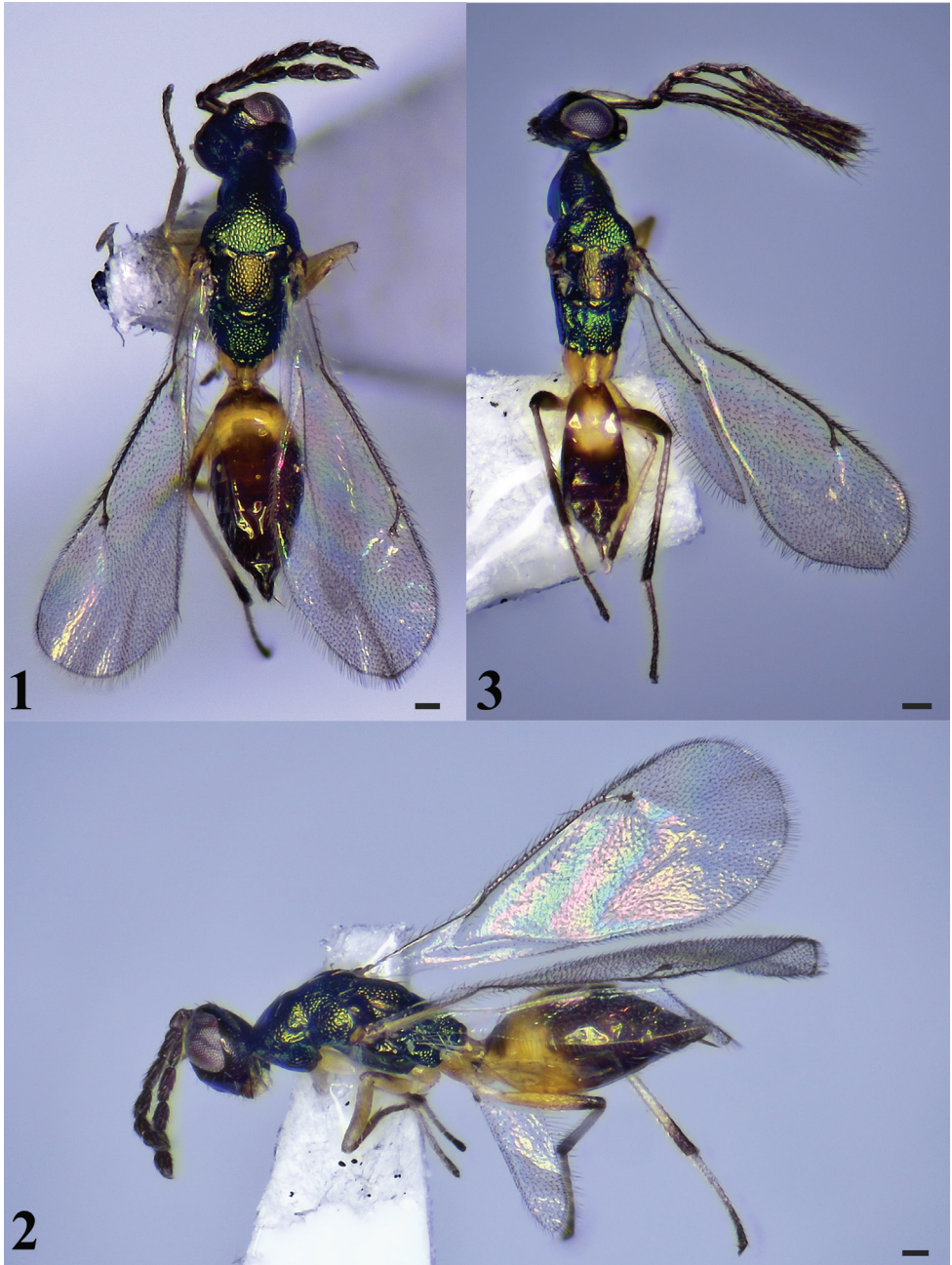
Hemiptarsenus tianshuiensis sp. nov.

<http://zoobank.org/E29DB39C-1E3B-4213-B1F4-61A82EAF6891>

Figs 1–8

Type material. *Holotype*, ♀ [NEFU; on card], CHINA, Gansu Province, Tianshui City, Maiji District, Maijishan National Geopark, 23.VII.2020, Jun-Jie Fan, by sweeping.

Paratypes: 2♀1♂; [1♀ on slide, 1♀1♂ on cards], same data as holotype.



Figures 1–3. *Hemiptarsenus tianshuiensis* sp. nov., female, holotype (1, 2), male, paratype (3) 1 habitus in dorsal view 2 habitus in lateral view 3 habitus in dorsal view. Scale bars: 100 μ m.

Diagnosis. Antennae dark brown with ventral surface of scape yellow. Metascutellum mostly smooth with anterior area reticulate. Propodeum about 0.7 \times as long as mesoscutellum measured medially, and strongly reticulate, median carina and plicae present. Mid and

hind leg tibiae yellowish-white with apical 1/3 dark brown, metafemur yellow with apical 1/4 dark brown. Petiole yellow. Gaster dark brown with a transverse yellow patch near base.

Description. Female. Length 1.8–2.0 mm (2.0 mm) mm, fore wing length 1.6–1.8 mm (1.8 mm) mm. Head dark metallic green. Eyes red-brown. Ocelli pale yellow. Scape yellow except dorsal surface dark brown, pedicel and flagellum dark brown. Mesosoma dark metallic green except mesoscutellum with golden-green tinge. Petiole yellow. Gaster dark brown with a transverse yellow patch near base. Fore leg mostly yellowish white with tarsomeres 1–3 brown, tarsomere 4 dark brown; mid leg with coxae and trochanters yellowish white, femur yellow with apical 1/2 brown on dorsal surface, tibiae yellowish-white with apical 1/3 dark brown, tarsomeres 1 and 2 yellowish white and tarsomeres 3 and 4 dark brown; hind leg similar to mid leg with femur apical 1/4 dark brown.

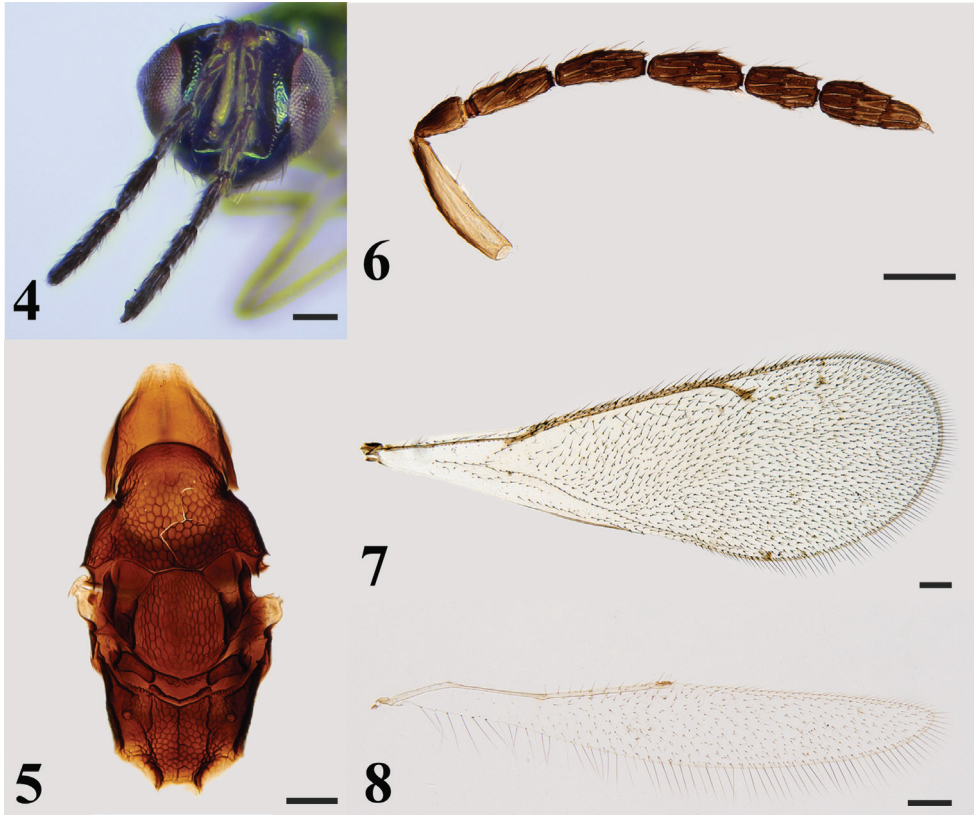
Head (Fig. 4) 1.2–1.3× (1.2×) as wide as high in frontal view and 1.9–2.1× (2.0×) as wide as long in dorsal view, micro-reticulate. POL 2.0× OOL. Eyes with short and dense setae. Malar sulcus present, malar space 0.34× eye height. Mandibles quadridentate. Antennae (Fig. 6) with scape slender and cylindrical, 4.3–4.6× (4.6×) as long as wide, extending far above vertex; pedicel 1.9–2.0× (1.9×) as long as wide and scape 2.4–2.6× (2.5×) as long as pedicel; funicle 4-segmented, F1 2.9–3.2× (3.0×) as long as wide and 1.3–1.4× (1.4×) as long as pedicel, F2 2.9–3.1× (2.9×) as long as wide, F3 and F4 2.6–2.8× (2.6×) and 2.0–2.1× (2.0×) as long as wide respectively; clava 2-segmented, 2.5–2.7× (2.6×) as long as wide, the first clavomere 1.8–1.9× (1.8×) as long as the second.

Mesosoma (Figs 1, 5) 2.0–2.2× (2.1×) as long as wide. Pronotum shorter than mesoscutum, reticulate. Notauli inconspicuous. Mesoscutum strongly reticulate, midlobe of mesoscutum with three pairs of long setae. Axillae mostly smooth and separated from each other. Mesoscutellum 1.2–1.3× (1.2×) as long as wide, shorter than mesoscutum, strongly reticulate, and with two pairs of long setae. Metascutellum mostly smooth with anterior area reticulate. Propodeum about 0.7 × as long as length of mesoscutellum measured medially, strongly reticulate, median carina and plicae present; spiracle separated from metanotum by a distance longer than diameter of spiracle; each propodeal callus with 13 setae. Prepectus with coarse reticulate sculpture. Metacoxa reticulate on dorsal surface.

Wings. Fore wing (Fig. 7) 2.7–2.9× (2.9×) as long as wide. Costal cell 13.7–14.0× (14.0×) as long as wide, with a row of black setae on dorsal surface. SMV with five setae on dorsal surface. Cubital vein straight at base. Speculum small, closed posteriorly. MV 1.3–1.4× (1.3×) as long as PMV. PMV 2.0–2.1× (2.0×) as long as STV. Hind wing (Fig. 8) about 6.4–6.9× (6.9×) as long as wide.

Metasoma (Fig. 1) 1.1–1.2× (1.1×) as long as length of mesosoma. Petiole longer than wide in dorsal view. Gaster ovate, 2.2–2.4× (2.3×) as long as wide. Ovipositor exerted beyond apex of gaster.

Male (Fig. 3). Similar to the female. Body length 1.6 mm, fore wing length 1.5 mm. Head 1.2× as wide as high in frontal view and about 1.9× as wide as long in dorsal view. POL 2.43× OOL. Malar space 0.5× eye height. Antennae dark brown with ventral surface of scape yellow, funicle with three long branches, with long setae. Relative measurements (length: width): scape = 33: 8; pedicel = 10: 7; F1 = 10: 6; F2 = 20: 4; F3 = 22: 4; F4 = 40: 7; clava = 40: 7. Fore wing 3.1× as long as wide. Hind wing about 7.1× as long as



Figures 4–8. *Hemiptarsenus tianshuiensis* sp. nov., female, holotype (**4**), paratype (**5–8**) **4** head in frontal view **5** mesosoma in dorsal view **6** antenna **7** fore wing **8** hind wing. Scale bars: 100 μ m.

wide. MV 1.3 \times as long as PMV. PMV 2.0 \times as long as STV. Metasoma almost as long as mesosoma. Petiole 1.7 \times as long as wide in dorsal view. Gaster ovate, 1.9 \times as long as wide.

Host. Unknown.

Distribution. China (Gansu).

Etymology. The specific epithet refers to the location of the type locality in Tianshui City.

***Hemiptarsenus longjiangensis* sp. nov.**

<http://zoobank.org/F4B950D8-204A-45CA-8CA6-46A96B867426>

Figs 9–15

Type material. *Holotype*, ♀ [NEFU; on card], CHINA, Heilongjiang Province, Yichun City, Dailing District, Liangshui National Nature Reserve, 30–31.VIII. 2019, Wen-Jian Li, Ting-Ting Zhao and Shu-Chen Deng, by yellow-pan trapping. *Paratypes*: 1♀ [on slide], CHINA, Heilongjiang Province, Shangzhi City, Maershan Town,



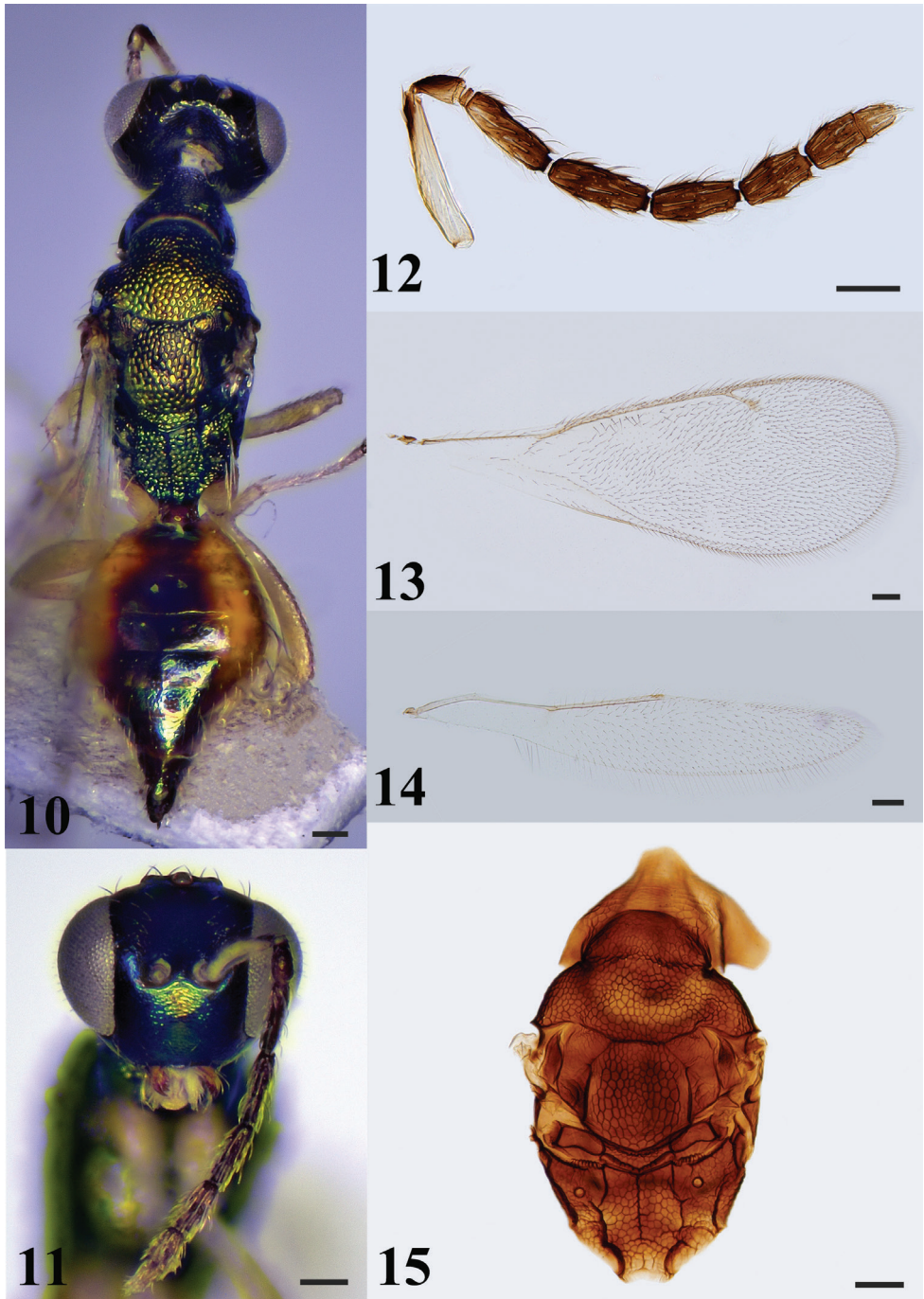
Figure 9. *Hemiptarsenus longjiangensis* sp. nov., female, holotype, habitus in lateral view. Scale bar: 100 μ m.

9.VII.2015, Ye Chen and Chao Zhang, by sweeping; 2♀ [on cards], CHINA, Heilongjiang Province, Yichun City, Dailing District, Liangshui National Nature Reserve, 1.VIII.2015, Si-Zhu Li, Xin-Yu Zhang and Xing-Yue Jin, by sweeping.

Diagnosis. Scape yellow with about apical 1/3 of dorsal surface dark brown, pedicel and flagellum dark brown. Metascutellum reticulate. Propodeum almost as long as length of mesoscutellum measured medially, strongly reticulate, median carina and plicae present. Gaster with a large, median, longitudinal, black patch from base to apex, margins of tergites 1–5 yellow. Metasoma almost as long as mesosoma.

Description. Female. Length 1.9–2.1 mm (2.1 mm), fore wing length 1.8 mm. Head and mesosoma dark metallic green with greenish-blue to golden-green tinge. Eyes gray. Ocelli pale yellow. Antennae dark brown except scape yellow with about apical 1/3 of dorsal surface dark brown. Mandibles brownish with teeth brown. Petiole dark brown. Gaster with a large median longitudinal black patch in middle of dorsal surface from base to apex, margins of tergites 1–5 yellow. Legs yellowish with all trochanters yellowish white. Ovipositor black. Wings hyaline with veins yellowish brown.

Head (Fig. 11) 1.3–1.5 \times (1.5 \times) as wide as high in frontal view and about 1.8–2.0 \times (1.9 \times) as wide as long in dorsal view. Lower face and vertex transversely reticulate, frons weakly reticulate. POL 1.7–1.8 \times (1.8 \times) OOL. Eyes with sparse, short pubescence. Malar sulcus present, malar space 0.26 \times eye height. Each mandible with two large teeth at apex and three small teeth above large teeth. Distance between toruli 0.8 \times diameter of torulus, 1.0 \times distance from torulus to eye margin. Antennae (Fig. 12) with scape slender and cylindrical, 5.6–5.7 \times (5.7 \times) as long as wide, extending far beyond



Figures 10–15. *Hemiptarsenus longjiangensis* sp. nov., female, holotype (10–14), paratype (15) 10 habitus in dorsal view 11 head in frontal view 12 antenna 13 fore wing 14 hind wing 15 mesosoma in dorsal view. Scale bars: 100 μ m.

vertex; pedicel 1.5–1.6× (1.6×) as long as wide and scape 3.6–3.7× (3.6×) as long as pedicel; funicle 4-segmented, F1 3.3–3.5× (3.5×) as long as wide and 2.2× as long as pedicel, F2 2.9–3.0× (3.0×) as long as wide, F3 and F4 2.4–2.6× (2.4×) and 1.8–2.1× (1.8×) as long as wide respectively; clava 2-segmented, 2.5–2.6× (2.5×) as long as wide, first clavomere 1.6–1.7× (1.6×) as long as second.

Mesosoma (Figs 10, 15) 1.8–2.0× (2.0×) as long as wide. Pronotum shorter than mesoscutum, reticulate. Notauli inconspicuous. Mesoscutum strongly reticulate, mid-lobe of mesoscutum with three pairs of long setae. Axillae reticulate and separate from each other. Mesoscutellum almost as long as wide, shorter than mesoscutum, strongly reticulate with two pairs of long setae. Metascutellum reticulate. Propodeum almost as long as length of mesoscutellum measured medially, strongly reticulate, median carina and plicae present; spiracle separated from metanotum by a distance longer than diameter of spiracle; each propodeal callus with nine setae. Prepectus with coarse reticulate sculpture. Metacoxa reticulate on dorsal surface.

Wings. Fore wing (Fig. 13) 2.7–2.9× (2.8×) as long as wide. Costal cell 15.4–16.0× (16.0×) as long as wide. SMV with 10 setae on dorsal surface. Cubital vein straight at base. Speculum small, closed posteriorly. MV 1.3–1.4× (1.3×) as long as PMV; PMV 1.9–2.0× (1.9×) as long as STV. Hind wing (Fig. 14) about 5.7–2.9× (5.9×) as long as wide.

Metasoma (Fig. 10) almost as long as mesosoma. Petiole short, transverse, about 0.5× as long as wide in dorsal view. Gaster ovate, 1.5–1.6× (1.5×) as long as wide. Ovipositor exerted beyond apex of gaster.

Male. Unknown.

Host. Unknown.

Distribution. China (Heilongjiang).

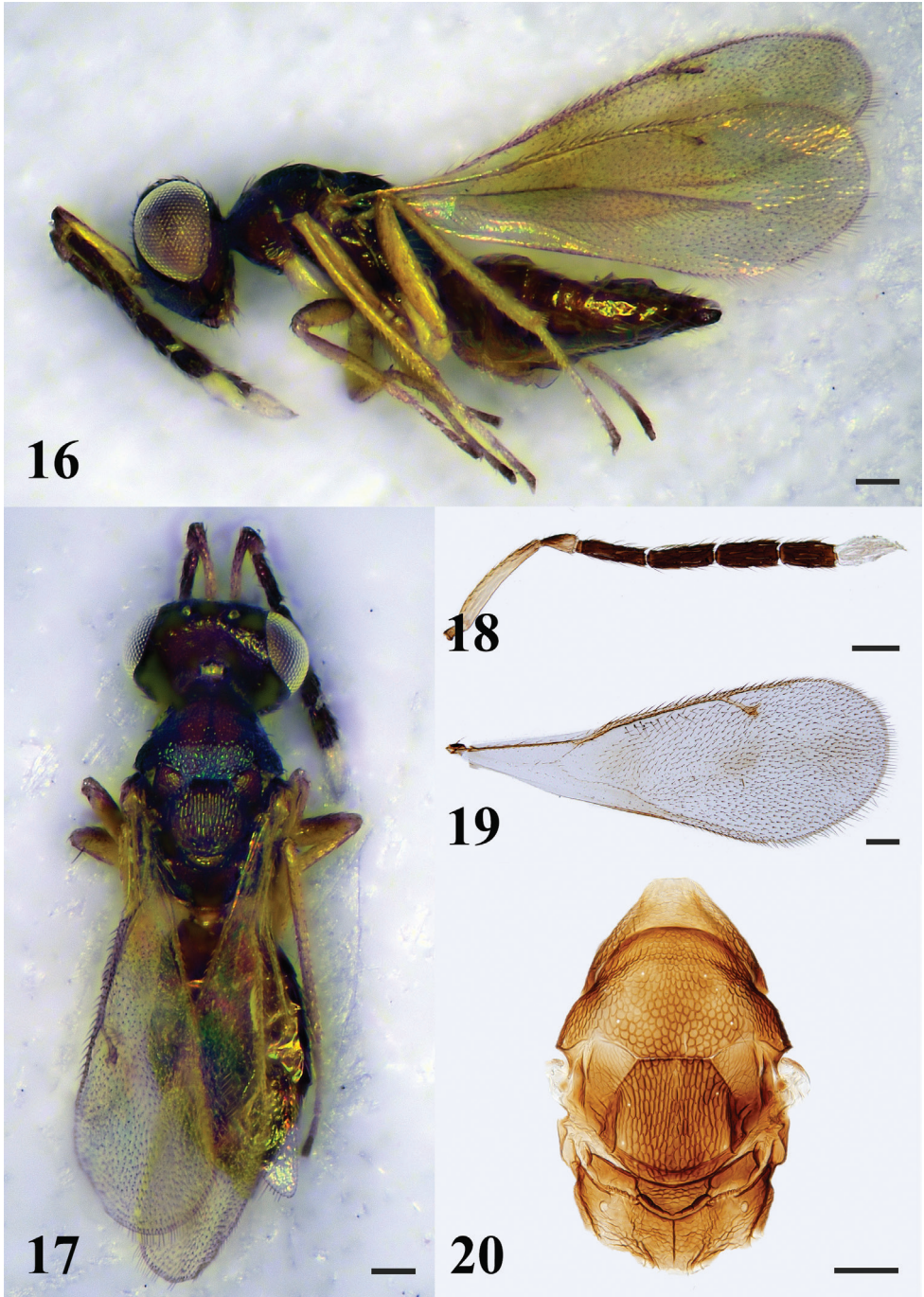
Etymology. The specific epithet refers to Heilongjiang Province where the type locality is located.

Hemiptarsenus jilinus Tao, 2021

Figs 16–20

Hemiptarsenus jilinus Tao, 2021: 175. Holotype, ♀, China, IMJAU, not examined.

Material examined. 11♀ [NEFU; 10 on cards, 1 on slide], CHINA, Liaoning Province, Fushun City, Shimengou, 18–20.VI.2012, Hui Geng, Xiang-Xiang Jin and Jiang Liu, by yellow-pan trapping; 1♀ [on card], CHINA, Heilongjiang Province, Yichun City, Dailing District, Liangshui National Nature Reserve, 30. VIII. 2019, Wen-Jian Li, Ting-Ting Zhao and Shu-Chen Deng, by sweeping; 1♀ [on card], CHINA, Heilongjiang Province, Yichun City, Dailing District, Liangshui National Nature Reserve, 30.VI.2018, Jun-Jie Fan, Guang-Xing Wang and Jun Wu, by sweeping; 2♀ [NEFU; 2 on cards], CHINA, Beijing, Baihuashan, 10–11.V.2012, Hui-Lin Han, Guo-Hao Zu and Jiang Liu, by yellow-pan trapping; 2♀ [NEFU; 2 on cards], CHINA, Hebei



Figures 16–20. *Hemiptarsenus jilinus* Tao, female **16** habitus in lateral view **17** habitus in dorsal view **18** antenna **19** fore wing **20** mesosoma in dorsal view. Scale bars: 100 μ m.

Province, Chengde City, Xinglong County, Wulingshan, 16–18.V.2017, Guang-Xing Wang and Wen-Jian Li, by yellow-pan trapping.

Diagnosis. Female. Head and mesosoma dark metallic green; gaster brown with or without yellowish patch near base. Antennae with funicle dark brown, scape and pedicel pale yellow or with dark on dorsal surface, clava white. Legs yellow with coxae and trochanters white. Mesoscutellum longitudinally sculptured. Metascutellum raised-reticulate. Propodeum shorter than mesoscutellum, with median carina and plicae complete. POL 1.6–1.7× OOL. Malar sulcus present, malar space 0.4–0.5× eye height. Antennae (Fig. 18) with scape slender and cylindrical, 6.7–8.2× as long as wide, extending far beyond vertex; pedicel 1.6–1.8× as long as wide; funicle 4-segmented, F1 2.9–3.7× as long as wide, F2 3.4–4.1× as long as wide, F3 and F4 2.3–2.5× and 2.2–2.3× as long as wide respectively; clava 2-segmented, 2.4–2.6× as long as wide. Fore wing (Fig. 19) 2.6–2.8× as long as wide. Costal cell 13.3–13.7× as long as wide. Speculum present, closed posteriorly. MV 1.1–1.3× as long as PMV; PMV 1.6–1.8× as long as STV. **Male.** See Tao et al. (2021).

Host. Primary parasitoid of *Chromatomyia horticola* (Goureau) (Diptera, Agromyzidae) (Tao et al. 2021).

Distribution. China (Jilin) (Tao et al. 2021); new records: Beijing, Heilongjiang, Liaoning, Hebei).

Acknowledgements

We thank the two reviewers and the subject editor for providing valuable comments on earlier drafts of this manuscript. We sincerely thank Dr Arkady Lelej (Federal Scientific Center of the East Asia Terrestrial Biodiversity, Russian Academy of Sciences, Russia) and Dr Ralph S. Peters (The Zoological Research Museum Alexander Koenig, Germany) for providing references. We are also grateful to Prof. Hui-Lin Han, Dr Hui Geng, Dr Guo-Hao Zu, Dr Xiang-Xiang Jin, Dr Wen-Jian Li, Dr Ye Chen, Mr Jiang Liu, Mr Jun Wu, Mr Guang-Xing Wang, Mr Chao Zhang, Miss Ting-Ting Zhao, Miss Shu-Chen Deng, Miss Xin-Yu Zhang, and Miss Xing-Yue Jin for specimen collection.

References

- Gibson GAP (1997) Morphology and terminology. In: Gibson GAP, Huber JT, Woolley JB (Eds) Annotated Keys to the Genera of Nearctic Chalcidoidea (Hymenoptera). NRC Research Press, Ottawa, 16–44.
- Hymenoptera Anatomy Consortium (2022) Hymenoptera Anatomy Ontology Portal. <http://glossary.hymao.org> [accessed 7 April 2022]
- Lee HS (1990) Differences in injury of *Liriomyza bryoniae* (Kalt.) on crops and the influence of the host plants to the parasitoids. *Yingyong Kunchong Xuebao* 10(4): 409–418.

- Noyes JS (1982) Collecting and preserving chalcid wasps (Hymenoptera: Chalcidoidea). *Journal of Natural History* 16: 315–334. <https://doi.org/10.1080/00222938200770261>
- Noyes JS (2019) Universal Chalcidoidea Database. World Wide Web electronic publication. <http://www.nhm.ac.uk/chalcidoids> [accessed 7 April 2022]
- Sheng JK, Zhong L, Wu Q (1989) The hymenopterous species of *Phytomyza horticola* Gourea from Jiangxi Province, in China. *Jiangxi Nongye Daxue Xuebao* 39(2): 22–31.
- Tao S-X, Huang K, Tian J, Ruan C-C (2021) A new species of *Hemiptarsenus* Westwood (Hymenoptera, Eulophidae) from China, with a key to Chinese species. *ZooKeys* 1033: 173–181. <https://doi.org/10.3897/zookeys.1033.62129>
- Westwood JO (1833) On the probable number of insect species in the creation; together with descriptions of several minute Hymenoptera. *Magazine of Natural History* 6: 116–123.
- Xu ZH, Chen XX, Rong LQ, He JH, Ma Y (2001) Parasitic wasps of leaf miner in vegetable field (I) – Eulophidae: Eulophinae and Elachertinae. *Entomological Journal of East China* 10(2): 5–10.
- Yang ZQ, Yao YX, Cao LM (2015) Chalcidoidea Parasitizing Forest Defoliators (Hymenoptera). Science Press, Beijing, 109–111.
- Zhu CD, Huang DW (2002) A taxonomic study on Eulophidae from Guangxi, China (Hymenoptera: Chalcidoidea). *Dong Wu Fen Lei Xue Bao* 27(3): 583–607.
- Zhu CD, LaSalle J, Huang DW (2000) Revision of Chinese species of *Hemiptarsenus* Westwood (Hymenoptera, Eulophidae). *Entomologia Sinica* 7(1): 1–11. <https://doi.org/10.1111/j.1744-7917.2000.tb00333.x>

Novel *in situ* observations of asexual reproduction in the carpet sea anemone, *Stichodactyla mertensii* (Stichodactylidae, Actiniaria)

Morgan F. Bennett-Smith¹, Micaela S. Justo¹, Michael L. Berumen¹,
Raquel Peixoto¹, Benjamin M. Titus^{2,3}

1 King Abdullah University of Science and Technology, Red Sea Research Center, 4700 Thuwal, 23955 Saudi Arabia **2** Department of Biological Sciences, University of Alabama, Tuscaloosa, AL 35899, USA **3** Dauphin Island Sea Lab, 101 Bienville Blvd, Dauphin Island, AL, 36528, USA

Corresponding author: Morgan F. Bennett-Smith (morgan.bennett-smith@kaust.edu.sa)

Academic editor: James Reimer | Received 30 March 2022 | Accepted 24 April 2022 | Published 27 May 2022

<http://zoobank.org/21CF48EC-C87F-4A0B-AF93-DEBFE6E3D959>

Citation: Bennett-Smith MF, Justo MS, Berumen ML, Peixoto R, Titus BM (2022) Novel *in situ* observations of asexual reproduction in the carpet sea anemone, *Stichodactyla mertensii* (Stichodactylidae, Actiniaria). ZooKeys 1103: 57–63. <https://doi.org/10.3897/zookeys.1103.84415>

Abstract

Merten's carpet sea anemone, *Stichodactyla mertensii* Brandt, 1835, is the largest known sea anemone species in the world, regularly exceeding one meter in oral disc diameter. A tropical species from the Indo-Pacific, *S. mertensii* drapes prominently over coral reef substrates and is a common host to numerous species of clownfishes and other symbionts throughout its range, which extends from the Red Sea through the Central Pacific Ocean. Long thought to reproduce via sexual reproduction only, recent genetic evidence suggests it may rarely reproduce asexually as well, although this process had never been confirmed through direct observation and the mechanism was yet to be described. Here, we directly observed and documented *in situ* asexual fragmentation via budding, in real time, by a Red Sea *S. mertensii* in a turbid inshore reef environment. While asexual reproduction is not unusual in sea anemones as a group, it is typically expected to be uncommon for large-bodied species. Herein, we describe *S. mertensii* fragmentation, provide high resolution images of the event from the Saudi Arabian coastline at multiple time points, and confirm asexual reproduction for this species.

Keywords

Actinians, clonality, fragmentation, Indian Ocean, reproduction, sea anemones

Introduction

Asexual reproduction is common in sea anemones (Anthozoa, Actiniaria), which have evolved a variety of different asexual modes including pedal laceration, binary fission, longitudinal fission, and budding (reviewed by Shick 1991). Asexual reproduction can lead to small clusters of two or three anemones or to expansive clonal aggregations of hundreds of individuals. Clonality can thus make important contributions to sea anemone population dynamics, especially for tropical species that serve as symbiotic hosts to a diverse suite of fishes and other invertebrates.

The Red Sea contains thousands of kilometers of fringing coral reef systems inhabited by tropical sea anemones, the largest of which serve as symbiotic hosts to clownfish. Yet only recently has there been clarity on the diversity of host anemone species that inhabit this region (Bennett-Smith et al. 2021). The largest species found in the Red Sea, *Stichodactyla mertensii* Brandt, 1835, is the largest known anemone species in the world, but has historically not been known to this region until only recently (Bennett-Smith et al. 2021). Although it is also possible that a range expansion has occurred, recent widespread documentation on surveys along the entire eastern coastline of the Red Sea indicates that *S. mertensii* is native to the region but remained unrecorded as a result of misidentifications in the literature (Bennett-Smith et al. 2021). In any case, despite *S. mertensii*'s widespread occurrence in the Red Sea, there have been few studies concerning its ecology or life history.

Stichodactyla mertensii is one of ten described clownfish-hosting anemone species found on Indo-Pacific coral reefs (reviewed by Titus et al. 2019). Only two, *Entacmaea quadricolor* (Leuckart in Rüppell & Leuckart, 1828) and *Heteractis magnifica* (Quoy & Gaimard, 1833) are known to reproduce clonally – a process well known to those in the aquarium trade who regularly propagate these species through binary fission by cutting the oral disc in half, resulting in two individuals. In the wild, *E. quadricolor* and *H. magnifica* regularly form clonal aggregations throughout their range via binary fission (Dunn 1981).

Stichodactyla mertensii was thought to reproduce sexually, not asexually, following the generalization that it had only ever been found solitarily and that smaller, facultatively clonal animals are more likely to reproduce asexually compared to their larger counterparts (reviewed by Titus et al. 2017). Recent work in the Red Sea provided an indication of low levels of potential clonality in *S. mertensii* populations through genetic sampling. Out of 122 individuals sampled by Emms et al. (2020), two were determined to be potential clones and both were found in waters surrounding or adjacent to the Arabian Peninsula (Saudi Arabia & Djibouti). However, direct confirmation and mechanisms for asexual reproduction had not been documented until now. Here, for the first time, we observed fragmentation via budding from the column in real time in a Red Sea *S. mertensii*. We photographed the specimen at several time points to track its asexual reproduction *in situ*. This evidence offers insight into the reproductive mechanisms of clonality in this species and expands our general knowledge of reproductive modes for the clownfish-hosting sea anemones.

Materials and methods

We conducted initial underwater surveys on SCUBA, near the campus of the King Abdullah University of Science and Technology (KAUST), in December 2021. During these surveys, we encountered several host anemone species, including *E. quadricolor* and *S. mertensii*.

To identify the host anemones located, we noted external morphological characteristics and used the dichotomous keys by Dunn (1981) and Fautin and Allen (1992). Morphological characteristics that were used to identify host anemones in the field included: the size and shape of the oral disc (flat, undulating, balled around the tentacles); the size, shape, color, and prevalence of verrucae (warty projections on the column) towards the pedal disc; the size, shape, density and uniformity of tentacles throughout the oral disc; the color pattern on the margins of the oral disc; the substratum on which the pedal disc was anchored (sand, rockwork, or rubble); and the coloration and appearance of the mouth. In the case of *S. mertensii*, this species has a large, flat oral disc, rounded, bulbous tentacle tips, longer tentacles around the mouth than at the periphery of the disc, and conspicuous verrucae along the column, extending to the pedal disc (Dunn 1981; Bennett-Smith et al. 2021).

One anemone identified as *S. mertensii* was observed in the process of asexually fragmenting via column budding. This individual was subsequently GPS-marked, located at the following coordinates: 22°16'41.32"N, 39°3'54.23"E (Fig. 1). The anemone was identified at a depth of 11 meters. The anemone was photographed *in situ* with a Canon R5 camera inside a Nauticam underwater housing, with two Sea and Sea underwater strobes.

After our initial observations, we returned to the same location again in February 2022. We followed the same procedure and again photographed and measured the individual on SCUBA, using the same equipment.

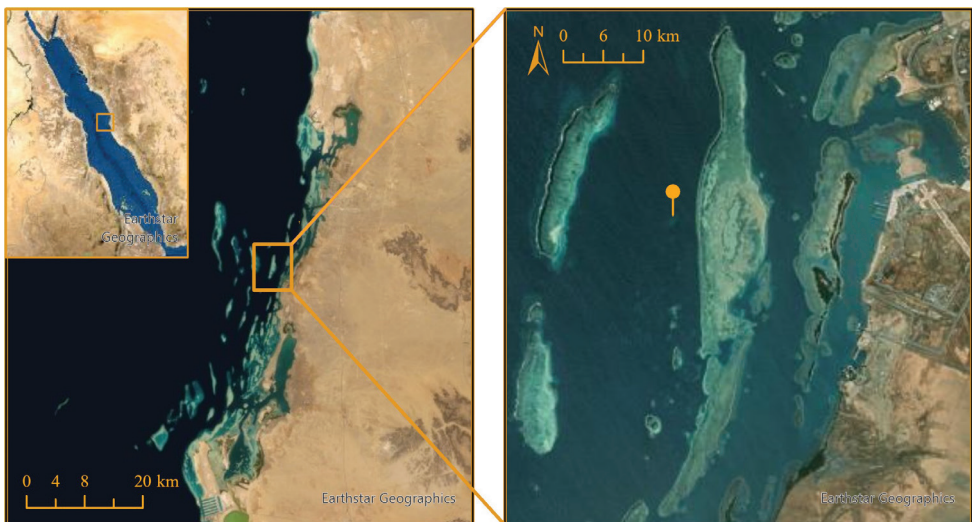


Figure 1. Location of observed *Stichodactyla mertensii* on an inshore Red Sea reef near the King Abdullah University of Science and Technology; Thuwal, Saudi Arabia.

Results

Description

Initial observation

The individual that was observed had two separate budding locations, both on the column of the animal (Figs 2, 3). When first observed (December 8, 2021), one fragmentation bud was already recognizable as a separate individual, around 6 cm in length, extending outwards, with tentacles fully developed, even though it was still attached to the column. The other bud was small, less than 2 cm in oral disc diameter and newly formed, with tentacles not extended (Fig. 3A).

Second observation

The second observation was made on February 11, 2022 (33 days after the first observation). The larger of the two fragmentation buds had grown to an oral disc diameter

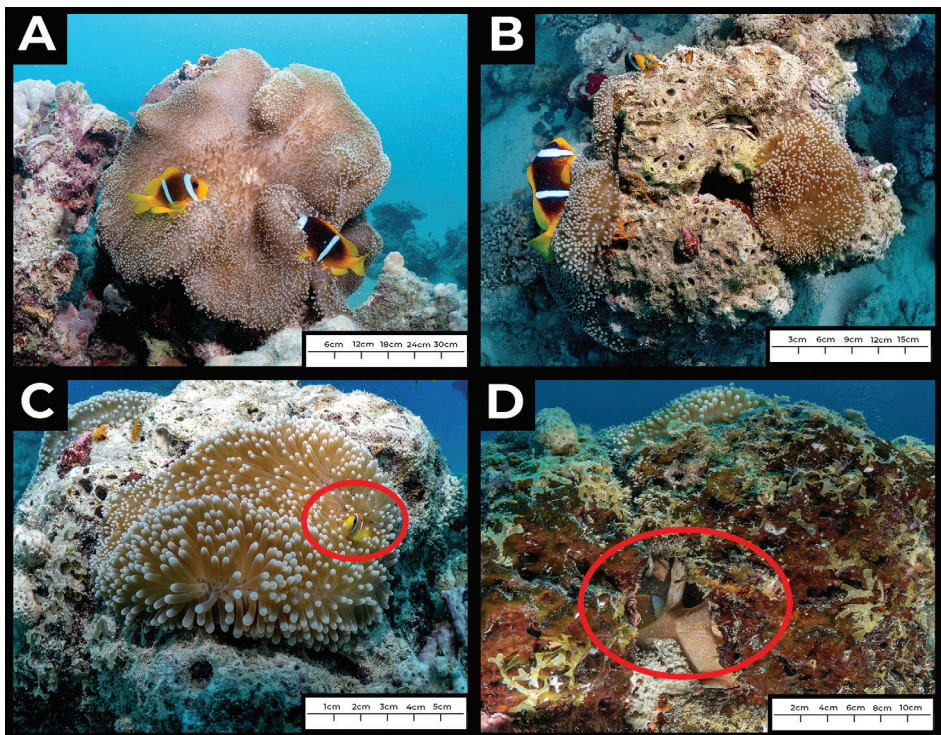


Figure 2. *In situ* images of asexual reproduction of *Stichodactyla mertensii* on an inshore reef near Thuwal, Saudi Arabia **A** the parent *S. mertensii* individual, with two *Amphiprion bicinctus* symbionts **B** top view of the parent individual (left, with anemonefish) and newly forming anemone bud (right) **C** anemonefish recruit (circled) in newly forming anemone bud **D** cross section of the reef rockwork, showing the column of the anemone from where the new fragmentation branches.

size of ~12 cm, showing an increase of about 6 cm in oral disc diameter (Fig. 2B, C). The smaller bud had grown from an initial disc diameter size of less than 2 cm to around 5 cm, an increase of 3 cm (Fig. 3B).

Notably, the larger bud appeared to be much closer to separating from the parent entirely, and was only connected to the column by a thin stalk (Fig. 2D).

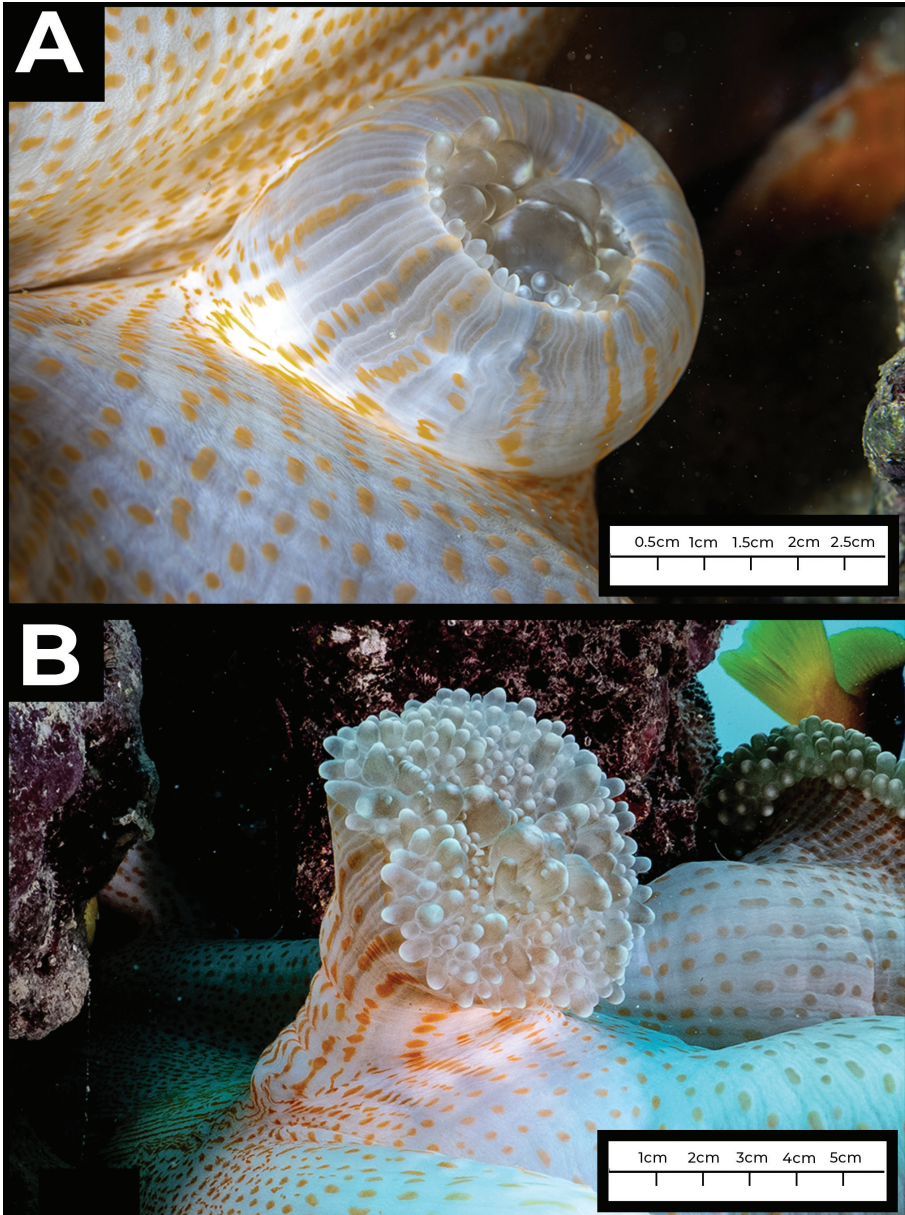


Figure 3. *In situ* macro images of new asexual bud on *Stichodactyla mertensii* near Thuwal, Saudi Arabi at two time points **A** initial observation, December 2021; bud oral disc diameter ~2 cm **B** second observation, February 2022; bud oral disc diameter ~5 cm.

Conclusions

These observations are the first of *in situ* asexual reproduction of *Stichodactyla mertensii* (and the first of any carpet anemone species in the Red Sea), yielding insight into the mechanisms by which these species reproduce clonally. Interestingly, *Stichodactyla mertensii* was not previously known to form clonal aggregations, and a recent survey effort covering several thousand km of Red Sea reefs did not reveal a single aggregation of any carpet anemone species (Bennett-Smith et al. 2021). Similarly, other large clownfish-hosting species from the genus *Stichodactyla*, like *Stichodactyla haddoni* (Saville-Kent, 1893) and *Stichodactyla gigantea* (Forsskål, 1775), do not form aggregations of individuals and are not thought to reproduce asexually. However, Titus et al. (2019) found *H. magnifica*, a species well known to reproduce asexually, to be well nested within a broader clade containing the members of the genus *Stichodactyla*. Additionally, *S. helianthus*, a smaller carpet anemone species found on coral reefs in the Tropical Western Atlantic, is a clonal species as well. Thus, it is possible that this reproductive mode has been overlooked in the Indo-Pacific members of the genus *Stichodactyla*. Our observations in the Red Sea confirm *S. mertensii* as the third species of clownfish-hosting sea anemone known to reproduce asexually, along with *E. quadricolor* and *H. magnifica*. The asexual reproductive strategies of other host anemones from the Red Sea and elsewhere in the Indo-Pacific, including *Stichodactyla haddoni*, *S. gigantea*, *Heteractis aurora* (Quoy & Gaimard, 1833), *Heteractis crispa* (Hemprich & Ehrenberg in Ehrenberg, 1834), *Heteractis malu* (Haddon & Shackleton, 1893) and *Macroactyla doreensis* (Quoy, Gaimard, 1833), also remain unclear. Increased observational effort and further molecular work on this group may clarify these questions, which have downstream implications for a range of host anemone-associated taxa.

Acknowledgements

We thank the King Abdullah University of Science and Technology Coastal and Marine Resources Core Lab for providing assistance in the field. Thank you to Nathalia Delgado Ordóñez, Inês Gonçalves Raimundo, and Viktor Nunes Peinemann for accompanying the initial survey dives. This work was supported by the King Abdullah University of Science and Technology (KAUST grant number BAS/1/1095-01-01 and KAUST Center Competitive Funding (CCF) FCC/1/1973-51-01), KAUST Office of the Provost, and US National Science Foundation Award to BMT (DEB-SBS 2205567).

References

- Bennett-Smith MF, Majoris JE, Titus BM, Berumen ML (2021) Clownfish hosting anemones (Anthozoa, Actiniaria) of the Red Sea: New associations and distributions, historical misidentifications, and morphological variability. *Marine Biodiversity Records* 14(1): 1–15. <https://doi.org/10.1186/s41200-021-00216-6>

- Brandt JF (1835) *Polypos, Acalephas Discophoras et Siphonophoras, nec non Echinodermata Continens*. Petropoli: Sumptibus Academiae, 76 pp. <https://doi.org/10.5962/bhl.title.10196>
- Dunn DF (1981) The clownfish sea anemones: Stichodactylidae (Coelenterata: Actiniaria) and other sea anemones symbiotic with pomacentrid fishes. *Transactions of the American Philosophical Society* 71(1): 3–115. <https://doi.org/10.2307/1006382>
- Ehrenberg CG (1834) Beiträge zur physiologischen Kenntniss der Corallenthiere im allgemeinen, und besonders des rothen Meeres, nebst einem Versuche zur physiologischen Systematik derselben. *Abhandlungen der Königlichen Akademie der Wissenschaften zu Berlin* 1: 225–380.
- Emms MA, Saenz-Agudelo P, Giles EC, Gatins R, Nanninga GB, Scott A, Hobbs JP, Frisch AJ, Mills SC, Beldade R, Berumen ML (2020) Comparative phylogeography of three host sea anemones in the Indo-Pacific. *Journal of Biogeography* 47(2): 487–500. <https://doi.org/10.1111/jbi.13775>
- Fautin DG, Allen GR (1992) *Field Guide to Anemonefishes and their Host Sea Anemones*. Western Australian Museum, Perth, 65 pp.
- Forsskål (1775) *Descriptiones Animalium* (Hauniae, Molleri).
- Haddon AC, Shackleton AM (1893) Description of some new species of Actiniaria from Torres Straits. *The Scientific Proceedings of the Royal Dublin Society*. Royal Dublin Society 8: 116–131.
- Quoy JRC, Gaimard P (1833) *Voyage de decouvertes de l’Astrolabe*. *Zoologie* •••: 4. [zoo-phytes] [Tastu, Paris.]
- Rüppell E, Leuckart FS (1828) *Atlas zu der Reise in nördlichen Afrika von Eduard Rüppell*. Neue Wirbellose Tiere des Roten Meers. Brenner, Frankfurt.
- Saville-Kent W (1893) *The Great Barrier Reef of Australia: its products and potentialities: containing an account, with copious coloured and photographic illustrations (the latter here produced for the first time), of the corals and coral reefs, pearl and pearl-shell, beche-de-mer, other fishing industries, and the marine fauna of the Australian Great Barrier Region*. Allen, 1893. <https://doi.org/10.5962/bhl.title.10161>
- Shick JM [Ed.] (1991) *A functional biology of sea anemones*. Springer Science & Business Media. <https://doi.org/10.1007/978-94-011-3080-6>
- Titus BM, Daly M, Macrander J, Del Rio A, Santos SR, Chadwick NE (2017) Contrasting abundance and contribution of clonal proliferation to the population structure of the corkscrew sea anemone *Bartholomea annulata* in the tropical Western Atlantic. *Invertebrate Biology* 136(1): 62–74. <https://doi.org/10.1111/ivb.12162>
- Titus BM, Benedict C, Laroche R, Gusmao LC, Van Deusen V, Chiodo T, Meyer CP, Berumen ML, Bartholomew A, Yanagi K, Reimer JD, Fujii T, Daly M, Rodriguez E (2019) Phylogenetic relationships of the clownfish-hosting sea anemones. *Molecular Phylogenetics and Evolution* 139: 106526. <https://doi.org/10.1016/j.ympev.2019.106526>

A braconid wasp (Hymenoptera, Braconidae) from the Lower Cretaceous amber of San Just, eastern Iberian Peninsula

Sergio Álvarez-Parra¹, Enrique Peñalver², Xavier Delclòs¹, Michael S. Engel^{3,4,5}

1 *Departament de Dinàmica de la Terra i de l'Oceà and Institut de Recerca de la Biodiversitat (IRBio), Facultat de Ciències de la Terra, Universitat de Barcelona, c/ Martí i Franquès s/n, 08028, Barcelona, Spain* **2** *Instituto Geológico y Minero de España-CSIC, c/ Cirilo Amorós 42, 46004, Valencia, Spain* **3** *Division of Entomology, Natural History Museum, University of Kansas, 1501 Crestline Drive – Suite 140, Lawrence, Kansas 66045-4415, USA* **4** *Department of Ecology and Evolutionary Biology, University of Kansas, Lawrence, Kansas 66045, USA* **5** *Division of Invertebrate Zoology, American Museum of Natural History, Central Park West at 79th Street, New York, New York 10024-5192, USA*

Corresponding author: Sergio Álvarez-Parra (sergio.alvarez-parra@ub.edu)

Academic editor: Kees van Achterberg | Received 11 March 2022 | Accepted 22 April 2022 | Published 30 May 2022

<http://zoobank.org/079C1F77-A3AA-4158-AE53-5F510C8FA0BE>

Citation: Álvarez-Parra S, Peñalver E, Delclòs X, Engel MS (2022) A braconid wasp (Hymenoptera, Braconidae) from the Lower Cretaceous amber of San Just, eastern Iberian Peninsula. ZooKeys 1103: 65–78. <https://doi.org/10.3897/zookeys.1103.83650>

Abstract

Braconid parasitoid wasps are a widely diversified group today, while their fossil record from the Mesozoic is currently poorly known. Here, we describe *Utrillabracon electropteron* Álvarez-Parra & Engel, **gen. et sp. nov.**, from the upper Albian (Lower Cretaceous) amber of San Just in the eastern Iberian Peninsula. The holotype specimen is incomplete, although the forewing and hind wing venation are well preserved. The new taxon is assigned to the subfamily †Protorhyssalinae (Braconidae) and, based on characteristics of the wing venation, seems to be closely related to *Protorhyssalus goldmani* Basibuyuk & Quicke, 1999 and *Diorhyssalus allani* (Brues, 1937), both from Upper Cretaceous ambers of North America. We discuss the taxonomy of the Cretaceous braconids, considering †Seneciobraconinae as a valid subfamily. We also comment on possible relationships within †Protorhyssalinae, although a phylogenetic analysis is necessary. Additionally, a checklist is included of braconids known from Cretaceous ambers.

Keywords

Albian, fossil, Ichneumonoidea, Protorhyssalinae, Spanish amber, taxonomy, wasp diversity, wing venation

Introduction

Braconidae are the second largest family of Hymenoptera in terms of species numbers (Chen and van Achterberg 2019), trailing just behind the closely related family, Ichneumonidae. Like ichneumonids, braconids are parasitoid wasps, with their larvae developing within or externally on other insects, typically Coleoptera, Diptera, and Lepidoptera, but actually encompassing a considerable breadth of hosts from aphids to other wasps, and even adult stages (e.g., Euphorinae) (Wharton 1993). Given that braconids attack the immatures of many agriculturally important pest species, they have been heavily employed in sustainable pest management programs throughout the world (e.g., Nomano et al. 2015).

Braconids belong to the superfamily Ichneumonoidea, which comprises the extant families Ichneumonidae, Braconidae, and Trachypetidae (Quicke et al. 2020), along with the extinct †Praeichneumonidae, a monogeneric family including five species known from Early Cretaceous compression fossils (Rasnitsyn 1983, 1990; Kopylov 2012). A putative fifth group, †Ichneumonimidae (Rasnitsyn 1975), has subsequently been considered to belong to Trigonalidae (Rasnitsyn 1988), while the Trachypetidae has been recently restored as a non-cyclostome braconid subfamily (Jasso-Martínez et al. 2022a, 2022b). The fossil record of Ichneumonoidea is most diverse in Cenozoic deposits but extends well into the Early Cretaceous, with Mesozoic fossils representing early diverging lineages of both Ichneumonidae and Braconidae, several of which have been difficult to place phylogenetically or to even confirm as monophyletic (Kopylov et al. 2021; Spasojevic et al. 2021; Viertler et al. 2022).

One notable example of these early lineages is the braconid subfamily †Protorhyssalinae, a group of parasitoid wasps almost exclusively known by amber inclusions from the Albian to the Campanian (Li et al. 2021). Braconidae are currently represented by 21 genera and 22 species in Cretaceous ambers (Table 1), besides other specimens preserved as compressions in Cretaceous rocks (Belokobylskij 2012). Only two braconid species have been previously reported from Cretaceous Spanish amber (Ortega-Blanco et al. 2009, 2011) (Fig. 1). Furthermore, other specimens of the family were found in lower Miocene compression outcrops from the eastern Iberian Peninsula (Peñalver and Martínez-Delclòs 2000; Álvarez-Parra and Peñalver 2019). Here, we describe a new genus and species of fossil wasp belonging to the subfamily †Protorhyssalinae included in amber from the upper Albian San Just in the eastern Iberian Peninsula. Although the specimen is incomplete, the wings are extraordinarily well preserved and allow for its proper placement and characterization relative to other protorhyssalines. We provide a description of the new species and compare it with the previously known genera of †Protorhyssalinae. In addition, we append comments on the diversity of the subfamily and putative phylogenetic groups among this assemblage of wasps.

Table 1. Checklist of species of Braconidae (Hymenoptera, Ichneumonoidea) from Cretaceous ambers. The two species marked with an asterisk need taxonomic revision. For Cretaceous compression fossils see Belokobylskij (2012).

Subfamily	Genus and species	Locality	Age	Reference
Aphidiinae	<i>Archephedrus stolamissus</i> Ortega-Blanco, Bennett, Delclòs, & Engel, 2009	Peñacerrada I, Spain	late Albian	Ortega-Blanco et al. (2009)
Brachistinae	" <i>Neoblacus</i> " (= <i>Blacus</i>) <i>facialis</i> Brues, 1937 *	Cedar Lake, Canada	Campanian	Brues (1937)
Euphorinae	" <i>Pygostolus</i> " <i>patriarchicus</i> Brues, 1937 *	Cedar Lake, Canada	Campanian	Brues (1937)
†Megalyrhyssalinae	<i>Megalyrhyssalus clavicornis</i> Belokobylskij & Jouault, 2021	Hukawng Valley, Myanmar	early Cenomanian	Belokobylskij and Jouault (2021)
†Protobraconinae	<i>Rhetinorhyssalites emersoni</i> Engel, Thomas, & Alqarni, 2017	Sayreville, USA	Turonian	Engel et al. (2017); Chen et al. (2021b)
	<i>Chainochora syntoma</i> Chen & van Achterberg, 2021	Hukawng Valley, Myanmar	early Cenomanian	Chen et al. (2021a)
	<i>Kleistochora dolichura</i> Chen & van Achterberg, 2021	Hukawng Valley, Myanmar	early Cenomanian	Chen et al. (2021a)
	<i>Protobracon robusticauda</i> Chen & van Achterberg, 2021	Hukawng Valley, Myanmar	early Cenomanian	Chen et al. (2021b)
	<i>Tibialobracon compressicornis</i> Chen & van Achterberg, 2021	Hukawng Valley, Myanmar	early Cenomanian	Chen et al. (2021b)
†Protorhyssalinae	<i>Diorhyssalus allani</i> (Brues, 1937)	Cedar Lake, Canada	Campanian	Brues, (1937); Engel (2016); Chen et al. (2021b)
	<i>Protorhyssalus goldmani</i> Basibuyuk & Quicke, 1999	Sayreville, USA	Turonian	Basibuyuk et al. (1999)
	<i>Protorhyssalodes arnaudi</i> Perrichot, Nel, & Quicke, 2009	Cadeuil, France	early Cenomanian	Perrichot et al. (2009); Chen et al. (2021b)
	<i>Archaeorhyssalus subsolanus</i> Engel, 2016	Hukawng Valley, Myanmar	early Cenomanian	Engel and Wang (2016)
	<i>Burmabracon gracilens</i> Li, Shih, & Ren, 2021	Hukawng Valley, Myanmar	early Cenomanian	Li et al. (2021)
	<i>Burmabracon grossus</i> Li, Shih, & Ren, 2021	Hukawng Valley, Myanmar	early Cenomanian	Li et al. (2021)
	<i>Protorhyssalopsis perrichoti</i> Ortega-Blanco, Delclòs, & Engel, 2011	Peñacerrada I, Spain	late Albian	Ortega-Blanco et al. (2011)
	<i>Utrillabracon electropteron</i> Álvarez-Parra & Engel, gen. et sp. n.	San Just, Spain	late Albian	This paper
†Seneciobraconinae	<i>Seneciobracon novalatus</i> Engel & Huang, 2018	Hukawng Valley, Myanmar	early Cenomanian	Engel et al. (2018)
<i>Incertae sedis</i>	<i>Aenigmabracon capdoliensis</i> Perrichot, Nel, & Quicke, 2009	Cadeuil, France	early Cenomanian	Perrichot et al. (2009)
	<i>Pyramidibracon clypeatus</i> Chen & van Achterberg, 2021	Hukawng Valley, Myanmar	early Cenomanian	Chen et al. (2021b)
	<i>Rhetinorhyssalus morticinus</i> Engel, 2016	Hukawng Valley, Myanmar	early Cenomanian	Engel (2016)
	<i>Stephanorhyssalus longiscapus</i> Belokobylskij & Jouault, 2021	Hukawng Valley, Myanmar	early Cenomanian	Belokobylskij and Jouault (2021)

Materials and methods

The amber material reported here comes from the San Just amber-bearing outcrop (Teruel Province, Aragón, Spain). The site is located near the Utrillas Municipality, in the Aliaga Sub-basin within the Maestrazgo Basin (Fig. 1). More than 30 amber-

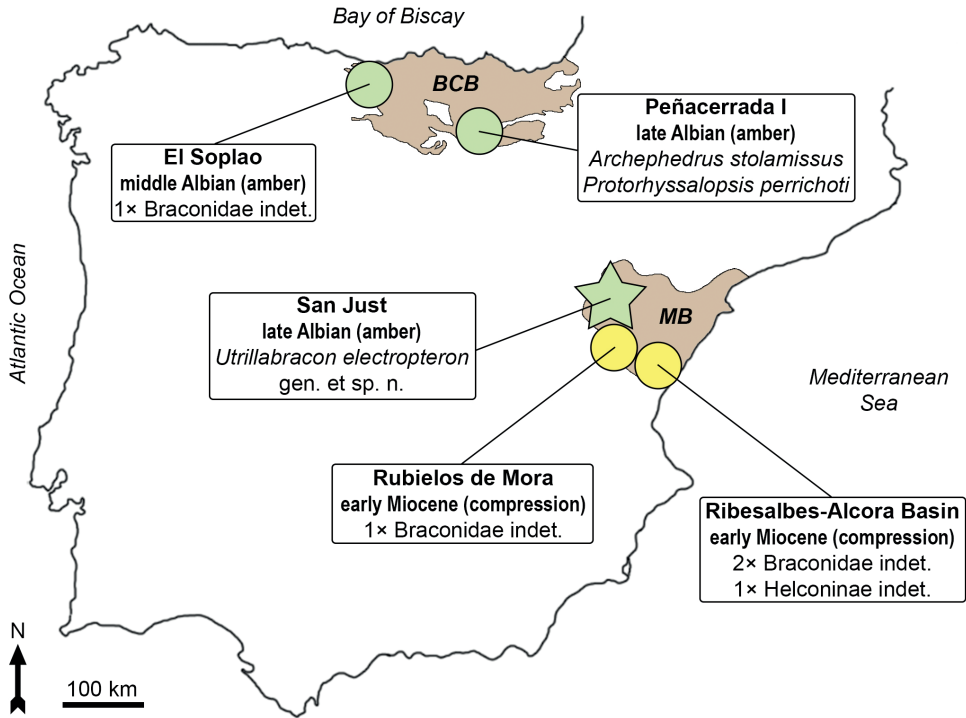


Figure 1. Map of the Iberian Peninsula showing the location of the amber and compression outcrops that have yielded braconid wasps. Basque-Cantabrian (BCB) and Maestrazgo (MB) basins are represented. The type locality the studied specimen is indicated with a star. The specimens from El Soplao and Rubielos de Mora are undescribed to date.

bearing outcrops have been reported in this basin, although only four of them have yielded bioinclusions (Álvarez-Parra et al. 2021). Stratigraphically, the San Just section has been assigned to the Escucha Formation (Peñalver et al. 2007). The amber-rich level is composed of grey-black marls with a high content of organic matter, charcoal, and fusinite and has been interpreted as a freshwater swamp plain (Peñalver et al. 2007; Villanueva-Amadoz et al. 2010). The site was dated as middle–earliest upper Albian based on palynological evidence (Villanueva-Amadoz et al. 2010). A new palynological study constrains the dating to the upper Albian (Eduardo Barrón pers. comm.). San Just is the type locality of 26 arthropod species (including the new species here described) and the Hymenoptera are represented by nine species in eight families (Santer et al. 2022). The amber piece was recovered during an excavation in 2012 (Government of Aragón permit 119/10-11-2012). The original amber piece was divided in four epoxy preparations to better examine the syninclusions. This process followed the methodology of Corral et al. (1999). The specimen was photographed and drawn using an Olympus CX41 compound microscope, with an attached digital camera sCMEX-20 and a camera lucida. Photographs were made using the software

ImageFocusAlpha v. 1.3.7.12967.20180920 and the figures were prepared using Photoshop CS6. Venational nomenclature is based on Huber and Sharkey (1993) and Ortega-Blanco et al. (2009). The specimen is deposited in the Museo Aragonés de Paleontología (Fundación Conjunto Paleontológico de Teruel-Dinópolis), Teruel, Spain. The fossil notation “MAP” corresponds to the number at the Museo Aragonés de Paleontología, while “SJE2012” is the field number.

Systematic paleontology

Family Braconidae Nees von Esenbeck, 1811

Subfamily †Protorhyssalinae Basibuyuk, Quicke, & van Achterberg, 1999

Protorhyssalinae Basibuyuk, Quicke, & van Achterberg, 1999: 211. Type genus: *Protorhyssalus* Basibuyuk & Quicke in Basibuyuk et al. (1999), by original designation.

Comments. Herein we restore the traditional concept of †Protorhyssalinae as recognized by Basibuyuk et al. (1999) and Chen and van Achterberg (2019). Belokobylskij and Jouault (2021) proposed a classification in which virtually all Cretaceous braconids are thrown into a paraphyletic group, rendering †Protorhyssalinae a meaningless grade. Admittedly, restoring †Protorhyssalinae still leaves the group paraphyletic but at least removes the more obviously derived groups and thereby narrows the challenge as to the affinities of the remaining genera. Nonetheless, while Belokobylskij and Jouault (2021) advocated for such a paraphyletic assemblage, they used plesiomorphic features along with autapomorphies to establish the subfamily †Megalyrhyssalinae. Unfortunately, †Megalyrhyssalinae is poorly justified and could be merely an autapomorphic form of the same protorhyssaline grade. By their own reasoning, they should have either not established such a subfamily or further divided †Protorhyssalinae to resolve the paraphyly. Under their conception of †Protorhyssalinae, †Megalyrhyssalinae would be a junior synonym. For now, we recognize the following subfamilies: †Protorhyssalinae, †Seneciobraconinae (*Seneciobracon*), and †Megalyrhyssalinae (*Megalyrhyssalus*), noting that the last may not be sufficiently justified but may well be worth considering once the full phylogeny of the genera comprising these groups is elucidated. Until such time it seems that further alterations of the subfamilial system in the absence of a cladistic framework would be unwarranted.

Included genera and species. *Archaeorhyssalus subsolanus* Engel, 2016; *Burmabracon gracilens* Li, Shih, & Ren, 2021; *B. grossus* Li, Shih, & Ren, 2021; *Diorhyssalus allani* (Brues, 1937); *Protorhyssalodes arnaudi* Perrichot, Nel, & Quicke, 2009; *Protorhyssalopsis perrichoti* Ortega-Blanco, Delclòs, & Engel, 2011; *Protorhyssalus goldmani* Basibuyuk & Quicke, 1999; and *Utrillabracon electropteron* Álvarez-Parra & Engel, gen. et sp. nov. *Cretorhyssalus brevis* Belokobylskij, 2012, *Magadanobracon rasnitsyni* Belokobylskij, 2012, and *M. zherikhini* Belokobylskij, 2012, known from compression fossils, were putatively assigned to †Protorhyssalinae *sensu* Belokobylskij (2012).

***Utrillabracon* Álvarez-Parra & Engel, gen. nov.**

<http://zoobank.org/C6FE19C1-A5D0-4780-9860-F611198EF09C>

Type species. *Utrillabracon electropteron* Álvarez-Parra & Engel, sp. nov.

Diagnosis. Forewing with margin bearing setae; pterostigma $4 \times$ longer than wide; 1Rs relatively long and curved; r-rs oblique, arising medially from pterostigma; r-rs several times longer than abscissa of M between 2Rs and m-cu; marginal cell reaching wing apex; rs-m nebulous; elongate, five-sided second submarginal cell, $3 \times$ longer than wide; 1M and m-cu of similar length; m-cu distinctly postfurcal; 2m-cu absent; cu-a slightly postfurcal and orthogonal. Hind wing with margin bearing setae; R1 distally widened with several hamuli beyond its apex; Sc + R not aligned with Rs; 2Cu present. Pretarsal claws present, without preapical tooth; arolium wide.

Etymology. The generic name is a combination of Utrillas, municipality where the San Just amber outcrop is located, and *Bracon* Fabricius, 1804, type genus of the family Braconidae. The gender of the name is masculine.

***Utrillabracon electropteron* Álvarez-Parra & Engel, sp. nov.**

<http://zoobank.org/59B73E2C-0514-4DA4-8A87-ABF61D6EF2A8>

Fig. 2

Material. Holotype. MAP-7819 (SJE2012 49-04), sex unknown, from San Just amber. The holotype is largely preserved as the forewings and hind wings. Some parts of the head, an antenna, and a leg are next to the wings. Undetermined cuticular fragments are visible near the wings. Deposited in the Museo Aragonés de Paleontología (Fundación Conjunto Paleontológico de Teruel-Dinópolis) in Teruel, Spain. Syninclusions include three other hymenopterans (probable serphitid, platygastriid, and stigmaphronid wasps). The holotype is prepared isolated in an epoxy prism of 20×15 mm.

Locality and horizon. San Just amber-bearing outcrop, Utrillas, Teruel, Spain; Maestrazgo Basin, Escucha Formation, upper Albian (Peñalver et al. 2007).

Diagnosis. As for the genus (*vide supra*).

Description. Head deformed and incomplete as preserved (Fig. 2A, B); antenna partially preserved with 11 flagellomeres covered by setae, multiporous plate sensilla not visible; only distal two maxillary palpomeres preserved, covered by fine setae. Forewings and venation rather complete (Fig. 2C), forewing base not preserved, more than 1.31 mm long and 0.53 mm in its maximum width, margin bearing setae; C + Sc + R fused anterobasally, extending along wing margin to pterostigma; pterostigma $4 \times$ longer than wide (0.33 mm vs 0.08 mm); elongate marginal cell, $3 \times$ longer than wide (0.57 mm vs 0.19 mm), reaching wing apex; 1Rs relatively long and curved; Rs + M slightly sinuous; first submarginal cell $2 \times$ longer than wide (0.31 mm vs 0.15 mm), pentagonal; 2Rs slightly sinuous; r-rs oblique, arising medially from pterostigma, 0.08 mm long; 3Rs extending nearly straight until wing margin, 0.55 mm long; r-rs several times longer than abscissa of M between 2Rs and m-cu; 1M curved, $2 \times$ longer

than 1Rs (0.14 mm vs 0.07 mm); 2M straight, 0.38 mm long; almost straight 3M, disappearing before wing margin; rs-m nebulous, 0.13 mm long; elongate, pentagonal second submarginal cell, 3 × longer than wide (0.38 mm vs 0.13 mm); trapezoidal third submarginal cell, 0.31 mm long; first discal cell almost 2 × longer than wide (0.21 mm vs 0.12 mm); m-cu distinctly postfurcal (absence of a vein 2Rs + M), 0.12 mm long; lacking 2m-cu; elongate second discal cell, 0.63 mm long; cu-a (nervulus) slightly postfurcal (therefore presence of an exceptionally short 1Cu_a), 0.06 mm long, perpendicular to 1Cu and A; 1Cu nearly straight, 0.14 mm long; 2Cu strongly curved basally separating 2Cu_a (0.05 mm long) and 2Cu_b, latter curved and directed towards wing margin (but without meeting margin); first subdiscal cell 2 × longer than wide (0.13 mm vs 0.07 mm); elongate and narrow second subdiscal cell; A tubular and nearly straight; 1a and 2a not visible. Hind wings and venation rather complete

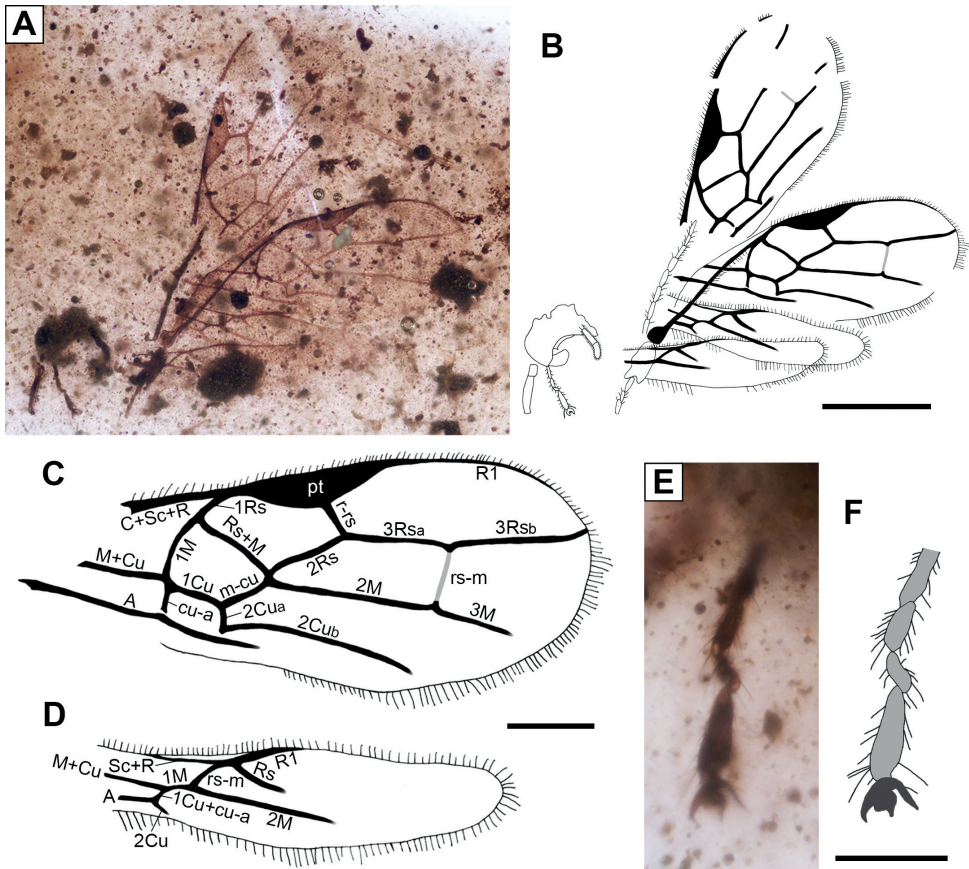


Figure 2. *Utrillabracon electropteron* Álvarez-Parra & Engel, gen. et sp. nov. (Braconidae, †Protorhyssalinae) from the upper Albian amber-bearing outcrop of San Just, specimen MAP-7819 (SJE2012 49-04). **A, B** photograph and drawing of preserved remains, both to the same scale **C** forewing venation **D** hind wing venation **E, F** photograph and drawing of tarsus and pretarsus, both to the same scale. Abbreviation: pt = pterostigma. Scale bars: 0.5 mm (**A, B**); 0.2 mm (**C, D**); 0.1 mm (**E, F**).

(Fig. 2D), hind wing base not preserved, more than 0.94 mm long and 0.23 mm at its maximum width, margin bearing setae; Sc + R fused anterobasally; R1 distally widened with several hamuli beyond its apex; Sc + R not aligned with Rs; 1M short, 0.05 long; rs-m oblique, 0.07 mm long; Rs and M ending as nebulous veins before margin; 1Cu + cu-a inclivitous, 0.03 mm long; short 2Cu, not contacting wing margin. Two fragments of legs visible: a partial femur and a tarsus; four distal tarsomeres preserved covered by fine setae (Fig. 2E, F), tarsomere III 0.06 mm long, tarsomere IV 0.04 mm long, tarsomere V 0.08 mm long; pretarsus with paired claws, preapical tooth absent, arolium wide.

Etymology. The specific epithet is a combination of the Greek ἤλεκτρον (*élektron*), meaning, “amber”, and πτερόν (*ptéron*), meaning, “winged creature”, and referring to the fact that the holotype is mainly preserved by the wings in amber.

Discussion

The newly reported San Just amber wasp can be assigned to Braconidae quite easily owing to the characteristic wing venation: Rs + M present and 2m-cu absent in the forewing and rs-m proximal to bifurcation of R1 and Rs in the hind wing (Huber and Sharkey 1993; Belokobylskij and Jouault 2021). The absence of 2m-cu in the forewing also serves to exclude the fossil from the plesiomorphic †Praeichneumonidae. Additionally, the Trachypetinae (formerly as family Trachypetidae) have rs-m distal to the separation of R1 and Rs (Quicke et al. 2020), and therefore the current fossil also does not accord with the circumscription of this group. Although many have noted that braconid wing venation can be quite variable, the current fossil from San Just cannot be ascribed to any other clade and is quite readily attributable to Braconidae. In fact, several Cretaceous braconids possess 2m-cu in the forewing, such as *Aenigmabracon capdoliensis* Perrichot, Nel, & Quicke, 2009 (subfamily *incertae sedis*), *Stephanorhysalus longiscapus* Belokobylskij & Jouault, 2021 (subfamily *incertae sedis*), and species of the subfamily †Eoichneumoninae, all of which likely retain this trait symplesiomorphically (Belokobylskij and Jouault 2021). Furthermore, some living species of the subfamilies Apozyginae, Doryctinae, and Rhyssalinae (all of crown-Braconidae) possess 2m-cu in the forewing (Tobias and Belokobylskij 1983), while some species of a few subfamilies of Ichneumonidae lack this vein (Tobias 1963). All of these cases are easily identified as secondary reappearances of the crossvein or “atavisms” based on the phylogenetic placement of the taxa in question (Belokobylskij and Jouault 2021).

The presence of a pentagonal (five-sided) second submarginal cell in the forewing and vein 2Cu in the hind wing indicates that *Utrillabracon electropteron* is currently best assigned to the subfamily †Protorhysalinae (Basibuyuk et al. 1999; Chen et al. 2021b), despite the fact that this group, even in its restricted sense, may be paraphyletic. Indeed, the overall venation of *Utrillabracon* accords broadly with that of †Protorhysalinae (Basibuyuk et al. 1999). The pentagonal second submarginal cell in the forewings is likely to be plesiomorphic in braconids. The other braconid subfamilies

with a Cretaceous record, such as Aphidiinae, †Seneciobraconinae, †Megalyrhyssalinae, and †Protobraconinae, lack 2Cu in the hind wing (Belokobylskij and Jouault 2021; Chen et al. 2021b). Several extant braconid subfamilies have 2Cu in the hind wing (Perrichot et al. 2009; Belokobylskij and Jouault 2021), and interestingly they are phylogenetically placed basal to all other crown-braconids (Apozyginae) or to the derived non-cyclostome lineage (Acampsohelconinae, Agathidinae, Meteorideinae, and Sigalphinae) (Chen and van Achterberg 2019). Furthermore, this character is also present in some †Eoichneumoninae (Braconidae), and in the ichneumonoid groups Trachypetinae (Braconidae), †Praeichneumonidae, and Ichneumonidae (Belokobylskij and Jouault 2021). Therefore, it is probable that the presence of 2Cu in the hind wing is symplesiomorphic across all of these lineages (Perrichot et al. 2009; Belokobylskij and Jouault 2021). The †Eoichneumoninae possess 2m-cu in the forewings (like the †Praeichneumonidae and the vast majority of Ichneumonidae) (Belokobylskij and Jouault 2021; Chen et al. 2021b), and quite unlike *U. electropteron*.

The San Just fossil may be easily distinguished from the two unplaced Canadian Late Cretaceous amber species “*Neoblacus*” (= *Blacus*) *facialis* Brues, 1937 and “*Pygostolus*” *patriarchicus* Brues, 1937. Both of these species need revision and likely do not belong to the genera to which Brues assigned them (Antropov et al. 2014; Chen et al. 2021b). Nonetheless, both are sufficiently known as to differentiate them from *U. electropteron*. The species *N.* (= *B.*) *facialis* lacks Rs + M and rs-m in the forewing (vs present), r-rs arises before the middle of the pterostigma and is perpendicular to the costal margin (vs inclivitous and arising pterostigmal midlength), and cu-a is distinctly postfurcal (vs slightly postfurcal) (Brues 1937). The pterostigma of *U. electropteron* seems to be similar to that of *N.* (= *B.*) *facialis*, as in both species it is 4 × longer than wide (Brues 1937). “*Pygostolus*” *patriarchicus* has a triangular pterostigma with basal and apical margins of equal length (vs pterostigma long and narrow), and cu-a postfurcal in the forewing (Brues 1937). The *incertae sedis* braconids *A. capdoliensis* and *S. longiscapus* differ from *U. electropteron* in the presence of 2m-cu and cu-a postfurcal in the forewing (Perrichot et al. 2009; Belokobylskij and Jouault 2021). *Pyramidibracon chypeatus* Chen & van Achterberg, 2021 and *Rhetinorhyssalus morticinus* Engel, 2016 are currently not assigned to a subfamily and differ from *U. electropteron* in several characters, such as cu-a strongly inclivitous in the forewing, Sc + R aligned with Rs, and both lack 2Cu in the hind wing (Engel 2016; Chen et al. 2021b).

Considering those genera currently assigned to †Protorhyssalinae, *U. electropteron* can be differentiated from them as summarized below. *Archaeorhyssalus subsolanus* lacks 1Rs (vs present), has a distinct 2Rs + M (vs absent), and m-cu antefurcal and contacting Rs + M (vs not contacting) in the forewing (Engel and Wang 2016). *Burmabracon gracilens*, *B. grossus*, and *Protorhyssalopsis perrichoti* have Sc + R aligned with Rs in the hind wing (vs not aligned), aside from a slew of further differences (Li et al. 2021; Ortega-Blanco et al. 2011). *Protorhyssalodes arnaudi* has cu-a distinctly postfurcal with 1Cu_a as long as cu-a (vs cu-a slightly postfurcal) in the forewing and also Sc + R aligned with Rs in the hind wing (Perrichot et al. 2009). The wing venation of *U. electropteron* is quite similar to that of *Protorhyssalus goldmani* and *Diorhyssalus allani* (Brues 1937; Basibuyuk et al. 1999; Engel 2016). *Utrillabracon electropteron*

shares with *P. goldmani* the marginal cell reaching the wing apex, vein m-cu postfurcal, and cu-a slightly postfurcal in the forewing, while differing in the length of the second submarginal cell (shorter in *P. goldmani*) and the length of r-rs in comparison to the abscissa of M between 2Rs and m-cu (similar length in *P. goldmani* and several times longer in *U. electropteron*) (Basibuyuk et al. 1999). Both species have Sc + R not aligned with Rs in the hind wing (Basibuyuk et al. 1999). In general, the venation of *U. electropteron* seems to be closest to that of *D. allani* (Brues 1937; Engel 2016). Particularly, the lengths of the second submarginal cell and r-rs (several times longer than the abscissa of M between 2Rs and m-cu) are similar in both, and they also have m-cu postfurcal (Brues 1937; Engel 2016). The characters present in *U. electropteron* that differ from *D. allani* are 1Rs curved (vs shorter and straight), rs-m nebulous (vs sclerotized), and cu-a orthogonal and slightly postfurcal (vs inclivitous and somewhat more postfurcal) (Brues 1937; Engel 2016). The hind wing of *D. allani* is poorly known (Engel 2016). Therefore, despite the similar venation of the San Just species with *D. allani*, we prefer to assign it to a new genus, as we think that the anatomical differences cannot be associated with variability between species. Furthermore, the San Just species and *D. allani* are separated by more than 20 Myr (Albian to Campanian), and a vast geographical distance (Iberian Peninsula vs western Canada).

Based on the similarities of the wing venations of *U. electropteron*, *P. goldmani*, and *D. allani*, it is possible that they were closely related. These three taxa may form a group within †Protorhyssalinae, supported by the following characters: 1Rs present, pterostigma long and narrow, r-rs arising medially from pterostigma, m-cu distinctly postfurcal, cu-a slightly postfurcal (1Cu_a shorter than cu-a) in the forewing, and Sc + R not aligned with Rs in the hind wing. The latter character is tenuous for *D. allani*, as the hind wings are poorly documented (Brues 1937; Engel 2016). Nonetheless, it is probable that the hind wing of *D. allani* also had 2Cu, based on the other anatomical similarities with *P. goldmani* and *U. electropteron*. A revision of the holotype of *D. allani* or the discovery of new specimens of the same morphotype may demonstrate the presence of 2Cu (and Sc + R not aligned with Rs) for the hind wing, thus corroborating its placement to †Protorhyssalinae. *Archaeorhyssalus subsolanus* has m-cu antefurcal, a distinctive character among protorhyssalines, and it may be that this genus belongs to a more derived clade between the generally plesiomorphic †Protorhyssalinae and the more derived †Seneciobraconinae. We refrain, however, from establishing another monogeneric subfamily for this genus until such time as more critical cladistic work has been undertaken. *Burmabracon gracilens*, *B. grossus*, *P. arnaudi*, and *P. perrichoti* share Sc + R aligned with Rs in the hind wing, a character that could be a potential apomorphy of a group formed by these four species. In any case, these groupings are based solely on observations of wing venation and a phylogenetic analysis incorporating larger suites of data is necessary to resolve monophyly (or lack thereof) for †Protorhyssalinae, relationships among the constituent groups, as well as the placement of the various extinct subfamilies among early diverging Braconidae. Basibuyuk et al. (1999) noted that the subfamily †Protorhyssalinae lacks apomorphies, and it is likely that it will be discovered to be a grade (Engel 2016; Chen and van Achterberg 2019), necessitating the removal of some genera to other or even new subfamilies (e.g., *Archaeorhyssalus*).

An interesting breadth of early braconid diversity is documented from Cretaceous amber inclusions and compression fossils (Table 1). Nonetheless, this diversity is trivial by comparison to the overwhelming diversity of present-day Braconidae (Chen and van Achterberg 2019). This may be the result of a Late Cretaceous diversification of the family, with little diversity present prior to this time. This may be partly the case as an incredible diversity of new potential hosts for braconids were appearing during the Late Cretaceous and into the Paleogene owing to the rise of several flower-associated insects at the time (Labandeira and Li 2021). However, there is likely also a considerable taphonomic bias against the capture and preservation of early fossil Braconidae (Martínez-Delclòs et al. 2004). Their typically diminutive size means that preservation in sediments requires exceptionally fine grains in order to have sufficient fidelity for their proper identification as braconids and despite the rich number of wasps included in amber, Cretaceous braconids are rare. This could be owing to the fact that braconids have little reason to be near resin flows except in the case of seeking or emerging from a host that was somehow present on or in trees exuding resins. Certainly, the family was present and widespread during the Cretaceous owing to their occurrence in deposits spanning Canada to Myanmar, and so the combination of potentially low abundances, lower than present species diversity, typically small body size necessitating exceptional preservational conditions, and biases away from resin-producing sources may account for their rarity. If this is the case, then it would also render challenging any direct exploration of their earliest history as fossils would likely continue to be rare.

Acknowledgements

We thank the Museo Aragonés de Paleontología (Fundación Conjunto Paleontológico de Teruel-Dinópolis) for the loan of the material reported herein. We are grateful to the Dirección General de Patrimonio Cultural of the Government of Aragón (Spain) for the permission to excavate in the San Just outcrop, and to Rafael López del Valle for the preparation of the amber piece. We also thank Sergey Belokobylskij, two anonymous reviewers, and the subject editor Kees van Achterberg for their generous and helpful comments that improved the manuscript. This study is a contribution to the project CRE CGL2017-84419 funded by the Spanish AEI/FEDER and UE. S.Á.-P. is grateful for support from the Secretaria d'Universitats i Recerca de la Generalitat de Catalunya (Spain) and the European Social Fund (2021FI_B2 00003).

References

- Álvarez-Parra S, Peñalver E (2019) Palaeontological study of the lacustrine oil-shales of the lower Miocene San Chils locality (Ribesalbes-Alcora Basin, Castellón province, Spain). *Spanish Journal of Palaeontology* 34(2): 187–203. <https://doi.org/10.7203/sjp.34.2.16093>
- Álvarez-Parra S, Pérez-de la Fuente R, Peñalver E, Barrón E, Alcalá L, Pérez-Cano J, Martín-Closas C, Trabelsi K, Meléndez N, López Del Valle R, Lozano RP, Peris D, Rodrigo A,

- Sarto i Monteys V, Bueno-Cebollada CA, Menor-Salván C, Philippe M, Sánchez-García A, Peña-Kairath C, Arillo A, Espílez E, Mampel L, Delclòs X (2021) Dinosaur bonebed amber from an original swamp forest soil. *eLife* 10: e72477. <https://doi.org/10.7554/eLife.72477>
- Antropov AV, Belokobylskij SA, Compton SG, Dlussky GM, Khalaim AI, Kolyada VA, Kozlov MA, Perfilieva KS, Rasnitsyn AP (2014) The wasps, bees and ants (Insecta: Vespidia = Hymenoptera) from the insect limestone (Late Eocene) of the Isle of Wight, UK. *Earth and Environmental Science Transactions of the Royal Society of Edinburgh* 104(3–4): 335–446. <https://doi.org/10.1017/S1755691014000103>
- Basibuyuk HH, Rasnitsyn AP, van Achterberg K, Fitton MG, Quicke DLJ (1999) A new, putatively primitive Cretaceous fossil braconid subfamily from New Jersey amber (Hymenoptera, Braconidae). *Zoologica Scripta* 28(1–2): 211–214. <https://doi.org/10.1046/j.1463-6409.1999.00006.x>
- Belokobylskij SA (2012) Cretaceous braconid wasps from the Magadan Province of Russia. *Acta Palaeontologica Polonica* 57(2): 351–361. <https://doi.org/10.4202/app.2010.0120>
- Belokobylskij SA, Jouault C (2021) Two new striking braconid genera (Hymenoptera: Braconidae) from the mid-Cretaceous Burmese amber. *Proceedings of the Geologists' Association* 132(4): 426–437. <https://doi.org/10.1016/j.pgeola.2021.04.003>
- Brues CT (1937) Superfamilies Ichneumonoidea, Serphoidea, and Chalcidoidea. In: Carpenter FM (Ed.) *Fossil Insects in Canadian Amber*. University of Toronto Studies, Geological Series 40: 27–44.
- Chen XX, van Achterberg C (2019) Systematics, phylogeny, and evolution of braconid wasps: 30 years of progress. *Annual Review of Entomology* 64(1): 335–358. <https://doi.org/10.1146/annurev-ento-011118-111856>
- Chen HY, van Achterberg C, Hong P (2021a) Two new genera of Protobraconinae (Hymenoptera, Braconidae) from mid-Cretaceous amber of northern Myanmar. *Cretaceous Research* 126: e104914. <https://doi.org/10.1016/j.cretres.2021.104914>
- Chen HY, van Achterberg C, Pang H, Liu JX (2021b) Three new genera of Braconidae (Hymenoptera) from mid-Cretaceous amber of northern Myanmar. *Cretaceous Research* 118: e104669. <https://doi.org/10.1016/j.cretres.2020.104669>
- Corral JC, López Del Valle R, Alonso J (1999) El ámbar cretácico de Álava (Cuenca Vasco-Cantábrica, norte de España). Su colecta y preparación. *Estudios del Museo de Ciencias Naturales de Álava* 14: 7–21.
- Engel MS (2016) Notes on Cretaceous amber Braconidae (Hymenoptera), with descriptions of two new genera. *Novitates Paleontologicae* 15(15): 1–7. <https://doi.org/10.17161/np.v0i15.5704>
- Engel MS, Wang B (2016) The first Oriental protorhyssaline wasp (Hymenoptera: Braconidae): A new genus and species in Upper Cretaceous amber from Myanmar. *Cretaceous Research* 63: 28–32. <https://doi.org/10.1016/j.cretres.2016.02.012>
- Engel MS, Thomas JC, Alqarni AS (2017) A new genus of protorhyssaline wasps in Raritan amber (Hymenoptera, Braconidae). *ZooKeys* 711: 103–111. <https://doi.org/10.3897/zookeys.711.20709>
- Engel MS, Huang D, Cai C, Alqarni AS (2018) A new lineage of braconid wasps in Burmese Cenomanian amber (Hymenoptera, Braconidae). *ZooKeys* 730: 75–86. <https://doi.org/10.3897/zookeys.730.22585>

- Huber JT, Sharkey MJ (1993) Structure. In: Goulet H, Huber JT (Eds) Hymenoptera of the World: An Identification Guide to Families. Agriculture Canada, Ottawa, 13–59.
- Jasso-Martínez JM, Quicke DLJ, Belokobylski SA, Santos BF, Fernández-Triana JL, Kula RR, Zaldívar-Riverón A (2022a) Mitochondrial phylogenomics and mitogenome organization in the parasitoid wasp family Braconidae (Hymenoptera: Ichneumonoidea). *BMC Ecology and Evolution* 22(1): e46. <https://doi.org/10.1186/s12862-022-01983-1>
- Jasso-Martínez JM, Santos BF, Zaldívar-Riverón A, Fernandez-Triana J, Sharanowski BJ, Richter R, Dettman JR, Blaimer BB, Brady SG, Kula RR (2022b) Phylogenomics of braconid wasps (Hymenoptera, Braconidae) sheds light on classification and the evolution of parasitoid life history traits. *Molecular Phylogenetics and Evolution* 107452: e107452. <https://doi.org/10.1016/j.ympev.2022.107452>
- Kopylov DS (2012) New species of Praeichneumonidae (Hymenoptera, Ichneumonoidea) from the lower Cretaceous of Transbaikalia. *Paleontological Journal* 46(1): 66–72. <https://doi.org/10.1134/S0031030112010078>
- Kopylov DS, Zhang Q, Zhang HC (2021) The Darwin wasps (Hymenoptera: Ichneumonidae) of Burmese amber. *Palaeoentomology* 4(6): 592–603. <https://doi.org/10.11646/palaeoentomology.4.6.8>
- Labandeira CC, Li L (2021) The history of insect parasitism and the Mid-Mesozoic Parasitoid Revolution. In: De Baets K, Huntley JW (Eds) The evolution and fossil record of parasitism: Identification and macroevolution of parasites. Springer, Topics in Geobiology 49(11): 377–533. https://doi.org/10.1007/978-3-030-42484-8_11
- Li L, Shih C, Yang J, Wang L, Li D, Ren D (2021) New amber record of Braconidae (Insecta: Hymenoptera) from the mid-Cretaceous of Myanmar. *Cretaceous Research* 124: e104794. <https://doi.org/10.1016/j.cretres.2021.104794>
- Martínez-Delclòs X, Briggs DE, Peñalver E (2004) Taphonomy of insects in carbonates and amber. *Palaeogeography, Palaeoclimatology, Palaeoecology* 203(1–2): 19–64. [https://doi.org/10.1016/S0031-0182\(03\)00643-6](https://doi.org/10.1016/S0031-0182(03)00643-6)
- Nees von Esenbeck CG (1811) Ichneumonides Adsciti, in genera et familias divisi. *Magazin Gesellschaft Naturforschender Freunde zu Berlin* 5: 1–37.
- Nomano FY, Mitsui H, Kimura MT (2015) Capacity of Japanese *Asobara* species (Hymenoptera; Braconidae) to parasitize a fruit pest *Drosophila suzukii* (Diptera; Drosophilidae). *Journal of Applied Entomology* 139(1–2): 105–113. <https://doi.org/10.1111/jen.12141>
- Ortega-Blanco J, Bennett DJ, Delclòs X, Engel MS (2009) A primitive aphidiine wasp in Albian amber from Spain and a Northern Hemisphere origin for the subfamily (Hymenoptera: Braconidae: Aphidiinae). *Journal of the Kansas Entomological Society* 82(4): 273–282. <https://doi.org/10.2317/JKES0812.08.1>
- Ortega-Blanco J, Delclòs X, Engel MS (2011) A protorhyssaline wasp in Early Cretaceous amber from Spain (Hymenoptera: Braconidae). *Journal of the Kansas Entomological Society* 84(1): 51–57. <https://doi.org/10.2317/JKES100728.1>
- Peñalver E, Martínez-Delclòs X (2000) Insectos del Mioceno Inferior de Ribesalbes (Castellón, España). *Hymenoptera. Treballs del Museu de Geologia de Barcelona* 9: 97–153.
- Peñalver E, Delclòs X, Soriano C (2007) A new rich amber outcrop with palaeobiological inclusions in the Lower Cretaceous of Spain. *Cretaceous Research* 28(5): 791–802. <https://doi.org/10.1016/j.cretres.2006.12.004>

- Perrichot V, Nel A, Quicke DLJ (2009) New braconid wasps from French Cretaceous amber (Hymenoptera, Braconidae): Synonymization with Eoichneumonidae and implications for the phylogeny of Ichneumonoidea. *Zoologica Scripta* 38(1): 79–88. <https://doi.org/10.1111/j.1463-6409.2008.00358.x>
- Quicke DLJ, Austin AD, Fagan-Jeffries EP, Hebert PD, Butcher BA (2020) Recognition of the Trachypetidae stat. n. as a new extant family of Ichneumonoidea (Hymenoptera), based on molecular and morphological evidence. *Systematic Entomology* 45(4): 771–782. <https://doi.org/10.1111/syen.12426>
- Rasnitsyn AP (1975) Hymenoptera Apocrita of Mesozoic. *Transactions of the Palaeontological Institute Academy of Sciences of the USSR* 147: 1–134. [In Russian]
- Rasnitsyn AP (1983) Ichneumonoidea (Hymenoptera) from the lower Cretaceous of Mongolia. *Contributions of the American Entomological Institute* 20: 259–265.
- Rasnitsyn AP (1988) An outline of evolution of the hymenopterous insects (order Vespida). *Oriental Insects* 22(1): 115–145. <https://doi.org/10.1080/00305316.1988.11835485>
- Rasnitsyn AP (1990) Hymenoptera. In: Ponomarenko AG (Ed.) *Late Mesozoic insects of Eastern Transbaikalian*. *Transactions of the Palaeontological Institute Academy of Sciences of the USSR* 239: 177–205. [In Russian]
- Santer M, Álvarez-Parra S, Nel A, Peñalver E, Delclòs X (2022) New insights into the enigmatic Cretaceous family Spathiopterygidae (Hymenoptera: Diaprioidea). *Cretaceous Research* 133: e105128. <https://doi.org/10.1016/j.cretres.2021.105128>
- Spasojevic T, Broad GR, Sääksjärvi IE, Schwarz M, Ito M, Korenko S, Klopstein S (2021) Mind the outgroup and bare branches in total-evidence dating: A case study of pimply Darwin wasps (Hymenoptera, Ichneumonidae). *Systematic Biology* 70(2): 322–339. <https://doi.org/10.1093/sysbio/syaa079>
- Tobias VI (1963) Ichneumonidae (Hymenoptera) with a venation type in the fore wings which resembles that in Braconidae. *Zoologicheskij Zhurnal* 42: 1513–1522. [In Russian with English summary]
- Tobias VI, Belokobylskij SA (1983) Aberrant wing venation in Braconidae (Hymenoptera) and its significance in study of the phylogeny of the family. *Entomologicheskoe Obozrenie* 62: 341–347. [In Russian]
- Viertler A, Klopstein S, Jouault C, Spasojevic T (2022) Darwin wasps (Hymenoptera, Ichneumonidae) in Lower Eocene amber from the Paris basin. *Journal of Hymenoptera Research* 89: 19–45. <https://doi.org/10.3897/jhr.89.80163>
- Villanueva-Amadoz U, Pons D, Diez JB, Ferrer J, Sender LM (2010) Angiosperm pollen grains of San Just site (Escucha Formation) from the Albian of the Iberian Range (northeastern Spain). *Review of Palaeobotany and Palynology* 162(3): 362–381. <https://doi.org/10.1016/j.revpalbo.2010.02.014>
- Wharton RA (1993) *Bionomics of the Braconidae*. *Annual Review of Entomology* 38(1): 121–143. <https://doi.org/10.1146/annurev.en.38.010193.001005>

An updated, illustrated inventory of the marine fishes of the US Virgin Islands

D. Ross Robertson¹, Carlos J. Estapé², Allison M. Estapé²,
Lee Richter³, Ernesto Peña¹, Benjamin Victor^{4,5}

1 *Smithsonian Tropical Research Institute, Balboa, Panama* **2** *197 Gulfview Drive, Islamorada, Florida, 33036, USA* **3** *National Park Service, 1300 Cruz Bay Creek, St. John, VI 00830, Virgin Islands, USA* **4** *Ocean Science Foundation, 4051 Glenwood, Irvine, CA 92604, USA* **5** *Guy Harvey Research Institute, Nova Southeastern University, 8000 North Ocean Drive, Dania Beach, FL 33004, USA*

Corresponding author: D. Ross Robertson (robertsondr@si.edu)

Academic editor: Caleb McMahan | Received 14 March 2022 | Accepted 9 May 2022 | Published 1 June 2022

<http://zoobank.org/F2333822-5B4F-45F4-8172-8E794AFBC316>

Citation: Robertson DR, Estapé CJ, Estapé AM, Richter L, Peña E, Victor B (2022) An updated, illustrated inventory of the marine fishes of the US Virgin Islands. ZooKeys 1103: 79–122. <https://doi.org/10.3897/zookeys.1103.83795>

Abstract

The US Virgin Islands (USVI) include St. John and St. Thomas on the Puerto Rican Platform (PRP) and St. Croix, isolated by 2000 m deep water 45 km south of that platform. Previous inventories of the marine fishes of these islands include a comprehensive 2014 checklist of the fishes of St. Croix and a list of the fishes of the PRP produced in 2000. The latter list noted the locations of many records of the plateau's fishes, allowing the construction of a combined inventory for St. John and St. Thomas. Those two islands are treated here as a single faunal unit because they are only 3.5 km apart on a shared shallow shelf with various islets and reefs in between. Here we provide updated information on those two USVI (St. Croix and St. John-Thomas) marine fish faunas. The additions to the St. Croix and St. John-Thomas inventories presented here are based on a combination of information from the two sources indicated above, more recent publications dealing with those faunas, a review of location records on various online sources of biogeographic data, and voucher photographs taken of fishes in the field by authors of this paper and other citizen scientists. This assessment increased the known fauna of St. Croix by 7.5% to 585 species. The inventory for St. John-Thomas increased by 39.9% from 401 species on the 2000 PRP list to 561 with the inclusion of records from other sources. On-site mtDNA (COI) barcodes are available for approximately one-third of the species of the St. John-Thomas fauna, but for only one species collected at St. Croix. A set of underwater photographs of 372 species (34 of them representing the sole record of a species) from St. John-Thomas and of 11 shallow-water species added to the St. Croix fauna is included. These represent occurrence vouchers and also are intended to facilitate future work that builds on the present compendium.

Keywords

Biodiversity, checklist, citizen science, DNA-barcode, photographic voucher, SCUBA survey

Introduction

The United States Virgin Islands (USVI) comprise a US territory adjacent to Puerto Rico, in the northeast Caribbean, that includes three large, inhabited islands, St. John, St. Thomas and St. Croix, and approximately 50 smaller islands and cays around them. The former two are situated only 3.5 km apart, in the center of the Puerto Rico Plateau (PRP), which has an area approximately twice the 9,100 km² of Puerto Rico Island and extends ~ 150 km eastwards from Puerto Rico. St. Croix is located south of St. John and St. Thomas, on its own insular platform, which is separated by 45 km of deep water from the southern edge of the PRP.

The fish fauna of St. Croix was comprehensively reviewed by Smith-Vaniz and Jelks (2014), who built upon an older list by Clavijo et al. (1980), using their own extensive collections of shallow fishes of the Buck Island Reef National Monument on the northern side of St. Croix (Smith-Vaniz et al. 2006), and a review of literature and examination of specimens of fishes collected at St. Croix that are lodged in various museums. In 2000, George Dennis produced an extensive (244 page; 500+ sources cited) U.S. Geological Survey report based on collections and observational records for marine and brackish-water fish from Puerto Rico, St. John and St. Thomas, and other islands on the PRP. Although never formally published in a scientific journal, and no longer available through the USGS source cited by Dennis et al. (2004), that compendium is available online (Dennis 2000).

Here we add new information to update the 2014 list for St. Croix and assemble an inventory for St. John and St. Thomas that includes and expands on data for those two islands contained in Dennis (2000). We extracted the additional information from museum records in online sources of biogeographic data, publications produced since Dennis (2000), digital images of live fishes obtained at the USVI, plus our recent collections and mtDNA barcode records obtained from the database BOLD. The great majority of the species in this compendium are marine, plus we include a small number of species found in fresh to brackish waters.

Materials and methods**Study sites**

St. Croix is a 215 km² island in the northeast corner of the Caribbean. It is isolated by ~ 45 km of deep water from the Puerto Rican Platform (**PRP**). Other islands of the Lesser Antilles chain lie within ~ 150 km to the east and southeast of St. Croix. The surrounding

shallow (above ~ 150 m depth) shelf of St. Croix, extending almost 20 km eastward, has approximately the same area as the island. In addition to exposed and sheltered coral reefs and soft bottoms, the island has extensive areas of seagrasses and mangroves.

St. John (area 50 km²) and St. Thomas (area 83 km²) are situated in the center of the shallow (to ~ 150 m deep) tongue of the PRP that extends 150 km eastwards from Puerto Rico. St. Thomas is closest to and 64 km from the main island of Puerto Rico. St. John and St. Thomas are separated from each other by only 3.5 km of water shallower than 20 m deep, with scattered islets and shallow reefs in between them. They have a similar range of habitats as St. Croix, with large areas of both sheltered and deeper shelf-edge coral reefs, rocky shores, seagrass beds and mangroves. Due to their proximity and similarity of habitats we treat them here as a single unit (hereafter St. John-Thomas). The shallow PRP associated with St. John-Thomas extends ~ 25 km north and ~ 15 km south of those islands and covers an area of ~ 2,100 km² (Rohmann et al. 2005).

Suppl. material 2: File S1 shows the bathymetry of bottom habitats on the above-150 m shelves of the USVI. The shelf area of the St. John-Thomas EEZ is not only much larger than that of St. Croix but also differs from the latter in containing a much greater diversity of areas of different depths. There are large expanses, in both absolute and relative terms, of habitat between 40–60 m deep to the north of St. Thomas and to the south of both islands. In contrast, most of the smaller shelf of St. Croix is shallower than 20 m deep.

Data sources

We reviewed and cited only publications from which we extracted information relating to the USVI fishes that were published after those cited by Dennis (2000) for St. John-Thomas, and after that by Smith-Vaniz and Jelks (2014) for St. Croix, plus a few earlier publications that contained additional relevant information.

Smith-Vaniz and Jelks (2014) published a comprehensive, annotated checklist of 544 fishes known from St. Croix. That checklist was based, in large part, on the yield of fishes from 106 rotenone stations obtained by Smith-Vaniz et al. (2006) and by later workers to document the shallow cryptobenthic fauna. That 2014 list identified questionable records, a few of which, as we show, have turned out to be valid. Smith-Vaniz and Jelks (2014). That checklist also excluded deep-water fishes not found above 200 m as well as Exocoetids and Myctophids. For completeness we have included any such species recorded by other sources among the additions noted here. We used the 2014 list of valid species and reviewed fishes listed by other surveys: a SCUBA study of the shallower parts (30–50 m depth) of a mesophotic coral ecosystem at the eastern end of the shelf (García-Sais et al. 2014); two JSL submersible dives off St. Croix to 30–600 m (Nelson and Appeldoorn (1985); and two ROV dives off St. Croix at depths greater than 800 m (Quattrini et al. 2017). In addition, we reviewed the records of fish species from St. Croix available from various online sources: the aggregators GBIF (<https://www.gbif.org/>), FishNet2 (<http://www.fishnet2.net/>), iDigBio (<https://www.idigbio.org/portal>), OBIS (<https://obis.org/>) and Vertnet (<http://vertnet.org/>), and the American

Museum of Natural History (AMNH; <https://www.amnh.org/research/vertebrate-zoology/ichthyology>). Those searches were made within a quadrat with latitudinal limits of 17.62°N to 17.85°N, and longitudinal limits of -64.4°W to -65.0°W, encompassing St. Croix and all of its platform. The sources of St. Croix records produced by those online searches were evaluated and museum records within the known geographic range of various species were accepted. Evaluation of individual records is necessary because aggregator information includes significant numbers of erroneous records.

Finally, the list includes shallow-reef fishes photographed by authors AME and CJE during a month spent at the island from 19 December 2020 to 13 January 2021. Suppl. material 3: File S2A presents a list, with georeferenced locations, of the 11 dive sites at which they together made 25 dives (total 47 hours duration per person) during that period (see also Fig. 1B and Suppl. material 4: File S3, a Google Earth © KMZ file that shows, for each of those sites, its location and georeferenced coordinates, and the number of dives and total dive time spent at that site). These photographs document a few species not previously recorded at the island, plus several not accepted by Smith-Vaniz and Jelks (2014) due to a lack of reliable information.

For St. John-Thomas we extracted a list of 401 species listed at those islands by Dennis (2000) and reviewed various publications dealing with fish records at and near those islands that were subsequently produced. Finally, we also used the same online data sources as for St. Croix (see above) to obtain records of fishes from the part of the Exclusive Economic Zone of the USVI that includes St. John-Thomas and extends between the northern and southern edges of the PRP. That irregularly shaped EEZ was obtained from Marineregions.org, which provides a standard set of global maps of EEZs (<https://www.marineregions.org/eezsearch.php>).

CJE and AME spent six months between 3 November 2020 and 29 May 2021 diving at both islands and photographing fishes to obtain voucher images of as many members of those islands' marine fish fauna as possible. File S2A presents a list, with georeferenced locations, of their dive sites at St. John (37) and St. Thomas (12), at which they made 113 joint dives (involving multiple dives at some sites) totaling 221 hours per person and 37 dives totaling 37 hours per person, respectively. Fig. 1A is a map with those 49 dive sites at St. John-Thomas indicated and File S2 provides additional information. Fig. 1A (and see File S2B) also indicates the location of sites from other sources at which additional species not recorded by CJE and AME were documented photographically by other divers.

Reef-associated bony fishes of the USVI

Greater Caribbean (GC) reef systems have reef-fish faunas that are dominated by members of typical, shallow-reef families of bony fishes extending down to depths of ~ 250–300 m (Baldwin et al. 2018). Here we focus on species belonging to those families, which have traditionally been viewed as reef fishes. We classed species living entirely or largely below 40 m depth as belonging to the deep-reef subset. Species classed here as shallow include both species restricted to depths shallower than 40 m

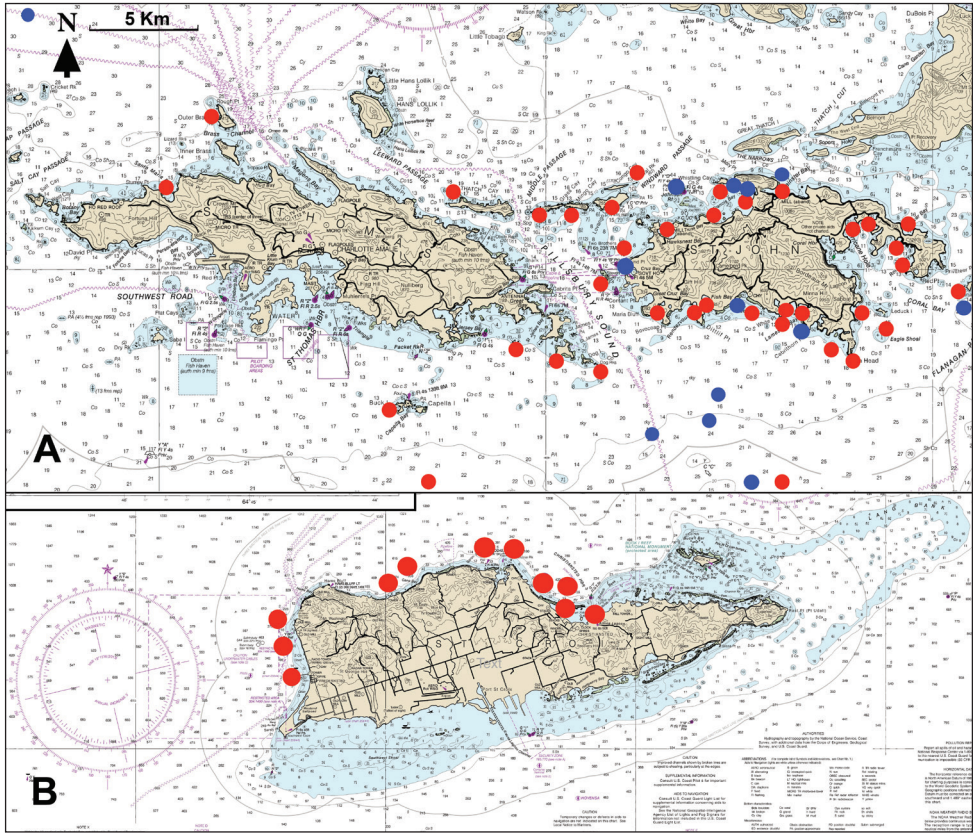


Figure 1. **A** dive sites generating fish-occurrence data at St. John and St. Thomas islands. Dive sites of CJE and AME are indicated by red symbols, and of other sources of voucher photographs by blue symbols. Note that some close-proximity sites are indicated by a single symbol. Symbols at the northern and southern edges of Fig. 1A are representative only, as their latitudes are outside the area of the map **B** dive sites of CJE and AME generating data at St. Croix. See Suppl. material 3: File S2A, B and Suppl. material 4: File S3 for further information. Base map in both cases: NOAA Chart 25641.

and those with depth ranges that extend above and below that level. These reef-associated fishes include not only benthic and demersal species found on hard-reef substrata, but also pelagic fishes that facultatively associate with reefs and benthic and demersal species that live on soft bottoms within and immediately around the fringes of reefs. Benthic species (e.g., eels, flatfishes) are restricted to life on and in different types of substrata, while demersal species (e.g., snappers and grunts) use both substratum habitats and the water column. Cryptobenthic species are visually cryptic and typically small. We followed Brandl et al. (2018) in classifying families dominated by small cryptobenthic coral-reef species as Core Coral Reef Fish families (CCRFs).

We also evaluate the ecological and zoogeographic composition of the two USVI fish faunas (St. Croix and St. John-Thomas) compared to the complete checklist of the regional fauna of reef-associated bony fishes, which includes 992 species in 342 genera and

84 families (Robertson and Tornabene 2021). These aspects of the fauna of the USVI are also compared with results from another recent comprehensive survey of the fish fauna of nearby Sint Eustatius, which is 170 km from St. Croix (Robertson et al. 2020).

mtDNA-barcode coverage of fishes collected in the USVI and Puerto Rico

Relatively few small marine locations have been comprehensively sampled for fish DNA barcoding, i.e., tissues sequenced for the mtDNA COI marker as a standard for identifying fishes, as compiled in the Barcode of Life Database, BOLD (Ward et al. 2009). Notably, BOLD not only includes a wide variety of projects, most of which are publicly available, but also regularly harvests all available COI sequences from GenBank. In contrast, GenBank does not harvest from BOLD, and BOLD sequences are generally submitted to GenBank only by request. As a result, only a fraction (~ 15% for GC fishes) of COI sequences on BOLD also are present on GenBank, despite its widespread use as the sole source for barcoding studies. BOLD further differs from GenBank by applying quality control to sequences and taxon identifications as data is entered, including sequences harvested from GenBank. It also has post-hoc quality control via a tagging and comment option on individual records. BOLD also includes a large number of private sequences, which can be assessed to a limited degree (with some metadata removed) via the BIN portal, which compiles all records, public and private, within a lineage, assigns a code, and presents some statistics, especially variance and nearest neighbor distances, as well as countries of origin.

The BOLD BIN code is a key advance enabling the compilation and comparison of mtDNA barcoding lists, since it supplies an independent identifier for a monophyletic genetic lineage, which is not the same as a species name. BOLD creates **BINs** (Barcode Index Numbers) by clustering barcode sequences algorithmically. The BIN often represents a particular species, but there are many exceptions to the “one-species, one BIN” concept: either multiple BINs per species, indicating genetically divergent populations within species (usually allopatric, but not always), a subset of which are putative new cryptic species awaiting morphological confirmation; or shared BINs by two or more species that retain shared or closely related haplotypes due to a short time since speciation, to incomplete lineage sorting, or to a small degree of hybridization.

Our broad assessment suggests that BOLD has a BIN that can be assigned (with widely varying degrees of confidence) to ~ 900 species of shallow-dwelling, reef-associated bony fishes from the GC. A list of sequences obtained in a particular area is obtained from BOLD by using a vector map in its search engine. The resulting list is from public projects (including all GenBank COI sequences), as well as whichever private projects the user has permission to access (often granted by an email request to the source of the sequence). In our case, we have been given access to all of the larger private projects in the region and barcodes for the vast majority (~ 90%) of sequence records in BOLD that could be evaluated in their respective BINs. The list of records from the geographic-area search on BOLD are individual sequences with metadata (including GenBank number if a sequence has one) and photographs of specimens (when available), together with a link to the BIN code to which it belongs. The species name originally submitted for

each is preserved, and the accuracy of the assignment can be assessed by examining the BIN to which it belongs, which has details on the various names applied to sequences in the BIN and by whom and where they were obtained. Accuracy assessments are critical, especially for more obscure species, since a “majority rules” decision is often inaccurate due to multiple identifications by inexperienced contributors, the tendency to repeat the species-level identification made by others as a shortcut, and the practice of assigning species-level names to submitted records that are from eggs, larvae, isolated tissue, or fish-market specimens. GenBank records are harvested by BOLD with whatever name is assigned in GenBank, often a preliminary one from submission, rather than the one later corrected or published in the subsequent literature.

Results

The island faunas

St. Croix: The checklist of Smith-Vaniz and Jelks (2014) included 544 species from 280 genera in 94 families. We obtained records of 41 species (belonging to 39 genera and 35 families; see Table 1) that were not included on that checklist, an increase of 7.5% in the number of species. Those new records included 19 deep-living species, six of them (11.1% of all deep species at St. Croix) resulting solely from observations by the JSL submersible (Nelson and Appeldoorn 1985; García-Sais et al. 2014) and an ROV (Remotely Operated Vehicle; Quattrini et al. 2017). It should be noted that almost all of that group belong to very deep taxa specifically excluded by Smith-Vaniz and Jelks (2014) from their list, which was focused primarily on shallower fishes. The remaining 22 species are shallow-water, reef-associated fishes. Ten of the latter group were photographed by AME and CJE (Table 1; Suppl. material 1: Plate S1). These additions include three species (*Eucinostomus melanopterus*, *Coryphopterus glaucofrenum* and *Opistognathus macrogathus*) that Smith-Vaniz and Jelks (2014) referred to but did not include in their checklist due to lack of confirmed records. Records of two mobulid rays consisted of identified photographs/videos provided by Mantatruster.org (<https://www.mantatruster.org/>) that were inspected by DRR. The list (Table 1, which includes source information) also includes records from museum collections that provide online data directly or indirectly through aggregators, which were included if consistent with the known geographic range of each of those species.

St. John-Thomas: Table 2 presents a list of species recorded from those islands together with the source(s) of each record (images, publications, DNA barcodes, or online museum records) and which species have a voucher image in the supplementary plates (Suppl. material 1: Plates S2–S18). In addition, for uncommon species (those encountered by AME, CJE, LR, or third-party photographers at three or fewer dive sites) the names of the sites at which those uncommon species were found are included, to aid future investigations. Dennis (2000) also included information on species that were collected using the ichthyocide Rotenone (see Table 2). Smith-Vaniz and Jelks (2014) list for St. Croix also included some species recorded at these St. John-Thomas as a result of collections using

Table 1. Species of fishes added to the St. Croix checklist of fishes of Smith-Vaniz and Jelks (2014).

Scientific name	Common name	Deep	Image plate	Literature source	Online source
Antennariidae					
<i>Fowlerichthys ocellatus</i> (Bloch & Schneider, 1801)	Ocellated Frogfish				TNHCI
Bathygadidae					
<i>Gadomus arcuatus</i> (Goode & Bean, 1886)	Doublethread Grenadier	yes		6	
Blenniidae					
<i>Hypleurochilus pseudoaequipinnis</i> Bath, 1994	Oyster Blenny		S1		
Bramidae					
<i>Eumegistus brevorti</i> (Poey, 1860)	Tropical Pomfret	yes			FIMNH
Chaenopsidae					
<i>Emblemariopsis leptocirris</i> Stephens, 1970	Fine-cirrus Blenny		S1		
Chimaeridae					
<i>Chimaera cubana</i> Howell Rivero, 1936	Cuban Chimaera	yes		1	
Etmopteridae					
<i>Etmopterus hillianus</i> (Poey, 1861)	Caribbean Lantern Shark	yes			FIMNH
Exocoetidae					
<i>Cheilopogon melanurus</i> (Valenciennes, 1847)	Atlantic Flyingfish				CF
<i>Cypselurus comatus</i> (Mitchill, 1815)	Clearwing Flyingfish				CF
Gempylidae					
<i>Lepidocybium flavobrunneum</i> (Smith, 1843)	Escolar	yes			NOAA
<i>Nesiarchus nasutus</i> Johnson, 1862	Black Gemfish	yes			NMNH
Gerreidae					
<i>Eucinostomus melanopterus</i> (Bleeker, 1863)	Flagfin Mojarra		S1	5,7*	
Gobiesocidae					
<i>Acyrtus lanthanum</i> Conway, Baldwin & White, 2014	Orange-spotted Clingfish				FIMNH
Gobiidae					
<i>Coryphopterus glaucofraenum</i> Gill, 1863	Bridled Goby		S1	2,5,7*	
<i>Coryphopterus kuna</i> Victor, 2007	Kuna Goby		S1		
<i>Oxyurichthys stigmalocephus</i> (Mead & Böhlke, 1958)	Spotfin Goby		S1		NOAA
Kyphosidae					
<i>Kyphosus cinerascens</i> (Forsskål, 1775)	Topsail Seachub		S1		
Macrouridae					
<i>Nezumia aequalis</i> (Günther, 1878)	Atlantic Blacktip Grenadier	yes		6	
Malakichthyidae					
<i>Verilus pseudomicrolepis</i> (Schultz, 1940)	False-smallscale Bass	yes			CAS
Mobulidae					
<i>Mobula cf birostris</i>	Giant Manta			4	
<i>Mobula tarapacana</i> (Philippi, 1892)	Sicklefin Devil Ray			4	
Muraenidae					
<i>Gymnothorax nigromarginatus</i> (Girard, 1858)	Blackedge Moray				CAS
Nemichthyidae					
<i>Nemichthys curvirostris</i> (Strömman, 1896)	Spottedbelly Snipe Eel	yes		6	
Neoscopelidae					
<i>Neoscopelus microchir</i> Matsubara, 1943	Shortfin Blackchin	yes		6	
Ophichthidae					
<i>Myrophis punctatus</i> Lütken, 1852	Speckled Worm Eel				MCZ
Ophidiidae					
<i>Monomitopus agassizii</i> (Goode & Bean, 1896)	Threespine Cusk-eel	yes			MCZ

Scientific name	Common name	Deep	Image plate	Literature source	Online source
Opistognathidae					
<i>Opistognathus macrognathus</i> Poey, 1860	Banded Jawfish		S1	5,7*	
Paralichthyidae					
<i>Syacium micrurum</i> Ranzani, 1842	Channel Flounder		S1		
Peristediidae					
<i>Peristedion longispatha</i> Goode & Bean, 1886	Widehead Armored Searobin	yes			MCZ
Pleuronectidae					
<i>Poecilopsetta inermis</i> (Breder, 1927)	Unarmed Deepwater Dab	yes			CAS, NMNH
Polymixiidae					
<i>Polymixia nobilis</i> Lowe, 1836	Noble Beardfish	yes		3	
Scombroptidae					
<i>Scombroptus oculatus</i> (Poey, 1860)	Atlantic Scombroptus	yes			FIMNH
Sparidae					
<i>Calamus calamus</i> (Valenciennes, 1830)	Saucereye Porgy			5	
Squalidae					
<i>Cirrhigaleus asper</i> (Merrett, 1973)	Roughskin Spiny Dogfish	yes			FIMNH
Stomiidae					
<i>Borostomia mononema</i> (Regan & Trewavas, 1929)	Sickle Snaggletooth	yes		8	
Synagropidae					
<i>Synagrops bellus</i> (Goode & Bean, 1896)	Blackmouth Bass	yes		6	
Syngnathidae					
<i>Hippocampus erectus</i> Perry, 1810	Lined Seahorse				NCSM
Synodontidae					
<i>Synodus foetens</i> (Linnaeus, 1766)	Inshore Lizardfish				ANSP
<i>Trachinocephalus myops</i> (Forster, 1801)	Snakefish		S1		
Trachipteridae					
<i>Zu cristatus</i> (Bonelli, 1820)	Scalloped Ribbonfish	yes		8	
Tripterygiidae					
<i>Enneanectes quadra</i> Victor, 2017	Squaretail Triplefin				FIMNH

Notes: Deep – restricted to depths below 40 m. Image Plate – see Suppl. material 1: Plate S1 for voucher images. Literature source – 1 Bunckley-Williams and Williams (2004); 2 Garcia-Sais et al. (2014); 3 Nelson and Appeldoorn (1985); 4 Mantatrust.org; 5 Pittman et al. (2008); 6 Quattrinni et al. (2017); 7 Smith-Vaniz and Jelks (2014) (asterisk indicates a species that was discussed by not included by those authors); 8 Clavijo et al. (1980). Online source - TNHCi (University of Texas at Austin, Biodiversity Center, Ichthyology collection; FIMNH (Florida Museum of Natural History); CF (Biological observations from the Dana Expedition Reports); NOAA (National Oceanographic and Atmospheric Administration); CAS (California Academy of Sciences); MCZ (Museum of Comparative Zoology); NMNH (National Museum of Natural History); NCSM (North Carolina State Museum of Natural Sciences); ANSP (Academy of Natural Sciences of Philadelphia). *Coryphopterus*: Smith-Vaniz et al. (2014) concluded that *C. tortugae*, but not *C. glaucofrenum*, was present at St. Croix. However, CJE and AME photographed both species at St. Croix, illustrated in Suppl. material 1: Plate S1.

that ichthyocide. Two ROV dives of Quattrinni et al. (2017) and four dives (including one to only 50 m depth on the PRP a little to the north of St. Thomas) by the JSL submersible at St. John-Thomas (Nelson and Appeldoorn 1985; Garcia-Sais 2005) yielded 75 species records. Of those 19 were of deep-living species, with 14 (28%) representing sole-source records of the 50 deep-living fishes currently known to occur at St. John-Thomas.

Table 2. Checklist of the fishes of St. John-Thomas islands.

Scientific name	Common name	Image Plate	Literature source	Online source	Uncommon (site code)	Ichthyocide	DNA
Acanthuridae							
<i>Acanthurus chirurgus</i> (Bloch, 1787)	Doctorfish	S2	2,4,8	1		1	
<i>Acanthurus coeruleus</i> Bloch & Schneider, 1801	Blue Tang	S2	2,4,5,8	1		1	YES
<i>Acanthurus tractus</i> Poey, 1860	Northern Ocean Surgeonfish	S2	2,4,5,8	1		1	YES
Achiridae							
<i>Gymnachirus nudus</i> Kaup, 1858	Flabby Sole	S2	2,11	1	SJ5, SJ18, SJ25		YES
Aetobatidae							
<i>Aetobatus narinari</i> (Euphrasen, 1790)	Spotted Eagle Ray	S2	2	1			
Albulidae							
<i>Albula goreensis</i> Valenciennes, 1847	Senegalese Bonefish				NOAA-BOLD		YES
<i>Albula vulpes</i> (Linnaeus, 1758)	Bonefish		2,4	1			YES
Anguillidae							
<i>Anguilla rostrata</i> (Lesueur, 1817)	American Eel		6	1			
Antennariidae							
<i>Antennarius multiocellatus</i> (Valenciennes, 1837)	Longlure Frogfish	S2	2	1		1	
<i>Antennarius paucinadiatus</i> Schultz, 1957	Dwarf Frogfish		2	1			
<i>Histrio histrio</i> (Linnaeus, 1758)	Sargassumfish	S2	12		O22		
Apogonidae							
<i>Apogon aurolineatus</i> (Mowbray, 1927)	Bridle Cardinalfish	S2	2,4	1			YES
<i>Apogon binotatus</i> (Poey, 1867)	Barred Cardinalfish	S2	2,4	1		1	
<i>Apogon lachneri</i> Böhlke, 1959	Whitestar Cardinalfish	S2	2,4	1	SJ2	1	
<i>Apogon maculatus</i> (Poey, 1860)	Flamefish	S2	2,4	1		1	YES
<i>Apogon phenax</i> Böhlke & Randall, 1968	Mimic Cardinalfish	S2	2,11			1	
<i>Apogon planifrons</i> Longley & Hildebrand, 1940	Pale Cardinalfish	S2	2	1		1	
<i>Apogon pseudomaculatus</i> Longley, 1932	Twospot Cardinalfish		2,4	1			
<i>Apogon quadrisquamatus</i> Longley, 1934	Sawcheek Cardinalfish	S2	2,4	1	SJ22, SJ25	1	YES
<i>Apogon robinsi</i> Böhlke & Randall, 1968	Roughlip Cardinalfish		2			-1	
<i>Apogon townsendi</i> (Breder, 1927)	Belted Cardinalfish	S2	2,4	1		1	YES
<i>Astrapogon puncticulatus</i> (Poey, 1867)	Blackfin Cardinalfish	S2	2	1			YES
<i>Astrapogon stellatus</i> (Cope, 1867)	Conchfish	S2	2,4	1	SJ5, SJ13		YES
<i>Paroncheilus affinis</i> (Poey, 1875)	Bigtooth Cardinalfish		2	1			

Scientific name	Common name	Image Plate	Literature source	Online source	Uncommon (site code)	Ichthyocide	DNA
<i>Phaeoptyx conklini</i> (Silvester, 1915)	Freckled Cardinalfish	S2	2	1		1	YES
<i>Phaeoptyx pigmentaria</i> (Poey, 1860)	Dusky Cardinalfish	S2	2	1		1	YES
<i>Phaeoptyx xenus</i> (Böhlke & Randall, 1968)	Sponge Cardinalfish	S2	2	1		1	YES
<i>Zapogon evermanni</i> (Jordan & Snyder, 1904)	Oddscales Cardinalfish	S2			SJ22		YES
Atherinidae							
<i>Atherina harringtonensis</i> Goode, 1877	Reef Silverside		2	1		1	YES
<i>Atherinomorus stipes</i> (Müller & Troschel, 1848)	Hardhead Silverside	S2	2,6	1		1	
Aulostomidae							
<i>Aulostomus maculatus</i> Valenciennes, 1841	Atlantic Trumpetfish	S2	2,4	1		1	
Balistidae							
<i>Balistes capriscus</i> Gmelin, 1789	Gray Triggerfish	S3	2				
<i>Balistes vetula</i> Linnaeus, 1758	Queen Triggerfish	S3	2,4,5,8	1		1	YES
<i>Canthidermis sufflamen</i> (Mitchill, 1815)	Ocean Triggerfish	S3	2	1	SJ33		
<i>Melichthys niger</i> (Bloch, 1786)	Black Durgon	S3	2,4	1	SJ33		
<i>Xanthichthys ringens</i> (Linnaeus, 1758)	Sargassum Triggerfish	S3	2,5	1	SJ33		
Belonidae							
<i>Ablennes hians</i> (Valenciennes, 1846)	Barred Needlefish	S3					
<i>Platybelone argalus argalus</i> (Lesueur, 1821)	Keeltail Needlefish	S3	2	1		1	
<i>Strongylura timucu</i> (Walbaum, 1792)	Timucú		2,6	1			
<i>Tylosurus acus</i> (Lacepède, 1803)	Atlantic Agujón				FIMNH, MCZ		
<i>Tylosurus crocodilus</i> (Péron & Lesueur, 1821)	Houndfish	S3	2	1			
Blenniidae							
<i>Entomacrodus nigricans</i> Gill, 1859	Pearl Blenny	S3	2	1		1	YES
<i>Hyppleurochilus pseudoaequipinnis</i> Bath, 1994	Oyster Blenny	S3	2,11	1			YES
<i>Hyppleurochilus springeri</i> Randall, 1966	Orangespotted Blenny	S3	2	1			
<i>Hypsoblennius invemar</i> Smith-Vaniz & Acero P., 1980	Tessellated Blenny	S3	11	1	ST11		YES
<i>Ophioblennius macclurei</i> (Silvester, 1915)	Redlip Blenny	S3	2,4	1		1	YES
<i>Parablennius marmoratus</i> (Poey, 1876)	Seaweed Blenny	S3	2,4	1		1	YES
<i>Scartella cristata</i> (Linnaeus, 1758)	Molly Miller	S3	2,4	1		1	YES
Bothidae							
<i>Bothus lunatus</i> (Linnaeus, 1758)	Peacock Flounder	S3	2,4	1		1	
<i>Bothus maculiferus</i> (Poey, 1860)	Mottled Flounder	S3			SJ3, SJ5, SJ28		

Scientific name	Common name	Image Plate	Literature source	Online source	Uncommon (site code)	Ichthyocide	DNA
<i>Bothus ocellatus</i> (Agassiz, 1831)	Eyed Flounder	S3	2,4	1			
<i>Bothus robinsi</i> Topp & Hoff, 1972	Twospot Flounder		2,3				
Bythitidae							
<i>Calamopteryx goslinei</i> Böhlke & Cohen, 1966	Longarm Brotula		2				-1
<i>Grammonus claudei</i> (de la Torre y Huerta, 1930)	Reef-cave Brotula		2	1			-1
<i>Petrotyx sanguineus</i> (Meek & Hildebrand, 1928)	Redfin Brotula		2	1			-1
Callionymidae							
<i>Callionymus bairdi</i> Jordan, 1888	Lancer Dragonet	S3	2,4	1			YES
<i>Chalinops pauciradiatus</i> (Gill, 1865)	Spotted Dragonet	S3	2	1	SJ28, SJ3, SJ5		YES
Carangidae							
<i>Alectis ciliaris</i> (Bloch, 1787)	African Pompano	S4	2	1	ST1, SJ13		
<i>Caranx bartholomaei</i> Cuvier, 1833	Yellow Jack	S4	2,4	1			
<i>Caranx crysos</i> (Mitchill, 1815)	Blue Runner	S4	2,4	1			
<i>Caranx hippos</i> (Linnaeus, 1766)	Crevalle Jack	S4			SJ29		
<i>Caranx latus</i> Agassiz, 1831	Horse-eye Jack	S4	2,6	1			
<i>Caranx lugubris</i> Poey, 1860	Black Jack	S4	2,4,5,8	1	SJ33		
<i>Caranx ruber</i> (Bloch, 1793)	Bar Jack	S4	2,4,8	1			1
<i>Chloroscombrus chrysurus</i> (Linnaeus, 1766)	Atlantic Bumper		2				
<i>Decapterus macarellus</i> (Cuviers, 1833)	Mackerel Scad	S4	2	1			
<i>Decapterus punctatus</i> (Cuvier, 1829)	Round Scad	S4	2	1			
<i>Decapterus tabl</i> Berry, 1968	Redtail Scad	S4			SJ11		
<i>Elagatis bipinnulata</i> (Quoy & Gaimard, 1825)	Rainbow Runner	S4	2	1	SJ33		
<i>Oligoplites saurus saurus</i> (Bloch & Schneider, 1801)	Leatherjack		2	1			
<i>Selar crumenophthalmus</i> (Bloch, 1793)	Bigeye Scad	S4	2	1	SJ13		
<i>Selene brownii</i> (Cuvier, 1816)	Caribbean Moonfish		2	1			
<i>Selene vomer</i> (Linnaeus, 1758)	Lookdown				FIMNH		
<i>Seriola dumerili</i> (Risso, 1810)	Greater Amberjack		2,5				
<i>Seriola rivoliana</i> Valenciennes, 1833	Almaco Jack	S4	2	1	SJ16, SJ23		
<i>Trachinotus falcatus</i> (Linnaeus, 1758)	Permit	S4	2	1	SJ22, SJ23		
<i>Trachinotus goodei</i> Jordan & Evermann, 1896	Palometa	S4	2,4	1	SJ23, SJ15		
Carcharhinidae							
<i>Carcharhinus acronotus</i> (Poey, 1860)	Blacknose Shark	S4	1,2,10	1	SJ35, SJ27, ST7		
<i>Carcharhinus falciformis</i> (Müller & Henle, 1839)	Silky Shark	S4			1, O1		
<i>Carcharhinus galapagensis</i> (Snodgrass & Heller, 1905)	Galapagos Shark		2				
<i>Carcharhinus limbatus</i> (Müller & Henle, 1839)	Blacktip Shark		1,2	1			

Scientific name	Common name	Image Plate	Literature source	Online source	Uncommon (site code)	Ichthyocide	DNA
<i>Carcharhinus longimanus</i> (Poey, 1861)	Oceanic Whitetip Shark			NMNH			
<i>Carcharhinus perezii</i> (Poey, 1876)	Reef Shark	S4	2,10	1	SJ13		
<i>Carcharhinus plumbeus</i> (Nardo, 1827)	Sandbar Shark			ANSP			
<i>Negaprion brevirostris</i> (Poey, 1868)	Lemon Shark	S4	1,2,6,10	1	SJ12, O2		
<i>Rhizoprionodon porosus</i> (Poey, 1861)	Caribbean Sharpnose Shark		1,2,10	1			
Centrophoridae							
<i>Centrophorus uyato</i> (Rafinesque, 1810)	Little Gulper Shark			CAS			
Centropomidae							
<i>Centropomus ensiferus</i> Poey, 1860	Swordspine Snook		6	1			
<i>Centropomus undecimalis</i> (Bloch, 1792)	Common Snook	S4	2,6	1			
Chaenopsidae							
<i>Acanthemblemaria aspera</i> (Longley, 1927)	Roughhead Blenny	S5	2	1	ST3		YES
<i>Acanthemblemaria maria</i> Böhlke, 1961	Secretary Blenny	S5	4	1			YES
<i>Acanthemblemaria spinosa</i> Metzelaar, 1919	Spinyhead Blenny	S5	2,4	1		1	YES
<i>Chaenopsis limbaughii</i> Robins & Randall, 1965	Yellowface Pikeblenny	S5	2,4	1			YES
<i>Chaenopsis ocellata</i> Poey, 1865	Bluethroat Pikeblenny		2,4	1			
<i>Coralliozetus cardonae</i> Evermann & Marsh, 1899	Twinhorn Blenny	S5	11	1			YES
<i>Emblemaria pandionis</i> Evermann & Marsh, 1900	Sailfin Blenny	S5	2,4	1			YES
<i>Emblemaria vitta</i> Williams, 2002	Ribbon Blenny	S5	2,3	1	ST6	-1	YES
<i>Emblemariaopsis bahamensis</i> Stephens, 1961	Blackhead Blenny	S5		1			YES
<i>Emblemariaopsis carib</i> Victor, 2010	Carib Blenny		2	1		-1	YES
<i>Emblemariaopsis leptocirris</i> Stephens, 1970	Fine-cirrus Blenny	S5	2,11			-1	YES
<i>Emblemariaopsis ruetzleri</i> Tyler & Tyler, 1997	Ruetzler's Blenny			BOLD, NMNH			YES
<i>Lucayablennius zingaro</i> (Böhlke, 1957)	Arrow Blenny	S5			SJ18, SJ19		
Chaetodontidae							
<i>Chaetodon capistratus</i> Linnaeus, 1758	Foureye Butterflyfish	S5	2,4,5,8	1		1	YES
<i>Chaetodon ocellatus</i> Bloch, 1787	Spotfin Butterflyfish	S5	2,4	1			
<i>Chaetodon sedentarius</i> Poey, 1860	Reef Butterflyfish	S5	2,4,5,8	1			
<i>Chaetodon striatus</i> Linnaeus, 1758	Banded Butterflyfish	S5	2,4	1		1	
<i>Prognathodes aculeatus</i> (Poey, 1860)	Longsnout Butterflyfish	S5	2,5,8	1			
<i>Prognathodes guyanensis</i> (Durand, 1960)	Guyana Butterflyfish		2,5,8,11				

Scientific name	Common name	Image Plate	Literature source	Online source	Uncommon (site code)	Ichthyocide	DNA
Chaunacidae							
<i>Chaunax pxtus</i> Fowler, 1946	Uniform Gaper		5				
<i>Chaunax suttkusi</i> Caruso, 1989	Pale-cavity Gaper			CAS			
Chlopsidae							
<i>Chlorhinus suensonii</i> Lütken, 1852	Seagrass Eel		2	1			
<i>Kaupichthys hyoproroides</i> (Strömman, 1896)	False Moray		2	1		-1	
<i>Kaupichthys nuchalis</i> Böhlke, 1967	Collared Eel		2,11	1			
Chlorophthalmidae							
<i>Parasudis truculenta</i> (Goode & Bean, 1896)	Longnose Greeneye		5				
Cichlidae							
<i>Oreochromis mossambicus</i> (Peters, 1852)	Mozambique Tilapia		6	1			
Cirrhitidae							
<i>Amblycirrhitus pinos</i> (Mowbray, 1927)	Redspotted Hawkfish	S5	2,4	1		1	
Clupeidae							
<i>Harengula clupeola</i> (Cuvier, 1829)	False Pilchard		2	1			YES
<i>Harengula humeralis</i> (Cuvier, 1829)	Redear Sardine	S5	2	1	SJ28, SJ13		YES
<i>Harengula jaguana</i> Poey, 1865	Scaled Sardine			FIMNH			
<i>Opisthonema oglinum</i> (Lesueur, 1818)	Atlantic Thread Herring			FIMNH			YES
<i>Sardinella aurita</i> Valenciennes, 1847	Spanish Sardine			FIMNH			
Congridae							
<i>Ariosoma balearicum</i> (Delaroche, 1809)	Bandtooth Conger		2				
<i>Conger triporiceps</i> Kanazawa, 1958	Manytooth Conger		4	1			
<i>Heteroconger longissimus</i> Günther, 1870	Brown Garden Eel	S5	2,4	1			
<i>Xenomystax bidentatus</i> (Reid, 1940)	Rabbit Conger			NMNH			
Coryphaenidae							
<i>Coryphaena equiselis</i> Linnaeus, 1758	Pompano Dolphinfish			ROM			
<i>Coryphaena hippurus</i> Linnaeus, 1758	Dolphinfish	S5	2	1			
Cynoglossidae							
<i>Symphurus anawak</i> Robins & Randall, 1965	Caribbean Tonguefish		2	1		1	
Dactylopteridae							
<i>Dactylopterus volitans</i> (Linnaeus, 1758)	Flying Gurnard	S5	4	1			YES
Dactyloscopidae							
<i>Dactyloscopus comptus</i> Dawson, 1982	Ornamented Stargazer		2,11	1			
<i>Dactyloscopus crossotus</i> Starks, 1913	Bigeye Stargazer			AMNH			
<i>Dactyloscopus poeyi</i> Gill, 1861	Shortchin Stargazer			FIMNH			
<i>Dactyloscopus tridigitatus</i> Gill, 1859	Sand Stargazer	S5	2	1		1	
<i>Gillellus greylae</i> Kanazawa, 1952	Arrow Stargazer		2			-1	
<i>Gillellus uranidea</i> Böhlke, 1968	Warteye Stargazer		2			-1	YES

Scientific name	Common name	Image Plate	Literature source	Online source	Uncommon (site code)	Ichthyocide	DNA
<i>Platygillellus rubrocinctus</i> (Longley, 1934)	Saddle Stargazer						
Dasyatidae							
<i>Hypanus americanus</i> (Hildebrand & Schroeder, 1928)	Southern Stingray	S5	1,2,4,10	1			
Diodontidae							
<i>Chilomycterus antennatus</i> (Cuvier, 1816)	Bridled Burrfish	S5	2,4	1	SJ18		
<i>Chilomycterus antillarum</i> Jordan & Rutter, 1897	Web Burrfish		2	1			
<i>Diodon holocanthus</i> Linnaeus, 1758	Balloonfish	S5	2,4	1	SJ11, SJ13	-1	
<i>Diodon hystrix</i> Linnaeus, 1758	Porcupinefish	S5	2,4	1		1	
Echeneidae							
<i>Echeneis naucrates</i> Linnaeus, 1758	Sharksucker	S6	2,4	1	SJ19, SJ23		YES
<i>Echeneis neucratoides</i> Zuiew, 1789	Whitefin Sharksucker	S6		1			
<i>Remora remora</i> (Linnaeus, 1758)	The Remora	S6		1	O3		YES
Eleotridae							
<i>Dormitorator maculatus</i> (Bloch, 1792)	Fat Sleeper	S6	6	1	SJ10		
<i>Eleotris perniger</i> (Cope, 1871)	Smallscaled Spinycheek Sleeper	S6	6	1	SJ10		
<i>Erotelis smaragdus</i> (Valenciennes, 1837)	Emerald Sleeper		6	1			
<i>Gobiomorus dormitor</i> Lacepède, 1800	Bigmouth Sleeper	S6		1			
Elopidae							
<i>Elops smithi</i> McBride, Rocha, Ruiz-Carus & Bowen, 2010	Malacho		2,6				YES
Engraulidae							
<i>Anchoa lyolepis</i> (Evermann & Marsh, 1900)	Dusky Anchovy		2	1			YES
Ephippidae							
<i>Chaetodipterus faber</i> (Broussonet, 1782)	Atlantic Spadefish	S6	2,4	1	SJ18, ST2		
Epigonidae							
<i>Epigonus pandionis</i> (Goode & Bean, 1881)	Caudal-ring Deepwater Cardinalfish			CAS			
Exocoetidae							
<i>Cheilopogon exsiliens</i> (Linnaeus, 1771)	Bandwing Flyingfish		2	1			
<i>Exocoetus obtusirostris</i> Günther, 1866	Oceanic Two-wing Flyingfish			MCZ			
<i>Hirundichthys affinis</i> (Günther, 1866)	Fourwing Flyingfish		2				
<i>Hirundichthys speculiger</i> (Valenciennes, 1847)	Mirrorwing Flyingfish		2	1			
<i>Prognichthys occidentalis</i> Parin, 1999	Bluntnose Flyingfish	S6					YES
Fistulariidae							
<i>Fistularia tabacaria</i> Linnaeus, 1758	Bluespotted Cornetfish	S6	2		O4		

Scientific name	Common name	Image Plate	Literature source	Online source	Uncommon (site code)	Ichthyocide	DNA
Galeocerdonidae							
<i>Galeocerdo cuvier</i> (Peron & Lesueur, 1822)	Tiger Shark		10				
Gempylidae							
<i>Epinnula magistralis</i> Poey, 1854	Domine		5	1			
Gerreidae							
<i>Eucinostomus argenteus</i> Baird & Girard, 1855	Spotfin Mojarra		2	1			YES
<i>Eucinostomus gula</i> (Quoy & Gaimard, 1824)	Silver Jenny	S6	4	1	SJ18, SJ13, SJ3		
<i>Eucinostomus harengulus</i> Goode & Bean, 1879	Tidewater Mojarra	S6		1	SJ28		
<i>Eucinostomus havana</i> (Nichols, 1912)	Bigeye Mojarra			FIMNH			
<i>Eucinostomus jonesii</i> (Günther, 1879)	Slender Mojarra	S6	4,6		SJ28		
<i>Eucinostomus lefroyi</i> (Goode, 1874)	Mottled Mojarra	S6			SJ28, SJ21		
<i>Eucinostomus melanopterus</i> (Bleeker, 1863)	Flagfin Mojarra	S6	4	1	SJ28		
<i>Eugerres brasilianus</i> (Cuvier, 1830)	Brazilian Mojarra		6,11	1			
<i>Gerres cinereus</i> (Walbaum, 1792)	Yellowfin Mojarra	S6	2,4,6	1			
Ginglymostomatidae							
<i>Ginglymostoma cirratum</i> (Bonnaterre, 1788)	Nurse Shark	S6	1,2,4,10	1			
Gobiesocidae							
<i>Acyrtops amplicirrus</i> Briggs, 1955	Flarenostril Clingfish		2				
<i>Acyrtops beryllinus</i> (Hildebrand & Ginsburg, 1927)	Emerald Clingfish		2	1			
<i>Acyrtus artius</i> Briggs, 1955	Papillate Clingfish		2				
<i>Acyrtus rubiginosus</i> (Poey, 1868)	Red Clingfish	S6		1	SJ23, SJ13, SJ5		YES
<i>Arcos nudus</i> (Linnaeus, 1758)	Padded Clingfish	S6	2	1	SJ23	1	
<i>Gobiesox nigripinnis</i> (Peters, 1859)	Dark-finned Clingfish	S6	2	1	SJ29		
<i>Gobiesox punctulatus</i> (Poey, 1876)	Stippled Clingfish	S6	2	1		1	YES
<i>Tomicodon cryptus</i> Williams & Tyler, 2003	Cryptic Clingfish	S6					YES
<i>Tomicodon fasciatus</i> (Peters, 1859)	Barred Clingfish		2	1		1	
<i>Tomicodon leurodiscus</i> Williams & Tyler, 2003	Smooth-suckered Clingfish		11	1			
<i>Tomicodon reitzae</i> Briggs, 2001	Accidental Clingfish	S6					YES
<i>Tomicodon rhabdodus</i> Smith-Vaniz, 1969	Antillean Clingfish	S6			O24		
<i>Tomicodon rupestris</i> (Poey, 1860)	Barred Clingfish		11	1			
Gobiidae							
<i>Awaous banana</i> (Valenciennes, 1837)	River Goby	S7		1	SJ10		
<i>Barbulifer ceuthoecus</i> (Jordan & Gilbert, 1884)	Bearded Goby		2	1			YES
<i>Bathygobius antillensis</i> Tornabene, Baldwin & Pezold, 2010	Antilles Frillfin	S7			SJ36		YES

Scientific name	Common name	Image Plate	Literature source	Online source	Uncommon (site code)	Ichthyocide	DNA
<i>Bathygobius curacao</i> (Metzelaar, 1919)	Notchtongue Goby		11	1			YES
<i>Bathygobius lacertus</i> (Poey, 1860)	Checkerboard Frillfin			FIMNH			YES
<i>Bathygobius mystacium</i> Ginsburg, 1947	Island Frillfin	S7			SJ21, SJ19		YES
<i>Bathygobius soporator</i> (Valenciennes, 1837)	Frillfin Goby		2,6,11	1			YES
<i>Bollmannia boqueronensis</i> Evermann & Marsh, 1899	White-eye Goby	S7	4		SJ19		YES
<i>Cerdale floridana</i> Longley, 1934	Pugjaw Wormfish	S7	2	1	SJ23	1	
<i>Coryphopterus alloides</i> Böhlke & Robins, 1960	Barfin Goby		2	1		-1	
<i>Coryphopterus dicrus</i> Böhlke & Robins, 1960	Colon Goby	S7	2,4	1		1	YES
<i>Coryphopterus eidolon</i> Böhlke & Robins, 1960	Pallid Goby	S7	2,4	1		1	YES
<i>Coryphopterus glaucofraenum</i> Gill, 1863	Bridled Goby	S7	2,4	1		1	YES
<i>Coryphopterus hyalinus</i> Böhlke & Robins, 1962	Glass Goby	S7	2	1		-1	YES
<i>Coryphopterus kuna</i> Victor, 2007	Kuna Goby	S7			SJ5, SJ12		
<i>Coryphopterus lipernes</i> Böhlke & Robins, 1962	Peppermint Goby	S7	2,4	1	ST6		YES
<i>Coryphopterus personatus</i> (Jordan & Thompson, 1905)	Masked Goby	S7	2	1		1	YES
<i>Coryphopterus thrix</i> Böhlke & Robins, 1960	Bartail Goby		2	1		1	YES
<i>Coryphopterus tortugae</i> (Jordan, 1904)	Sand Goby	S7		1			YES
<i>Coryphopterus venezuelae</i> Cervigón, 1966	Venezuela Goby	S7		1			YES
<i>Ctenogobius boleosoma</i> (Jordan & Gilbert, 1882)	Darter Goby	S7	6	1	SJ28		YES
<i>Ctenogobius saepepallens</i> (Gilbert & Randall, 1968)	Dash Goby	S7	2,4	1			YES
<i>Ctenogobius smaragdus</i> (Valenciennes, 1837)	Emerald Goby		11				
<i>Ctenogobius stigmaturus</i> (Goode & Bean, 1882)	Spottail Goby	S7			SJ28		YES
<i>Elacatinus chancei</i> (Beebe & Hollister, 1933)	Shortstripe Goby	S7	2,4	1			YES
<i>Elacatinus evelynae</i> (Böhlke & Robins, 1968)	Sharknose Goby	S7	2,4	1		1	YES
<i>Elacatinus prochilos</i> (Böhlke & Robins, 1968)	Broadstripe Goby	S7		1			YES
<i>Evorthodus lyricus</i> (Girard, 1858)	Lyre Goby		6	1			
<i>Ginsburgellus novemlineatus</i> (Fowler, 1950)	Nineline Goby	S7		1	SJ23, SJ5		YES
<i>Gnatholepis thompsoni</i> Jordan, 1904	Goldspot Goby	S7	2,4	1		1	YES
<i>Gobionellus oceanicus</i> (Pallas, 1770)	Highfin Goby	S7		1	SJ28		
<i>Gobiosoma grosvenori</i> (Robins, 1964)	Rockcut Goby		4	1			

Scientific name	Common name	Image Plate	Literature source	Online source	Uncommon (site code)	Ichthyocide	DNA
<i>Lophogobius cyprinoides</i> (Pallas, 1770)	Crested Goby	S8	6	1	SJ28		
<i>Lythrypnus elason</i> Böhlke & Robins, 1960	Dwarf Goby	S8	2	AMNH	ST5	1	YES
<i>Lythrypnus minimus</i> Garzón-Ferreira & Acero P, 1988	Pygmy Goby	S8					YES
<i>Lythrypnus nesiotus</i> Böhlke & Robins, 1960	Island Goby	S8	2	1	SJ34	1	YES
<i>Lythrypnus spilus</i> Böhlke & Robins, 1960	Bluegold Goby	S8			ST3		
<i>Microgobius carri</i> Fowler, 1945	Seminole Goby	S8	2,4	1	SJ19, SJ25	1	YES
<i>Microgobius signatus</i> Poey, 1876	Signal Goby	S8		1	SJ28, SJ22, SJ3		YES
<i>Nes longus</i> (Nichols, 1914)	Orangespotted Goby	S8	4	1			YES
<i>Oxyurichthys stigmaliobius</i> (Mead & Böhlke, 1958)	Spotfin Goby	S8	4	1	SJ5, SJ19, SJ28		
<i>Palatogobius paradoxus</i> Gilbert, 1971	Mauve Goby		2,11	1			
<i>Priolepis hipoliti</i> (Metzelaar, 1922)	Rusty Goby	S8	2,4	1		1	
<i>Pilotris celsa</i> Böhlke, 1963	Highspine Goby		2	1			
<i>Preteleotris helenae</i> (Randall, 1968)	Hovering Dartfish	S8	2,4	1			
<i>Risor ruber</i> (Rosén, 1911)	Tusked Goby	S8	2	1		1	YES
<i>Sicydium plumieri</i> (Bloch, 1786)	Sirajo Goby	S8	6	1	SJ10		YES
<i>Sicydium punctatum</i> Perugia, 1896	Spotted Algae-eating Goby	S8		1	SJ10		YES
<i>Tigriogobius dilepis</i> (Robins & Böhlke, 1964)	Orangesided Goby		4	1			
<i>Tigriogobius multifasciatus</i> (Steindachner, 1876)	Greenbanded Goby	S8	2	1			YES
<i>Tigriogobius pallens</i> (Ginsburg, 1939)	Semiscaled Goby	S8			SJ23		
<i>Tigriogobius saucrus</i> (Robins, 1960)	Leopard Goby	S8	2	1		1	YES
Grammatidae							
<i>Gramma linki</i> Starck & Colin, 1978	Yellowcheek Basslet		2,5,8			1	
<i>Gramma loreto</i> Poey, 1868	Fairy Basslet	S8	2,4	1			YES
Haemulidae							
<i>Anisotremus surinamensis</i> (Bloch, 1791)	Black Margate	S9	2,4,5,8	1		1	YES
<i>Anisotremus virginicus</i> (Linnaeus, 1758)	Porkfish	S9	2,5,6,8	1			YES
<i>Brachygenys chrysargyrea</i> (Günther, 1859)	Smallmouth Grunt	S9	2,4	1		1	YES
<i>Emmelichthys atlanticus</i> Schultz, 1945	Bonnetmouth	S9	2		ST8		
<i>Haemulon album</i> Cuvier, 1830	Margate	S9	2,4	1	SJ7		
<i>Haemulon aurolineatum</i> Cuvier, 1830	Tomtate	S9	2,4,5,8	1		1	YES
<i>Haemulon carbonarium</i> Poey, 1860	Caesar Grunt	S9	2,4	1		1	
<i>Haemulon flavolineatum</i> (Desmarest, 1823)	French Grunt	S9	2,4,5,8	1		1	YES
<i>Haemulon macrostoma</i> Günther, 1859	Spanish Grunt	S9	2,4	1		1	
<i>Haemulon melanurum</i> (Linnaeus, 1758)	Cottonwick	S9	2	1	O5		YES

Scientific name	Common name	Image Plate	Literature source	Online source	Uncommon (site code)	Ichthyocide	DNA
<i>Haemulon parra</i> (Desmarest, 1823)	Sailors Choice	S9	2,4	1	SJ1, SJ21		YES
<i>Haemulon plumieri</i> (Lacepède, 1801)	White Grunt	S9	2,4	1		1	YES
<i>Haemulon sciurus</i> (Shaw, 1803)	Bluestriped Grunt	S9	2,4,5	1		1	YES
<i>Haemulon striatum</i> (Linnaeus, 1758)	Striped Grunt		2,4	1			YES
<i>Haemulon vittatum</i> (Poey, 1860)	Boga	S9	2,4	1	ST6, ST8, ST2	1	
Hemiramphidae							
<i>Euleptorhamphus velox</i> Poey, 1868	Flying Halfbeak			MCZ			
<i>Hemiramphus balao</i> Lesueur, 1821	Balao			MCZ			
<i>Hemiramphus brasiliensis</i> (Linnaeus, 1758)	Ballyhoo	S9	2	1			
<i>Hyporhamphus unifasciatus</i> (Ranzani, 1841)	Atlantic Silverstripe Halfbeak		2	1			
Hexanchidae							
<i>Heptranchias perlo</i> (Bonnaterra, 1788)	Sharpnose Sevengill Shark			FIMNH			
<i>Hexanchus vitulus</i> Springer & Waller, 1969	Atlantic Sixgill Shark			FIMNH			
Holocentridae							
<i>Holocentrus adscensionis</i> (Osbeck, 1765)	Squirrelfish	S9	2,4,5,8	1		1	YES
<i>Holocentrus rufus</i> (Walbaum, 1792)	Longspine Squirrelfish	S9	2,4,5,8	1		1	
<i>Myripristis jacobus</i> Cuvier, 1829	Blackbar Soldierfish	S9	2,4,5,8	1		1	
<i>Neoniphon coruscum</i> (Poey, 1860)	Reef Squirrelfish	S9	2,4,5,8	1		1	YES
<i>Neoniphon marianus</i> (Cuvier, 1829)	Longjaw Squirrelfish	S9	2,4,5,8	1		1	
<i>Neoniphon vexillarium</i> (Poey, 1860)	Dusky Squirrelfish	S9	2,4	1		1	
<i>Ostichthys trachypoma</i> (Günther, 1859)	Bigeye Soldierfish		2,5,8	1			
<i>Plectrypops retrospinis</i> (Guichenot, 1853)	Cardinal Soldierfish	S9	2,5,8	1	SJ9, SJ22, ST3	1	
<i>Sargocentron bullisi</i> (Woods, 1955)	Deepwater Squirrelfish		2,11	1			
Ipnopidae							
<i>Bathypterois bigelowi</i> Mead, 1958	Spottail Tripodfish			CAS			
<i>Bathypterois phenax</i> Parr, 1928	Blackfin Spiderfish		9				
<i>Bathypterois viridensis</i> (Roule, 1916)	Twobanded Tripodfish		9				
<i>Ipnopis murrayi</i> Günther, 1878	Grیدهye Fish		9				
Istiophoridae							
<i>Istiophorus platypterus</i> (Shaw, 1792)	Sailfish	S9	2				
<i>Kajikia albigata</i> (Poey, 1860)	White Marlin	S9	2				
<i>Makaira nigricans</i> Lacepède, 1802	Blue Marlin		2				YES
<i>Tetrapturus pfluegeri</i> Robins & de Sylva, 1963	Longbill Spearfish		2				

Scientific name	Common name	Image Plate	Literature source	Online source	Uncommon (site code)	Ichthyocide	DNA
Kyphosidae							
<i>Kyphosus cinerascens</i> (Forsskål, 1775)	Topsail Seachub	S10					
<i>Kyphosus sectatrix</i> (Linnaeus, 1758)	Bermuda Chub	S10	2,4	1			
<i>Kyphosus vaigiensis</i> (Quoy & Gaimard, 1825)	Yellow Chub	S10		1			
Labridae							
Labrinae							
<i>Bodianus rufus</i> (Linnaeus, 1758)	Spanish Hogfish	S10	2,4,5,8	1			YES
<i>Clepticus parvae</i> (Bloch & Schneider, 1801)	Creole Wrasse	S10	2,4,5,8	1			YES
<i>Decodon puellaris</i> (Poey, 1860)	Red Hogfish		2	1			
<i>Doratonotus megalepis</i> Günther, 1862	Dwarf Wrasse		2	1			
<i>Halichoeres bivittatus</i> (Bloch, 1791)	Slippery Dick	S10	2,4	1		1	YES
<i>Halichoeres caudalis</i> (Poey, 1860)	Painted Wrasse			NOAA			
<i>Halichoeres cyanocephalus</i> (Bloch, 1791)	Yellowcheek Wrasse		2	1			
<i>Halichoeres garnoti</i> (Valenciennes, 1839)	Yellowhead Wrasse	S10	2,4	1		1	YES
<i>Halichoeres maculipinna</i> (Müller & Troschel, 1848)	Clown Wrasse	S10	2,4	1		1	
<i>Halichoeres pictus</i> (Poey, 1860)	Rainbow Wrasse	S10	2,4	1		1	
<i>Halichoeres poeyi</i> (Steindachner, 1867)	Blackear Wrasse	S10	2,4	1			
<i>Halichoeres radiatus</i> (Linnaeus, 1758)	Puddingwife	S10	2,4	1		1	YES
<i>Lachnolaimus maximus</i> (Walbaum, 1792)	Hogfish	S10	2,4,5,8	1			
<i>Thalassoma bifasciatum</i> (Bloch, 1791)	Bluehead	S10	2,4	1		1	
<i>Xyrichtys martinicensis</i> Valenciennes, 1840	Rosy Razorfish	S10	2,4	1			
<i>Xyrichtys novacula</i> (Linnaeus, 1758)	Pearly Razorfish	S10	2,4	1			YES
<i>Xyrichtys splendens</i> Castelnau, 1855	Green Razorfish	S10	2,4	1			
Scarinae							
<i>Cryptotomus roseus</i> Cope, 1871	Bluelip Parrotfish	S10	2,4	1			YES
<i>Scarus coelestinus</i> Valenciennes, 1840	Midnight Parrotfish	S10	2	1	O6	1	
<i>Scarus coeruleus</i> (Edwards, 1771)	Blue Parrotfish		2,4	1		1	
<i>Scarus guacamaia</i> Cuvier, 1829	Rainbow Parrotfish	S10	2,4	1	SJ28, SJ33, O2		
<i>Scarus iseri</i> (Bloch, 1789)	Striped Parrotfish	S10	2,4	1		1	YES
<i>Scarus taeniopterus</i> Lesson, 1829	Princess Parrotfish	S10	2,4,5,8	1		1	YES
<i>Scarus vetula</i> Bloch & Schneider, 1801	Queen Parrotfish	S10	2,4	1		1	YES
<i>Sparisoma atomarium</i> (Poey, 1861)	Greenblotch Parrotfish	S11	2,4	1			
<i>Sparisoma aurofrenatum</i> (Valenciennes, 1840)	Redband Parrotfish	S11	2,4,5,8	1		1	YES
<i>Sparisoma chrysopterygum</i> (Bloch & Schneider, 1801)	Redtail Parrotfish	S11	2,4	1		1	YES
<i>Sparisoma radians</i> (Valenciennes, 1840)	Bucktooth Parrotfish	S11	2,4	1		1	YES
<i>Sparisoma rubripinne</i> (Valenciennes, 1840)	Yellowtail Parrotfish	S11	2,4	1		1	YES

Scientific name	Common name	Image Plate	Literature source	Online source	Uncommon (site code)	Ichthyocide	DNA
<i>Sparisoma viride</i> (Bonnaterre, 1788)	Stoplight Parrotfish	S11	2,4,5,8	1		1	YES
Labrisomidae							
<i>Brockius albigenys</i> Beebe & Tee-Van, 1928	Whitecheek Blenny		DNA		Berry Bay, St. John		YES
<i>Brockius nigricinctus</i> (Howell Rivero, 1936)	Spotcheek Blenny	S11		1	SJ21		YES
<i>Gobioclinus bucciferus</i> (Poey, 1868)	Puffcheek Blenny	S11	2	1			YES
<i>Gobioclinus filamentosus</i> (Springer, 1960)	Quillfin Blenny	S11	3,11	1	O7		YES
<i>Gobioclinus gobio</i> (Valenciennes, 1836)	Palehead Blenny	S11	2	1		1	YES
<i>Gobioclinus guppyi</i> (Norman, 1922)	Mimic Blenny	S11	2	1		-1	YES
<i>Gobioclinus bairdianus</i> (Beebe & Tee-Van, 1928)	Longfin Blenny	S11	2	1	SJ12	1	YES
<i>Labrisomus cricota</i> Sazima, Gasparini & Moura, 2002	Mock Blenny	S11			SJ10		
<i>Labrisomus nuchipinnis</i> (Quoy & Gaimard, 1824)	Hairy Blenny	S11	2,4	1		1	YES
<i>Malacoctenus aurolineatus</i> Smith, 1957	Goldline Blenny	S11	2,4	1		1	YES
<i>Malacoctenus boehlkei</i> Springer, 1959	Diamond Blenny	S11	2,4	1		1	YES
<i>Malacoctenus erdmani</i> Smith, 1957	Imitator Blenny	S11			SJ23		YES
<i>Malacoctenus gilli</i> (Steindachner, 1867)	Dusky Blenny	S11	2,4	1			YES
<i>Malacoctenus macropus</i> (Poey, 1868)	Rosy Blenny	S11	2,4	1			YES
<i>Malacoctenus triangulatus</i> Springer, 1959	Saddled Blenny	S11	2,4	1		1	YES
<i>Malacoctenus versicolor</i> (Poey, 1876)	Barfin Blenny	S11	2,4	1	SJ23, SJ12		YES
<i>Nemaclinus atelestos</i> Böhlke & Springer, 1975	Threadfin Blenny		2,11	1			
<i>Paraclinus barbatus</i> Springer, 1955	Goatee Blenny		2,11				
<i>Paraclinus cingulatus</i> (Evermann & Marsh, 1899)	Coral Blenny		2				
<i>Paraclinus fasciatus</i> (Steindachner, 1876)	Banded Blenny	S11	2		SJ12		
<i>Paraclinus nigripinnis</i> (Steindachner, 1867)	Blackfin Blenny	S11	2	1	SJ12		YES
<i>Starksia culebrae</i> (Evermann & Marsh, 1899)	Culebra Blenny	S11	2	1	ST2, SJ13		YES
<i>Starksia hassi</i> Klausewitz, 1958	Ringed Blenny	S11	2,11	1	SJ24	1	
<i>Starksia lepicoelia</i> Böhlke & Springer, 1961	Blackcheek Blenny		2	1		1	
<i>Starksia nanodes</i> Böhlke & Springer, 1961	Dwarf Blenny		2	1			
<i>Starksia williamsi</i> Baldwin & Castillo, 2011	Williams's Blenny	S11			SJ2, SJ13		YES
<i>Stathmonotus gymnodermis</i> Springer, 1955	Naked Blenny		2	1			
<i>Stathmonotus stabli</i> (Evermann & Marsh, 1899)	Southern Eelgrass Blenny		2	1			

Scientific name	Common name	Image Plate	Literature source	Online source	Uncommon (site code)	Ichthyocide	DNA
Latilidae							
<i>Caulolatilus cyanops</i> Poey, 1866	Blackline Tilefish		2				
Lobotidae							
<i>Lobotes surinamensis</i> (Bloch, 1790)	Atlantic Tripletail	S11	2	1	O18		
Lutjanidae							
<i>Apsilus dentatus</i> Guichenot, 1853	Black Snapper		2				
<i>Etelis oculatus</i> (Valenciennes, 1828)	Queen Snapper	S12	2,5,8				YES
<i>Lutjanus analis</i> (Cuvier, 1828)	Mutton Snapper	S12	2,4,5,8	1			YES
<i>Lutjanus apodus</i> (Walbaum, 1792)	Schoolmaster	S12	2,4,5,6,8	1		1	YES
<i>Lutjanus buccanella</i> (Cuvier, 1828)	Blackfin Snapper	S12	2,5,8	1			YES
<i>Lutjanus cyanopterus</i> (Cuvier, 1828)	Cubera Snapper	S12	2,4	1			YES
<i>Lutjanus griseus</i> (Linnaeus, 1758)	Gray Snapper	S12	2,4,6	1		1	
<i>Lutjanus jocu</i> (Bloch & Schneider, 1801)	Dog Snapper	S12	2,4,5,8	1			YES
<i>Lutjanus mahogoni</i> (Cuvier, 1828)	Mahogany Snapper	S12	2,4	1		1	YES
<i>Lutjanus purpureus</i> (Poey, 1866)	Caribbean Red Snapper		2	1			
<i>Lutjanus synagris</i> (Linnaeus, 1758)	Lane Snapper	S12	2,4	1			YES
<i>Lutjanus vivanus</i> (Cuvier, 1828)	Silk Snapper	S12	2,5,8	1			YES
<i>Ocyurus chrysurus</i> (Bloch, 1791)	Yellowtail Snapper	S12	2,4	1		1	YES
<i>Pristipomoides macrophthalmus</i> (Müller & Troschel, 1848)	Cardinal Snapper		2				
<i>Rhomboplites aurorubens</i> (Cuvier, 1829)	Vermilion Snapper	S12	2		SJ20		
Malacanthidae							
<i>Malacanthus plumieri</i> (Bloch, 1786)	Sand Tilefish	S12	2,4,5,8	1		1	
Megalopidae							
<i>Megalops atlanticus</i> Valenciennes, 1847	Tarpon	S12	2,6	1			
Mobulidae							
<i>Mobula birostris</i> (Walbaum, 1792)	Giant Manta	S12	2				
<i>Mobula cf. birostris</i>	Caribbean Manta	S12				SJ12	
Monacanthidae							
<i>Aluterus monoceros</i> (Linnaeus, 1758)	Unicorn Filefish	S12				O23	
<i>Aluterus schoepfii</i> (Walbaum, 1792)	Orange Filefish	S12		1	SJ34		
<i>Aluterus scriptus</i> (Osbeck, 1765)	Scrawled Filefish	S12	4	1			
<i>Cantherbines macrocerus</i> (Hollard, 1853)	Whitespotted Filefish	S12	2	1			YES
<i>Cantherbines pullus</i> (Ranzani, 1842)	Orangespotted Filefish	S12	2,4	1		1	
<i>Monacanthus ciliatus</i> (Mitchill, 1818)	Fringed Filefish	S12	2,4	1			YES
<i>Monacanthus tuckeri</i> Bean, 1906	Slender Filefish	S12	2,4	1			
<i>Stephanolepis hispidus</i> (Linnaeus, 1766)	Planehead Filefish				FIMNH		
<i>Stephanolepis setifer</i> (Bennett, 1831)	Pygmy Filefish		2				
Moringuidae							
<i>Moringua edwardsi</i> (Jordan & Bollman, 1889)	Spaghetti Eel		2	1			-1

Scientific name	Common name	Image Plate	Literature source	Online source	Uncommon (site code)	Ichthyocide	DNA
Mugilidae							
<i>Dajaus monticola</i> (Bancroft, 1834)	Mountain Mullet	S13	6	1	SJ10		
<i>Mugil curema</i> Valenciennes, 1836	White Mullet	S13	2,6		SJ21		YES
<i>Mugil rubrioculus</i> Harrison, Nirchio, Oliveira, Ron & Gaviria, 2007	Redeye Mullet	S13	DNA				YES
<i>Mugil trichodon</i> Poey, 1875	Fantail Mullet			ROM			
Mullidae							
<i>Mulloidichthys martinicus</i> (Cuvier, 1829)	Yellow Goatfish	S13	2,4,6	1		1	YES
<i>Pseudupeneus maculatus</i> (Bloch, 1793)	Spotted Goatfish	S13	2,4,5,8	1		1	
Muraenidae							
<i>Echidna catenata</i> (Bloch, 1795)	Chain Moray	S13	2,4	1	SJ21, SJ10	1	
<i>Enchelycore carychroa</i> Böhlke & Böhlke, 1976	Chestnut Moray	S13	2	1	SJ5	1	
<i>Enchelycore nigricans</i> (Bonnaterre, 1788)	Viper Moray	S13	2	1	SJ9	1	
<i>Gymnothorax conspersus</i> Poey, 1867	Saddled Moray			ANSP			
<i>Gymnothorax funebris</i> Ranzani, 1839	Green Moray	S13	2,4	1		1	YES
<i>Gymnothorax maderensis</i> (Johnson, 1862)	Sharktooth Moray		2	1			
<i>Gymnothorax miliaris</i> (Kaup, 1856)	Goldentail Moray	S13	2,4	1		1	
<i>Gymnothorax moringa</i> (Cuvier, 1829)	Spotted Moray	S13	2,4			1	YES
<i>Gymnothorax vicinus</i> (Castelnau, 1855)	Purplemouth Moray	S13	2,4	1		1	
<i>Uropterygius macularius</i> (Lesueur, 1825)	Marbled Moray	S13	2	1		1	
Myctophidae							
<i>Centrobranchus nigroocellatus</i> (Günther, 1873)	Roundnose Lanternfish			ROM			
Neoscopelidae							
<i>Neoscopelus macrolepidotus</i> Johnson, 1863	Largescale Blackchin			CAS			
Nomeidae							
<i>Penes cyanophrys</i> Valenciennes, 1833	Freckled Driftfish		2	1			
Ogcocephalidae							
<i>Ogcocephalus nasutus</i> (Cuvier, 1829)	Shortnose Batfish		2	1			
<i>Ogcocephalus pumilus</i> Bradbury, 1980	Dwarf Batfish			CAS			
Ophichthidae							
<i>Abliia egmontis</i> (Jordan, 1884)	Key Worm Eel		2	1			
<i>Aprognathodon platyventris</i> Böhlke, 1967	Stripe Eel		2	1			
<i>Callechebys guineensis</i> (Osório, 1893)	Shorttail Snake Eel		11	1			
<i>Echiophis intertinctus</i> (Richardson, 1848)	Spotted Spoon-nose Eel		2				
<i>Ichthyapus ophioneus</i> (Evermann & Marsh, 1900)	Surf Eel			FIMNH			
<i>Myrichthys breviceps</i> (Richardson, 1848)	Sharptail Eel	S13	2		SJ13		

Scientific name	Common name	Image Plate	Literature source	Online source	Uncommon (site code)	Ichthyocide	DNA
<i>Myrichthys ocellatus</i> (Lesueur, 1825)	Goldspotted Eel		2	1			
<i>Myrophis anterodorsalis</i> McCosker, Böhlke & Böhlke, 1989	Longfin Worm Eel	S13			SJ28		
<i>Myrophis platyrhynchus</i> Breder, 1927	Broadnose Worm Eel		2	1			YES
<i>Myrophis punctatus</i> Lütken, 1852	Speckled Worm Eel		2,11	1			
Ophidiidae							
<i>Brotula barbata</i> (Bloch & Schneider, 1801)	Atlantic Bearded Brotula		2	1		-1	
<i>Lepophidium pheromystax</i> Robins, 1960	Upsilon Cusk-eel		2	1			
<i>Luciobrotula corethromycter</i> * Cohen, 1964	Broomnose Cusk-eel		9				
<i>Ophidion holbrookii</i> Putnam, 1874	Bank Cusk-eel		2,3,11	1		-1	
<i>Parophidion schmidti</i> (Woods & Kanazawa, 1951)	Dusky Cusk-eel			1			
<i>Xyelacyba myersi</i> * Cohen, 1961	Gargoyle Cusk-eel		9				
Opistognathidae							
<i>Lonchopisthus micrognathus</i> (Poey, 1860)	Swordtail Jawfish	S13	4	1	SJ28, SJ19		YES
<i>Opistognathus aurifrons</i> (Jordan & Thompson, 1905)	Yellowhead Jawfish	S13	2,4	1			YES
<i>Opistognathus macrognathus</i> Poey, 1860	Banded Jawfish	S13	2,4,11	1	SJ5, SJ13, SJ19		
<i>Opistognathus maxillosus</i> Poey, 1860	Mottled Jawfish	S13	2	1	SJ5, SJ13, SJ19	1	
<i>Opistognathus whitehursti</i> (Longley, 1927)	Dusky Jawfish	S13		1	SJ12		
Ostraciidae							
<i>Acanthostracion polygonium</i> Poey, 1876	Honeycomb Cowfish	S13	2	1			
<i>Acanthostracion quadricornis</i> (Linnaeus, 1758)	Scrawled Cowfish	S13	2	1			
<i>Lactophrys bicaudalis</i> (Linnaeus, 1758)	Spotted Trunkfish	S13	2,4	1			
<i>Lactophrys trigonus</i> (Linnaeus, 1758)	Trunkfish	S13	2,4	1			
<i>Lactophrys triquetus</i> (Linnaeus, 1758)	Smooth Trunkfish	S13	2,4	1		1	
Paralichthyidae							
<i>Citharichthys cornutus</i> (Günther, 1880)	Horned Whiff				FMNH		
<i>Citharichthys uhleri</i> Jordan, 1889	Voodoo Whiff				FMNH		
<i>Cyclopssetta fimbriata</i> (Goode & Bean, 1885)	Spotfin Flounder	S14	2	1	SJ12, O14		
<i>Syacium micurum</i> Ranzani, 1842	Channel Flounder		2	1			YES
Parazenidae							
<i>Cyttopsis rosea</i> (Lowe, 1843)	Red Dory		5				
Pempheridae							
<i>Pempheris schomburgkii</i> Müller & Troschel, 1848	Glassy Sweeper	S14	2,4	1	SJ13, ST3, SJ15		YES

Scientific name	Common name	Image Plate	Literature source	Online source	Uncommon (site code)	Ichthyocide	DNA
Poeciliidae							
<i>Poecilia reticulata</i> Peters, 1859	Guppy	S14		1	SJ10		
Polymixiidae							
<i>Polymixia lowei</i> Günther, 1859	Beardfish			FIMNH, CAS			
<i>Polymixia nobilis</i> Lowe, 1836	Noble Beardfish		5,8				
Polynemidae							
<i>Polydactylus virginicus</i> (Linnaeus, 1758)	Barbu			FIMNH			
Pomacanthidae							
<i>Centropyge argi</i> Woods & Kanazawa, 1951	Cherubfish	S14	2,4,5,8	1	O21		
<i>Holacanthus ciliaris</i> (Linnaeus, 1758)	Queen Angelfish	S14	2,4	1		1	YES
<i>Holacanthus tricolor</i> (Bloch, 1795)	Rock Beauty	S14	2,4,5,8	1		1	
<i>Pomacanthus arcuatus</i> (Linnaeus, 1758)	Gray Angelfish	S14	2,4,5,8	1		1	
<i>Pomacanthus paru</i> (Bloch, 1787)	French Angelfish	S14	2,4,5	1		1	
Pomacentridae							
<i>Abudefduf saxatilis</i> (Linnaeus, 1758)	Sergeant Major	S14	2,4,6	1		1	YES
<i>Abudefduf taurus</i> (Müller & Troschel, 1848)	Night Sergeant	S14	2,4	1		1	
<i>Azurina cyanea</i> (Poey, 1860)	Blue Chromis	S14	2,4,8	1		1	YES
<i>Azurina multilineata</i> (Guichenot, 1853)	Brown Chromis	S14	2,4,5,8	1		1	YES
<i>Chromis insolata</i> (Cuvier, 1830)	Sunshinetail	S14	2,5,8	1	O20		
<i>Microspathodon chrysurus</i> (Cuvier, 1830)	Yellowtail Damselfish	S14	2,4,5	1		1	
<i>Stegastes adustus</i> (Troschel, 1865)	Dusky Damselfish	S14	2,4,6	1		1	
<i>Stegastes diencaeus</i> (Jordan & Rutter, 1897)	Longfin Damselfish	S14	2,4	1			YES
<i>Stegastes leucostictus</i> (Müller & Troschel, 1848)	Beaugregory	S14	2,4	1		1	YES
<i>Stegastes partitus</i> (Poey, 1868)	Bicolor Damselfish	S14	2,4,5,8	1		1	YES
<i>Stegastes planifrons</i> (Cuvier, 1830)	Threespot Damselfish	S14	2,4	1		1	YES
<i>Stegastes xanthurus</i> (Poey, 1860)	Cocoa Damselfish	S14	2,4	1		1	YES
Priacanthidae							
<i>Heteropriacanthus cruentatus</i> (Lacepède, 1801)	Glasseye Snapper	S15	2,4	1		1	YES
<i>Priacanthus arenatus</i> Cuvier, 1829	Bigeye	S15	2	1	SJ24		
<i>Pristigenys alta</i> (Gill, 1862)	Short Bigeye		2	1			
Rachycentridae							
<i>Rachycentron canadum</i> (Linnaeus, 1766)	Cobia	S15			ST3		
Rhincodontidae							
<i>Rhincodon typus</i> Smith, 1828	Whale Shark	S15					
Rivulidae							
<i>Kryptolebias marmoratus</i> (Poey, 1880)	Mangrove Rivulus		6	1			

Scientific name	Common name	Image Plate	Literature source	Online source	Uncommon (site code)	Ichthyocide	DNA
Sciaenidae							
<i>Cornula batabana</i> (Poey, 1860)	Blue Croaker		2,11	1			
<i>Eques lanceolatus</i> (Linnaeus, 1758)	Jackknife-fish	S15	2,4	1	SJ30		
<i>Eques punctatus</i> Bloch & Schneider, 1801	Spotted Drum	S15	2,4	1		1	
<i>Odontoscion dentex</i> (Cuvier, 1830)	Reef Croaker	S15	2,4	1		1	
<i>Pareques acuminatus</i> (Bloch & Schneider, 1801)	High-hat	S15	2,4	1		1	YES
<i>Umbrina coroides</i> Cuvier, 1830	Sand Drum		2	1			
Scomberesocidae							
<i>Scomberesox saurus</i> (Walbaum, 1792)	Atlantic Saury				KU		
Scombridae							
<i>Acanthocybium solandri</i> (Cuvier, 1832)	Wahoo	S15	2				
<i>Euthynnus alletteratus</i> (Rafinesque, 1810)	Little Tunny	S15	2	1			YES
<i>Katsuwonus pelamis</i> (Linnaeus, 1758)	Skipjack Tuna	S15	2				
<i>Scomberomorus brasiliensis</i> Collette, Russo & Zavala-Camin, 1978	Serra		2	1			
<i>Scomberomorus cavalla</i> (Cuvier, 1829)	King Mackerel	S15	2		SJ4, ST6		
<i>Scomberomorus regalis</i> (Bloch, 1793)	Cero	S15	2,4	1			
<i>Thunnus albacares</i> (Bonnaterre, 1788)	Yellowfin Tuna	S15	2				
<i>Thunnus atlanticus</i> (Lesson, 1831)	Blackfin Tuna	S15	2	1			
Scorpaenidae							
<i>Pontinus castor</i> Poey, 1860	Longsnout Scorpionfish		2	1			
<i>Pterois volitans</i> (Linnaeus, 1758)	Red Lionfish	S15		1			YES
<i>Scorpaena albifimbria</i> Evermann & Marsh, 1900	Coral Scorpionfish	S15	2,11	1	O8		
<i>Scorpaena bergii</i> Evermann & Marsh, 1900	Goosehead Scorpionfish				FIMNH		
<i>Scorpaena brasiliensis</i> Cuvier, 1829	Barbfish		2,11	1			
<i>Scorpaena calcarata</i> Goode & Bean, 1882	Smoothhead Scorpionfish		2,11	1			
<i>Scorpaena grandicornis</i> Cuvier, 1829	Plumed Scorpionfish		2,6	1			
<i>Scorpaena inermis</i> Cuvier, 1829	Mushroom Scorpionfish	S15	2	1	SJ5		
<i>Scorpaena plumieri</i> Bloch, 1789	Spotted Scorpionfish	S15	2,4	1		1	
<i>Scorpaenodes caribbaeus</i> Meek & Hildebrand, 1928	Reef Scorpionfish	S15	2	1	SJ34, SJ23, SJ13	1	
Serranidae							
<i>Alphestes afer</i> (Bloch, 1793)	Mutton Hamlet	S16	2	1	SJ23	1	
<i>Bullisichthys caribbaeus</i> Rivas, 1971	Pugnose Bass		5,8				
<i>Cephalopholis cruentata</i> (Lacepède, 1802)	Graysby	S16	2,4,5,8	1		1	YES
<i>Cephalopholis fulva</i> (Linnaeus, 1758)	Coney	S16	2,4,5,8	1		1	
<i>Diplectrum bivittatum</i> (Valenciennes, 1828)	Dwarf Sand Perch	S16	2	1		1	YES
<i>Diplectrum formosum</i> (Linnaeus, 1766)	Sand Perch		4	1			

Scientific name	Common name	Image Plate	Literature source	Online source	Uncommon (site code)	Ichthyocide	DNA
<i>Epinephelus adscensionis</i> (Osbeck, 1765)	Rock Hind	S16	2,4	1	SJ22, SJ15	1	
<i>Epinephelus guttatus</i> (Linnaeus, 1758)	Red Hind	S16	2,4,5,8	1		1	
<i>Epinephelus itajara</i> (Lichtenstein, 1822)	Atlantic Goliath Grouper	S16	2				
<i>Epinephelus morio</i> (Valenciennes, 1828)	Red Grouper	S16	2	1			
<i>Epinephelus striatus</i> (Bloch, 1792)	Nassau Grouper	S16	2,4,5,8	1		1	YES
<i>Hypoplectrus aberrans</i> Poey, 1868	Yellowbelly Hamlet	S16	2,4	1		1	
<i>Hypoplectrus chlorurus</i> (Cuvier, 1828)	Yellowtail Hamlet	S16	2,4,5,8	1			
<i>Hypoplectrus guttavarius</i> (Poey, 1852)	Shy Hamlet	S16	2,4	1	SJ19, ST6		
<i>Hypoplectrus indigo</i> (Poey, 1851)	Indigo Hamlet	S16	2,4	1			
<i>Hypoplectrus nigricans</i> (Poey, 1852)	Black Hamlet	S16	2,4	1		1	
<i>Hypoplectrus puella</i> (Cuvier, 1828)	Barred Hamlet	S16	2,4	1		1	
<i>Hypoplectrus unicolor</i> (Walbaum, 1792)	Butter Hamlet	S16	2,4	1		1	
<i>Hyporhamphus mystacinus</i> (Poey, 1852)	Misty Grouper		2,8				
<i>Liopropoma mowbrayi</i> Woods & Kanazawa, 1951	Cave Basslet		2,5				
<i>Liopropoma rubre</i> Poey, 1861	Peppermint Basslet	S16	2,4	1	ST1, SJ9, SJ13	1	
<i>Mycteroperca acutirostris</i> (Valenciennes, 1828)	Western Comb Grouper		2	1			
<i>Mycteroperca bonaci</i> (Poey, 1860)	Black Grouper	S17	2	1	SJ33, O9, O10		
<i>Mycteroperca interstitialis</i> (Poey, 1860)	Yellowmouth Grouper	S17	2,4,5	1	SJ7		YES
<i>Mycteroperca tigris</i> (Valenciennes, 1833)	Tiger Grouper	S17	2,5,8	1	O11, O12, O13	1	
<i>Mycteroperca venenosa</i> (Linnaeus, 1758)	Yellowfin Grouper	S17	2,4,5,8	1		1	YES
<i>Paranthias furcifer</i> (Valenciennes, 1828)	Atlantic Creolefish	S17	2,5,8	1	SJ33		
<i>Pronotogrammus martinicensis</i> (Guichenot, 1868)	Roughtongue Bass		5				
<i>Rypticus bistrispinus</i> (Mitchill, 1818)	Freckled Soapfish	S17			O14		
<i>Rypticus carpenteri</i> Baldwin & Weigt, 2012	Slope Soapfish	S17					
<i>Rypticus saponaceus</i> (Bloch & Schneider, 1801)	Greater Soapfish	S17	2,4	1		1	
<i>Rypticus subbifrenatus</i> Gill, 1861	Spotted Soapfish		2	1		1	
<i>Schulzeia beta</i> (Hildebrand, 1940)	School Bass	S17	2	1	O19		YES
<i>Serraniculus pumilio</i> Ginsburg, 1952	Pygmy Sea Bass	S17	11	1	SJ19		YES
<i>Serranus annularis</i> (Günther, 1880)	Orangeback Bass	S17	2,11	1	O17		
<i>Serranus baldwini</i> (Evermann & Marsh, 1899)	Lantern Bass	S17	2,4	1	SJ32, SJ12, SJ22		YES
<i>Serranus luciopercanus</i> Poey, 1852	Crosshatch Bass		2,5,8				
<i>Serranus phoebe</i> Poey, 1851	Tattler		2	1			
<i>Serranus tabacarius</i> (Cuvier, 1829)	Tobaccofish	S17	2,4	1			YES
<i>Serranus tigrinus</i> (Bloch, 1790)	Harlequin Bass	S17	2,4	1		1	
<i>Serranus tortugarum</i> Longley, 1935	Chalk Bass	S17	2,4,5	1			YES

Scientific name	Common name	Image Plate	Literature source	Online source	Uncommon (site code)	Ichthyocide	DNA
Sparidae							
<i>Archosargus rhomboidalis</i> (Linnaeus, 1758)	Sea Bream	S17	2,8	1	SJ13, SJ3		
<i>Calamus bajonado</i> (Bloch & Schneider, 1801)	Jolthead Porgy	S17	2	1			
<i>Calamus calamus</i> (Valenciennes, 1830)	Saucereye Porgy	S17	2,4	1			
<i>Calamus penna</i> (Valenciennes, 1830)	Sheepshead Porgy	S17	2,4	1			
<i>Calamus pennatula</i> Guichenot, 1868	Pluma Porgy	S17	2,4	1			YES
<i>Calamus proridens</i> Jordan & Gilbert, 1884	Littlehead Porgy			CMN			
<i>Diplodus caudimaculatus</i> (Poey, 1860)	Silver Porgy	S17	2,4,11	1	ST6		
Sphyraenidae							
<i>Sphyraena barracuda</i> (Edwards, 1771)	Great Barracuda	S17	2,4,5,6,8	1			YES
<i>Sphyraena borealis</i> DeKay, 1842	Sennet	S17	2	1	SJ13, SJ12, SJ21		
Sphyrnidae							
<i>Sphyrna lewini</i> (Griffith & Smith, 1834)	Scalloped Hammerhead		10	1			
<i>Sphyrna mokarran</i> (Rüppell, 1837)	Great Hammerhead		10				
Spratelloididae							
<i>Jenkinsia lamprotaenia</i> (Gosse, 1851)	Dwarf Herring		2,6	1		1	YES
<i>Jenkinsia parvula</i> Cervigón & Velazquez, 1978	Shortstriped Round Herring		2				
<i>Jenkinsia stolifera</i> (Jordan & Gilbert, 1884)	Shortband Herring		2				
Squalidae							
<i>Squalus cubensis</i> Howell Rivero, 1936	Cuban Dogfish				FMNH		
Sternoptychidae							
<i>Sonoda paucilampa</i> Grey, 1960	Deepsea Hatchetfish				NMNH		
Stomiidae							
<i>Astronesthes similis</i> Parr, 1927	Similar Snaggletooth				NMNH		
Syngnathidae							
<i>Amphelikurtus dendriticus</i> (Barbour, 1905)	Pipehorse	S18			SJ12		
<i>Bryx dunckeri</i> (Metzelaar, 1919)	Pugnose Pipefish	S18	2	1	SJ13	1	YES
<i>Cosmocampus brachycephalus</i> (Poey, 1868)	Crested Pipefish		2			1	
<i>Cosmocampus elucens</i> (Poey, 1868)	Shortfin Pipefish	S18	2,4	1	SJ19		
<i>Cosmocampus profundus</i> (Herald, 1965)	Deepwater Pipefish		2				
<i>Halicampus crinitus</i> (Jenyns, 1842)	Banded Pipefish	S18			SJ34, SJ13, SJ22		
<i>Hippocampus erectus</i> Perry, 1810	Lined Seahorse		11	1			YES
<i>Hippocampus reidi</i> Ginsburg, 1933	Longsnout Seahorse	S18	4	1	SJ19		YES
<i>Microphis lineatus</i> (Kaup, 1856)	Opposum Pipefish	S18			O23		
<i>Pseudophallus mindii</i> (Meek & Hildebrand, 1923)	Freshwater Pipefish		11				

Scientific name	Common name	Image Plate	Literature source	Online source	Uncommon (site code)	Ichthyocide	DNA
<i>Syngnathus caribbaeus</i> Dawson, 1979	Caribbean Pipefish	S18	2		SJ21		
<i>Syngnathus dawsoni</i> (Herald, 1969)	Antillean Pipefish		2,4,11	1			
<i>Syngnathus pelagicus</i> Linnaeus, 1758	Sargassum Pipefish			ROM			
Synodontidae							
<i>Saurida brasiliensis</i> Norman, 1935	Largescale Lizardfish		2				
<i>Saurida suspicio</i> Breder, 1927	Doubtful Lizardfish	S18	2	1	SJ5, SJ13		YES
<i>Synodus foetens</i> (Linnaeus, 1766)	Inshore Lizardfish	S18	2	1	SJ5, SJ13	1	YES
<i>Synodus intermedius</i> (Spix & Agassiz, 1829)	Sand Diver	S18	2,4	1		1	YES
<i>Synodus poeyi</i> Jordan, 1887	Offshore Lizardfish		2				
<i>Synodus synodus</i> (Linnaeus, 1758)	Red Lizardfish	S18	2	1	SJ11, SJ21	1	
<i>Trachinocephalus myops</i> (Forster, 1801)	Snakefish			CAS			
Tetraodontidae							
<i>Canthigaster rostrata</i> (Bloch, 1786)	Sharppose Puffer	S18	2,4,5,8	1		1	
<i>Sphoeroides spengleri</i> (Bloch, 1785)	Bandtail Puffer	S18	2,4	1		1	YES
<i>Sphoeroides testudineus</i> (Linnaeus, 1758)	Checkered Puffer	S18	2,4,6	1	O15	1	
Triakidae							
<i>Mustelus canis</i> (Mitchill, 1815)	Smooth Dogfish			FIMNH			
Triglidae							
<i>Peristedion longispatha</i> Goode & Bean, 1886	Widehead Armored Searobin			CAS			
Tripterygiidae							
<i>Enneanectes altivelis</i> Rosenblatt, 1960	Lofty Triplefin	S18	2	1		1	
<i>Enneanectes atrorus</i> Rosenblatt, 1960	Blackedge Triplefin		2,11	1			
<i>Enneanectes boehlkei</i> Rosenblatt, 1960	Roughhead Triplefin	S18	2	1		-1	YES
<i>Enneanectes jordani</i> (Evermann & Marsh, 1899)	Mimic Triplefin	S18	2	1	SJ21		
<i>Enneanectes matador</i> Victor, 2013	Matador Triplefin	S18		1			YES
Xiphiidae							
<i>Xiphias gladius</i> Linnaeus, 1758	Swordfish	S18					

Notes: Image voucher – supplementary plate number is given; photographer name is imbedded in each image. Literature source – 1 DeAngelis et al. (2008); 2 Dennis (2000); 3 Dennis et al. (2004); 4 Friedlander et al. (2013); 5 Garcia-Sais (2005); 6 Loftus (2003); 7 Mantatrust.org pers. comm. to DRR; 8 Nelson and Appledorn (1985); 9 Quatrinni et al. (2017); 10 Recksiek et al. (2006), 11 Smith-Vaniz and Jelks (2014); 12 Rogers et al. (2010). Online source – 1 indicates that an aggregator source exists, with the source named whenever it represents the sole voucher: AMNH (American Museum of Natural History); NOAA (National Oceanographic and Atmospheric Administration); BOLD (Barcode of Life); FIMNH (Florida Museum of Natural History); MCZ (Museum of Comparative Zoology); NMNH (National Museum of Natural History); ANSP (Academy of Natural Sciences of Philadelphia); CAS (California Academy of Sciences); ROM (Royal Ontario Museum); KUBI (University of Kansas Biodiversity Institute); CMN (Canadian Museum of Nature). Uncommon – species seen at 3 or less named sites by CJE and AME (see Suppl material 3: File S2a, b (for site codes) and Suppl. material 4: File S3). Ichthyocide – species collected by this method as noted in Dennis (2000); parentheses indicate ichthyocide was the only collection method noted by Dennis (2000). Gobiidae – we follow Thacker (2009) in including *Cerdale* and *Ptereleotris* among the Gobiidae. *Hypoplectrus* – we follow Puebla et al. (2022) in treating *H. maculiferus* as a synonym of *H. aberrans*.

Table 3. Fishes from St. John-Thomas recorded by different sources.

Types of fish taxa recorded	Species	Genera	Families
Total from all sources	561	296	108
From Literature sources All	451	251	89
Dennis 2000 All	401	216	79
Sole source is Dennis 2000	164	126	55
Sources other than Dennis 2000	50	44	25
From Online sources All	453	253	97
Online sources only	50	46	42
From Images All	371	20	73
Images only	34	29	20
Deep species All sources	49	44	33
Recorded by Dennis 2000	19	18	13
Uncommon shallow species	138	104	45
Ichthyocide Collection All	173	99	45
Ichthyocide only	18	15	11
mtDNA BARCODES	Species	Genera	Families
St. John-Thomas	156	93	41
Sole record is from barcode data	1	1	1
Puerto Rico	90	50	25
St. John-Thomas but not Puerto Rico	113	61	24
Puerto Rico but not St. John-Thomas	47	18	8
St. Croix	1	1	1
British Virgin Islands	3	2	1
All sites combined	207	112	49

Notes: Data sources (literature, online sources, images) are listed in Table 2. Deep species are those exclusively or typically found below 40 m depth. Uncommon shallow species are those found at 1–3 sites by CJE, AME, LR, and third-party photographers as indicated in Table 2. Ichthyocide collection: recorded as being collected with rotenone by a source cited by Dennis (2000). Ichthyocide only: the only collection method listed for a species from St. John-Thomas by Dennis (2000). DNA barcodes: (see Suppl. material 7: File S6). The single DNA Barcoded species collected at St. Croix (see Suppl. material 7: File S6) is not known from St. John-Thomas. The St. John-Thomas species count includes four identified only to genus. DNA barcode data for *Pterois volitans* are not included in this table.

Dennis (2000) listed 401 species from 216 genera and 79 families from those two islands (Table 2). We found records of an additional 159 species, producing an increase of 39.7% in the number of species, 37.0% in the number of genera and 36.7% in the number of families known from there (Table 3). The additions include 34 species for which the only source is a voucher image, 50 species recorded in post-2000 publications, and 49 species recorded only by online sources of museum (and other) data (Table 3). Of the 561 in Table 2, 24.6% were uncommon. Although 30.1% were collected using rotenone, species accounts by Dennis (2000) mentioned no other collecting method for only 10.4% of that subgroup of species. The 561 include three non-natives to the area (*Oreochromis niloticus*, *Poecilia reticulata* and *Pterois volitans*), 11 freshwater/estuarine species (*Anguilla rostratus*, *Dormitator maculatus*, *Eleotris perniger*, *Gobiomorus dormitor*, *Awaous banana*, *Sicydium plumieri*, *Sicydium punctatum*, *Dajaus monticola*, *Microphis lineatus* and *Pseudophallus mindii*) and 547 marine species native to the GC.

Table 4. Taxonomic comparisons of St. John-Thomas and St. Croix marine fish faunas.

Site	Species	Genera	Families
Both US Virgin Islands			
Entire fauna (n)	679	345	122
Shallow fishes (n)	590	279	90
Deep fishes (n)	89	77	54
St. John-Thomas			
Entire Fauna (n)	547	283	105
Percent of USVI fauna	80.6	82.0	86.0
Percent only at St. John-Thomas	19.3	15.5	10.5
Shallow fishes (n)	497	245	86
Percent of USVI shallow fauna	84.2	86.6	94.5
Percent only at St. John-Thomas	13.0	7.4	1.9
Deep fishes (n)	50	44	34
Percent of USVI deep fauna	56.2	57.1	63.0
Percent only at St. John-Thomas	70.0	50.0	26.5
St. Croix			
Entire fauna (n)	573	301	112
Percent of USVI fauna	84.5	87.2	91.8
Percent only at St. Croix	23.4	20.4	15.5
Shallow fishes (n)	519	256	88
Percent of USVI fauna	88.0	91.8	97.8
Percent only at St. Croix	18.3	13.1	2.7
Deep fishes (n)	54	50	39
Percent of USVI deep fauna	61.4	64.9	62.2
Percent only St. Croix	72.2	60.0	41.0

Notes: USVI fauna = combined fauna of St. John-Thomas and St. Croix, with exotic and primarily freshwater species excluded. Some genera and families have a deep member in one site but not the other, which affects USVI totals for deep and shallow genera and families. Shallow fishes: species exclusively or commonly found shallower than 40 m. Deep fishes: species exclusively or largely found deeper than 40 m (see methods for further details).

Comparative taxonomic composition of the USVI fish faunas (Table 4, Suppl. material 5: File S4)

The species richness of the USVI marine fauna (i.e., the combined St. John-Thomas plus St. Croix faunas) was 15–20% greater than that of either of the two insular faunas (Table 4). Those two faunas had slightly higher relative rates of richness of genera and families than of species. The larger size of the USVI fauna of species derives from ~ 1/5 of species in each insular fauna not being present in the other, with lower proportions of genera and families also being recorded only at one of the two islands. Relative faunal richness at all three taxonomic levels and the relative abundance of taxa present at only one island were ~ 5% higher at St. Croix than St. John-Thomas. In both island faunas the relative representation of species, genera, and families in the entire USVI fauna was substantially greater among shallow species than deep species. The deep fauna was much smaller than the shallow fauna at each island and there was much less overlap in occurrence of species, genera, and families between the two insular deep faunas than between their shallow faunas (Table 4).

Table 5. Abundance of ecotypes of reef-associated bony fishes in the Greater Caribbean and the USVI.

	Region	St. John-Thomas	St. Croix
All species (n)	992	470	493
Pelagic species % of fauna	8.0	10.4	10.3
Non-pelagic species % of fauna	92.0	89.6	89.7
Demersal species %	34.6	46.3	45.0
Benthic species %	65.4	53.7	55.0
Cryptobenthic species %	64.6	53.0	54.3
Small cryptobenthic species %	42.6	31.6	32.5
CCRF species %	45.9	36.3	35.7
SHALLOW NON-PELAGIC SPECIES (n)	772	400	424
Percent of fauna	84.6	95.0	95.9
Demersal species %	34.9	45.3	44.0
Benthic species %	65.1	54.7	56.0
Cryptobenthic species %	64.0	54.3	55.2
Small cryptobenthic species %	42.5	33.3	34.0
CCRF species %	46.0	37.5	37.3
DEEP NON-PELAGIC SPECIES (n)	141	21	18
Percent of fauna	15.4	5.0	4.2
Demersal species %	33.3	66.7	66.7
Benthic species %	66.7	33.3	33.3
Cryptobenthic species %	66.7	33.3	33.3
Small cryptobenthic species %	43.3	4.8	0
CCRF species %	45.4	19.0	0

Notes: Data for the region pattern are from Robertson and Tornabene (2021), for St. Croix are from Robertson et al. (2022), and for St. John-Thomas are in File S5. Bold percentages indicate whether the value(s) for either the region or the USVI islands were > 5% higher than the value(s) for the other group in each case.

Table 6. Zoogeographic composition of the USVI and Sint Eustatius faunas. Percentage of species in each category. Non-native species are not included.

Site (n)	Northwest Atlantic	Western Atlantic	Trans-Atlantic	Atlantic & Indo-Pacific
St. Croix (534)	41.6	33.9	13.9	10.6
St. John-Thomas (558)	39.5	36.5	14.0	10.0
Sint Eustatius (406)	41.1	33.3	15.3	10.3

Notes: St. Croix data are from Smith-Vaniz and Jelks 2014. Sint Eustatius values are from Robertson et al. (2020). St. John-Thomas values are from the present study. Northwest Atlantic = Greater Caribbean, with or without range extensions to the north of that region. Western Atlantic = Northwestern Atlantic + Brazil. Trans-Atlantic = anywhere in the western Atlantic + any of the islands of the central Atlantic and/or the Eastern Atlantic. Atlantic & Indo-Pacific = Anywhere in the Western Atlantic + anywhere in the Indo-Pacific.

Ecotypic structure of the USVI reef-fish faunas vs. the region (Table 5, Suppl. material 6: File S5)

We compared the ecotypic structure of the St. John-Thomas and St. Croix faunas of reef-associated fishes with that of the GC fauna (see Robertson and Tornabene 2021). Both St. Croix and St. John-Thomas have faunas that are almost half the size of the total regional

fauna, with the listed St. John-Thomas fauna being ~ 5% smaller than that of St. Croix (Table 5). Compared to the GC fauna both islands have slightly higher percentages of pelagic species, distinctly higher percentages of demersal species, and correspondingly lower percentages of benthic, cryptobenthic, small cryptobenthic, and CCRF species. These differences for non-pelagic types apply to each entire USVI fauna, and to both shallow- and deep-reef subgroups of those faunas. Both USVI sites also have markedly lower relative abundances (~ 1/3) of deep-reef species than the regional fauna. The relative abundances of different ecotypes are remarkably similar at both islands, except for the presence of a few deep cryptobenthic and CCRF species detected only at St. John-Thomas.

Zoogeographic structure of the USVI faunas (Table 6)

The zoogeographic structures of the faunas of the two USVI sites and nearby Sint Eustatius are quite similar (Table 6). Species that are endemic to the Greater Caribbean and, in a few cases, surrounding areas are the largest group in all three faunas, with West Atlantic species also found in Brazil being the second largest by a small margin in each case. The two smallest groups in each case are Trans-Atlantic and Atlantic & Indo-Pacific. The ranks of those four groups are the same in all three faunas, a measure of their strong similarities.

mtDNA-Barcode Coverage (Tables 2, 3; Suppl. material 7: File S6)

Table 2 indicates which members of the St. John-Thomas fauna have mtDNA-barcode sequences on the BOLD database derived from specimens collected at that site. Table 3 presents a summary of taxa that have sequences obtained from St. John-Thomas, Puerto Rico, the British Virgin Islands and St. Croix, singly and in combination. File S6 provides technical information about those barcode data for the various species. We obtained local DNA-barcodes for 156 fish species in 156 BINs from St. John-Thomas, with one additional from St. Croix, and three additional species from around the British Virgin Islands (total 160 species). Of these, two are only from GenBank records harvested by BOLD, and 10 are added from specimens collected in offshore larval plankton tows described in Lamkin et al. (2009). We obtained 91 species records (including one non-native, *Pterois volitans*) for Puerto Rico, 44 of them shared with the Virgin Islands. Of the 91, 27 are added from Harms-Tuohy et al. (2016), 14 from GenBank records harvested by BOLD, and seven from other sources, including the University of Kansas (UKFBJ), Smithsonian (Birmingham/Lessios; BSMUA & BSOPA), the Guy Harvey Research Institute (Hanner et al. 2011; EBFSF), and the Museum and Art Gallery of the Northern Territory (GOBY) in Australia.

The available DNA-barcode sequence records from specimens collected at St. John-Thomas represent coverage of 27.8% of the species, 31.4% of the genera and 38% of the families of fishes known from that site. Barcode records represent the sole source of information on the presence of one species known from those islands and are also available for another four species currently identifiable only to genus. Distinctly fewer species have been barcoded from fish taken at Puerto Rico, and there are almost no

such data available from either St. Croix or the British Virgin Islands. Barcode records from Puerto Rico and the British Virgin Islands exist for 52 species occurring in St. John-Thomas but not sequenced from there, bringing the total PRP DNA-barcoded species to 36.5% of St. John-Thomas fauna. All but seven of the 200 barcoded species are reef-associated bony fishes. The vast majority (98.5%) of barcoded species are shallow forms. Deep-living species are especially under-represented among the barcoded forms: only three of 51 such species have barcode data (File S6).

Discussion

St. Croix

The species records we have added increased the size of that island's fauna by 7.5%. Almost a third of the additions arise from voucher photographs of shallow-reef species photographed by CJE and AME (and provided by Mantatrust.org). Those include several not accepted by Smith-Vaniz and Jelks (2014) due to inadequate information available at that time. Cryptobenthic fishes, which, by definition, are generally difficult to observe, are a major component of Greater Caribbean reef-fish faunas, including that of St. Croix. Such species comprised all but one of those added by CJE and AME. The exception, *Kyphosus cinerascens*, may have been misidentified previously, since the taxonomic status and global distributions of members of the genus were only comprehensively reviewed by Knudsen and Clements (2016), after Smith-Vaniz and Jelks (2014) published their checklist. Almost half the additions were deep-living species, one third of which were recorded only by submersible or ROV, with the remainder coming from online and literature records.

The process of obtaining location records is an ongoing one for online aggregators, which have vastly increased the amounts of data they host during the last half decade. Although the aggregators offer such information, and are involved in collaborative data sharing, such sharing is sufficiently incomplete that it is necessary to examine records from multiple aggregators to obtain a comprehensive picture of all the data available for any particular site. Even “old” data becomes newly available on the aggregators from time to time and needs to be included in faunal inventories of well-studied sites. The increase in faunal size, although not large in percentage terms, demonstrates the utility of citizen-science efforts to provide photographic vouchers, of reviews of submersible and ROV studies of deep-living fishes, and of periodic evaluations of information available online from aggregators.

St. John-Thomas

Although the 401 species list for this site extracted from Dennis (2000) was substantial (74% the size of Smith-Vaniz and Jelks (2014) count for St. Croix), our use of the same methods as those that produced an increase in the St. Croix fauna produced a much larger increase in the St. John-Thomas fauna: 40% vs. 7.5% for St. Croix. Dennis (2000) was

the sole source for 29% of species recorded in our expanded list of the St. John-Thomas fauna. Records from additional sources brought the size of the St. John-Thomas fauna to within 5% of the size of the St. Croix fauna. Citizen-scientists' photographic records accounted for 22% of the new additions and data only available from online databases for 33%, while other literature sources provided the sole records for 32% of the additional species. Multiple types of sources accounted for the remaining 13% of new records.

The size, and taxonomic- and ecotypic structure of the two USVI marine faunas

Both insular marine faunas are over 80% the size of the combined USVI fauna in terms of species richness. Species found at only one of the two islands represent ~ 20% of each fauna. For shallow species the size of each insular fauna is 85–90% that of the combined fauna, with correspondingly lower rates of occurrence at only one island. Two factors may contribute to these differences between the island faunas: variation in ecological conditions between the islands and inadequate sampling. The possibility of differing ecological conditions seems small as both islands have the same range of large-scale habitat types, although those vary in abundance between the islands. The shelf area of St. John-Thomas is close to 10 times the size of the St. Croix shelf, yet the former has the smaller known fauna. At both islands the great majority of sampling has occurred in quite shallow water, often very close to shore in the case of St. John-Thomas. Shelf habitats likely are under-sampled at both islands, strongly so at St. John-Thomas, where there are large areas of habitat between 40–60 m depth some distance from the islands on both the northern and southern parts of the PRP. At St. Croix most shallow sampling has occurred in and near the Buck Island Reef National Monument, rather than spread around different parts of the platform and different sides of the island. Hence both insular faunas likely are larger than indicated here, particularly in the case of St. John-Thomas.

Review of the two USVI marine species lists show that species not shared between the two islands are distributed through many genera and families (Suppl. material 5: File S4; Table 4). None are endemic to either USVI island and single-island endemics are rare amongst the Greater Caribbean fauna and limited to highly isolated islands such as Cayman. Most species in that region have geographic ranges much larger than the USVIs. The larger size of the St. Croix fauna, particularly of cryptobenthic species can be attributed to a greater effort to find such species. This was done using rotenone during two intensive sampling campaigns that occurred ~ 40 y after rotenone sampling at St. John-Thomas, plus some subsequent minor efforts in the shallow part of a Buck Island Reef National Monument that, in its entirety constitutes ~ 1/3 of the St. Croix insular platform: 46% (262) of the native marine species known from St. Croix are shallow species collected using rotenone (Smith-Vaniz and Jelks 2014), vs. 31.7% (173) of such species from St. John-Thomas. Later sampling by Pittman et al. (2008) at the same small, shallow St. Croix site as studied by Smith-Vaniz et al. (2006) added 10.9% more species to the tally of the first two series of collections. Smith-Vaniz and Jelks (2014) produced a list of 41 species from 22 families that, at that time, were known from St. John-Thomas but not St. Croix. Since then, five of the 35 shallow species on that table have been added to the St. Croix fauna (Table 1 here), together with two others that were listed as unconfirmed

by those authors. Photographic sampling of shallow reef fishes at St. John-Thomas by CJE, AME and other citizen scientists, by itself increased the size of the fauna registered by Dennis (2000) by 8.5%. Finally, the species composition of local reef-fish faunas can change substantially through time at intensively sampled sites, for varying reasons (e.g., see changes registered by Starck et al. 2017 over a 50y period), highlighting the utility of temporally dispersed sampling. With further sampling many shallow species currently known from only one of the USVI should be expected to be found at the other, in which case the shallow faunas of each island would be 10–15% larger than the current figures.

The deep-species fauna represents only 13.1% of the entire (shallow plus deep) USVI fauna and deep species exhibit much lower rates of faunal overlap between the two islands than occurs among shallow species. The two islands have experienced low rates of exploration of deep habitats, particularly deep reefs, by submersibles and ROVs, which were limited to observational studies. The few ROV (Quattrini et al. 2017) and submersible dives (Nelson and Appeldoorn 1985; Garcia-Sais 2005) were the sole source of only 11.1% and 28% of records of deep fishes at St. Croix and St. John-Thomas, respectively. The edges of the insular platforms of the two USVIs are < 50 km apart and the suite of deep species involved have ranges much larger than the area occupied by the USVI. Low levels of sampling can account for the small size of both USVI deep faunas, particularly the deep-reef component, and to the low level of overlap between the deep faunas of the two islands.

At both USVI sites the deep-reef species represent only 4.2–5% of the entire local reef-fish fauna, i.e., ~ 1/3 of the percentage for the GC regional fauna (Robertson et al. 2022). In contrast, when intensive submersible collecting and observations have been aimed specifically at assessing the diversity of deep-reef fish faunas, such as has occurred at other Caribbean islands (Curacao, Roatan and Sint Eustatius), the inventory of deep-reef species at individual islands has increased ~ 9 fold, with such species representing 16% of the entire (shallow plus deep) reef-fish fauna at the most intensively sampled island (Robertson et al. 2022), i.e., more than three times the level at each USVI. Similar sampling at both USVI undoubtedly will increase the absolute and relative sizes of their deep-reef faunas. Smith-Vaniz and Jelks (2014) concluded that there was no indication at the time of their study that the St. Croix fauna had reached asymptotic size. The additions reported here and patterns of variation in faunal composition between the two islands support that view for St. John-Thomas as well as St. Croix.

Reef-associated bony fishes comprised 84% and 91%, respectively, of the faunas of St. John-Thomas and St. Croix, and the St. John-Thomas reef-fish fauna was 94.3% the size of the equivalent fauna of St. Croix. The ecotypic structure of those two USVI reef-fish faunas was very similar, with both differing from the broad structure of the GC regional fauna by having larger proportions of pelagic and demersal species that are readily visible to observers and correspondingly smaller proportions of cryptic species. Similarities in the zoogeographic structures and sizes of the two USVI faunas support the view that both can be considered to be sampled with a similar level of efficiency, at least in terms of their shallow faunas.

mtDNA-barcode coverage

In terms of the availability of DNA-barcodes for marine fishes, the Greater Caribbean currently is the most well-sampled large marine biogeographic region in the tropics, with ~ 90% of the shore-fishes barcoded and up to 95% of the shallow reef-associated species (Victor et al. 2015). However, several specific locations account for the vast majority of sequences. Those include Florida, Yucatan (Mexico), Belize, Panama, and Curacao; with species lists published for Yucatan by Valdez-Moreno et al. (2010) and lists for additional locations in Weigt et al. (2012). The Puerto Rican Plateau has been only lightly sampled, with information derived mostly from older collections by author BV at St. John-Thomas and Puerto Rico, and from a set of lionfish stomach contents from La Parguera in Puerto Rico sequenced by Harms-Tuohy et al. (2016). The latter identified 39 species from 16 families. A few additional sequences come from open-ocean sampling for larvae around the USVI, by Lamkin et al. (2009). The older collections from St. Thomas and Puerto Rico were collected by BV for recruitment and otolith studies as well as some taxonomic reviews (e.g., the genera *Coryphopterus* and *Emblemariopsis*). The recent additions of 19 species from St. John were collected by CJE and AME mainly for DNA confirmation of the species identification of diagnostic underwater photographs that serve as vouchers here, mostly of cryptobenthic fishes. No collections at St. John-Thomas or elsewhere on the PRP that provided DNA barcodes were expressly made for assembling an inventory of fish species- hence the absence of some of the most abundant and widespread shallow reef fishes in the barcode list presented here (e.g., the Bluehead Wrasse, *Thalassoma bifasciatum*).

We cannot directly compare barcode coverage of fishes at St. John-Thomas with that at other intensively barcoded locations noted above because neither the number of barcoded species nor the local species inventory have been comparably evaluated at any of those sites. The results of the present assessment of DNA-barcode coverage for the USVI and the remainder of the PRP highlight the usefulness of the DNA-barcode database for ancillary projects. Accumulating sequences for unrelated purposes, such as taxonomic reviews, stomach-content studies, larval or e-DNA surveys (environmental DNA, where water is sampled for dissolved DNA sequences), augments the general DNA-barcode coverage for specific biogeographic regions and helps confirm species identifications for faunal surveys.

Permits

Collections from St. John in 2021 were made under National Park Service Collecting Permit VIIS-2021-SCI-0006: We especially thank Thomas Kelley (Virgin Islands NP/ Virgin Islands Coral Reef NM) for facilitating that work.

Acknowledgements

CJE and AME greatly appreciate the assistance, knowledge, photographic contributions, and camaraderie of various people and organizations in the USVI: Alasdair Dunlap-Smith for logistical support, help with collections and photographic contributions; Miguel Andres Goolishian Hernandez for assistance with diving and photo contributions; the owners and staff of Low Key Watersports' on St. John and to St. Croix Ultimate Bluewater Adventures on St. Croix; Bogie's Villa for logistical support at St. John. Thanks to Caroline Rogers, Chris Rapchick, Serenity Mitchell, Spencer Riley, Max Koestenblatt, Cristina Kessler, Jenny Keith, Nicole Krampitz, Sara Richter and Jamie Irving (see File S2C) for contributing voucher images, to Rafe Boulon for information about USVI fishes and to Guy Stevens and Nicole Pelletier of Mantatrust.org for providing photographic documentation of mobulid rays at the USVI. We also appreciate the cooperation of J. Lamkin, as well as T. Girard, E. Malka, A. Shiroza, L. Vasquez-Yeomans, and G. Zapfe for providing information on larvae from the NOAA SEFSC NMFS Miami Larval Fish collection (funded by NOAA's Coral Reef Conservation Program, NOAA NMFS SEFSC, and University of Miami's Cooperative Institute for Marine and Atmospheric Studies). Thanks also to Andrew Bentley (Biodiversity Institute, University of Kansas), Amy Driskell (LAB, National Museum of Natural History), Chelsea Harms-Tuohy (Isla Mar Research Expeditions, Rincon, PR) and Eric Post (FFWCC, Fish and Wildlife Research Institute, FL) for access to barcodes and information and discussion for assigning them to species.

References

- Baldwin CC, Tornabene L, Robertson DR (2018) Below the mesophotic. *Scientific Reports* 8: e4920. <https://doi.org/10.1038/s41598-018-23067-1>
- Brandl SJ, Goatley CHR, Bellwood DR, Tornabene L (2018) The hidden half: Ecology and evolution of cryptobenthic fishes on coral reefs. *Biological Reviews of the Cambridge Philosophical Society* 93(4): 1846–1873. <https://doi.org/10.1111/brv.12423>
- Bunckley-Williams L, Williams EH (2004) New Locality, Depth, and Size Records and Species Character Modifications of Some Caribbean Deep-Reef/Shallow Slope Fishes and a New Host and Locality Record for the Chimaera Cestodarian. *Caribbean Journal of Science* 40: 88–119.
- Clavijo IE, Yntema JA, Ogden JC (1980) An annotated list of the fishes of St. Croix, U.S. Virgin Islands. West Indies Lab, Special Publication, 2nd edn. West Indies Laboratory, Christiansted, 49 pp. <https://doi.org/10.5281/zenodo.5510695>
- DeAngelis BM, McCandless CT, Kohler NE, Recksiek CW, Skomal GB (2008) First characterization of shark nursery habitat in the United States Virgin Islands: Evidence of habitat partitioning by two shark species. *Marine Ecology Progress Series* 358: 257–271. <https://doi.org/10.3354/meps07308>
- Dennis GD (2000) Annotated checklist of shallow-water marine fishes from the Puerto Rico Plateau including Puerto Rico, Culebra, Vieques, St. Thomas, St. John, Tortola, Virgin Gorda and Anegada. Florida Caribbean Science Center, Gainesville, [244 + 26] 286 pp. <https://doi.org/10.5281/zenodo.5770763>

- Dennis GD, Hensley D, Colin PL, Kimmel JJ (2004) New Records of Marine Fishes from the Puerto Rican Plateau. *Caribbean Journal of Science* 40: 70–87. <https://doi.org/10.5281/zenodo.5512853>
- Friedlander AM, Jeffrey CFG, Hile SD, Pittman SJ, Monaco ME, Caldow C [Eds] (2013) Coral reef ecosystems of St. John, U.S. Virgin Islands: Spatial and temporal patterns in fish and benthic communities (2001–2009). NOAA Technical Memorandum 152. Silver Spring, MD, 150 pp. <https://repository.library.noaa.gov/view/noaa/789>
- García-Sais JR (2005) Inventory and Atlas of Corals and Coral Reefs, with Emphasis on Deep-Water Coral Reefs from the U. S. Caribbean EEZ Final Report; Caribbean Fishery Management Council San Juan, Puerto Rico, 214 pp. http://sedarweb.org/docs/wsupp/S26_RD_02_deep_reefs_report_2005.pdf
- García-Sais JR, Williams SM, Sabater-Clavell J, Esteves R, Carlo M (2014) Mesophotic benthic habitats and associated reef communities at Lang Bank, St. Croix, USVI. Final Report; Caribbean Fishery Management Council San Juan, Puerto Rico, 124 pp.
- Hanner R, Floyd R, Bernard A, Collette BB, Shivji M (2011) DNA barcoding of billfishes. *Mitochondrial DNA* 22(sup1, S1): 27–36. <https://doi.org/10.3109/19401736.2011.596833>
- Harms-Tuohy CA, Schizas NV, Appeldoorn RS (2016) Use of DNA metabarcoding for stomach content analysis in the invasive lionfish *Pterois volitans* in Puerto Rico. *Marine Ecology Progress Series* 558: 181–191. <https://doi.org/10.3354/meps11738>
- Knudsen SW, Clements KC (2016) World-wide species distributions in the family Kyphosidae (Teleostei: Perciformes). *Molecular Phylogenetics and Evolution* 101: 252–266. <https://doi.org/10.1016/j.ympev.2016.04.037>
- Lamkin JT, Gerard TL, Malca E, Shiroza A, Muhling BA, Davis N, Fuenmayor F, Whitecraft S, Johns L, Smith R, Melo N, Rawson G, Idrisi N, Smith T, Brown K (2009) USVI larval reef fish supply study: 2007-08 report. Coral Reef Conservation Program (U.S.). U.S. Dept. of Commerce, National Oceanic and Atmospheric Administration, Southeast Fisheries Science Center, Miami, 43 pp. <https://repository.library.noaa.gov/view/noaa/548>
- Loftus WF (2003) Inventory of fishes in inland fresh and brackish-water habitats of Virgin Island National Park. Final Report, U.S. Inventory and Monitoring Program 3207–24F29 VIIS-1102, 52 pp. <https://irma.nps.gov/DataStore/Reference/Profile/2175778>
- Nelson WR, Appeldoorn RS (1985) Cruise Report R/V Seward Johnson. A Submersible Survey of the Continental Slope of Puerto Rico and the U.S. Virgin Islands, 1–23 October 1985, 76 pp. https://link.springer.com/chapter/10.1007/978-3-319-92735-0_7
- Pittman SJ, Hile SD, Jeffrey CFG, Caldow C, Kendall MS, Monaco ME, Hillis-Starr Z (2008) Fish assemblages and benthic habitats of Buck Island Reef National Monument (St. Croix, U.S. Virgin Islands) and the surrounding seascape: A characterization of spatial and temporal patterns. NOAA Technical Memorandum NOS NCCOS 71. Silver Spring, MD, 96 pp. https://coastalscience.noaa.gov/data_reports/fish-assemblages-and-benthic-habitats-of-buck-island-reef-national-monument-st-croix-u-s-virgin-islands-and-the-surrounding-seascape-a-characterization-of-spatial-and-temporal-patterns-2/
- Puebla O, Coulmance F, Estape CJ, Morgan Estape A, Robertson DR (2022) A review of 263 years of taxonomic research on *Hypoplectrus* (Perciformes: Serranidae), with a redescription of *Hypoplectrus affinis* (Poey, 1861). *Zootaxa* 5093(2): 101–141. <https://doi.org/10.11646/zootaxa.5093.2.1>

- Quattrini AM, Demopoulos AWJ, Singer R, Roa-Varon A, Chaytor JD (2017) Demersal fish assemblages on seamounts and other rugged features in the northeastern Caribbean. Deep-sea Research. Part I, Oceanographic Research Papers 123: 90–104. <https://doi.org/10.1016/j.dsr.2017.03.009>
- Recksiek C, Wetherbee BM, DeAngelis B (2006) Assessment of the Status of Shark Populations in the USVI. Final Report. University of Rhode Island, Kingston, 22 pp. https://www.ncei.noaa.gov/data/oceans/coris/library/NOAA/CRCP/project/1413/NA04NMF4630343_FinalReport_shark_usvi.pdf
- Robertson DR, Tornabene L (2021) Reef-associated Bony Fishes of the Greater Caribbean: a Checklist (Version 4) [Data set]. Zenodo. <https://doi.org/10.5281/zenodo.5592149>
- Robertson DR, Estapé CJ, Estapé AM, Peña E, Tornabene L, Baldwin CC (2020) The marine fishes of St Eustatius Island, northeastern Caribbean: an annotated, photographic catalog. Zookeys 1007: 145–180. <https://doi.org/10.3897/zookeys.1007.58515>
- Robertson DR, Tornabene L, Lardizabal CC, Baldwin CC (2022) Submersibles greatly enhance research on the diversity of deep-reef fishes in the Greater Caribbean. Frontiers in Marine Science 8: e800250. <https://doi.org/10.3389/fmars.2021.800250>
- Rogers CS, Pietsch TW, Randall JE, Arnold RJ (2010) The Sargassum Frog-fish (*Histrio histrio* Linnaeus) Observed in Mangroves in St. John, U.S. Virgin Islands. Coral Reefs 29(3): 577. <https://doi.org/10.1007/s00338-010-0636-z>
- Rohmann SO, Hayes JJ, Newhall RC, Monaco ME, Grigg RW (2005) The area of potential shallow-water tropical and subtropical coral ecosystems in the United States. Coral Reefs 24(3): 370–383. <https://doi.org/10.1007/s00338-005-0014-4>
- Smith-Vaniz W, Jelks HL (2014) Marine and inland fishes of St. Croix, U. S. Virgin Islands: an annotated checklist. Zootaxa 3803: 1–120. <https://doi.org/10.11646/zootaxa.3803.1.1>
- Smith-Vaniz W, Jelks HL, Rocha LA (2006) Relevance of cryptic fishes in biodiversity assessments: A case study at Buck Island Reef National Monument, St. Croix. Bulletin of Marine Science 79: 17–48. <https://www.ingentaconnect.com/content/umrsmas/bull-mar/2006/00000079/00000001/art00002>
- Starck WA, Estapé CJ, Morgan Estapé A (2017) The fishes of Alligator Reef and environs in the Florida Keys: A half-century update. Journal of the Ocean Science Foundation 27: 74–117. <https://doi.org/10.5281/ZENODO.851651>
- Thacker CE (2009) Phylogeny of Gobioidae and placement within Acanthomorpha, with a new classification and investigation of diversification and character evolution. Copeia 2009(1): 93–104. <https://doi.org/10.1643/CI-08-004>
- Valdez-Moreno M, Vásquez-Yeomans L, Elías-Gutiérrez M, Ivanova NV, Hebert PDN (2010) Using DNA barcodes to connect adults and early life stages of marine fishes from the Yucatan Peninsula, Mexico: Potential in fisheries management. Marine and Freshwater Research 61(6): 655–671. <https://doi.org/10.1071/MF09222>
- Victor BC, Valdez-Moreno M, Vasquez-Yeomans L (2015) Status of DNA Barcoding Coverage for the Tropical Western Atlantic Shore-fishes and Reef Fishes. DNA Barcodes 3(1): 89–93. <https://doi.org/10.1515/dna-2015-0011>

Ward RD, Hanner R, Hebert PDN (2009) The campaign to DNA barcode all fishes, FISH-BOL. *Journal of Fish Biology* 74(2): 329–356. <https://doi.org/10.1111/j.1095-8649.2008.02080.x>

Weigt LA, Baldwin CC, Driskell A, Smith DG, Ormos A, Reyler EA (2012) Using DNA Barcoding to Assess Caribbean Reef Fish Biodiversity: Expanding Taxonomic and Geographic Coverage. *PLoS ONE* 7(7): e41059. <https://doi.org/10.1371/journal.pone.0041059>

Supplementary material 1

Plates S1–S18

Authors: D. Ross Robertson, Carlos J. Estapé, Allison M. Estapé, Lee Richter, Ernesto Peña, Benjamin Victor

Data type: images (jpg, images in ZIP arhiv)

Explanation note: Fishes of St. Croix (Plate S1), fishes of St. John-Thomas (Plates S2–S18).

Copyright notice: This dataset is made available under the Open Database License (<http://opendatacommons.org/licenses/odbl/1.0/>). The Open Database License (ODbL) is a license agreement intended to allow users to freely share, modify, and use this Dataset while maintaining this same freedom for others, provided that the original source and author(s) are credited.

Link: <https://doi.org/10.3897/zookeys.1103.83795.suppl1>

Supplementary material 2

File S1

Authors: D. Ross Robertson, Carlos J. Estapé, Allison M. Estapé, Lee Richter, Ernesto Peña, Benjamin Victor

Data type: image (jpg file)

Explanation note: Bathymetry of the US Virgin Islands.

Copyright notice: This dataset is made available under the Open Database License (<http://opendatacommons.org/licenses/odbl/1.0/>). The Open Database License (ODbL) is a license agreement intended to allow users to freely share, modify, and use this Dataset while maintaining this same freedom for others, provided that the original source and author(s) are credited.

Link: <https://doi.org/10.3897/zookeys.1103.83795.suppl2>

Supplementary material 3

File S2

Authors: D. Ross Robertson, Carlos J. Estapé, Allison M. Estapé, Lee Richter, Ernesto Peña, Benjamin Victor

Data type: GPS data (excel file)

Explanation note: File S2A: Georeferencing coordinates and site codes for dive sites of authors Carlos and Allison Estapé at St John, St Thomas and St. Croix during 2021. File S2B: Georeferencing coordinates and site codes for dive sites used by non-author photographers at St John-Thomas. File S2C: Names and emails of third party Citizen Scientists who provided voucher images of various St John-Thomas fishes.

Copyright notice: This dataset is made available under the Open Database License (<http://opendatacommons.org/licenses/odbl/1.0/>). The Open Database License (ODbL) is a license agreement intended to allow users to freely share, modify, and use this Dataset while maintaining this same freedom for others, provided that the original source and author(s) are credited.

Link: <https://doi.org/10.3897/zookeys.1103.83795.suppl3>

Supplementary material 4

File S3

Authors: D. Ross Robertson, Carlos J. Estapé, Allison M. Estapé, Lee Richter, Ernesto Peña, Benjamin Victor

Data type: GPS data (kmz. file)

Explanation note: KMZ file of USVI dive sites.

Copyright notice: This dataset is made available under the Open Database License (<http://opendatacommons.org/licenses/odbl/1.0/>). The Open Database License (ODbL) is a license agreement intended to allow users to freely share, modify, and use this Dataset while maintaining this same freedom for others, provided that the original source and author(s) are credited.

Link: <https://doi.org/10.3897/zookeys.1103.83795.suppl4>

Supplementary material 5

File S4

Authors: D. Ross Robertson, Carlos J. Estapé, Allison M. Estapé, Lee Richter, Ernesto Peña, Benjamin Victor

Data type: occurrences (excel file)

Explanation note: File S4. Native marine fish faunas of St. John-Thomas and St. Croix.

Copyright notice: This dataset is made available under the Open Database License (<http://opendatacommons.org/licenses/odbl/1.0/>). The Open Database License (ODbL) is a license agreement intended to allow users to freely share, modify, and use this Dataset while maintaining this same freedom for others, provided that the original source and author(s) are credited.

Link: <https://doi.org/10.3897/zookeys.1103.83795.suppl5>

Supplementary material 6

File S5

Authors: D. Ross Robertson, Carlos J. Estapé, Allison M. Estapé, Lee Richter, Ernesto Peña, Benjamin Victor

Data type: occurrences (excel file)

Explanation note: Ecological Characteristics of Reef-Associated Bony Fishes from St John-Thomas. See Methods of paper for details.

Copyright notice: This dataset is made available under the Open Database License (<http://opendatacommons.org/licenses/odbl/1.0/>). The Open Database License (ODbL) is a license agreement intended to allow users to freely share, modify, and use this Dataset while maintaining this same freedom for others, provided that the original source and author(s) are credited.

Link: <https://doi.org/10.3897/zookeys.1103.83795.suppl6>

Supplementary material 7

File S6

Authors: D. Ross Robertson, Carlos J. Estapé, Allison M. Estapé, Lee Richter, Ernesto Peña, Benjamin Victor

Data type: genomic (excel file)

Explanation note: File S6: mtDNA-Barcode information for fishes from islands on the Puerto Rico Platform (St John-Thomas, Puerto Rico and the British Virgin Islands) and St. Croix. For coding of differently colored highlighting see bottom of table. For explanations of "Reef Associated" and "Deep" see main text.

Copyright notice: This dataset is made available under the Open Database License (<http://opendatacommons.org/licenses/odbl/1.0/>). The Open Database License (ODbL) is a license agreement intended to allow users to freely share, modify, and use this Dataset while maintaining this same freedom for others, provided that the original source and author(s) are credited.

Link: <https://doi.org/10.3897/zookeys.1103.83795.suppl7>

Descriptions of two new flightless species of *Pseudocsikia* Schimmel & Platia (Coleoptera, Elateridae, Dimini) from Taiwan Island, China, with a definition of the *formosana* species-group

Lu Qiu¹, Robin Kundrata²

1 Engineering Research Center for Forest and Grassland Disaster Prevention and Reduction, Mianyang Normal University, Mianxing West Road, 621000, Mianyang, China **2** Department of Zoology, Faculty of Science, Palacky University, 17. listopadu 50, 77146, Olomouc, Czech Republic

Corresponding author: Lu Qiu (123church@163.com)

Academic editor: Hume Douglas | Received 18 March 2022 | Accepted 10 May 2022 | Published 1 June 2022

<http://zoobank.org/58199DE7-FAD7-43E1-A029-DC969C6E9BFC>

Citation: Qiu L, Kundrata R (2022) Descriptions of two new flightless species of *Pseudocsikia* Schimmel & Platia (Coleoptera, Elateridae, Dimini) from Taiwan Island, China, with a definition of the *formosana* species-group. ZooKeys 1103: 123–138. <https://doi.org/10.3897/zookeys.1103.84015>

Abstract

Two new flightless click beetle species, *Pseudocsikia choui* **sp. nov.** and *Pseudocsikia chanjuan* **sp. nov.**, are described and illustrated from Taiwan, China. Their habitus and diagnostic characters are illustrated. The two species most resemble *P. formosana*, which is endemic to Taiwan, by the strongly protruding pronotal anterior angles accompanied by pits and the shape of aedeagus. They can be all grouped as the *P. formosana*-species group. A key to the species of the *P. formosana*-species group and an updated checklist of Chinese *Pseudocsikia* with supplementary notes on type localities are provided. The discovery of two new species highlights the potential species-richness of the flightless click-beetles on Taiwan Island.

Keywords

China, Dendrometrinae, Elateroidea, flightlessness, new species, Taiwan

Introduction

Pseudocsikia Schimmel & Platia, 1991 (Elateridae, Dendrometrinae, Dimini) is a small genus of click-beetles known from China, Myanmar, Laos, India, and Nepal (Kundrata et al. 2018). Schimmel and Platia (1991) established this genus for two species, *P. rustica* Schimmel & Platia, 1991 and *P. laticollis* Schimmel & Platia, 1991, both from Nepal. Later, Schimmel (1993, 1996a) transferred five species from other genera to *Pseudocsikia*: *Csikia formosana* Ôhira, 1972 from Taiwan Island, China, *Csikia manipurensis* Schimmel & Platia, 1992 from India, *Penia birmanica* Candèze, 1888 and *Penia fausta* Candèze, 1888 from Myanmar, and *Penia dorsalis* Fleutiaux, 1936 from Laos. Schimmel (1996b, 2006) described three more species in the genus, *Pseudocsikia gaoligongshana* Schimmel, 1996 and *P. turnai* Schimmel, 2006 from mainland China, and *P. phongsalyana* Schimmel, 2006 from Laos. Hence, 10 species are currently included in this genus (Kundrata et al. 2018).

Although several works (Schimmel and Platia 1991; Schimmel 1993, 1996a, 1996b, 2006) contributed to the knowledge of *Pseudocsikia*, the generic concept remains been vague. Only Schimmel and Platia (1991) and Schimmel (1996a) fundamentally defined the genus. According to these works, *Pseudocsikia* can be distinguished among Dimini by the following combination of characters: pronotum widest near the middle, as wide as or wider than elytra, hind angles long, pointed and extended straight toward the base of elytra, elytra short, arched laterally in dorsal view, tarsomeres III–IV lobate ventrally, metacoxal plate covering near half or more of metatrochanter.

Here, we describe two new *Pseudocsikia* species from Taiwan Island, China. Both species are flightless and share many similar characters with *P. formosana*, which is also known from Taiwan. A species group is defined to include these three species. The discovery of these species suggests that the flightless Dimini in China can be species-rich not only in the mainland habitats but also on continental islands.

Material and methods

The specimens were softened in hot water, and genital segments were excised and dissected after treatment in 80 °C 10% KOH for 10 min. Habitus images were photographed using a Canon EOS RP + Mount Adapter EF-EOS R + a Laowa 25 mm F2.8 2.5–5× Ultra Macro Lens (for Canon EF); diagnostic characters were made using a Leica M205A stereomicroscope and a Leica DFC 550. All figures (Figs 1–5) were modified in Adobe Photoshop CC 2019. Body length was measured from the anterior margin of the head to the apex of the elytra, pronotal length was measured at midline, pronotal width was measured both at the widest point and between hind angles, and body width was measured at the widest place of the elytra. The generic concept of *Pseudocsikia* follows Schimmel and Platia (1991) and Schimmel (1996a). The holotypes of the new species are deposited in the Invertebrate Collection of Mianyang Normal Uni-

versity, Mianyang, Sichuan, China (MYNU). The holotype and one paratype of *P. formosana* are deposited in the Bernice Pauahi Bishop Museum, Honolulu, Hawaii, USA (BPBM). The collecting data is quoted verbatim (in Chinese) in quotation marks. Translation of the data, as well as additional information, is given in square brackets.

Systematics

Genus *Pseudocsikia* Schimmel & Platia, 1991

Chinese common name: 伪斯叩甲属

Pseudocsikia Schimmel & Platia, 1991: 357 (original description); Schimmel 1996a: 203 (revision); Cate et al. 2007: 186 (catalogue); Kundrata et al. 2018: 65 (catalogue).

Type species. *Pseudocsikia rustica* Schimmel & Platia, 1991.

Pseudocsikia formosana-species group, here defined

Diagnosis. Anterior angles of pronotum lateroapically protruded, with anterior edge of pronotum mesally concave in dorsal view. Each protrusion with sides almost parallel in dorsal view, with concavity laterally and a deep pit at basal portion (Figs 2E, 3C, 4C). Hypomeron with long carination parallel to pronotosternal suture and following curved outline of anterior protrusion of hypomeron, with small pit on the inside edge (Figs 2F, 3D, 4D). Male genitalia (Fig. 5) with robust median lobe, distal half enlarged, variously shaped. Parameres short, stout, about half as long as median lobe. Phallobase with thickened outlines, and medially with longitudinal line.

Remarks. The *P. formosana*-species group is known only from Taiwan and is possibly endemic. All three species are easily distinguished from congeners by the structure of anterior angles of pronotum, which are stoutly protruded, with a abrupt concavity laterally, and with a large deep pit at the basal portion of each protrusion. Such characters are not present in the type species of *Pseudocsikia*, *P. rustica* (Schimmel and Platia 1991), or any other *Pseudocsikia* species (Schimmel and Platia 1991; Schimmel 1993, 1996a, 1996b, 2006). Within Dimini, protruded anterior angles of pronotum can be found in several other Dimini, like for example, *Platiana* Schimmel, 1993 or most species of *Parapenia* Suzuki, 1982 (Suzuki 1982; Schimmel 1996a), but the protrusions in these species are more or less gradually narrowed to a point, and either with larger pits located anteriorly or with only small, shallow pits. These unique characters of Taiwanese *Pseudocsikia* suggest a possible need for a new genus to accommodate them. However, they should be kept in *Pseudocsikia* until evidence from a detailed revision or phylogeny is available.

Species included. *Pseudocsikia formosana* (Ôhira, 1972), *P. choui* sp. nov., *P. chanjuan* sp. nov.

Distribution. China (Taiwan).

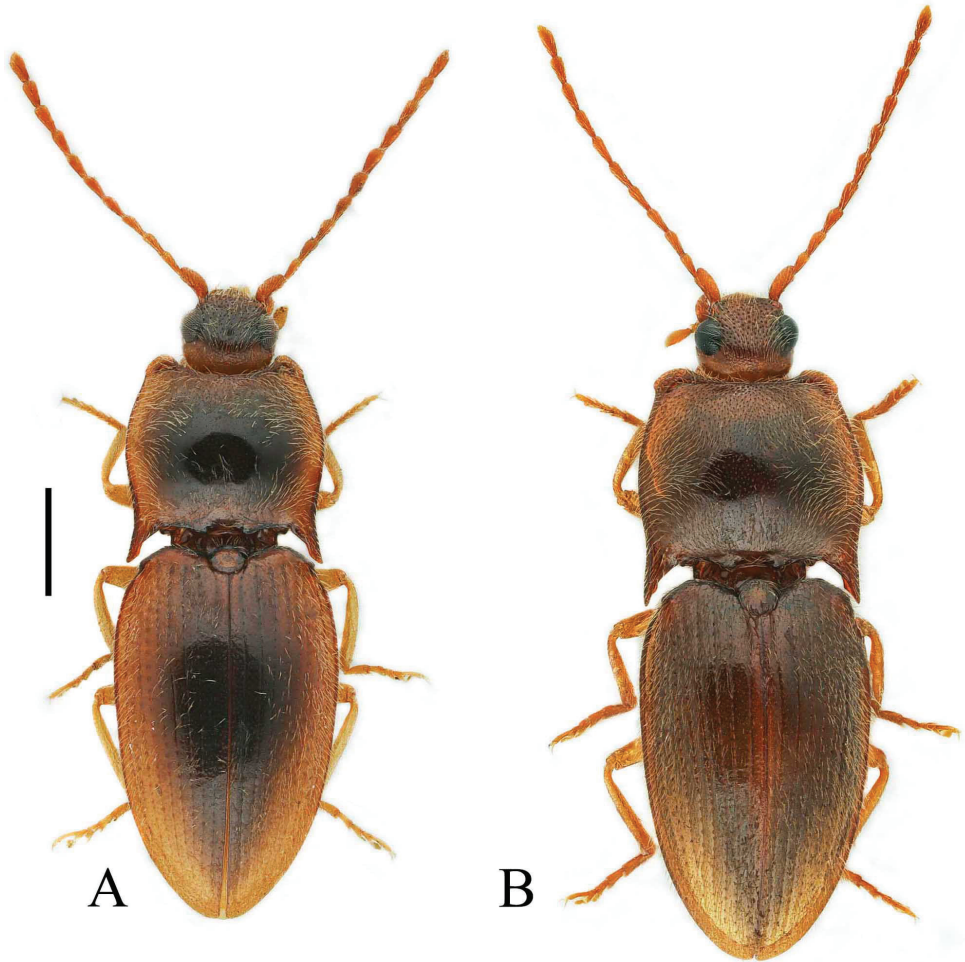


Figure 1. Habitus of *Pseudocsikia* spp. **A** *Pseudocsikia choui* sp. nov., male holotype, dorsal view **B** *Pseudocsikia chanjuan* sp. nov., male holotype, dorsal view. Scale bar: 1.0 mm.

***Pseudocsikia choui* sp. nov.**

<http://zoobank.org/9AD84855-59B9-4C47-9734-FC6A2AAC723E>

Figs 1A, 3A–H, 5A–F

Type material. *Holotype*, male, “2017.IX.13,台湾嘉义县阿里山二万坪, 2000m, 周文一” [Erwanping, Mount Alishan, Chiayi County, Taiwan, 2000 m, 13.IX.2017, Wen-I Chou leg.], “*Pseudocsikia choui* sp. nov. 周氏伪斯叩甲 HOLOTYPE des. Qiu et Kundrata 2022” (MYNU).

Diagnosis. Head, pronotum, and elytra dark brown, with paler lateral portions of pronotum and elytra, legs yellow (Fig. 1A). Antennomere II subequal in length to antennomere III. Pronotum (Fig. 3A) smooth, with sparse punctures (intervals usually equal to 4–6 puncture diameters). Anterior angle of pronotum with apex of protrusion closer to

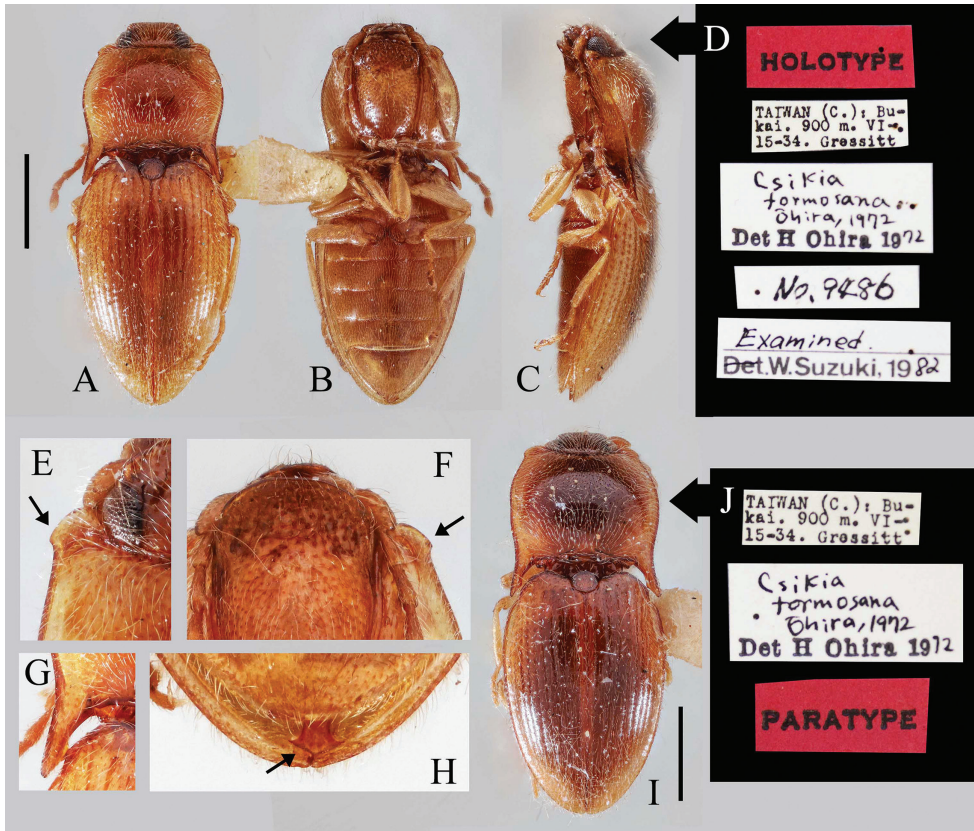


Figure 2. Habitus and characters of *Pseudocsikia formosana* (Ohira, 1972) **A–H** male holotype **A** habitus, dorsal view **B** habitus, ventral view **C** habitus, lateral view **D** labels **E** anterior protrusion of pronotum (indicated by an arrow), dorsal view **F** anterior protrusion of hypomeron (indicated by an arrow), ventral view **G** posterior angle of pronotum, dorsal view **H** abdominal tip, ventral view (arrow indicates the apex of median lobe) **I, J** paratype of an unknown sex **I** habitus, dorsal view **J** labels. Scale bars: 1.0 mm (**A–C, I**); **E–H** not to scale. All photos provided by Jeremy Frank (BPBM).

inner angle. Posterior angles divergent. Metaventricle sparsely punctate, intervals between punctures on average subequal to 2–5 puncture diameters. Metacoxal plate (Fig. 3G) enlarged mesally, sparsely punctate. Tergite IX (Fig. 5B) subtriangular, with two narrow lobes. Aedeagus with median lobe with acute lateral projections near midlength, narrowed to apex, apex blunt with small acute lateral projections. Paramere with apex pointed and projecting laterad. Phallobase with basal angles rounded (Fig. 5D).

Comparison. This species superficially resembles *P. fimosana* by the pale coloration of its pronotum and elytral sides and by the sparse punctures of pronotum, but it can be easily distinguished from the latter by the larger body length (5.9 mm, while 4.0 mm in *P. formosana*), darker coloration of pronotum and elytra medially, more forwardly protruded anterior angles of pronotum (pointing more outward in the pronotum of *P. formosana*), and shorter and more divergent posterior angle of pronotum (longer, more robust and nearly straight in *P. formosana*). The shape of aedeagus also readily differentiates these two

species. Based on the illustration of Ôhira (1972: fig. 3), the distal half of the median lobe of *P. formosana* has four large acute processes laterally, and its apex is somewhat rectangular; and the paramere of *P. formosana* has the apex rounded and slightly outward.

Description (male holotype). Body smooth, surface covered with curved, semi-erect, and moderately long pubescence. Body length 5.9 mm; width 2.2 mm; antenna length 3.0 mm; pronotum length 1.4 mm, pronotum width 1.9 mm (measured at posterior angles), elytra length 3.5 mm.

Body brown, pubescence yellow (Fig. 1A). Head dark brown, antennae yellowish brown, labrum and mandibles brown, remaining mouthparts yellowish brown. Pronotum dark brown centrally; lateral, anterior and hind portions, and hind angles yellowish brown, with darker outlined margins. Scutellar shield brown, with dark outlined margins, especially anteriorly. Elytra dark brown centrally, yellowish brown laterally; yellowish-brown portions gradually lightened toward apices, basal margins of elytra dark outlined. Underside reddish brown, prosternum darker than hypomeron, sternites VI–VII and legs yellow.

Head including eyes 0.5 times as wide as pronotum. Supra-antennal carinae short, directed mesad and fading medially so that median portion of frontoclypeus is not formed by sharp carina; frontoclypeus overhanging base of labrum in lateral view. Head surface sparsely punctate; punctures small, intervals between punctures mostly equal 2–3 puncture diameters. Maxillary palpus with palpomere III longer than wide. Antenna (Fig. 3E) surpassing hind angle of pronotum by about one antennomere; scape robust and longest, remaining antennomeres subequal in length; ultimate antennomere obliquely truncate, with apex rounded.

Pronotum (Fig. 3A) wider than long (measured at midline), widest near middle. In lateral view, pronotum convex. Anterior angles of pronotum protruding (Fig. 3C); protrusion of anterior angle subquadrate, inner angle more protruded than outer angle, posterior part of protrusion with deep, crescent-shape pit. Lateral margins of pronotum arched medially, sides near middle narrowing anteriorly and posteriorly, anteriorly narrowing more sharply than posteriorly; posterior angles (Fig. 3F) long, slightly divergent, apical portion of posterior angle slightly enlarged, then narrowed, apex blunt. Disc of pronotum sparsely covered with small, shallow punctures; intervals between punctures on average subequal to four to six puncture diameters; interstices smooth. Pubescence mostly directed outwards; basal portion directed anteriorly.

Hypomeron (Fig. 3B) more densely punctate than pronotum, punctures small and shallow, intervals between punctures on average subequal to 3–4 puncture diameters; apex of hypomeron strongly protruded, margin wrinkled. Pronotosternal sutures nearly straight, anterior excavation wide, long carination paralleled with suture from base of hypomeron and reaching anterior protrusion of hypomeron, forming hook-shaped carination anteriorly, end of the carination slightly extending backwards, with a small pit partly enclosed by curving hook of carination (Fig. 3D). Prosternum (Fig. 3B) including prosternal process about 2.00 times as long as wide; chin piece with large, dense punctures, intervals between punctures approximately one puncture diameter; punctures in remaining area sparser and smaller, intervals between punctures 3–6

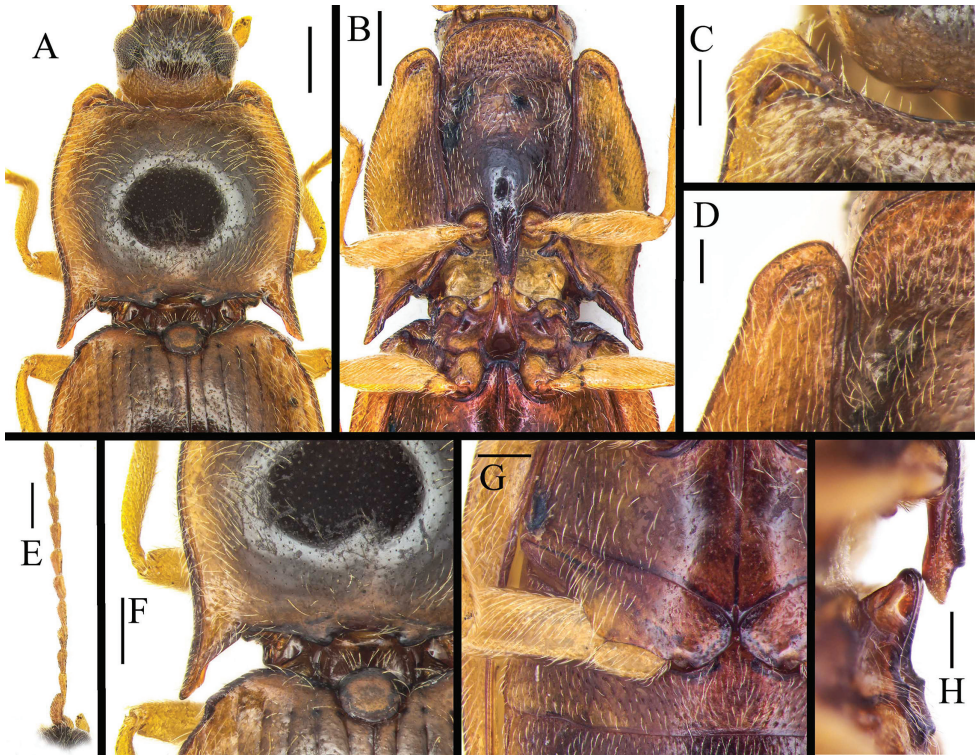


Figure 3. Characters of *Pseudocsikia choui* sp. nov., male, holotype **A** pronotum, dorsal view **B** pro- and mesothorax, ventral view **C** anterior protrusion of pronotum, dorsal view **D** anterior protrusion of hypomerion, ventral view **E** antenna **F** posterior angle of pronotum, dorsal view **G** metacoxal plate, ventral view **H** prosternal process, lateral view. Scale bars: 0.5 mm (**A, B, E, F**); 0.2 mm (**C, D, G, H**).

puncture diameters, punctures on prosternal process sparse, small. Prosternal process (Fig. 3H) with ventral surface horizontal in lateral view, with elongate notch ventroapically, roundly enlarged dorsoapically.

Scutellar shield (Fig. 3F) suboval, about 1.2 times as wide as long; anterior margin rounded, posterior margin slightly pointed. Mesoventrite (Fig. 3B) with deep procoxal rests. Mesoventral process elevated, hind margin wide. Mesanepisternum with large, curved lateral extensions of procoxal rests. Metaventrite medially with sparse punctures, intervals between punctures on average subequal to 3–5 puncture diameters. Anterior portion of discrimen with sharp groove, occupying half-length of metaventrite. Metacoxal plate enlarged inward, narrowed laterad (Fig. 3G), surface with very sparse punctures.

Elytra (Fig. 1A) elongate, together 1.6 times as long as wide, widest at 1/3 of their length from base. Humeri (Fig. 3A, F) elevated. Sides from humeri roundly widened to 1/3 of elytral length in dorsal view, then gradually narrowed towards apices; apices slightly independently rounded. Elytral striae shallow, formed by lines of small punctures, intervals between punctures in stria on average subequal to 2–3 puncture diameters. Interstriae flat, smooth, with some micropunctures. Hind wings

absent. Abdomen with ventrites more densely punctate than pronotum, intervals between punctures on average subequal to 2–3 puncture diameters; pubescence directed backwards. Apical ventrite with blunt apex. Tergite VIII (Fig. 5C) subtriangular, 1.6 times as long as wide, distal margin pointed medially, apically covered with sparse pubescence. Sternite VIII with two dark colored lobes, shape as Fig. 5C, with long setae, remaining portion membranous. Tergite IX (Fig. 5B) subtriangular, 1.3 times as long as wide, medially deeply emarginate; two lobes elongate, lateral sides with long setae; tergite X (Fig. 5B) membranous, exceeding apices of lobes of tergite IX. Sternite IX (Fig. 5A) slightly stout, 2.7 times as long as wide, apically widely rounded and setose.

Aedeagus (Fig. 5D–F) with robust median lobe, two times as long as one paramere; distal half of median lobe arrow-shaped, apex with small protrusion, apex blunt, laterally with small acute projections; long, needle-like sclerite present on ventral side of median lobe. Paramere stout, reaching half of median lobe; apex pointed outward. Phallobase subquadrate, margins thickened, medially with longitudinal thickened line, basal angles rounded.

Female. Unknown.

Immature stages. Unknown.

Distribution. China: Taiwan (Chiayi).

Etymology. The specific patronymic epithet is dedicated to Dr Wen-I Chou (Taiwan, China), the collector of the holotype.

***Pseudocsikia chanjuan* sp. nov.**

<http://zoobank.org/835DC83E-6E39-437D-8A81-7C78F81757A9>

Figs 1B, 4A–H, 5G–L

Type material. *Holotype*, male, “2017.IX.16, 台湾台东县金峰乡太麻里山, 1300 m, 周文一” [Mount Taimalishan, Taitung County, Taiwan, 1300 m, 16.IX.2017, Wen-I Chou leg.], “*Pseudocsikia chanjuan* sp. nov. 婵娟伪斯叩甲 HOLOTYPE des. Qiu et Kundrata 2022” (MYNU).

Diagnosis. Pronotum and elytra almost unicolored brown, but with paler apices of elytra and lateral margins of pronotum (in dry specimen condition), legs yellow (Fig. 1B). Antennomere II shorter than the length of antennomere III. Pronotum (Fig. 4A) with dense punctures (intervals usually subequal to 2–4 puncture diameters). Anterior angle of pronotum with the protrusion outward at outer angle. Posterior angle straight. Metaventricle densely punctate, intervals between punctures on average subequal to 2–3 puncture diameters. Metacoxal plate (Fig. 4G) short internally, surface densely covered with punctures. Tergite IX (Fig. 5H) suboval, with two robust lobes. Median lobe with small lateral pointed process near midlength, apical portion rounded and enlarged. Paramere with rounded apex and small process subapically. Phallobase subtrapezoidal, with slightly pointed basal angles (Fig. 5J).

Comparison. This species can be distinguished from *P. formosana* and *P. choui* sp. nov. by the denser punctures of pronotum and larger body size (6.3 mm versus 4.0–5.9 mm). This new species can be further distinguished from *P. choui* sp. nov. by

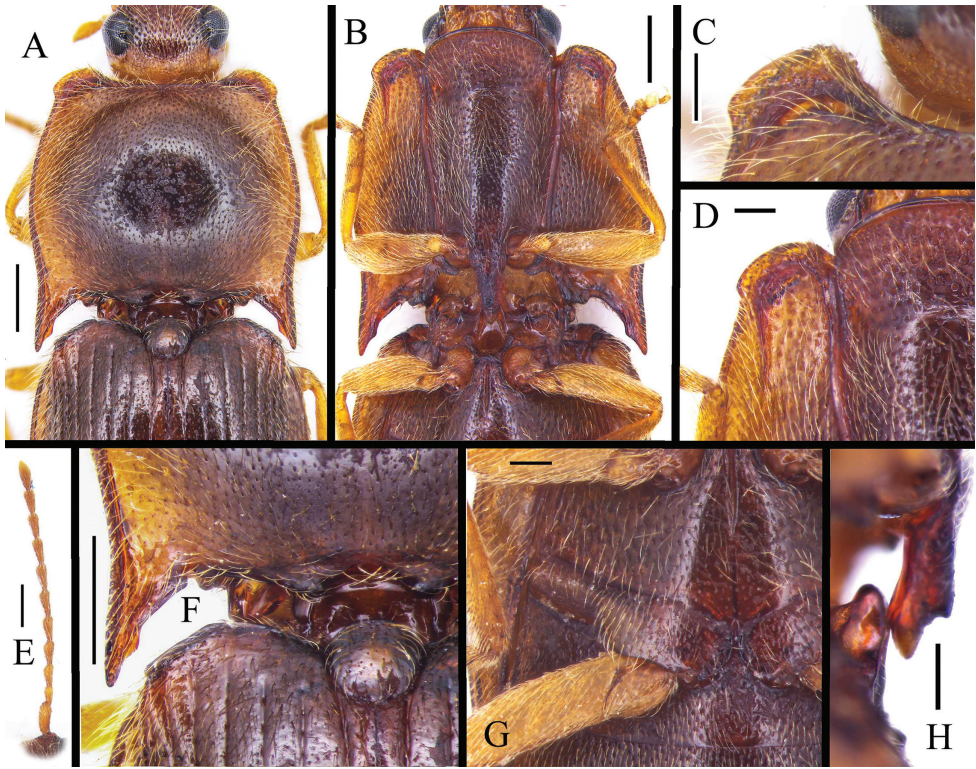


Figure 4. Characters of *Pseudocsikia chanjuan* sp. nov., male, holotype **A** pronotum, dorsal view **B** pronotum and mesothorax, ventral view **C** anterior protrusion of pronotum, dorsal view **D** anterior protrusion of hypomeron, ventral view **E** antenna **F** posterior angle of pronotum, dorsal view **G** metacoxal plate, ventral view **H** prosternal process, lateral view. Scale bars: 0.5 mm (**A, B, E, F**); 0.2 mm (**C, D, G, H**).

the more outwardly protruded anterior angles of pronotum, and the larger and straight posterior angle of pronotum. The shape of aedeagus also differs from these. The median lobe of *P. chanjuan* sp. nov. has a slightly enlarged and rounded apex and two small acute processes laterally near midlength, its paramere is rounded at apex but with small process subapically, and the phallobase is less rounded basally than those of the other two species.

Description (male holotype). Body smooth, surface covered with curved, semi-erect, and moderately long pubescence. Body length 6.3 mm; width 2.3 mm; antenna length 3.3 mm; pronotum length 1.7 mm, width 2.1 mm (measured at hind angles), elytra length 3.7 mm.

Body generally brown, pubescence yellow (Fig. 1B). Head (including antennae and mouthparts), pronotum, elytra (except apical portions), underside (except last two sternites and lateral portion of abdomen) brown. Pronotum with paler lateral margins (in dry condition). Legs, apical portion of elytra, the last two sternites, and lateral portion of abdomen yellowish brown.

Head including eyes 0.5 times as wide as pronotum. Supra-antennal carinae short, directed mesad and fading medially so that median portion of frontoclypeus is not

formed by sharp carina; frontoclypeus overhanging base of labrum in lateral view. Head surface with intervals between punctures mostly equal 1–2 puncture diameters. Maxillary palpus with palpomere III longer than wide. Antenna (Fig. 4E) simple, surpassing hind angle of pronotum about $1\frac{1}{2}$ antennomeres; scape robust and longest, antennomere II shortest, antennomere III longer than antennomere II, antennomeres IV–X subequal in length, ratio of antennomeres II–IV and XI = 1: 1.1: 1.3: 1.5, ultimate antennomere tapered apically, apex pointed.

Pronotum (Fig. 4A) large, subquadrate, wider than long (measured at midlines), widest near middle. In lateral view, pronotum convex. Anterior angles (Fig. 4C) of pronotum protruded, protrusion of anterior angle subquadrate, inner angle protruded almost same degree as outer angle; protrusion with deep, narrow and curved gap. Lateral margins of pronotum roundly arched medially, sides near middle more or less evenly narrowing anterad and posterad in similar degree, posterior angle (Fig. 4F) straight, less divergent, pointing straightly toward elytra, apex blunt, inner margin with small protrusion. Disc of pronotum densely covered with small, deep punctures; intervals between punctures on average subequal to 2–4 puncture diameters; interstices smooth. Pubescence directed outwards; basal portion directed forwards.

Hypomeron (Fig. 4B) more densely punctate than pronotum, punctures moderate and deep, intervals between punctures on average subequal to 1–2 puncture diameters, apex of hypomeron strongly protruded, margin wrinkled. Pronotosternal sutures nearly straight, anterior excavation deep and narrow; long carination paralleled with suture from base of hypomeron and reaching anterior protrusion of hypomeron, forming elongate U-shaped carination anteriorly; end of the carination extending backwards, with a straight, elongate pit partly enclosed by curving hook of carination (Fig. 4D). Prosternum (Fig. 4B) including prosteral process 2.2 times as long as wide; chin piece with dense and large punctures, intervals between punctures on average subequal to half to one puncture diameter; punctures in remaining area slightly sparser and smaller, intervals between punctures on average subequal to 1–2 puncture diameters. Prosteral process (Fig. 4H) ventrally straight in lateral view, ventroapically with notch; small process in notch acutely enlarged dorsoapically.

Scutellar shield (Fig. 4A, F) suboval, about 1.2 times as wide as long; anterior margin rounded, posterior margin slightly pointed.

Mesoventrite (Fig. 4B) with procoxal rests. Mesoventral process elevated, hind margin narrow. Mesanepisternum with large, curved lateral extensions of procoxal rests. Metaventrite medially with dense punctures, intervals between punctures on average subequal to 2–3 puncture diameters. Anterior portion of discrimen with needle-like groove, occupying half-length of metaventrite. Metacoxal plate enlarged inward, strongly reduced outward (Fig. 4G), surface densely punctate.

Elytra (Fig. 1B) elongate, together 1.7 times as long as wide, widest at $\frac{1}{3}$ of their length from base. Humeri (Fig. 4A, F) elevated, sides from humeri roundly widened to $\frac{1}{3}$ of elytral length, then gradually narrowed towards apices; apices slightly independently rounded. Elytral striae shallow, formed by lines of small punctures, intervals between punctures in stria on average subequal to 2–4 puncture diameters. Interstriae flat, smooth, with some micropunctures. Hind wings absent. Abdomen with ventrites

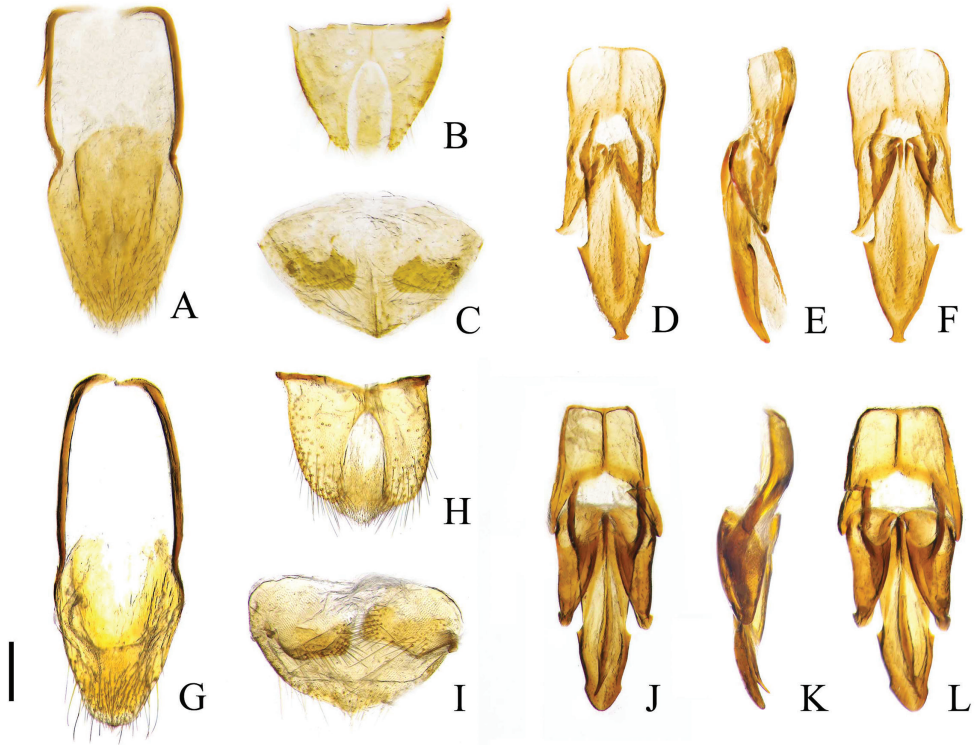


Figure 5. Characters of *Pseudocsikia* spp. **A–F** *Pseudocsikia choui* sp. nov., male holotype **G–L** *Pseudocsikia chanjuan* sp. nov., male, holotype **A, G** abdominal sternite IX, dorsal view **B, H** abdominal tergites IX–X, dorsal view **C, I** abdominal sternite VIII and tergite VIII, ventral view **D, J** aedeagus, ventral view **E, K** aedeagus, lateral view **F, L** aedeagus, dorsal view. Scale bar: 0.2 mm.

more densely punctate than pronotum, intervals between punctures on average subequal to one puncture diameter; pubescence directed backwards. Apical ventrite with rounded apex. Tergite VIII (Fig. 5I) subtriangular, 1.7 times as long as wide, distal margin pointed medially, apically covered with sparse pubescence, basal angles rounded. Sternite VIII (Fig. 5I) with two dark-colored lobes, shape as Fig. 5I with long setae, remaining portion membranous. Tergite IX (Fig. 5H) semi-oval, 1.2 times as long as wide, medially deeply and widely emarginate; two lobes robust, lateral sides with long setae; tergite X (Fig. 5H) membranous, exceeded apices of lobes of tergite IX. Sternite IX (Fig. 5G) relatively narrow, 2.66 times as long as wide, apically truncate and setose.

Aedeagus (Fig. 5J–L) with robust median lobe, 1.7 times as long as one paramere; distal half of median lobe gradually narrowed to a rounded point, with one small pointed processes on each lateral side near midlength, apical portion enlarged, apex bluntly rounded; median lobe with long, needle-like ventral sclerite. Paramere stout, slightly exceeding half of median lobe; apex rounded, with small process subapically. Phallobase trapezoidal, margins thickened, medially with longitudinal thickened line, basal angles angled.

Female. Unknown.

Immature stages. Unknown.

Distribution. China: Taiwan (Taitung).

Etymology. The specific epithet *Chanjuan* is derived from the Chinese 婵娟 [chán juān], which means “beauty”.

***Pseudocsikia formosana* (Ôhira, 1972)**

Fig. 2A–J

Csikia formosana Ôhira, 1972: 8 (original description); Bouwer 1991: 57 (checklist); Jiang 1993: 146 (catalogue); Suzuki 1999: 120 (catalogue).

Pseudocsikia formosana (Ôhira, 1972): Schimmel 1993: 255 (new combination); Schimmel 1996a: 204 (diagnosis); Cate et al. 2007: 186 (catalogue); Kundrata et al. 2018: 66 (catalogue).

Type material. *Holotype* of *Csikia formosana* Ôhira, 1972, male, “TAIWAN (C.): Bu-kai. 900 m. VI.15–34. Gressitt”, “*Csikia formosana* Ôhira, 1972 Det H Ohira 1972”, “HOLOTYPE”, “No. 9486”, “Examined. Det. W. Suzuki, 1982” (BPBM). One *paratype* of *Csikia formosana* Ôhira, 1972, sex unknown, “TAIWAN (C.): Bu-kai. 900 m. VI-15-34. Gressitt”, “*Csikia formosana* Ohira, 1972 Det H Ohira 1972”, “PARATYPE” (BPBM).

Diagnosis. (based on Ôhira 1972 and the figures of holotype and one paratype provided by BPBM). Body length 4.0 mm, width 1.7 mm (based on holotype; see Ôhira 1972). Body reddish brown (examined paratype darker than holotype; Fig. 2A–C, I), outer margins of pronotum and elytra, underside, and legs paler. Antenna exceeding posterior angle of pronotum by about apical two antennomeres (Ôhira 1972). Antennomere II slightly shorter than antennomere III (Ôhira 1972). Punctures on pronotum of moderate size, intervals between punctures mostly equal 3–5 puncture diameters, anterior protrusion of pronotum with apex laterad of center (Fig. 2E, F). Posterior angle (Fig. 2G) of pronotum long, straight and robust, apex blunt, inner margin with obtuse protrusion subapically.

Aedeagus with robust median lobe, twice as long as paramere; with large acute lateral processes near midlength, apex rectangular, with large subapical spines laterally (Fig. 2H) (needle-like ventral sclerite not mentioned in Ôhira 1972 and not observable in this study). Paramere stout, reaching half length of median lobe; apex rounded, slightly outwards. Phallobase subquadrate, margins thickened, medially with longitudinal thickened line, basal angles rounded (based on Ôhira 1972: fig. 3).

Distribution. China: Taiwan (Nantou).

Checklist of *Pseudocsikia* species from China, with notes on their type localities

***Pseudocsikia formosana* (Ôhira, 1972)**

Chinese common name: 台湾伪斯叩甲.

Type locality: “Bukai” (Ôhira 1972).

Note: Bukai is an old name of Fatyu [法治] (or Wuchieh [武界]) (Chu and Yamanaka 1973), Ren'ai township [仁爱乡], Nantou County [南投县], Taiwan.

***Pseudocsikia gaoligongshana* Schimmel, 1996**

Chinese common name: 高黎贡伪斯叩甲.

Type locality: “Yunnan, Gaoligongshan, 100 km westlich von Baoshan [100 km W of Baoshan]” (Schimmel 1996b).

Note: Gaoligongshan [高黎贡山] is an extensive mountain range lying on the border of Yunnan, China and Myanmar; the exact locality information of the holotype is unknown. However, according to the original paper, the holotype was collected 100 km west of Baoshan, which is near Tengchong.

***Pseudocsikia turnai* Schimmel, 2006**

Chinese common name: 图氏伪斯叩甲.

Type locality: “China: Hubei-Provinz, 30 km nordostlich von Hefeng, Mulinzi [30 km NE of Hefeng, Mulinzi]” (Schimmel 2006).

Note: Mulinzi [木林子] is a nature reserve in Hefeng County [鹤峰县], Enshi City [恩施市], Hubei.

***Pseudocsikia choui* Qiu & Kundrata, sp. nov.**

Chinese common name: 周氏伪斯叩甲.

Type locality: Erwanping, Mount Alishan, Chiayi County, Taiwan, 2000 m (this work).

***Pseudocsikia chanjuan* Qiu & Kundrata, sp. nov.**

Chinese common name: 婵娟伪斯叩甲.

Type locality: Mount Taimalishan, Taitung County, Taiwan, 1300 m (this work).

Key to species of *Pseudocsikia formosana*-species group

- 1 Pronotum with anterior angles widely and strongly protruded with lateral concavity, with large pits at posterior part of protrusion in dorsal view..... **2 (*P. formosana*-species group)**
- Pronotum with anterior angles not protruded or simply, gradually and narrowly protruded, and without large pits at posterior part of protrusion if protruded..... **other species of *Pseudocsikia***
- 2 Pronotum densely punctate, with average interval between punctures 2–4 puncture diameters (Fig. 4A); median lobe of aedeagus with one small point-

- ed process on each side near midlength, apex simply enlarged, widely rounded, without acute projections (Fig. 5J) *P. chanjuan* sp. nov.
- Pronotum sparsely punctate, with average intervals between punctures 3–6 puncture diameters (Figs 2A, 3A); median lobe of aedeagus with one large acute lateral projection on each lateral side near midlength, apically or subapically with lateral acute projections..... **3**
- 3 Median lobe of aedeagus with narrowed apical portion, apex additionally with blunt protrusion with small acute lateral projections; apex of paramere acute and pointing laterad (Fig. 5D) *P. choui* sp. nov.
- Median lobe of aedeagus with large rectangular apical portion, apex blunt, without protrusion, but with two large acute projections preapically; apex of paramere rounded (Ôhira 1972: fig. 3) *P. formosana*

Discussion

In China, the tribe Dimini is represented not only by the lineages with flying species, but also by flightless ones, such as those from genera *Dima* Charpentier, 1825, *Neodima* Schimmel & Platia, 1992, and *Sinodima* Kundrata, Sormova & Qiu, 2019 (Qiu et al. 2018; Kundrata et al. 2019a, 2019b). Most of these flightless species are known from the western mountains of China (12 spp. of *Dima* and four spp. of *Neodima*) (Qiu et al. 2018, 2020; Ruan et al. 2018; Kundrata et al. 2019b; Qiu 2021), with very few species from central (one sp. of *Dima* and one sp. of *Sinodima*) and eastern China (two spp. of *Dima*) (Suzuki 1979; Qiu et al. 2018; Ruan et al. 2018; Kundrata et al. 2019a). Previously only one flightless species of Dimini was formally reported by Suzuki (1979) from Taiwan Island, i.e., *Dima nebriomorpha* Suzuki, 1979. The two flightless Dimini species from Taiwan described in this paper are morphologically similar to but also readily distinguishable from *Pseudocsikia formosana*. The original description of *P. formosana* did not reveal whether it has reduced hind wings or not (Ôhira 1972), but based on the similarity of the elytral humeri and metaventrite between *P. formosana* and the two new species, we suppose that *P. formosana* also lacks or has reduced hind wings. The most notable characters supporting this hypothesis are the globose elytra and abdomen, the rounded elytra shoulders, and a relatively short metaventrite. These all are typical characters for the flightless species in Coleoptera (Smith 1964). The discovery of two more non-flying species in Taiwan indicates that the diverse flightless Dimini may be present not only on mainland East Asia but also on islands.

Acknowledgements

We thank Wen-I Chou (Taiwan, China) for collecting and providing the specimens of the new species for our study and Jeremy Frank (BPBM) for providing the type photographs of *P. formosana*. We are also grateful to Yu-Tang Wang (Taiwan, China)

and Hao Xu (MYNU) for help locating the name “Bukai”, and to Yong-Ying Ruan, Tamás Németh, and Hume Douglas (Editor) for their critical remarks on the manuscript. This research was supported by the Grant from Mianyang Normal University (no. QD2021A29).

References

- Bouwer R (1991) Beschreibung einer neuen *Csikia*-Art von Sumatra (Coleoptera: Elateridae). *Entomologische Zeitschrift mit Insektenbörse* 101: 53–58.
- Cate PC, Sánchez-Ruiz A, Löbl I, Smetana A (2007) Elateridae. In: Löbl I, Smetana A (Eds) *Catalogue of Palaearctic Coleoptera, Volume 4*. Apollo Books, Stenstrup, 89–209.
- Chu Y-I, Yamanaka T (1973) A check List of the present and old name of insect collected localities in Taiwan. *Annual of the National Taiwan Museum* 18: 121–150.
- Jiang S-H (1993) A catalogue of the Chinese Elateridae. Beijing Agricultural University Publishing House, Beijing, 136–162.
- Kundrata R, Musalkova M, Kubackzova M (2018) Annotated catalogue of the click-beetle tribe Dimini (Coleoptera: Elateridae: Dendrometrinae). *Zootaxa* 4412(1): 1–75. <https://doi.org/10.11646/zootaxa.4412.1.1>
- Kundrata R, Sormova E, Qiu L (2019a) *Sinodima jenisi* gen. et sp. nov., a new wingless click-beetle from the mountains of Hunan, China (Elateridae: Dendrometrinae: Dimini). *Journal of Asia-Pacific Entomology* 22(1): 15–18. <https://doi.org/10.1016/j.aspen.2018.11.016>
- Kundrata R, Sormova E, Qiu L, Prosvirov AS (2019b) Revision of the flightless click-beetle genus *Neodima* Schimmel & Platia (Elateridae: Dimini) endemic to China, with comments on its systematic position. *Zootaxa* 4604(1): 42–58. <https://doi.org/10.11646/zootaxa.4604.1.2>
- Ôhira H (1972) Elaterid-beetles from Taiwan in Bishop Museum (Coleoptera). *Pacific Insects* 14: 1–14.
- Qiu L (2021) A new *Neodima* species (Coleoptera: Elateridae: Dimini), with notes on the distribution and morphology of the genus. *Zootaxa* 5067(1): 115–121. <https://doi.org/10.11646/zootaxa.5067.1.7>
- Qiu L, Sormova E, Ruan Y, Kundrata R (2018) A new species of *Dima* (Coleoptera: Elateridae: Dimini), with a checklist and identification key to the Chinese species. *Annales Zoologici* 68(3): 441–450. <https://doi.org/10.3161/00034541ANZ2018.68.3.006>
- Qiu L, Németh T, Prosvirov AS, Kundrata R (2020) *Dima spicata* Schimmel, 1999 (Elateridae: Dimini), a morphologically remarkable species endemic to China. *Zootaxa* 4768(3): 415–424. <https://doi.org/10.11646/zootaxa.4768.3.8>
- Ruan Y, Kundrata R, Sormova E, Qiu L, Zhang M, Jiang S (2018) Description of two new species of *Dima* Charpentier, 1825 from China (Coleoptera: Elateridae: Dendrometrinae). *Zootaxa* 4526(4): 589–599. <https://doi.org/10.11646/zootaxa.4526.4.10>
- Schimmel R (1993) Neue Arten sowie eine neue Gattung der Unterfamilie Diminae Candèze, 1863 aus Ostasien und dem Balkan (Coleoptera: Elateridae). *Koleopterologische Rundschau* 63: 245–259.

- Schimmel R (1996a) Das Monophylum Diminae Candèze, 1863 (Insecta: Coleoptera: Elateridae). Pollichia-Buch 33: 1–370.
- Schimmel R (1996b) Neue und wenig bekannte Elateriden aus Griechenland und Ostasien (Coleoptera: Elateridae). Koleopterologische Rundschau 66: 161–177.
- Schimmel R (2006) Neue Megapenthini-, Physorhinini-, Diminae- und Senodoniina-Arten aus Südostasien (Insecta: Coleoptera, Elateridae). Mitteilungen der Pollichia 92: 107–130.
- Schimmel R, Platia G (1991) Revision der Subtribus Dimina Candèze, 1863 aus dem Himalaya, mit Bestimmungstabellen der Gattungen und Arten (Coleoptera: Elateridae). Entomologica Basiliensia 14: 261–382.
- Smith DS (1964) The structure and development of flightless Coleoptera: A light and electron microscopic study of the wings, thoracic exoskeleton and rudimentary flight musculature. Journal of Morphology 114(1): 107–183. <https://doi.org/10.1002/jmor.1051140106>
- Suzuki W (1979) A new elaterid beetle of the genus *Dima* from Central Taiwan. Bulletin of the National Science Museum 5: 207–210.
- Suzuki W (1982) A new denticolline genus, *Parapenia*, from the Indo-chinese subregion (Coleoptera: Elateridae). Transactions of the Shikoku Entomological Society 16: 83–94.
- Suzuki W (1999) Catalogue of the family Elateridae (Coleoptera) of Taiwan. Miscellaneous Reports of the Hiwa Museum for Natural History 38: 1–348.

A new species in the *Cyrtodactylus oldhami* group (Squamata, Gekkonidae) from Kanchanaburi Province, western Thailand

Siriporn Yodthong¹, Attapol Rujirawan¹, Bryan L. Stuart²,
L. Lee Grismer³, Akrachai Aksornneam¹,
Korkhwan Termprayoon¹, Natee Ampai⁴, Anchalee Aowphol¹

1 Department of Zoology, Faculty of Science, Kasetsart University, Bangkok 10900, Thailand **2** North Carolina Museum of Natural Sciences, 11 West Jones Street, Raleigh, North Carolina 27601, USA **3** Herpetology Laboratory, Department of Biology, La Sierra University, 4500 Riverwalk Parkway, Riverside, California 92505, USA **4** Department of Biology, Faculty of Science, Srinakharinwirot University, Bangkok 10110, Thailand

Corresponding author: Anchalee Aowphol (fsciocl@ku.ac.th)

Academic editor: Thomas Ziegler | Received 31 March 2022 | Accepted 10 May 2022 | Published 2 June 2022

<http://zoobank.org/23C7C818-5D08-44DF-B473-0D60824B07C1>

Citation: Yodthong S, Rujirawan A, Stuart BL, Grismer LL, Aksornneam A, Termprayoon K, Ampai N, Aowphol A (2022) A new species in the *Cyrtodactylus oldhami* group (Squamata, Gekkonidae) from Kanchanaburi Province, western Thailand. ZooKeys 1103: 139–169. <https://doi.org/10.3897/zookeys.1103.84672>

Abstract

Cyrtodactylus monilatus **sp. nov.** is described from Si Sawat District, Kanchanaburi Province, in western Thailand. The new species superficially resembles *C. zebraicus* Taylor, 1962 from southern Thailand. However, differences between the new species from *C. zebraicus* and other congeners were supported by an integrative taxonomic analysis of molecular and morphological data. Phylogenetic analyses based on the mitochondrial NADH dehydrogenase subunit 2 (ND2) gene showed that the new species is a member of the *C. oldhami* group and closely related to *Cyrtodactylus* sp. MT468911 from Thong Pha Phum National Park, Thong Pha Phum District, Kanchanaburi Province. Uncorrected pairwise genetic divergences (*p*-distances) between the new species and its congeners, including *C. zebraicus*, ranged from 7.7–17.7%. *Cyrtodactylus monilatus* **sp. nov.** can also be distinguished from all members of the *C. oldhami* group by having a unique combination of morphological characters, including a snout to vent length of 53.7–63.3 mm in adult males and 58.6–75.8 mm in adult females; 22–34 paravertebral tubercles; 34–42 ventral scales; 30–39 enlarged contiguous femoropreloacal scales; femoral pores and preloacal pores absent in both sexes; four or five rows of postpreloacal scales; enlarged median subcaudal scales absent; weak ventrolateral folds present; 4–7 rows of paired, paravertebral, dark-brown blotches edged in yellow or yellowish white; and two rows of small, diffuse, yellow or yellowish white spots on flanks. The new species occurs in a narrow range of forest at mid to low elevations associated with karst landscapes in the Tenasserim mountain range.

Keywords

Cyrtodactylus monilatus sp. nov., *Cyrtodactylus zebraicus*, integrative taxonomy, mitochondrial DNA, morphology, phylogeny, Southeast Asia

Introduction

The Bent-toed Gecko genus *Cyrtodactylus* Gray, 1827 is the third largest vertebrate genus in the world and one of the most species-rich radiations of gekkonid lizards (Grismer et al. 2021b). The genus is widely distributed from South and Southeast Asia into northern Australia and Melanesia (Grismer et al. 2021b; Uetz et al. 2022), where it occupies a broad variety of habitats associated with karst landscapes and forested areas (Grismer et al. 2021a). The genus *Cyrtodactylus* is monophyletic and currently contains 330 recognized species (Uetz et al. 2022) within 32 monophyletic species groups that have been delimited based on molecular data (Grismer et al. 2022). Most of the known species diversity is in mainland Southeast Asia (Wood et al. 2012; Grismer et al. 2018b, 2021b; Uetz et al. 2022), including Thailand, which is home to 39 species or nearly 9% of the described diversity (e.g., Chomdej et al. 2020; Grismer et al. 2020; Termprayoon et al. 2021; Uetz et al. 2022). Although the number of recognized species in the genus has rapidly increased in recent years, the true species diversity of the genus is still underestimated, and many known molecular lineages await formal description as species (Brennan et al. 2017; Chomdej et al. 2021; Grismer et al. 2021b).

The *Cyrtodactylus oldhami* group is restricted to a narrow geographic range on the Thai-Malay Peninsula and Myanmar northward into Kanchanaburi Province in western Thailand (Panitvong et al. 2014; Pauwels et al. 2016; Connette et al. 2017; Grismer et al. 2018b, 2021b). The *oldhami* group is one of the most taxonomically diverse species groups of *Cyrtodactylus* in Thailand. The group is monophyletic and contains at least seven nominal species (Grismer et al. 2021b), of which five occur in Thailand, i.e., *C. oldhami* (Theobald, 1876), *C. saiyok* Panitvong, Sumontha, Tunprasert & Pauwels, 2014, *C. sanook* Pauwels, Sumontha, Latinne & Grismer, 2013, *C. thirakhupti* Pauwels, Bauer, Sumontha & Chanhome, 2004, and *C. zebraicus* Taylor, 1962. *Cyrtodactylus phetchaburiensis* Pauwels, Sumontha & Bauer, 2016 from southern Thailand may also belong to the *oldhami* group, based on morphological characters (Pauwels et al. 2016), but this hypothesis remains untested by molecular data. Two additional species in the group are known from Myanmar, i.e., *C. lenya* Mulcahy, Thura & Zug, 2017, and *C. payarhtanensis* Mulcahy, Thura & Zug, 2017. The members of the *oldhami* group are morphologically variable, especially in color pattern, but the group is morphologically diagnosable from the other species groups (see Grismer et al. 2018b).

Cyrtodactylus peguensis zebraicus Taylor, 1962 was originally described from Ron Phibun (“Ronpibon”) District, Nakhon Si Thammarat Province in southern Thailand. The taxonomic status of this species was long uncertain, and often confused with *C. peguensis* (Boulenger, 1893). Grismer et al. (2018a) redescribed *C. peguensis* based on new collections from its type (and only known) locality at Bago Region, Taikkyi

Township, Yangon (north) District, Myanmar. In addition, they also studied specimens of *C. peguensis zebraicus* from southern Thailand (Nakhon Si Thammarat, Surat Thani, and Trang provinces) and compared them to other species in the *C. peguensis* group. Their phylogenetic results revealed that *C. zebraicus* is not closely related to *C. peguensis*, but rather belongs within the *C. oldhami* group. As such, Grismer et al. (2018a) elevated *C. peguensis zebraicus* to full species status (as *C. zebraicus*) and removed it from the synonymy of *C. peguensis*.

During our fieldwork in 2019 and 2021, we collected *Cyrtodactylus* specimens of the *C. oldhami* group from three localities in Si Sawat District, Kanchanaburi Province, western Thailand. These specimens closely resembled *C. zebraicus* in body size, color pattern and habitat usage. The taxonomic status of the Si Sawat specimens was investigated using mitochondrial DNA and morphological data. The datasets corroborated differences in the Si Sawat specimens from *C. zebraicus* and other species of the *C. oldhami* group. Herein, we describe this population as a new species.

Materials and methods

Sampling

A total of 22 specimens (eleven adult males, nine adult females, and two juveniles) of the Si Sawat *Cyrtodactylus* were collected by hand during fieldwork in April and November 2019, and November 2021 from Si Sawat District, Kanchanaburi Province, western Thailand (Fig. 1). Geographical coordinates and elevation were recorded with a Garmin GPSMAP 64s. Ambient air temperature and relative humidity were collected using a Kestrel 4000 Weather Meter. Photographs were taken to document the color pattern of specimens in life prior to preservation. The specimens were humanely euthanized using cardiac injection of tricaine methanesulfonate (MS-222) solution (Simmons 2015). Liver tissue was collected from each individual, preserved in 95% ethyl alcohol, and stored at -20 °C for genetic analysis. Voucher specimens were then initially fixed in 10% buffered formalin and later transferred to 70% ethyl alcohol for long-term preservation. All specimens were deposited in the herpetological collection of the Zoological Museum, Kasetsart University, Bangkok, Thailand (ZMKU). The holotype of *C. zebraicus* was examined in the holdings of the Field Museum of Natural History, Chicago (FMNH).

Molecular analyses

Total genomic DNA were extracted from preserved liver tissue of nine individuals of the Si Sawat species (Table 1) using the NucleoSpin Tissue DNA Extraction Kit (Macherey-Nagel Inc., Düren, Germany). A 1,355–1,394 base pair (bp) fragment of mitochondrial (mt) DNA that encodes the complete NADH dehydrogenase subunit 2 (ND2) gene and partial flanking tRNA genes was amplified by the polymerase chain reaction (PCR) under the following conditions: initial denaturation at 95 °C for

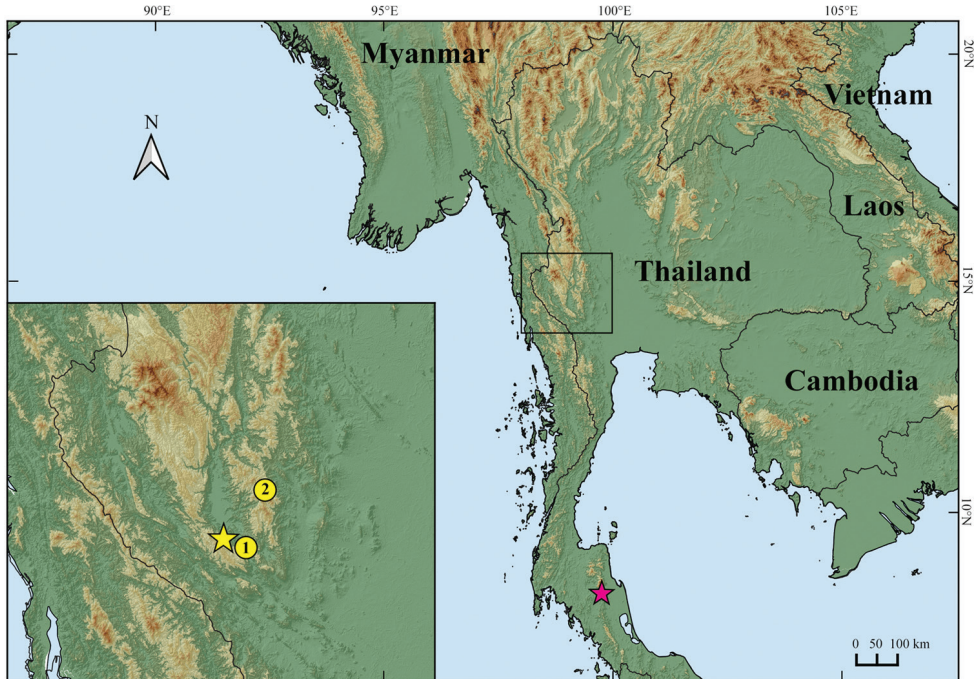


Figure 1. Map illustrating the type locality at Tham Phrathat Protection Unit (yellow star) and paratype localities (yellow cycle) at Erawan Waterfall (1) and at Tham Than Lot Noi-Tham Than Lot Yai Nature Trail (2), Si Sawat District, Kanchanaburi Province, Thailand of *Cyrtodactylus monilatus* sp. nov., and the type locality (pink star) at Ron Phibun (= “Ronpibon”) District, Nakhon Si Thammarat Province, Thailand of *C. zebraicus* (“*C. peguensis zebraicus*”).

2 min, followed by 33 cycles of a second denaturation at 95 °C for 35 s, annealing at 54 °C for 35 s, extension at 72 °C for 35 s, and final extension at 72 °C for 10 min using the primer pair L4437b (AAGCTTTCGGGCCCCATRCC; Macey et al. 1997) and H5934 (AGRGTGCCAATGTCTTTGTGRTT; Macey et al. 1997). PCR products were purified using the QIAquick PCR Purification Kit (Qiagen Ltd., Hilden, Germany) and sequenced in both directions on an ABI 3730XL sequencers by Sangon Biotech Inc. (Shanghai, China) using BigDye version 3 chemistry and the amplifying primers. DNA sequences were edited and aligned using Geneious R11 (Biomatter, Ltd., Auckland, New Zealand). The protein-coding region of the ND2 sequence was aligned and translated to amino acids to verify that the desired protein-coding genes were correctly sequenced and edited. All novel sequences were deposited in GenBank under the accession numbers ON231266–ON231274 (Table 1).

All available ND2 sequences of related species in the genus *Cyrtodactylus* from Myanmar–Thai populations and the outgroups *Dixonius siamensis* (Boulenger, 1899), *Gekko gecko* (Linnaeus, 1758), *G. kaengkrahanense* (Sumontha, Pauwels, Kunya, Limlikhitaksorn, Ruksue, Taokratok, Ansermet & Chanhom, 2012), and *Hemidactylus frenatus* Duméril & Bibron, 1836 were downloaded from GenBank following Grismer

Table 1. Specimens used in this study, including localities, museum numbers and GenBank accession numbers of the mitochondrial NADH dehydrogenase subunit 2 gene and flanking tRNA regions.

Species	Locality	Voucher No.	Accession No.	Reference
Ingroup				
<i>Cyrtodactylus amphipetraeus</i>	Tha Ra Rak Waterfall, Mae Sot Dist., Tak Prov., Thailand	ZMMU R 16626	MT550630	Chomdej et al. (2020)
<i>Cyrtodactylus brevipalmatus</i>	Khao Ramrome, Ron Phibun Dist., Nakhon Si Thammarat Prov., Thailand	AUP-00573	MT468899	Chomdej et al. (2021)
<i>Cyrtodactylus dammathetensis</i>	Dammathet Cave, 19.8 km east of Mawlamyine, Mawlamyine Dist., Mon State, Myanmar	LSUHC 12864	MF872278	Grismer et al. (2018b)
<i>Cyrtodactylus doisuthep</i>	Doi Suthep, Mueang Dist., Chiang Mai Prov., Thailand	AUP-00777	MT497801	Chomdej et al. (2021)
<i>Cyrtodactylus dummuui</i>	Chiang Dao, Chiang Mai Prov., Thailand	AUP-00768	MW713972	Grismer et al. (2021b)
<i>Cyrtodactylus erythropros</i>	Coral Cave, Pang Mapha Dist., Mae Hong Son Prov., Thailand	AUP-00771	MT497806	Chomdej et al. (2021)
<i>Cyrtodactylus interdigitalis</i>	Nakai Dist., Khammouan Prov., Laos	FMNH 255454	JQ889181	Johnson et al. (2012)
<i>Cyrtodactylus inthanon</i>	Tiger Head mountain, Doi Inthanon National Park, Chom Thong Dist., Chiang Mai Prov., Thailand	AUP-00156	MT497800	Chomdej et al. (2021)
<i>Cyrtodactylus lenya</i>	The proposed Lenya National Park Extension, Tanintharyi Region, Myanmar	USNM 587789	KY041652	Connette et al. (2017)
<i>Cyrtodactylus lenya</i>	The proposed Lenya National Park Extension, Tanintharyi Region, Myanmar	USNM 587788	KY041653	Connette et al. (2017)
<i>Cyrtodactylus lenya</i>	The proposed Lenya National Park Extension, Tanintharyi Region, Myanmar	CAS 260233	KY041655	Connette et al. (2017)
<i>Cyrtodactylus linnoensis</i>	Linno Cave region 5 km south-west of Hpa-an, Hpa-an Dist., Kayin State, Myanmar	LSUHC 12825	MF872295	Grismer et al. (2018b)
<i>Cyrtodactylus linnwayensis</i>	12.7 km north-east of Ywangan, Linn-Way Village, Yum Twing Gyi Cave, Taunggyi Dist., Shan State, Myanmar	BYU 52214	MF872280	Grismer et al. (2018b)
<i>Cyrtodactylus maelanoi</i>	Tha Pha Pum Subdist., Mae La Noi Dist., Mae Hong Son Prov., Thailand	ZMKU R 00858	MT823267	Grismer et al. (2020)
<i>Cyrtodactylus monilatus</i> sp. nov.	Chaloem Rattanakosin National Park, Khao Chor Subdist., Si Sawat Dist., Kanchanaburi Prov., Thailand	ZMKU R 00923	–	This study
<i>Cyrtodactylus monilatus</i> sp. nov.	Chaloem Rattanakosin National Park, Khao Chor Subdist., Si Sawat Dist., Kanchanaburi Prov., Thailand	ZMKU R 00924	–	This study
<i>Cyrtodactylus monilatus</i> sp. nov.	Chaloem Rattanakosin National Park, Khao Chor Subdist., Si Sawat Dist., Kanchanaburi Prov., Thailand	ZMKU R 00925	–	This study
<i>Cyrtodactylus monilatus</i> sp. nov.	Chaloem Rattanakosin National Park, Khao Chor Subdist., Si Sawat Dist., Kanchanaburi Prov., Thailand	ZMKU R 00926	ON231266	This study
<i>Cyrtodactylus monilatus</i> sp. nov.	Erawan National Park, Tha Kradan Subdist., Si Sawat Dist., Kanchanaburi Prov., Thailand	ZMKU R 00927	ON231267	This study
<i>Cyrtodactylus monilatus</i> sp. nov.	Erawan National Park, Tha Kradan Subdist., Si Sawat Dist., Kanchanaburi Prov., Thailand	ZMKU R 00928	–	This study
<i>Cyrtodactylus monilatus</i> sp. nov.	Erawan National Park, Tha Kradan Subdist., Si Sawat Dist., Kanchanaburi Prov., Thailand	ZMKU R 00929	–	This study
<i>Cyrtodactylus monilatus</i> sp. nov.	Erawan National Park, Tha Kradan Subdist., Si Sawat Dist., Kanchanaburi Prov., Thailand	ZMKU R 00930	–	This study

Species	Locality	Voucher No.	Accession No.	Reference
<i>Cyrtodactylus monilatus</i> sp. nov.	Erawan National Park, Tha Kradan Subdist., Si Sawat Dist., Kanchanaburi Prov., Thailand	ZMKU R 00931	–	This study
<i>Cyrtodactylus monilatus</i> sp. nov.	Erawan National Park, Tha Kradan Subdist., Si Sawat Dist., Kanchanaburi Prov., Thailand	ZMKU R 00932	–	This study
<i>Cyrtodactylus monilatus</i> sp. nov.	Erawan National Park, Tha Kradan Subdist., Si Sawat Dist., Kanchanaburi Prov., Thailand	ZMKU R 00933	–	This study
<i>Cyrtodactylus monilatus</i> sp. nov.	Erawan National Park, Tha Kradan Subdist., Si Sawat Dist., Kanchanaburi Prov., Thailand	ZMKU R 00934	–	This study
<i>Cyrtodactylus monilatus</i> sp. nov.	Erawan National Park, Tha Kradan Subdist., Si Sawat Dist., Kanchanaburi Prov., Thailand	ZMKU R 00935	–	This study
<i>Cyrtodactylus monilatus</i> sp. nov.	Erawan National Park, Tha Kradan Subdist., Si Sawat Dist., Kanchanaburi Prov., Thailand	ZMKU R 00936	ON231268	This study
<i>Cyrtodactylus monilatus</i> sp. nov.	Erawan National Park, Tha Kradan Subdist., Si Sawat Dist., Kanchanaburi Prov., Thailand	ZMKU R 00937	–	This study
<i>Cyrtodactylus monilatus</i> sp. nov.	Erawan National Park, Tha Kradan Subdist., Si Sawat Dist., Kanchanaburi Prov., Thailand	ZMKU R 00938	–	This study
<i>Cyrtodactylus monilatus</i> sp. nov.	Erawan National Park, Tha Kradan Subdist., Si Sawat Dist., Kanchanaburi Prov., Thailand	ZMKU R 00939	ON231269	This study
<i>Cyrtodactylus monilatus</i> sp. nov.	Erawan National Park, Tha Kradan Subdist., Si Sawat Dist., Kanchanaburi Prov., Thailand	ZMKU R 00940	ON231270	This study
<i>Cyrtodactylus monilatus</i> sp. nov.	Erawan National Park, Tha Kradan Subdist., Si Sawat Dist., Kanchanaburi Prov., Thailand	ZMKU R 00941	ON231271	This study
<i>Cyrtodactylus monilatus</i> sp. nov.	Erawan National Park, Tha Kradan Subdist., Si Sawat Dist., Kanchanaburi Prov., Thailand	ZMKU R 00942	ON23172	This study
<i>Cyrtodactylus monilatus</i> sp. nov.	Erawan National Park, Tha Kradan Subdist., Si Sawat Dist., Kanchanaburi Prov., Thailand	ZMKU R 00943	ON231273	This study
<i>Cyrtodactylus monilatus</i> sp. nov.	Erawan National Park, Tha Kradan Subdist., Si Sawat Dist., Kanchanaburi Prov., Thailand	ZMKU R 00944	ON231274	This study
<i>Cyrtodactylus</i> cf. <i>oldhami</i>	Suan Phueng Distc., Ratchburi Prov., Thailand	HLM 0307	MW713967	Grismer et al. (2021b)
<i>Cyrtodactylus oldhami</i>	Kraburi Dist., Phang-nga Prov., Thailand	MS 460	MF872301	Grismer et al. (2018b)
<i>Cyrtodactylus oldhami</i>	Muang Dist., Ranoong Prov., Thailand	MS 585	MF872302	Grismer et al. (2018b)
<i>Cyrtodactylus oldhami</i>	Chumpon Prov., Thailand	LSUHC 9486	MH940241	Murdoch et al. (2019)
<i>Cyrtodactylus payarhtanensis</i>	in the proposed Lenya National Park, Tanintharyi Region, Myanmar	USNM 587409	KY041656	Connette et al. (2017)
<i>Cyrtodactylus payarhtanensis</i>	in the proposed Lenya National Park, Tanintharyi Region, Myanmar	USNM 587792	KY041657	Connette et al. (2017)
<i>Cyrtodactylus payarhtanensis</i>	in the proposed Lenya National Park, Tanintharyi Region, Myanmar	USNM 587791	KY041658	Connette et al. (2017)
<i>Cyrtodactylus pharbaungensis</i>	Pharpoun Cave, 38.4 km south-east of Mawlamyine, Mawlamyine Dist., Mon State, Myanmar	BYU 52215	MF872303	Grismer et al. (2018b)

Species	Locality	Voucher No.	Accession No.	Reference
<i>Cyrtodactylus sadanensis</i>	Sadan Cave, 17 km south-east of Hpa-an, Hpa-an Dist., Kayin State, Myanmar	LSUHC 12853	MF872324	Grismer et al. (2018b)
<i>Cyrtodactylus sadansinensis</i>	Sadan Sin Cave 10.5 km north-west of Mawlamyine, Mawlamyine Dist., Mon State, Myanmar	BYU 52220	MF872325	Grismer et al. (2018b)
<i>Cyrtodactylus sai yok</i>	Sai Yok National Park, Kanchanaburi Prov., Thailand	MS 484	MF872308	Grismer et al. (2018b)
<i>Cyrtodactylus sai yok</i>	Sai Yok National Park, Kanchanaburi Prov., Thailand	MS 480	MF872309	Grismer et al. (2018b)
<i>Cyrtodactylus sai yok</i>	Sai Yok Dist., Kanchanaburi Prov., Thailand	AUP-00773	MT497805	Chomdej et al. (2021)
<i>Cyrtodactylus sanook</i>	Tham Sanook, Muang Dist., Chumphon Prov., Thailand	AUP-00570	MT468898	Chomdej et al. (2021)
<i>Cyrtodactylus sanpelensis</i>	Sanpel Cave, 21.3 km south-east of Mawlamyine, Mawlamyine Dist., Mon State, Myanmar	LSUHC 12886	MF872343	Grismer et al. (2018b)
<i>Cyrtodactylus shwetawngorum</i>	5.3 km north of Pyinyang Village at the Apache Cement factory mining site, Mandalay Region, Myanmar	BYU 52227	MF872348	Grismer et al. (2018b)
<i>Cyrtodactylus</i> sp.	Moe Cham Pae Dist., Mae Hong Son Prov., Thailand	HLM 0357	MW713961	Grismer et al. (2021b)
<i>Cyrtodactylus</i> sp.	Krabi, Trang Prov., Thailand	HLM 0358	MW713969	Grismer et al. (2021b)
<i>Cyrtodactylus</i> sp. MT468910	Thong Pha Phum National Park, Thong Pha Phum Dist., Kanchanaburi Prov., Thailand	AUP-01718	MT468910	Chomdej et al. (2021)
<i>Cyrtodactylus</i> sp. MT468911	Near Vajiralongkorn dam, Thong Pha Phum National Park, Thong Pha Phum Dist., Kanchanaburi Prov., Thailand	AUP-01722	MT468911	Chomdej et al. (2021)
<i>Cyrtodactylus thirakhupti</i>	Tham Khao Sonk hill, Surat Thani Prov., Thailand	ZMKU R 00732/LSUHC 12467	MF872357	Grismer et al. (2018b)
<i>Cyrtodactylus thirakhupti</i>	Tham Khao Sonk hill, Surat Thani Prov., Thailand	ZMKU R 00733/LSUHC 12468	MF872358	Grismer et al. (2018b)
<i>Cyrtodactylus tigroides</i>	Ban Tha Sao, Sai-Yok Dist., Kanchanaburi Prov., Thailand	IRSNB2380	JX440562	Wood et al. (2012)
<i>Cyrtodactylus tigroides</i>	Wang Krachae Subdist., Sai Yok Dist., Kanchanaburi Prov., Thailand	AUP-00776	MT497804	Chomdej et al. (2021)
<i>Cyrtodactylus yathepyanensis</i>	Yathe Pyan Cave, 9 km south-west of Hpa-an, Hpa-an Dist., Kayin State, Myanmar	LSUHC 12823	MF872367	Grismer et al. (2018b)
<i>Cyrtodactylus zebranicus</i>	Mueang Krabi, Krabi, Thailand	HLM 0344	MW713971	Grismer et al. (2021b)
<i>Cyrtodactylus zebranicus</i>	Khao Luang National Park, Thailand	CUMZR 2005.07.30.54	GU550727	Siler et al. (2010)
<i>Cyrtodactylus zebranicus</i>	Ron Phibun, Nakhon Si Thammarat, Thailand	FMNH 178286	–	This study
Outgroup				
<i>Dixonius siamensis</i>	Thong Pha Phum National Park, Thong Pha Phum Dist., Kanchanaburi Prov., Thailand	AUP-01724	MT468896	Chomdej et al. (2021)
<i>Gekko gekko</i>	Shwettaw wildlife sanctuary, Mimbun Township, Magway Div., Myanmar	CAS 213628	JN019053	Rösler et al. (2011)
<i>Gekko kaengkrachanense</i>	Thong Pha Phum National Park, Thong Pha Phum Dist., Kanchanaburi Prov., Thailand	AUP-01710	MT468895	Chomdej et al. (2021)
<i>Hemidactylus frenatus</i>	Rathegala, Sri Lanka	AMB 7420	EU268359	Bauer et al. (2008)

et al. (2018b, 2021b) and Chomdej et al. (2021) (Table 1). The downloaded sequences were aligned to the newly-generated sequences of the new species using the MUSCLE plug-in as implemented in Geneious R11. The alignment was edited by eye and trimmed with the gaps partially deleted to ensure that did not disrupt the coding region. Phylogenetic relationships were constructed using Maximum Likelihood (ML) and Bayesian Inference (BI) analysis. The dataset was partitioned by codon position and a separate partition for the tRNAs. The best partitioning scheme and models of evolution were selected using ModelFinder function in IQ-TREE (Kalyanamoorthy et al. 2017) with the Bayesian Information Criterion (BIC). The best-fit partitioning scheme and models of evolution are listed in Table 2. The ML analysis was performed using the IQ-TREE webserver (Trifinopoulos et al. 2016), with 1,000 bootstrap pseudoreplicates using the ultrafast bootstrap (UFB) approximation algorithm (Hoang et al. 2017). Nodes with UFB ≥ 95 were considered to be strongly supported (Minh et al. 2013).

The BI analysis was performed on CIPRES Science Gateway (Miller et al. 2010) using MrBayes v3.2.6 on XSEDE (Ronquist et al. 2012) with the partitioning scheme and models of evolution most closely approximating those calculated in IQ-TREE for the ML analysis. Two simultaneous runs each with four chains were performed using Markov chain Monte Carlo (MCMC). MCMC chains were run for 20 million genera-

Table 2. Models of molecular evolution selected for the maximum likelihood and Bayesian analyses.

Gene	Model selected	Model applied for ML	Model applied for BI
ND2			
1 st position	TVM+F+I+G4	TVM+F+I+G4	GTR+I+ Γ
2 nd position	TPM3u+F+I+G4	TPM3u+F+I+G4	GTR+I+ Γ
3 rd position	TIM3+F+G4	TIM3+F+G4	GTR+I+ Γ
tRNAs	TIMe+G4	TIMe+G4	GTR+I+ Γ

tions using the default priors, chain temperature set to 0.1, trees sampled every 1,000 generations, and the first 25% of trees discarded as burn-in. The convergence of the two simultaneous runs, and stationary states of each parameter, were assessed based on the standard deviation of split frequencies (< 0.01) and the effective sample sizes (ESS) scores were above 200 in Tracer v1.7.1 (Rambaut et al. 2018). A 50% majority-rule consensus of the sampled trees was constructed to calculate the posterior probabilities (PP) of the tree nodes. Nodes with PP ≥ 0.95 were considered to be strongly supported (Huelsenbeck and Ronquist 2001; Wilcox et al. 2002). Uncorrected pairwise sequence divergences (p -distances) were calculated in MEGA 11 (Tamura et al. 2021) using the pairwise deletion option.

Morphological analyses

Mensural, meristic, and qualitative characters were taken using a Nikon SMZ 745 Zoom Stereomicroscope. Measurements were taken on the left side of the body when possible, with digital calipers (Mitutoyo CD-6" ASX Digimatic Caliper, Japan) to

the nearest 0.1 mm. Characters and abbreviations were modified from Grismer et al. (2018a, 2018b). Morphological measurements were as follows:

SVL	Snout to vent length, taken from the tip of snout to the vent;
HL	Head length, the distance from the posterior margin of the retroarticular process of the lower jaw to the tip of the snout;
HW	Head width, measured at the angle of the jaws;
HD	Head depth, the maximum height of head measured from the occiput to the mandibles;
ED	Eye diameter, the greatest horizontal diameter of the eyeball;
EE	Eye to ear distance, measured from the anterior edge of the ear opening to the posterior edge of the eyeball;
ES	Eye to snout distance, measured from anterior most margin of the eyeball to the tip of snout;
EN	Eye to nostril distance, measured from the anterior margin of the eyeball to the posterior margin of the external nares;
IO	Interorbital distance, measured between the anterior edges of the orbit;
EL	Ear diameter, the greatest vertical distance of the ear opening;
IN	Internarial distance, measured between the nares across the rostrum;
FL	Forearm length, taken on the dorsal surface from the posterior margin of the elbow while flexed 90° to the inflection of the flexed wrist;
TBL	Tibia length, taken on the ventral surface from the posterior surface of the knee while flexed 90° to the base of the heel;
AG	Axilla to groin length, taken from the posterior margin of the forelimb at its insertion point on the body to the anterior margin of the hind limb at its insertion point on the body;
TL	Tail length, taken from the vent to the tip of the tail, original and regenerated;
TW	Tail width, taken at the base of the tail immediately posterior to the post-coecal swelling.

Meristic characters were taken on both right and left (R/L) sides when possible. The presence, absence, and/or numbers of the characters were recorded as follows:

SL	The numbers of supralabial scales, counted from the largest scale immediately below the posterior margin of the eyeball to the rostral scales;
SL-mideye	The numbers of supralabial scales, counted from the largest scale immediately below the middle of the eyeball to the rostral scales;
IL	The numbers of infralabial scales, counted from the largest scale immediately below the posterior margin of the eyeball to the mental scales;
IL-mideye	The numbers of infralabial scales, counted from the largest scale immediately below the middle of the eyeball to the mental scales;
PVT	The number of paravertebral tubercles between limb insertions, counted in a straight line immediately left of the vertebral column;

LRT	The number of longitudinal rows of dorsal tubercles, counted transversely across the center of the dorsum from one ventrolateral fold to the other;
VS	The number of longitudinal rows of ventral scales, counted transversely across the center of the abdomen from one ventrolateral fold to the other;
4FLE	The number of expanded subdigital lamellae proximal to the digital inflection on the fourth finger, counted from the base of the first phalanx where it contacts the body of the hand to the largest scale on the digital inflection;
4FLU	The number of small, unmodified subdigital lamellae distal to the digital inflection on the fourth finger, counted from the digital inflection to the claw;
4FL	The total number of subdigital lamellae beneath the fourth finger;
4TLE	The number of expanded subdigital lamellae proximal to the digital inflection on the fourth toe, counted from the base of the first phalanx where it contacts the body of the foot to the largest scale on the digital inflection;
4TLU	The number of small, unmodified subdigital lamellae distal to the digital inflection on the fourth toe, counted from the digital inflection to the claw;
4TL	The total number of subdigital lamellae beneath the fourth toe;
FPS	The number continuous femoropreloacal scales in males and females;
PP	Presence or absence preloacal pores in males and females;
PPS	The number of rows of post-preloacal scales on the midline between the enlarged preloacal scales and the vent;
PPT	The number of postcloacal tubercles;
BB	The number of body bands between the nuchal loop (dark band running from eye to eye) and the hind limb insertions not including the nape or postsacral bands;
LCB	The number of light caudal bands on an original tail;
DCB	The number of dark caudal bands on an original tail.

Non-meristic morphological characters examined were the degree of body tuberculation, weak tuberculation refers to low and weakly keeled dorsal body tubercles whereas prominent tuberculation refers to raised and prominently keeled dorsal body tubercles; body tubercles extending past the base of the tail or not; enlarged femoral scales and preloacal scales contiguous or separated by a diastema at the base of the femora; a preloacal depression or groove present or absent; transversely expanded, median subcaudal scales present or absent; and the relative length to width ratio of the transversely expanded, median subcaudal scales. Color pattern characters evaluated were the nuchal loop being continuous from eye to eye, or separated medially into paravertebral blotches; the dorsal body bands bearing paired, paravertebral elements or fused medially; dark dorsal body bands edged with light-colored tubercles or not; dark markings present or absent in the dorsal interspace; ventrolateral body folds weak or prominent; top of head bearing combinations of dark diffuse mottling or dark distinct blotches overlain with a light-colored reticulating network or not; light-colored caudal bands encircling tail or not; and regenerated tail bearing a pattern of distinct, dark spots or not.

Morphological comparisons were based on examination of the holotype of *C. zebraicus* (FMNH 178286) as well as data taken from the original and expanded descriptions of species in the literature (Theobald 1876; Taylor 1962; Pauwels et al. 2004; Pauwels et al. 2013; Panitvong et al. 2014; Connette et al. 2017; Grismer et al. 2018a).

Results

Molecular analyses

The total aligned dataset contained 1,444 mtDNA characters with gaps from 50 individuals of *Cyrtodactylus* species and four individuals of the outgroup species. The standard deviation of split frequencies among the two BI runs was 0.001410, and the ESS of all parameters were $\geq 10,325.8$, indicating that the two runs had been sufficiently sampled and converged. The maximum likelihood value of the best ML tree was $\ln L = -19,837.548$. The 50% majority rule consensus tree from BI analysis and the best ML tree had identical ingroup topologies, and so the ML topology was used herein (Fig. 2).

In both analyses, the Si Sawat species represented a deeply divergent mtDNA lineage and a strongly supported monophyletic group (1.0 PP, 100 UFB; Fig. 2) nested within the *C. oldhami* group containing *C. lenya*, *C. oldhami*, *C. payarhtanensis*, *C. sanook*, *C. saiyok*, *Cyrtodactylus* sp. MW713969, *Cyrtodactylus* sp. MT468910, *Cyrtodactylus* sp. MT468911, *C. thirakhupti*, and *C. zebraicus*. The Si Sawat species was strongly supported as the sister taxon to *Cyrtodactylus* sp. MT468911 from Thong Pha Phum National Park, Thong Pha Phum District, Kanchanaburi Province, Thailand (1.0 PP, 100 UFB; Fig. 2). The phylogenies also revealed that the current concept of *C. oldhami* is non-monophyletic.

The uncorrected pairwise sequence divergences (p -distances) between the Si Sawat species and all others in the *C. oldhami* species group used in this study are given in Table 3. The sequence divergences within the Si Sawat species were low, ranging from 0.0–1.2% (mean = 0.3%). However, the Si Sawat species had uncorrected p -distances of 7.7–17.7% from other members of the *C. oldhami* group, 7.7–8.0% (mean = 7.7%) from the sister taxon *Cyrtodactylus* sp. MT468911, and 17.3–17.7% (mean = 17.6%) from *C. zebraicus*, which it closely resembles in color pattern (Table 3).

Taxonomy

Based on the results of mtDNA and morphological comparisons (see below), the *Cyrtodactylus* specimens from Si Sawat District, Kanchanaburi Province, western Thailand distinctly differed from *C. zebraicus* and other species of the *oldhami* group. Thus, we hypothesize that the Si Sawat specimens represent a distinct species that is described as new, as follows.

Table 3. Uncorrected pairwise sequence divergences (*p*-distances) in the mitochondrial NADH dehydrogenase subunit 2 gene and flanking tRNA regions of *Cyrtodactylus monilatus* sp. nov. and related species. 1 = *Cyrtodactylus monilatus* sp. nov., 2 = *Cyrtodactylus* sp. MT468911, 3 = *Cyrtodactylus* cf. *oldhami*, 4 = *Cyrtodactylus* sp. MT 468910, 5 = *Cyrtodactylus* sp. MW713969, 6 = *C. thirakbhupti*, 7 = *C. payarbtanensis*, 8 = *C. sanook*, 9 = *C. oldhami* MF872302, 10 = *C. oldhami* MF872301, 11 = *C. oldhami* MH940241, 12 = *C. saijok*, 13 = *C. lenya*, and 14 = *C. zebraicus*.

No.	1	2	3	4	5	6	7	8	9	10	11	12	13	14
1	0.3 (0.0–1.2)													
2	7.7 (7.7–8.0)	–												
3	11.5 (11.2–11.7)	10.8 (10.8)	–											
4	11.6 (11.4–11.7)	11.2 (11.2)	1.8 (1.8)	–										
5	11.8 (11.7–12.0)	10.0 (10.0)	9.3 (9.3)	9.3 (9.3)	–									
6	12.0 (11.4–12.4)	11.3 (11.1–11.4)	9.0 (9.0)	9.2 (9.1–9.2)	9.7 (9.7)	0.0 (0.0)								
7	12.3 (11.7–13.2)	11.1 (10.7–11.9)	10.6 (10.2–11.4)	10.9 (10.5–11.6)	7.4 (7.1–8.1)	8.3 (7.7–9.7)	0.1 (0.0–0.1)							
8	12.7 (12.6–12.8)	12.1 (12.1)	9.9 (9.9)	9.6 (9.6)	6.0 (6.0)	7.1 (7.0–7.2)	8.02 (7.7–8.7)	–						
9	12.8 (12.7–12.9)	11.3 (11.3)	9.7 (9.7)	9.9 (9.9)	6.5 (6.5)	6.9 (6.6–7.2)	7.7 (7.4–8.3)	7.7 (7.7)	–					
10	12.3 (12.13–12.57)	11.6 (11.58)	9.7 (9.7)	9.53 (9.53)	5.49 (5.49)	7.17 (6.61–7.18)	9.1 (8.63–9.97)	7.4 (7.43)	7.8 (7.8)	–				
11	13.0 (12.7–13.2)	12.1 (12.1)	9.3 (9.3)	9.3 (9.3)	10.7 (10.7)	10.8 (10.4–11.2)	11.2 (10.9–11.7)	11.0 (11.0)	10.6 (10.6)	11.4 (11.4)	–			
12	15.4 (15.2–15.6)	14.6 (14.3–14.8)	14.2 (14.1–14.3)	14.8 (14.7–14.9)	14.4 (14.2–14.6)	14.9 (14.6–15.2)	14.8 (14.1–16.4)	15.1 (14.9–15.3)	14.6 (14.4–14.8)	15.5 (15.2–15.8)	15.3 (15.0–15.5)	0.1 (0.1–0.2)		
13	16 (16.6–17.0)	15.1 (15.0–15.1)	16.5 (16.4–16.6)	16.6 (16.4–16.7)	15.5 (15.4–15.7)	14.9 (14.1–15.6)	16.3 (15.6–17.6)	16.9 (16.7–17.1)	16.1 (16.0–16.1)	16.7 (16.6–16.8)	17.5 (17.3–17.6)	16.1 (15.7–16.4)	0.5 (0.2–0.6)	
14	17.6 (17.3–17.7)	16.3 (16.2–16.3)	16.8 (16.6–16.9)	17.0 (16.9–17.0)	16.9 (16.8–16.9)	16.3 (15.3–17.2)	17.7 (16.7–19.2)	17.5 (17.5)	17.3 (17.2–17.4)	17.2 (17.2–17.4)	17.4 (17.2–17.6)	17.2 (15.7–16.4)	13.2 (13.0–13.2)	6.0 (6.0)

***Cyrtodactylus monilatus* sp. nov.**

<http://zoobank.org/8F2DB395-0234-47D5-B272-0778D34ABE95>

Common English name: Kanchanaburi Spotted Bent-toed Gecko

Figs 3–5, 7

Material examined. Holotype. ZMKU R 00943, adult male (Figs 3, 4), collected from Thailand, Kanchanaburi Province, Si Sawat District, Tha Kradan Subdistrict, Erawan National Park, Tham (= cave) Phrathat Protection Unit (14°23.754'N, 99°04.751'E, 699 m elevation), 19 November 2021, by Siriporn Yodthong, Attapol Rujirawan, Akrachai Aksornneam, and Natee Ampai.

Paratypes (Fig. 5). Seven adult males (ZMKU R 00934–00939, ZMKU R 00944) and three adult females (ZMKU R 00940–00942), same data as holotype. Three adult males (ZMKU R 00928–00930) and two adult females (ZMKU R 00931–00932), same data as holotype except collected on 26 November 2019, by Siriporn Yodthong, Attapol Rujirawan, Akrachai Aksornneam, and Korkhwan Termprayoon. One adult female (ZMKU R 00927), collected from Thailand, Kanchanaburi Province, Si Sawat District, Tha Kradan Subdistrict, Erawan National Park, Erawan Waterfall (14°22.315'N, 99°08.806'E, 82 m elevation) on 25 November 2019 by Siriporn Yodthong, Attapol Rujirawan, Akrachai Aksornneam, and Korkhwan Termprayoon. Three adult females (ZMKU R 00924–00926), collected from Thailand, Kanchanaburi Province, Si Sawat District, Khao Chot Subdistrict, Chaloeam Ratanakosin National Park, Tham Than Lot Noi-Tham Than Lot Yai Nature Trail (14°40.158'N, 99°17.436'E, 526 m elevation) on 20 April 2019 by Siriporn Yodthong, Akrachai Aksornneam, Korkhwan Termprayoon, and Natee Ampai.

Referred specimens. One juvenile (ZMKU R 00923), collected from Thailand, Kanchanaburi Province, Si Sawat District, Khao Chot Subdistrict, Chaloeam Ratanakosin National Park, Tham Than Lot Noi-Tham Than Lot Yai Nature Trail (14° 39.767'N, 99°18.314'E, 233 m elevation) on 19 April 2019 by Siriporn Yodthong, Akrachai Aksornneam, Korkhwan Termprayoon, and Natee Ampai. One juvenile (ZMKU R 00933), same data as holotype except collected on 26 November 2019 by Siriporn Yodthong, Attapol Rujirawan, Akrachai Aksornneam, and Korkhwan Termprayoon.

Etymology. The specific epithet *monilatus* is taken from *monile* (L.) for necklace or string of beads and *latus* (L.) for flank, in reference to the new species having two rows of small, diffuse, yellow or yellowish white spots on the flanks that resemble a beaded necklace. These spots are an important color pattern difference between the new species and *C. zebraicus*. We propose “Kanchanaburi Spotted Bent-toed Gecko” for the common English name and “ตุ๊กแกปลายจุดเมืองกาญจน์” (Took kae pa lai jud mueang kan) for the common Thai name of the new species.

Diagnosis. *Cyrtodactylus monilatus* sp. nov. is assigned to the *C. oldhami* group on the basis of its recovered phylogenetic position (Fig. 1). This species can be distinguished from all other species of the *C. oldhami* group (sensu Grismer et al. 2021b) by having the following combination of characters: (1) a medium-sized *Cyrtodactylus*, SVL 53.7–63.3 mm in adult males, 58.6–75.8 mm in adult females; (2) 10–13 supralabial and 8–11 infrala-

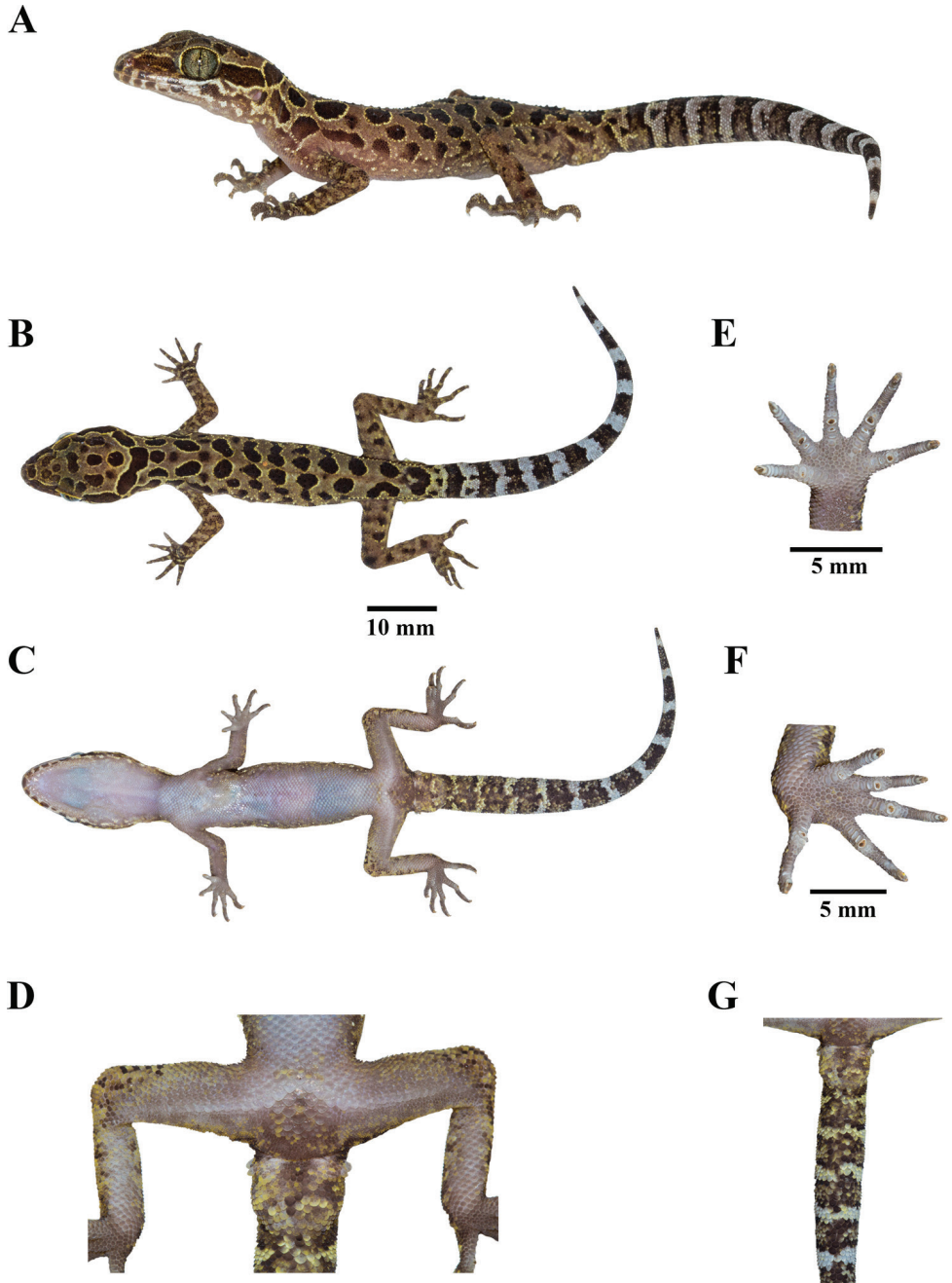


Figure 3. Adult male holotype of *Cyrtodactylus monilatus* sp. nov. (ZMKU R 00943) in life from Tham Phrathat Protection Unit, Si Sawat District, Kanchanaburi Province, Thailand **A** lateral view **B** dorsal view **C** ventral view **D** preloacal region showing distribution of continuous, enlarged femoropreloacal scales **E** palmar view of the left hand **F** plantar view of the left foot, and **G** ventral view of tail showing not enlarged median subcaudal scales.

bial scales; (3) 22–34 paravertebral tubercles; (4) 16–21 longitudinal rows of dorsal tubercles; (5) 34–42 ventral scales; (6) 12–16 total subdigital lamellae on the fourth finger; (7) 15–19 total subdigital lamellae on the fourth toe; (8) 30–39 contiguous enlarged femoropreloacal scales; (9) femoral pores and preloacal pores absent in both sexes; (10) four or five rows of postpreloacal scales; (11) preloacal groove or depression absent; (12) enlarged median subcaudal scales absent; (13) 9–12 dark and light caudal bands encircling the original tail; (14) weak ventrolateral folds present; (15) subconical to slightly prominent trihedral keeled tubercles on body that extend past the base of the tail but no further than 1/3 of anterior portion of tail; (16) top of head bearing large, dark-brown blotches edged in yellow or yellowish white with no light-colored network; (17) 4–7 dorsal body bands composed of paired, paravertebral, dark-brown blotches edged in yellow or yellowish white; and (18) two rows of small, diffuse, yellow or yellowish white spots on flanks.

Description of holotype (Figs 3, 4). Adult male with 56.4 mm SVL; head moderate in length (HL/SVL 0.29), wide (HW/HL 0.65), slightly flattened (HD/HL 0.40), distinct from neck, and triangular in dorsal profile; lores concave anteriorly, inflated posteriorly; frontal region flattened, prefrontal region slightly concave, canthus rostralis rounded; snout rather elongate (ES/HL 0.40), rounded in rostral region, eye to snout distance slightly greater than head depth; eye large (ED/HL 0.29), eyeball slightly protuberant, eye diameter less than the eye to ear distance, pupil vertical; ear opening elliptical, obliquely oriented, moderate in size (EL/HL 0.09); eye to ear distance greater than eye diameter; rostral large, subrectangular, height 1.6 mm, shorter than wide, 2.8 mm, medially divided by dorsal a furrow, reaching to approximately half-way down rostral height, bordered posteriorly by supranasals and internasal, laterally by first supralabials and nostrils; external nares at anterior angle of snout, directed lateroposteriorly, bordered anteriorly by rostral, dorsally by large supranasal, posteriorly by two small postnasals, ventrally by first supralabial; internarial distance narrow; supranasals subrectangular, separated by two small internasals, bordered anteriorly by rostral, laterally by nostrils, posteriorly by four small scales; two internasals, subpentagonal, vertically arranged, slightly protruding rostral, bordered posteriorly by three small scales; 8/7 (right/left) supralabials extending to below midpoint of eye, 12/11 to below the posterior margin of the eyeball, subrectangular anteriorly, elliptical shape posteriorly; 5/7 infralabials extending to below midpoint of eye, 9/10 to below the posterior margin of the eyeball, larger than supralabials, tapering smoothly posteriorly; scales of frontonasal, prefrontal and lores, small, relatively raised, domed, slightly larger than granular scales on top of head and occiput; scales on occiput intermixed with scattered, slightly larger, more rounded, dome to subconical tubercles, more prominent tubercles between occiput and above ear opening; dorsal supraciliaries crenulated, not elongate or keeled; mental large, triangular, 2.4 mm in width, 1.8 mm in length, bordered laterally by first infralabials and posteriorly by large, right and left trapezoidal postmentals that contact medially for 66% of their length posterior to mental; one row of slightly enlarged chin shields extending posteriorly to sixth (right) and seventh (left) infralabial; and gular and throat scales small, granular, grading posteriorly into larger, flat, smooth, imbricate, pectoral and ventral scales.

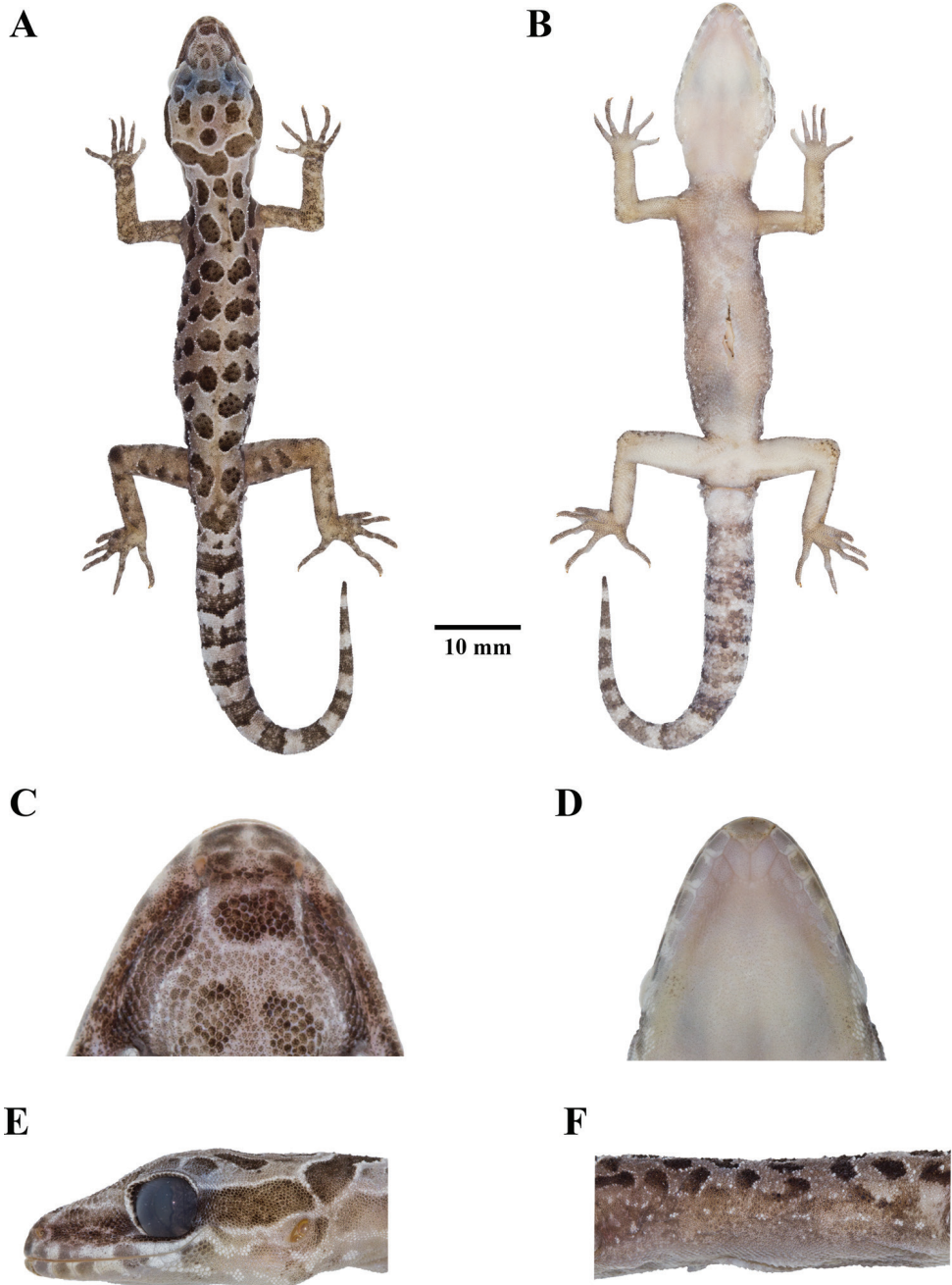


Figure 4. Adult male holotype of *Cyrtodactylus monilatus* sp. nov. (ZMKU R 00943) in preservation **A** dorsal view **B** ventral view **C** dorsal view showing the rostral, supranasal, and internasal scales **D** ventral view showing the mental and postmental scales **E** lateral view of head of the left side **F** lateral view of flank of the left side.

Body slender, relatively short (AG/SVL 0.44), with weak ventrolateral folds; scales on dorsum small, mostly homogenous, granular, interspersed with larger, irregularly arranged, slightly prominent trihedral keeled tubercles; tubercles extending from occiput beyond to the base of the tail but not farther than 1/3 of tail; tubercles on occiput, nape and anterior of body at level above shoulder smaller, subconical; those mid-dorsally and on the posterior section of the body larger, being more dense, slightly more prominently keeled, and more regularly arrange in sacral region and tail base; tubercles on flanks sparse; approximately 16 longitudinal rows of dorsal tubercles; approximately 28 paravertebral tubercles; 38 flat, imbricate, smooth ventral scales, those near midline larger than those laterally and dorsal scales; femoral scales enlarged, extending along 2/3 of femora and contiguous with enlarged precloacal scales; precloacal scales smooth, approximately twice the size of femoral scales; 33 contiguous femoroprecloacal scales; femoral pores and precloacal pores absent; four rows of enlarged postprecloacal scales; and precloacal groove or depression absent.

Limbs moderately slender; forelimbs relatively short (FL/SVL 0.15); scales on dorsal surface domed to subconical, granular, slightly larger than those on body, interspersed with sparsely enlarged, subconical and trihedrally keeled tubercles; dorsal scales of wrist and palm flat, smooth, round, imbricate; ventral scales of palm flat, weakly rounded, slightly raised, not imbricate, smaller than those on body; 16/16 (right/left) total subdigital lamellae on fourth finger, 4/4 proximal subdigital lamellae rectangular with rounded to weakly rounded corners, broadly expanded proximal to joint inflection on fourth finger, 12/12 distal subdigital lamellae, slightly expanded immediately distal to joint, becoming gradually more expanded near the claw; digits well-developed, relatively long, inflected at basal interphalangeal joints; digits slightly narrower distal to inflections; no interdigital webbing; claw well-developed, relatively short, claw base sheathed by a dorsal and ventral scales; hind limbs more robust than forelimbs, moderate in length (TBL/SVL 0.18); dorsal scales domed to subconical, granular, interspersed with enlarged subconical and trihedrally keeled tubercles, and anterior part of thigh covered by flat, slightly larger, imbricate scales; ventral scales of femora flat, smooth, imbricate, smaller than those on body; small postfemoral scales form an abrupt union with large, flat ventral scales of posteroventral margin of thigh; ventral scales of tibia flat, imbricate; dorsal scales of plantar surface relatively smooth, rounded, imbricate; ventral scales of plantar surface low flat, weakly rounded; 18/19 (right/left) total subdigital lamellae on fourth toe, 5/6 proximal subdigital lamellae, rectangular with rounded to weakly rounded corners, broadly expanded proximal to joint inflection on fourth toe, 13/13 distal subdigital lamellae, slightly expanded immediately distal to joint, becoming gradually more expanded near the claw; digits well-developed, relatively long, inflected at basal, interphalangeal joints; and claw well-developed, relatively short, claw base sheathed by a dorsal and ventral scales.

Tail 58.1 mm in length, original, slightly longer than SVL (TL/SVL 1.03), moderate in proportions, segmented, cylindrical, wide anteriorly, 4.6 mm in width at base, tapering to a tip, covered with small scales on the dorsal surface but slightly larger scales on ventral surface; dorsal scales of tail base granular, round, becoming larger, flatter, subimbricate posteriorly; those on tail base bearing trihedrally keeled tubercles

forming paravertebral rows, four dorsal longitudinal tubercles rows, two transverse rows of dorsal tubercles extend from tail base to posterior margin of third caudal band, 7.1 mm from tail base, approximately 1/8 of tail; no enlarged median row of transverse scales on subcaudal region; no caudal furrow; base of tail forming hemipenial swelling; 2/2 (right/left) postcloacal tubercles on the enlarged smooth hemipenial swelling; and postcloacal tubercles approximately equal size.

Coloration of holotype in life (Fig. 3). Dorsal ground color of head, body, and limbs yellowish brown; top of head bearing large, dark-brown blotches edged in yellow; superciliary scales yellow; wide dark-brown stripe edged in yellow on canthus, extending from posterior margin of nostril to anterior margin of orbit; wide, discontinuous, dark-brown nuchal loop edged in yellow, extending from posterior margin of one orbit, across occiput to posterior margin of the other orbit; three large, dark-brown blotches edged in yellow on nape; seven paravertebral blotches on right and six on left between limb insertions resulting in five anterior bands of paired, paravertebral, dark-brown blotches, remaining bands composed of one and two, unpaired, paravertebral, blotches; all dorsal bands terminate on upper flanks with a series of dark-brown, irregularly shaped blotches of varying sizes edged in yellow and yellowish white; two similarly colored postsacral bands, anterior composed of paravertebral blotches and posterior composed of confluent blotches; 11 dark-brown caudal bands and 11 white caudal bands; all caudal bands encircle the tail; dorsal portion of forelimbs bearing irregularly shaped dark markings with dull-yellow spots; dorsal portion of hind limbs mottled with yellow spots and small, poorly defined, dark-brown blotches; supralabial and infralabial scales off-white with darker markings; suborbital region to forelimb insertions covered with irregularly shaped dark-brown and yellowish white markings; lower flanks bearing two rows of small, diffuse, yellowish white spots; all ventral surfaces generally greyish white, immaculate, except for ventral surface of knee, precloacal and postcloacal regions, and hemipenial swellings which bear dark and yellow to yellowish white markings.

Coloration of holotype in preservation (Fig. 4). Color pattern of head, body, limbs, and tail similar to that in life with some fading. Ground color of head, body, and limbs light-beige; dark body and dark caudal bands lighter than in life; yellow coloration on dorsal and ventral surface fade to off-white; and all ventral surfaces light-beige.

Variations. Morphometric, meristic and color pattern characters of the type series and referred specimens of *C. monilatus* sp. nov. are presented in Tables 4–6. All paratypes approximate the holotype in general aspects of morphology, with variations in coloration and banding (Fig. 5). Dorsal ground color varies from beige, brown, to yellowish brown. Edge of dark-brown blotches on dorsum varies from yellow to yellowish white. Pattern on top of head of one specimen (ZMKU R 00926) has faint, poorly-defined, dark, irregularly shaped blotches. One specimen (ZMKU R 00926) has a faint, poorly-defined, dark stripe on canthus region. Nuchal loop patterns of three specimens (ZMKU R 00925–00927) are completely continuous. Dorsal body bands of one specimen (ZMKU R 00925) comprise four bands, seven specimens (ZMKU R 00923, ZMKU R 00924, ZMKU R 00926, ZMKU R 00929, ZMKU R 00933, ZMKU R 00941 and ZMKU R 00944) have five bands, and nine specimens (ZMKU R00927,

ZMKU R 00930–00931, ZMKU R 00934, ZMKU R 00937–00940 and ZMKU R 00942) have six bands. Ventral ground color varies from beige to greyish white.

Internasal scales of ten specimens (ZMKU R 00923–00924, ZMKU R 00926, ZMKU R 00930, ZMKU R 00933, ZMKU R 00935, ZMKU R 00937, ZMKU R 00940–00941, ZMKU R 00944) are single and eight specimens (ZMKU R 00925, ZMKU R 00928–00929, ZMKU R 00932, ZMKU R 00934, ZMKU R 00936, ZMKU R 00938, ZMKU R 00942) are absent. Regenerated tail covered with flat, imbricate, round scales; enlarge median subcaudal scales absent; ground color of regenerated tail varies from beige, yellowish brown, brown to dark-brown bearing brown and dark markings; dark and light caudal bands absent (Fig. 5). Females have larger body SVL than males (Table 4). In life, coloration and banding pattern of juvenile specimens (ZMKU R 00923 and ZMKU R 00933) resemble that of the adults.

Distribution and natural history. *Cyrtodactylus monilatus* sp. nov. is currently known from only three localities in Si Sawat District, Kanchanaburi Province, western Thailand: Tham Phrathat Protection Unit, Erawan Waterfall in Erawan National Park, and Tham Than Lot Noi-Tham Than Lot Yai Nature Trail in Chaloeem Ratanakosin National Park (Figs 1, 6). All individuals were found in karst forests with mixed deciduous trees, and dry evergreen trees at 82–699 m elevation. These areas are surrounded by agricultural lands (orchards, rubber plantation, and pasture lands) and human residential areas. Specimens ($N = 22$) were collected at night (1900–2100 hr) during the dry season (November–April) on the forest floor (54.6%; $N = 12$), on

Table 4. Descriptive measurements in millimeters of the type series of *Cyrtodactylus monilatus* sp. nov. Abbreviations are defined in the text.

Characters	Holotype male	Holotype and paratype males		Paratype females	
	$N = 1$	$N = 11$		$N = 9$	
		Min–Max	Mean \pm SD	Min–Max	Mean \pm SD
SVL	56.4	53.7–63.3	58.0 \pm 3.4	58.6–75.8	68.7 \pm 5.6
HL	16.4	15.5–18.10	16.6 \pm 0.9	16.8–22.0	19.3 \pm 1.7
HW	10.6	10.1–12.1	11.0 \pm 0.6	11.5–15.4	13.3 \pm 1.2
HD	6.5	5.8–7.5	6.6 \pm 0.6	6.4–9.1	7.7 \pm 0.9
ED	4.8	4.3–5.3	4.7 \pm 0.4	4.8–5.4	5.2 \pm 0.3
EE	5.1	4.0–5.3	4.9 \pm 0.4	5.1–6.7	5.9 \pm 0.6
ES	6.6	5.9–7.4	6.6 \pm 0.4	6.5–8.8	7.4 \pm 0.7
EN	5.2	4.3–5.4	4.9 \pm 0.3	4.8–6.5	5.5 \pm 0.5
IO	5.3	5.1–6.4	5.7 \pm 0.4	5.7–7.6	6.6 \pm 0.7
EL	1.5	1.1–1.8	1.4 \pm 0.2	1.3–1.7	1.5 \pm 0.2
IN	1.9	1.7–2.1	1.9 \pm 0.1	1.8–2.4	2.1 \pm 0.2
AG	24.7	22.3–27.8	25.4 \pm 1.7	26.1–34.4	31.1 \pm 2.8
FL	8.3	8.0–9.6	8.8 \pm 0.5	9.1–11.8	10.4 \pm 1.0
TBL	10.4	9.8–11.7	10.8 \pm 0.7	11.4–14.1	12.8 \pm 1.0
TL (original)	58.1	58.1–62.10 ^a	59.9 \pm 1.7 ^a	64.0–77.7 ^c	71.4 \pm 5.7 ^c
TL (regenerated)	NA	41.8–60.0 ^b	49.5 \pm 5.8 ^b	25.7–55.1 ^d	42.8 \pm 12.9 ^d
TW	4.6	4.0–5.4	4.9 \pm 0.5	4.5–5.3	4.9 \pm 0.3
TD	4.0	4.0–5.6	4.7 \pm 0.5	4.3–5.4	4.8 \pm 0.4

^a $N = 4$; ^b $N = 7$; ^c $N = 5$; ^d $N = 4$

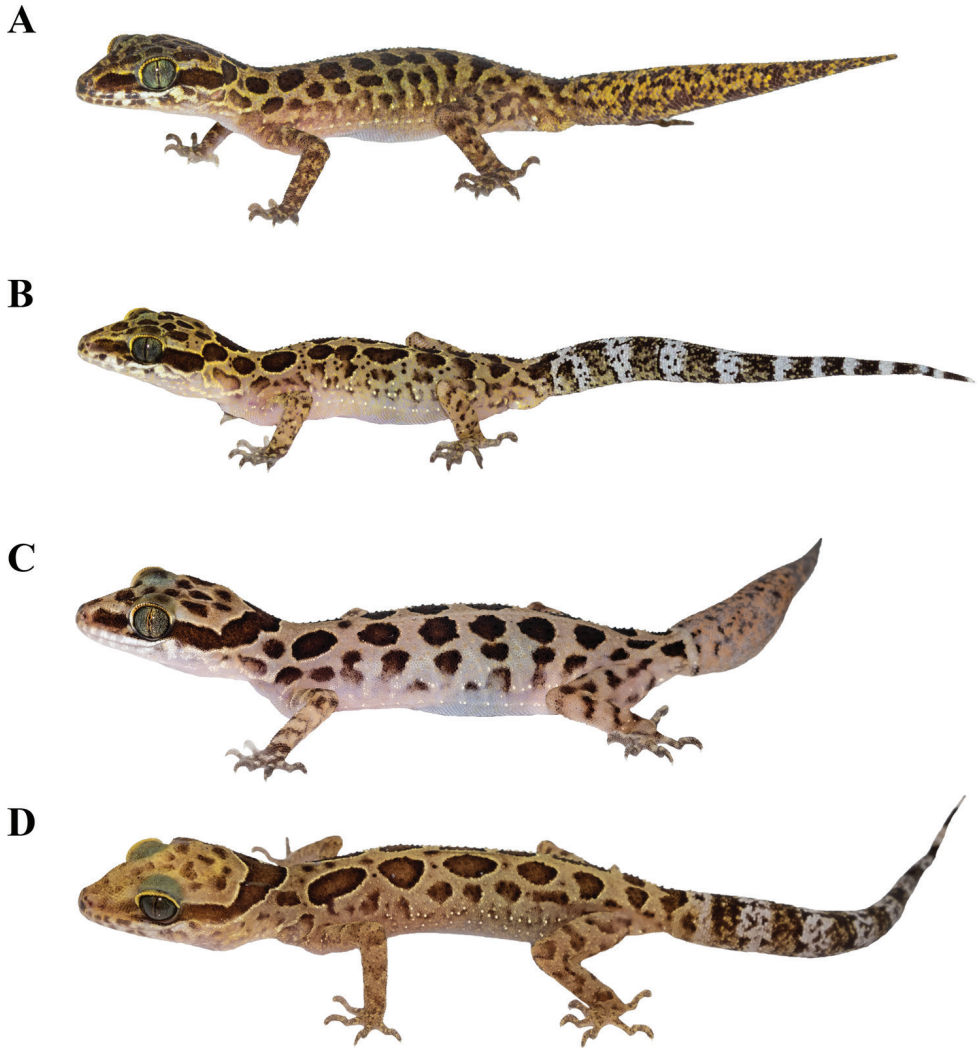


Figure 5. Paratypes of *Cyrtodactylus monilatus* sp. nov. in life showing variation in color pattern **A** adult male (ZMKU R 00935) **B** adult male (ZMKU R 00944) from Tham Phrathat Protection Unit **C** adult female (ZMKU R 00927) from Erawan Waterfall **D** adult female (ZMKU R 00926) from Tham Than Lot Noi-Tham Than Lot Yai Nature Trail, Si Sawat District, Kanchanaburi Province, Thailand.

karst boulder outcrops (22.7%; $N = 5$), and on shrub or bamboo twigs with ≤ 100 cm above ground level (22.7%; $N = 5$). The range in altitude at which the specimens were collected suggests that elevation has little to do with their distribution. It is likely that karst forests are the ecological factor that determines where they occur.

At Tham Phrathat Protection Unit, the holotype (ZMKU R 00943) was found on 19 November 2021 on the forest floor covered with leaf litter, at a temperature 24.0 °C and relative humidity 90.0%. On the previous day with temperatures between

24.2–24.4 °C and relative humidity between 82.6–83.9%, three specimens (ZMKU R 00937, ZMKU R 00939–00940) were found on the forest floor covered with leaf litter, two specimens (ZMKU R 00934–00935) were found on shrub twigs with ≤ 10 cm above ground level, and three specimens (ZMKU R 00936, ZMKU R 00938 and ZMKU R 00941) were found on the karst boulder outcrops, including one gravid female (ZMKU R 00942) containing two eggs (externally visible). Juveniles and immatures (SVL < 50 mm) were found on the forest floor and on the karst boulder outcrops but not collected. During November of the previous year (2019) at a temperature 25.9 °C and relative humidity of 54.3%, one specimen (ZMKU R 00929) was found on the twig of a shrub approximately 30 cm above ground level, another specimen (ZMKU R 00930) was found on bamboo twig around 100 cm above ground level, and three specimens (ZMKU R 00928, ZMKU R 00931–00932) were found on the forest floor covered with leaf litter, including one juvenile (ZMKU R 00933). Other sympatric lizard species found at this locality included *Acanthosaura crucigera* Boulenger, 1885, *Cnemaspis huaseesom* Grismer, Sumontha, Cota, Grismer, Wood, Pauwels & Kunya, 2010, *Cyrtodactylus tigroides* Bauer, Sumontha & Pauwels, 2003, *Dixonius hangseesom*

Table 5. Meristic characters (right/left) and color patterns of *Cyrtodactylus monilatus* sp. nov. Abbreviations are defined in the text. Key: NA = data unavailable or unapplicable.

Characters	Holotype	Holotype and paratypes
	N = 1	N = 20 Min–Max
SL	12/11	10–13
SL-mideye	8/7	6–9
IL	9/10	8–11
IL-mideye	5/7	5–8
Body tubercles pointed and keeled	Yes	Yes
PVT	28	25–34
LRT	16	16–21
VS	38	34–42
4FLU	12/12	9–12
4FLE	4/4	3–5
4FL	16/16	12–16
4TLU	13/13	10–13
4TLE	5/6	4–6
4TL	18/19	15–19
Enlarge femoral and precloacal scales continuous	Yes	Yes
FPS	33	30–39*
PP	Absent	Absent
PPS	4	4–5
PPT	2/2	2–3
Enlarged median subcaudal scales	No	No
Nuchal loop discontinuous	Yes	Yes & No
Paravertebral elements not in contact	Yes	Yes
BB	6	4–7
DCB	11	9–12
LCB	11	9–12

* N = 19, data from ZMKU R 00934 was not included because its FPS has a defect.

Bauer, Sumontha, Grossmann, Pauwels & Vogel, 2004, *Dixonius siamensis* (Boulenger, 1899), *Eutropis macularia* (Blyth, 1853), *Gehyra mutilata* (Wiegmann, 1834), and *Subdoluseps bowringii* (Günther, 1864).

At Erawan Waterfall, one gravid female (ZMKU R 00927) contained two eggs (externally visible) and was found on the forest floor near the waterfall stream during November 2019. Other sympatric lizard species found at this locality included *Draco taeniopterus* (Günther, 1861) and *Sphenomorphus maculatus* (Blyth, 1853).

At Tham Than Lot Noi-Tham Than Lot Yai Nature Trail, one juvenile specimen (ZMKU R 00923) was found on karst boulder outcrops at a temperature 27.1 °C and relative humidity 72.0%, another adult female (ZMKU R 00925) was found on dry twig on the forest floor, and one gravid female (ZMKU R 00926) containing two eggs (externally visible) was found on the forest floor covered with leaf litter at a temperature 31.9 °C and relative humidity 56.9%. Other sympatric lizard species found at this locality included *Cyrtodactylus* sp., *Dixonius siamensis*, *Draco taeniopterus*, and *Sphenomorphus maculatus*.

Comparisons. *Cyrtodactylus monilatus* sp. nov. is differentiated from all seven species of *C. oldhami* group and two additional species, *C. phetchaburiensis* and *C. surin* by having a unique combination of morphological characters, its phylogenetic placement

Table 6. Meristic characters (right/left) and color patterns of the referred specimens of *Cyrtodactylus monilatus* sp. nov. Abbreviations are defined in the text. Key: NA = data unavailable or unapplicable.

Characters	ZMKU R 00933	ZMKU R 00923	Min–Max
Age	Juvenile	Juvenile	<i>N</i> = 2
SVL	40.6	31.3	31.3–40.6
SL	12/11	12/10	10–12
SL-mideye	8/7	8/7	7–8
IL	10/9	8/8	8–10
IL-mideye	7/6	5/6	5–7
Body tubercles pointed and keeled	Yes	Yes	Yes
PVT	22	27	22–27
LRT	16	17	16–17
VS	34	40	34–40
4FLU	11/11	10/10	10–11
4FLE	4/4	4/4	4
4FL	15/15	14/14	14–15
4TLU	12/12	11/11	11–12
4TLE	6/5	6/6	5–6
4TL	18/17	17/17	17–18
Enlarge femoral and precloacal scales continuous	Yes	Yes	Yes
FPS	33	33	33
PPS	5	5	5
PPT	2/3	2/2	2–3
Enlarged median subcaudal scales	NA	No	No
Nuchal loop discontinuous	Yes	Yes	Yes
Paravertebral elements not in contact	Yes	Yes	Yes
BB	6	5	5–6
DCB	NA	10	10
LCB	NA	11	11

(Fig. 2), and having uncorrected pairwise sequence divergences in mtDNA from all other members of the *oldhami* group of 7.7–17.7%, (Table 3).

Cyrtodactylus monilatus sp. nov. differs from *C. lenya* Mulcahy, Thura & Zug, 2017 by having 25–34 paravertebral tubercles (vs. 39–41 tubercles); 34–42 ventral scales (vs. 29 scales); enlarged median subcaudal scales absent (vs. present); top of head bearing dark-brown blotches edged in yellow or yellowish white (vs. indistinctly mottled); dorsal body bands composed of paired, paravertebral, dark-brown blotches edged in yellow or yellowish white (vs. broad dark-brown dorsal bands with narrow chocolate brown

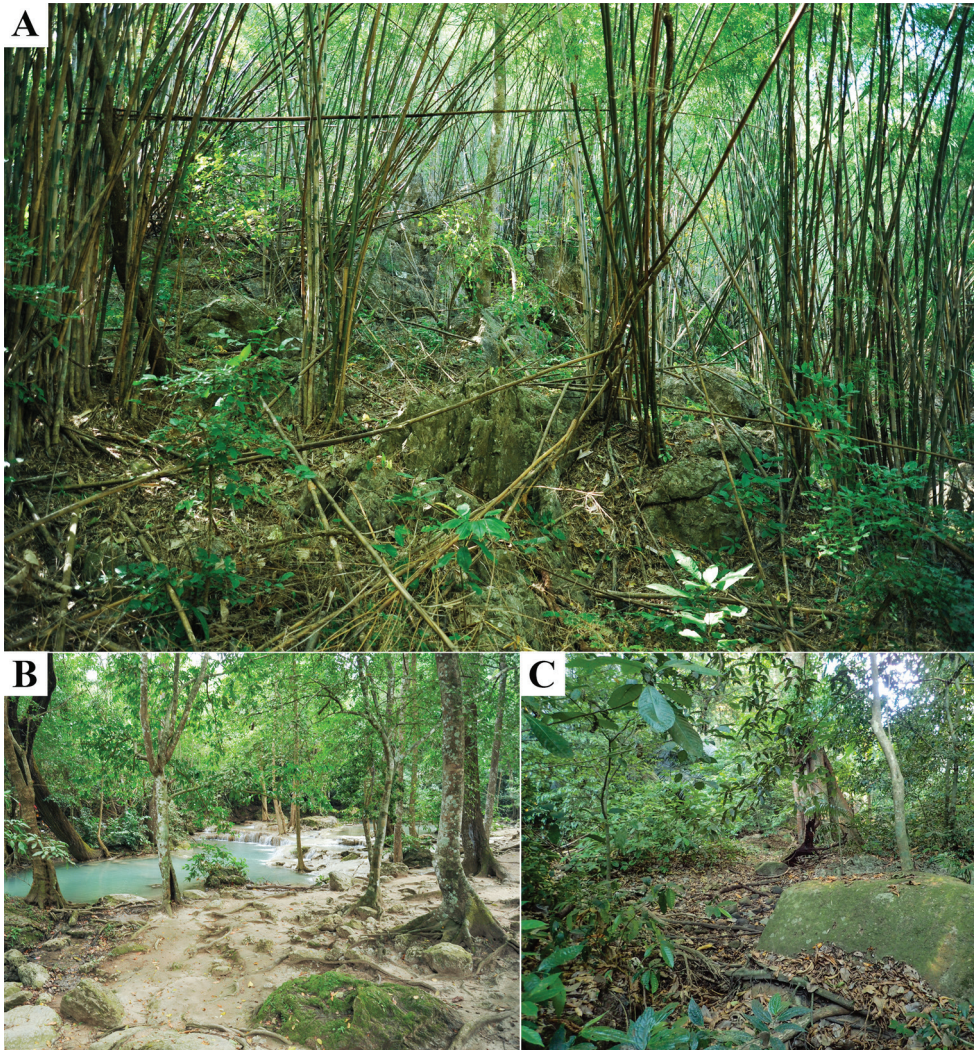


Figure 6. Sampling localities of *Cyrtodactylus monilatus* sp. nov. **A** the type locality in Tham Phrathat Protection Unit **B** Erawan Waterfall **C** Tham Than Lot Noi-Tham Than Lot Yai Nature Trail, Si Sawat District, Kanchanaburi Province, Thailand.

borders fore and aft, alternating with narrower medium to light-brown interspaces); and two rows of small, diffuse, yellow or yellowish white spots on flanks present (vs. absent).

Cyrtodactylus monilatus sp. nov. differs from *C. oldhami* (Theobald, 1876) by having 16–21 longitudinal rows of dorsal tubercles (vs. 30 rows); precloacal pores absent in both sexes (vs. present in males); top of head bearing large, dark-brown blotches edged in yellow or yellowish white (vs. uniform brown); and dorsal body bands composed of paired, paravertebral, dark-brown blotches edged in yellow or yellowish white (vs. elongated or rounded spots arranged in four longitudinal lines).

Cyrtodactylus monilatus sp. nov. differs from *C. payarhtanensis* Mulcahy, Thura & Zug, 2017 by being smaller, SVL 53.7–63.3 mm in adult males, 58.6–75.8 mm in adult females (vs. 61–80 mm in adult males, 74–83 mm in adult females); 22–34 paravertebral tubercles (vs. 40–45 tubercles); 34–42 ventral scales (vs. 26–32 scales); 15–19 total subdigital lamellae on the fourth toe (vs. 12 or 13); enlarged median subcaudal scales absent (vs. present); top of head bearing dark-brown blotches edged in yellow or yellowish white (vs. indistinctly mottled, dusky brown marks); dorsal body bands composed of paired, paravertebral, dark-brown blotches edged in yellow or yellowish white (vs. irregularly shaped and edged dark-brown); and two rows of small, diffuse, yellow or yellowish white spots on flanks present (vs. absent).

Cyrtodactylus monilatus sp. nov. differs from *C. phetchaburiensis* Pauwels, Sumontha & Bauer, 2016 which is not in the phylogeny by lacking precloacal pores in both sexes (vs. present in males); enlarged median subcaudal scales absent (vs. present); and dorsal body bands composed of paired, paravertebral, dark-brown blotches edged in yellow or yellowish white (vs. absent).

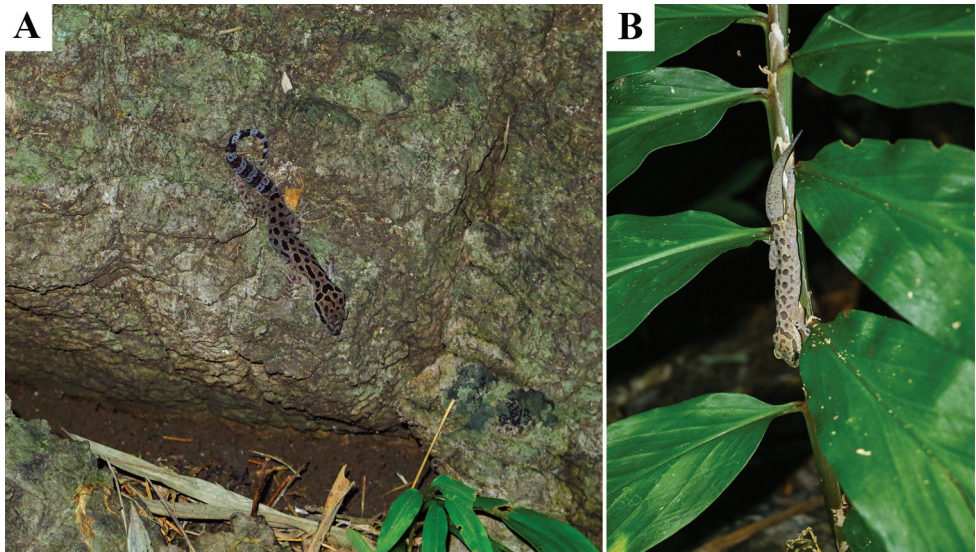


Figure 7. Habitat of *Cyrtodactylus monilatus* sp. nov. Tham Phrathat Protection Unit, Si Sawat District, Kanchanaburi Province, Thailand **A** adult female (ZMKU R 00941) on boulder outcrops **B** adult male (not collected) on shrub.

Cyrtodactylus monilatus sp. nov. differs from *C. saiyok* Panitvong, Sumontha, Tunprasert & Pauwels, 2014 by having 34–42 ventral scales (vs. 23–24 scales); precloacal pores absent in both sexes (vs. present in males); enlarged median subcaudal scales absent (vs. present); and dorsal body bands composed of paired, paravertebral, dark-brown blotches edged in yellow or yellowish white (vs. irregular, medially interrupted or not, black).

Cyrtodactylus monilatus sp. nov. differs from *C. sanook* Pauwels, Sumontha, Latinne & Grismer, 2013 by being smaller, SVL 53.7–63.3 mm in adult males (vs. 72.9–79.5 mm); precloacal pores absent in both sexes (vs. present in males); enlarged median subcaudal scales absent (vs. present); and dorsal body bands composed of paired, paravertebral, dark-brown blotches edged in thin yellow or yellowish white (vs. irregular pale narrow bands).

Cyrtodactylus monilatus sp. nov. differs from *C. surin* Chan-ard & Makchai, 2011 which is not in the phylogeny by having 34–42 ventral scales (vs. 25 ventral scales); enlarged median subcaudal scales absent (vs. present); and precloacal pores absent in both sexes (vs. present in males).

Cyrtodactylus monilatus sp. nov. differs from *C. thirakhupti* Pauwels, Bauer, Sumontha & Chanhome, 2004 by being smaller, SVL 53.7–63.3 mm in adult males (vs. 72.0–79.6 mm in adult males); 16–21 longitudinal rows of dorsal tubercles (vs. 14 rows); enlarged median subcaudal scales absent (vs. present); and dorsal body bands composed of paired, paravertebral, dark-brown blotches edged in yellow or yellowish white (vs. yellowish bands with very dark brown borders).

Cyrtodactylus monilatus sp. nov. differs from *C. zebraicus* Taylor, 1962 by having precloacal pores absent in both sexes (vs. present in males; Fig. 8); four or five rows of postprecloacal scales (vs. two rows); and two rows of small, diffuse, yellow or yellowish white spots on flanks present (vs. their absence; Fig. 8; Grismer et al. 2018a: fig. 4A; Bringsøe, 2020: fig. 1; Grismer et al. 2021b: fig. 28B).

Discussion

The combination of morphological and molecular phylogenetic evidence in this study corroborated the hypothesis that the Si Sawat population should be recognized as a distinct species, described here as *Cyrtodactylus monilatus* sp. nov., and that this new species is a member of the *C. oldhami* group. Morphologically, the new species superficially resembles *C. zebraicus* from southern Thailand in body shape and color pattern, but phylogenetically they are not closely related. Moreover, our phylogenetic analyses of the *C. oldhami* group indicated that populations in Thailand that are currently referred to *C. oldhami* are not monophyletic and likely represent additional, undescribed species (Chomdej et al. 2021; Grismer et al. 2021b). Unfortunately, the type locality of *C. oldhami* is uncertain (Annandale 1905, 1913; Das et al. 1998; Pauwels et al. 2016; Uetz et al. 2022) and so the concept of *C. oldhami* is limited to the original description of the holotype (Theobald 1876). It is therefore possible that none of the “*C. oldhami*” samples in our phylogenetic analyses represent true *C. oldhami*. Comparisons of the holotype to all specimens from Thailand and Myanmar currently referred to *C. oldhami* are necessary before further taxonomic partitioning of *C. oldhami* can be done.

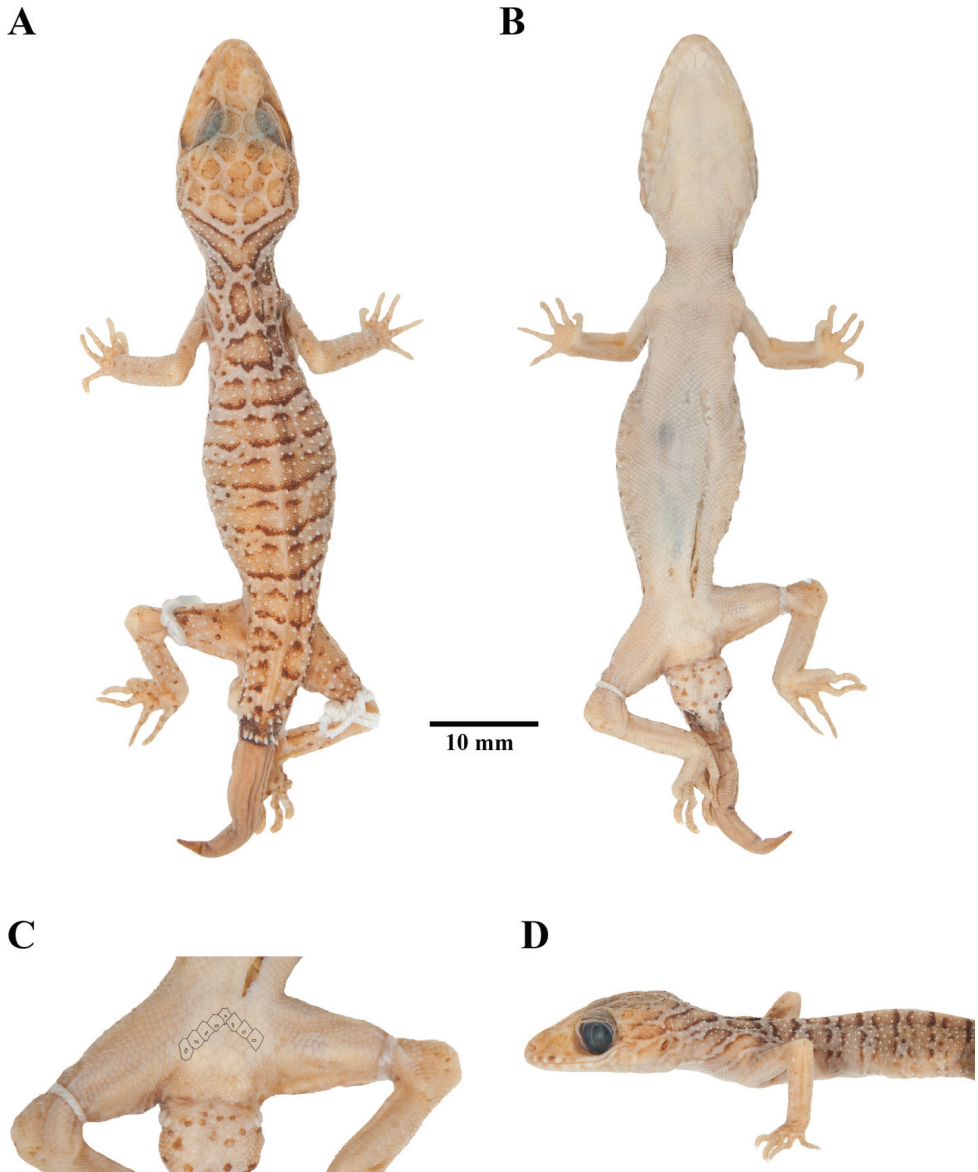


Figure 8. Adult male holotype of *Cyrtodactylus zebraicus* (FMNH 178286) from Ron Phibun District, Nakhon Si Thammarat Province, Thailand, in preservation **A** dorsal view **B** ventral view **C** preloacal region showing distribution of preloacal pores **D** lateral view of the left side.

Cyrtodactylus phetchaburiensis and *C. surin* were described from the Isthmus of Kra area (Phetchaburi Province and Surin Island, Phang-nga Provinces, respectively) based only on morphological data (Chan-ard and Makchai 2011; Pauwels et al. 2016). These two species can be tentatively assigned to the *C. oldhami* group based on their morphological appearances and geographic distributions (Pauwels et al. 2016; personal observation). However, genetic data are needed to verify their taxonomic status and phylogenetic

placement. The discovery of *Cyrtodactylus monilatus* sp. nov. brings the number of species in the *C. oldhami* group to eight and the total number of *Cyrtodactylus* in Thailand to 40 (Termprayoon et al. 2021; Uetz et al. 2022). *Cyrtodactylus monilatus* sp. nov. is currently known only from the kart forests in Si Sawat District, Kanchanaburi Province in western Thailand. Additional field surveys and sampling in western Thailand and nearby areas including the Thai-Myanmar border, as well as re-evaluation of existing museum specimens, are needed to determine the actual geographic range of the new species.

Acknowledgements

This work was financially supported by the Office of the Ministry of Higher Education, Science, Research and Innovation; and the Thailand Science Research and Innovation through the Kasetsart University Reinventing University Program 2021. AR and AA were supported by Kasetsart University Research and Development Institute (KURDI), the Department of Zoology, Faculty of Science, Kasetsart University and Office of the Permanent Secretary, Ministry of Higher Education, Science, Research and Innovation (Grant No. RGNS 64-038). NA was supported by Srinakharinwirot University Research (Grant No. 596/2564). The study was ethical reviews and approvals by the Institutional Animal Care and Use Committee of Faculty of Science, Kasetsart University (project number ACKU61-SCI-008 and ACKU64-SCI-005) and the Department of National Parks, Wildlife and Plant Conservation, Thailand provided research permission (No. 0907.4/3328 and No. 0907.4/20535). We would like to thank Suchai Horradee (Chaloem Rattanakosin National Park), Porayoot Vaivong and Peerawat Sirothphiphat (Erawan National Park) for facilitating the fieldwork. Sang Nguyen and Han Ngo improved the manuscript.

References

- Annandale N (1905) Contributions to Oriental herpetology II. Notes on Oriental lizards in the Indian Museum, with a list of the species recorded from British India and Ceylon. Part I. Journal and Proceedings of the Asiatic Society of Bengal n.s. 1(3): 81–97.
- Annandale N (1913) The Indian geckos of the genus *Gymnodactylus*. Records of the Indian Museum 9: 309–326. [pls XVI, XVII]
- Bauer AM, Giri VB, Greenbaum E, Jackman TR, Dharne MS, Shouche YS (2008) On the Systematics of the Gekkonid Genus *Teratolepis* Günther, 1869: Another One Bites the Dust. Hamadryad 33(1): 13–27.
- Boulenger GA (1893) Concluding report on the reptiles and batrachians obtained in Burma by Signor L. Fea, dealing with a collection made in Pegu and Karin Hills in 1887–1888. Annali del Museo Civico di Storia Naturale di Genova 13(2): 304–347.
- Brennan IG, Bauer AM, Tri NV, Wang YY, Wang WZ, Zhang YP, Murphy RW (2017) Barcoding utility in a mega-diverse, cross-continental genus: Keeping pace with *Cyrtodactylus* geckos. Scientific Reports 7(1): e5592. <https://doi.org/10.1038/s41598-017-05261-9>

- Bringsøe H (2020) Observation on *Cyrtodactylus zebraicus* Taylor, 1962 tolerating a contactpoisonous plant in southern Thailand. *Sauria* 42(2): 54–56.
- Chan-ard T, Makchai S (2011) A New Insular Species of *Cyrtodactylus* Gray, 1827 (Squamata, Gekkonidae), from the Surin Islands, Phang-nga Province, Southern Thailand. *The Thailand Natural History Museum Journal* 5(1): 7–15.
- Chomdej S, Suwanapoom C, Pawangkhanant P, Pradit W, Nazarov RA, Grismer LL, Poyarkov NA (2020) A new species *Cyrtodactylus* Gray (Squamata: Gekkonidae) from western Thailand and the phylogenetic placement of *C. inthanon* and *C. doisuthep*. *Zootaxa* 4838(2): 179–209. <https://doi.org/10.11646/zootaxa.4838.2.2>
- Chomdej S, Pradit W, Suwanapoom C, Pawangkhanant P, Nganvongpanit K, Poyarkov NA, Che J, Gao YC, Gong SP (2021) Phylogenetic analyses of distantly related clades of bent-toed geckos (genus *Cyrtodactylus*) reveal an unprecedented amount of cryptic diversity in northern and western Thailand. *Scientific Reports* 11(1): e2328. <https://doi.org/10.1038/s41598-020-70640-8>
- Connette GM, Oswald P, Thura MK, Connette KJJ, Grindley ME, Songer M, Zug GR, Mulcahy DG (2017) Rapid forest clearing in a Myanmar proposed national park threatens two newly discovered species of geckos (Gekkonidae: *Cyrtodactylus*). *PLoS ONE* 12(4): e0174432. <https://doi.org/10.1371/journal.pone.0174432>
- Das I, Dattagupta B, Gayen NC (1998) History and catalogue of reptile types in the collection of the Zoological Survey of India. *Journal of Southeast Asian History* 3(2): 121–172.
- Grismer LL, Wood Jr PL, Quah ESH, Murdoch ML, Grismer MS, Herr MW, Espinoza RE, Brown RM, Lin A (2018a) A phylogenetic taxonomy of the *Cyrtodactylus peguensis* group (Reptilia: Squamata: Gekkonidae) with descriptions of two new species from Myanmar. *PeerJ* 6: e5575. <https://doi.org/10.7717/peerj.5575>
- Grismer LL, Wood Jr PL, Thura MK, Zin T, Quah ESH, Murdoch ML, Grismer MS, Lin A, Kyaw H, Lwin N (2018b) Twelve new species of *Cyrtodactylus* Gray (Squamata: Gekkonidae) from isolated limestone habitats in east-central and southern Myanmar demonstrate high localized diversity and unprecedented microendemism. *Zoological Journal of the Linnean Society* 182(4): 862–959. <https://doi.org/10.1093/zoolinnean/zlx057>
- Grismer LL, Rujirawan A, Termprayoon K, Ampai N, Yodthong S, Wood Jr PL, Oaks JR, Aowphol A (2020) A new species of *Cyrtodactylus* Gray (Squamata; Gekkonidae) from the Thai Highlands with a discussion on the evolution of habitat preference. *Zootaxa* 4852(4): 401–427. <https://doi.org/10.11646/zootaxa.4852.4.1>
- Grismer L, Wood Jr PL, Poyarkov NA, Le MD, Karunarathna S, Chomdej S, Suwanapoom C, Qi S, Liu S, Che J, Quah ESH, Kraus F, Oliver PM, Riyanto A, Pauwels OSG, Grismer JL (2021a) Karstic landscapes are foci of species diversity in the world's third-largest vertebrate genus *Cyrtodactylus* Gray, 1827 (Reptilia: Squamata; Gekkonidae). *Diversity (Basel)* 13(5): 183. <https://doi.org/10.3390/d13050183>
- Grismer LL, Wood Jr PL, Poyarkov NA, Le MD, Kraus F, Agarwal I, Oliver PM, Nguyen SN, Nguyen TQ, Karunarathna S, Welton LJ, Stuart BL, Luu VQ, Bauer AM, O'Connell KA, Quah ESH, Chan KO, Ziegler T, Ngo H, Nazarov RA, Aowphol A, Chomdej S, Suwanapoom C, Siler CD, Anuar S, Tri NV, Grismer JL (2021b) Phylogenetic partitioning of the third-largest vertebrate genus in the world, *Cyrtodactylus* Gray, 1827 (Reptilia; Squa-

- mata; Gekkonidae) and its relevance to taxonomy and conservation. *Vertebrate Zoology* 71: 101–154. <https://doi.org/10.3897/vertebrate-zoology.71.e59307>
- Grismer LL, Poyarkov NA, Quah ESH, Grismer JL, Wood Jr PL (2022) The biogeography of bent-toed geckos, *Cyrtodactylus* (Squamata: Gekkonidae). *PeerJ* 10: e13153. <https://doi.org/10.7717/peerj.13153>
- Hoang DT, Chernomor O, von Haeseler A, Minh BQ, Vinh LS (2017) UFBoot2: Improving the ultrafast bootstrap approximation. *Molecular Biology and Evolution* 35(2): 518–522. <https://doi.org/10.1093/molbev/msx281>
- Huelsenbeck J, Ronquist F (2001) MRBAYES: Bayesian inference of phylogeny. *Bioinformatics (Oxford, England)* 17(8): 754–755. <https://doi.org/10.1093/bioinformatics/17.8.754>
- Johnson CB, Quah ESH, Anuar S, Muin MA, Wood Jr PL, Grismer JL, Greer LF, Chan KO, Ahmad N, Bauer AM, Grismer LL (2012) Phylogeography, geographic variation, and taxonomy of the Bent-toed Gecko *Cyrtodactylus quadrivirgatus* Taylor, 1962 from Peninsular Malaysia with the description of a new swamp dwelling species. *Zootaxa* 3406: 39–58. <https://doi.org/10.11646/zootaxa.3406.1.3>
- Kalyaanamoorthy S, Minh BQ, Wong TK, von Haeseler A, Jermin LS (2017) ModelFinder: Fast model selection for accurate phylogenetic estimates. *Nature Methods* 14(6): 587–589. <https://doi.org/10.1038/nmeth.4285>
- Macey JR, Larson A, Ananjeva NB, Papenfuss TJ (1997) Evolutionary shifts in three major structural features of the mitochondrial genome among iguanian lizards. *Journal of Molecular Evolution* 44(6): 660–674. <https://doi.org/10.1007/PL00006190>
- Miller MA, Pfeiffer W, Schwartz T (2010) Creating the CIPRES Science Gateway for inference of large phylogenetic trees. In: *Proceedings of the Gateway Computing Environments Workshop (GCE)*, 14 November 2010, New Orleans, 8 pp. <https://doi.org/10.1109/GCE.2010.5676129>
- Minh BQ, Nguyen MAT, Haeseler A (2013) Ultrafast approximation for phylogenetic bootstrap. *Molecular Biology and Evolution* 30(5): 1188–1195. <https://doi.org/10.1093/molbev/mst024>
- Murdoch ML, Grismer LL, Wood Jr PL, Neang T, Poyarkov NA, Tri NV, Nazarov RA, Aowphol A, Pauwels OSG, Nguyen HN, Grismer JL (2019) Six new species of the *Cyrtodactylus intermedius* complex (Squamata: Gekkonidae) from the Cardamom Mountains and associated highlands of Southeast Asia. *Zootaxa* 4554(1): 001–062. <https://doi.org/10.11646/zootaxa.4554.1.1>
- Panitvong N, Sumontha M, Tunprasert J, Pauwels OSG (2014) *Cyrtodactylus saiyok* sp. nov., a new dry evergreen forest-dwelling bent-toed gecko (Squamata: Gekkonidae) from Kanchanaburi Province, western Thailand. *Zootaxa* 3869(1): 064–074. <https://doi.org/10.11646/zootaxa.3869.1.6>
- Pauwels OSG, Bauer AM, Sumontha M, Chanhome L (2004) *Cyrtodactylus thirakhupti* (Squamata: Gekkonidae), a new cave-dwelling gecko from southern Thailand. *Zootaxa* 772(1): 1–11. <https://doi.org/10.11646/zootaxa.772.1.1>
- Pauwels OSG, Sumontha M, Latinne A, Grismer LL (2013) *Cyrtodactylus sanook* (Squamata: Gekkonidae), a new cave-dwelling gecko from Chumphon Province, southern Thailand. *Zootaxa* 3635(3): 275–285. <https://doi.org/10.11646/zootaxa.3635.3.7>
- Pauwels OSG, Sumontha M, Bauer AM (2016) A new bent-toed gecko (Squamata: Gekkonidae: *Cyrtodactylus*) from Phetchaburi Province, Thailand. *Zootaxa* 4088(3): 409–419. <https://doi.org/10.11646/zootaxa.4088.3.6>

- Rambaut A, Drummond AJ, Xie D, Baele G, Suchard MA (2018) Posterior summarisation in Bayesian phylogenetics using Tracer 1.7. *Systematic Biology* 67(5): 901–904. <https://doi.org/10.1093/sysbio/syy032>
- Ronquist F, Teslenko M, van der Mark P, Ayres DL, Darling A, Höhna S, Larget B, Liu L, Suchard MA, Huelsenbeck JP (2012) MrBayes 3.2: Efficient Bayesian phylogenetic inference and model choice across a large model space. *Systematic Biology* 61(3): 539–542. <https://doi.org/10.1093/sysbio/sys029>
- Rösler H, Bauer AM, Heinicke MP, Greenbaum E, Jackman T, Nguyen TQ, Ziegler T, Rösler H (2011) Phylogeny, taxonomy, and zoogeography of the genus *Gekko* Laurenti, 1768 with the revalidation of *G. reevesii* Gray, 1831 (Sauria: Gekkonidae). *Zootaxa* 2989(1): 1–50. <https://doi.org/10.11646/zootaxa.2989.1.1>
- Siler CD, Oaks JR, Esselstyn JA, Diesmos AC, Brown RM (2010) Phylogeny and biogeography of Philippine bent-toed geckos (Gekkonidae: *Cyrtodactylus*) contradict a prevailing model of Pleistocene diversification. *Molecular Phylogenetics and Evolution* 55(2): 699–710. <https://doi.org/10.1016/j.ympev.2010.01.027>
- Simmons JE (2015) *Herpetological Collecting and Collections Management*, 3rd ed. Society for the Study of Amphibians and Reptiles Herpetological Circular No. 42. Salt Lake City, UT, 191 pp.
- Tamura K, Stecher G, Kumar S (2021) MEGA11: Molecular evolutionary genetics analysis version 11. *Molecular Biology and Evolution* 38(7): 3022–3027. <https://doi.org/10.1093/molbev/msab120>
- Taylor EH (1962) New oriental reptiles. *The University of Kansas Science Bulletin* 43: 209–263. <https://doi.org/10.5962/bhl.part.13346>
- Termprayoon K, Rujirawan A, Ampai N, Wood Jr PL, Aowphol A (2021) A new insular species of the *Cyrtodactylus pulchellus* group (Reptilia, Gekkonidae) from Tarutao Island, southern Thailand revealed by morphological and genetic evidence. *ZooKeys* 1070: 101–134. <https://doi.org/10.3897/zookeys.1070.73659>
- Theobald W (1876) *Descriptive catalogue of the reptiles of British India*. Thacker, Spink & Co., Calcutta, [xiii +] 238 pp. <https://doi.org/10.5962/bhl.title.5483>
- Trifinopoulos J, Nguyen LT, von Haeseler A, Minh BQ (2016) W-IQ-TREE: A fast online phylogenetic tool for maximum likelihood analysis. *Nucleic Acids Research* 44(W1): W232–W235. <https://doi.org/10.1093/nar/gkw256>
- Uetz P, Freed P, Hosek J (2022) *The Reptile Database*. <https://reptile-database.org> [accessed 31 March 2022]
- Wilcox TP, Zwickl DJ, Heath TA, Hillis DM (2002) Phylogenetic relationships of the dwarf boas and a comparison of Bayesian and bootstrap measures of phylogenetic support. *Molecular Phylogenetics and Evolution* 25(2): 361–371. [https://doi.org/10.1016/S1055-7903\(02\)00244-0](https://doi.org/10.1016/S1055-7903(02)00244-0)
- Wood Jr PL, Heinicke MP, Jackman TR, Bauer AM (2012) Phylogeny of bent-toed geckos (*Cyrtodactylus*) reveals a west to east pattern of diversification. *Molecular Phylogenetics and Evolution* 65(3): 992–1003. <https://doi.org/10.1016/j.ympev.2012.08.025>

Cave-inhabiting Cheliferidae (Arachnida, Pseudoscorpiones) from Thailand, with description of four new species of *Metachelifer* Redikorzev

Yun-Chun Li¹, Ai-Min Shi²

1 College of Life Science, China West Normal University, Nanchong, Sichuan 637009, China **2** Key Laboratory of Southwest China Wildlife Resources Conservation, Institute of Rare Animals & Plants, China West Normal University, Nanchong, Sichuan 637009, China

Corresponding author: Yun-Chun Li (liyc2260@cwnu.edu.cn)

Academic editor: Jana Christophoryová | Received 3 December 2021 | Accepted 13 May 2022 | Published 3 June 2022

<http://zoobank.org/50A8B929-B506-4C21-AD58-A507E5089AE2>

Citation: Li Y-C, Shi A-M (2022) Cave-inhabiting Cheliferidae (Arachnida, Pseudoscorpiones) from Thailand, with description of four new species of *Metachelifer* Redikorzev. ZooKeys 1103: 171–188. <https://doi.org/10.3897/zookeys.1103.78808>

Abstract

Four new species of the genus *Metachelifer* Redikorzev, 1938 are described from caves in the provinces of Tak (*M. takensis* **sp. nov.** and *M. thailandicus* **sp. nov.**), Chiangmai (*M. mahnerti* **sp. nov.**), and Nakhon Ratchasima (*M. cheni* **sp. nov.**). An identification key is provided to all known world representatives of the genus *Metachelifer*.

Keywords

Identification key, pseudoscorpion, Southeast Asia, taxonomy, troglobiont

Introduction

The pseudoscorpion genus *Metachelifer* Redikorzev, 1938 belongs to the family Cheliferidae Risso, 1827 and the subfamily Cheliferinae. This subfamily contains 57 genera that are mostly distributed in Africa, southern Europe, central Asia, North America,

and South America (World Pseudoscorpiones Catalog 2022). At present, *Metachelifer* contains three species which are confined to Asia: *M. duboscqui* Redikorzev, 1938 from Cambodia, Laos, Philippines, and Vietnam; *M. macrotuberculatus* (Krumpál, 1987) and *M. nepalensis* (Beier, 1974) from Nepal (Redikorzev 1938; Beier 1974; Krumpál 1987).

Males of the genus *Metachelifer* can be characterized by the carapace surface with tubercles; coxa IV with an anterolateral process and coxal sac; sternite III uplifted laterally and extending to short thorns; leg I tarsus lateral claw shorter than mesal one; subterminal seta simple (Redikorzev 1938; Dashdamirov 2006). While identifying pseudoscorpion specimens collected from Thailand in 2014–2016, four new cave-inhabiting species of *Metachelifer* were found and are described here.

Materials and methods

The specimens were examined with a Leica M205FA stereomicroscope and an Olympus CX31 compound microscope. The specimens are preserved in 75% ethanol. They were cleared in lactic acid for 12–24 h at room temperature and, after the study, washed in distilled water and returned to alcohol. Photographs were taken using a Canon 6D Mark II camera fitted with a Laowa 25 mm f/2.8 2.5–5 × and 100 mm F2.8 2.0 × ultra macro lens. The final high depth of field images were stacked from 30 to 80 single photos using Helicon Focus 7.6.1., and CorelDRAW 2018 and SAI 2 software were used to draw the figures. The type specimens of the new species are deposited in the collection of the Museum of China West Normal University (MCWNU; Sichuan, China) and Muséum national d'Histoire naturelle (MNHN; Paris, France).

Pseudoscorpion terminology and measurements mostly follow Chamberlin (1931) with some minor modifications to the terminology of the trichobothria (Harvey 1992) and chelicera (Judson 2007). The following abbreviations are used for the trichobothria: *b* = basal; *sb* = sub-basal; *st* = sub-terminal; *t* = terminal; *ib* = interior basal; *isb* = interior sub-basal; *ist* = interior sub-terminal; *it* = interior terminal; *eb* = exterior basal; *esb* = exterior sub-basal; *est* = exterior sub-terminal; *et* = exterior terminal.

Results

Cheliferidae Risso, 1827

Cheliferinae Risso, 1827

Metachelifer Redikorzev, 1938

Metachelifer Redikorzev, 1938: 108.

Type species. *Metachelifer duboscqui* Redikorzev, 1938, by monotypy.

Identification key to the species of *Metachelifer*

- 1 Carapace slightly broader than long 2
 – Carapace slightly longer than broad 3
 2 Tergite XI with two tactile setae; pedipalpal femur $4.49 \times$ longer than broad (1.08/0.24 mm) *M. macrotuberculatus* (Krumpál, 1987)
 – Tergite XI without tactile setae; pedipalpal femur $5.22 \times$ longer than broad (1.41/0.27 mm) *M. nepalensis* (Beier, 1974)
 3 Fixed and movable chelal fingers with at least 57 teeth; trichobothrium *st* distinctly closer to *sb* than to *t* 4
 – Fixed and movable chelal fingers with 35 teeth; trichobothrium *st* midway between *sb* and *t* *M. duboscqui* Redikorzev, 1938
 4 Tergite XI with two tactile setae 5
 – Tergite XI without tactile setae *M. mahnerti* Li & Shi, sp. nov.
 5 Venom ducts very short, not extending past *et* (Figs 1G, 4F); posterior genital operculum of female without lyrifissures 6
 – Venom ducts long, extending past *et* (Fig. 3G); posterior genital operculum of female with eight lyrifissures *M. takensis* Li & Shi, sp. nov.
 6 Carapace with 100–101 setae; coxal sac occupying 1/2 of coxal length; anterior genital operculum of female with tubular setae
 *M. cheni* Li & Shi, sp. nov.
 – Carapace with 86–88 setae; coxal sac occupying only 2/5 of coxal length; anterior genital operculum of female without tubular setae
 *M. thailandicus* Li & Shi, sp. nov.

***Metachelifer cheni* sp. nov.**

<http://zoobank.org/06F1B0AB-CAE5-461F-A445-53C976611A5C>

Figs 1, 5A, B

Type material. *Holotype* male: Thailand, Nakhon Ratchasima Province, Pak Chong district, Musee Village, Wat Dewaroop Song Cave 3, $14^{\circ}33.714'N$, $101^{\circ}24.049'E$, 402 m a.s.l., 24 Oct. 2014, Yun-Chun Li and Zhi-Gang Chen leg., in MCWNU (Ms20141014-01). *Paratypes*: 3 males, 7 females, 7 tritonymphs, collected with the holotype, in MCWNU (Ms20141014-01); 1 male, 2 females, 1 tritonymph, collected with the holotype, in MNHN.

Diagnosis. Troglobiont habitus. This new species is distinguished from other members of the genus *Metachelifer* by the following combination of characters: carapace with 100–101 setae; coxal sac occupying 1/2 of coxal length; male anterior genital operculum without tubular setae; female anterior genital operculum with 31 setae (24 of them tubular) and two lyrifissures; posterior operculum with 12 setae, without lyrifissures.

Etymology. Latinized adjective, derived from the last name of the collector, Zhi-Gang Chen.

Description. Adult male (Fig. 5A). Carapace, pedipalps and tergites I–III brown, remaining parts yellowish brown (Fig. 5A).

Carapace (Fig. 1A): $1.14\text{--}1.16 \times$ longer than broad, with a pair of well-developed eyes, length of eyes 0.09 mm, breadth 0.03 mm, carapace surface evenly and strongly granular. Median and posterior furrows prominent, regularly granular. Dorsal setae of carapace, borne on larger but relatively inconspicuous tubercles. With 100–101 denticuloclavate setae, including 8 on anterior margin and 11–12 on posterior margin. **Coxae:** manducatory process with 4 setae (1 long apical, 2 rather short subapical setae, and 1 suboral seta at base of medial margin). Pedipalpal coxa with 10 (non-denticulate) + 7–8 (denticulate) setae, coxa I 14–16, II 15, III 18–19, IV with an anterolateral process and 30–36 setae. Coxal sac occupying only 1/2 of coxal length, atrium well developed (Fig. 1E). **Chelicera** (Fig. 1B): $1.85\text{--}1.91 \times$ longer than broad, hand with 5 setae and 1 lyrifissure dorsally, movable finger with 1 submedial seta (1 specimen with 2 submedial setae) and 2–3 teeth (Fig. 1B). Galea with a short, broad stump on left chelicera (clearly broken). Serrula exterior with about 21–22 blades. Rallum with 3 blades, anterior 1 weakly denticulate distally. **Pedipalp** (Fig. 1F–H): all segments with well-developed granulations, except for chelal fingers, which are smooth; dorsal setae short and prominently denticuloclavate. Trochanter $1.92\text{--}1.95 \times$, femur $6.55\text{--}6.57 \times$, patella $5.29\text{--}5.33 \times$ longer than broad. Femur $1.13\text{--}1.14 \times$ longer than patella. Chela with pedicel $6.10\text{--}6.12 \times$, hand with pedicel $3.06\text{--}3.08 \times$ longer than broad; movable chelal finger $1.03\text{--}1.04 \times$ longer than hand with pedicel length. Fixed finger with 64–66 small cusped teeth, movable finger with 63–65 teeth; venom apparatus present in both chelal fingers very short (Fig. 1G). Fixed chelal finger with 8 trichobothria and movable finger with 4, *eb-esb* (retrolateral view) and *ib-isb* (dorsal view) at the base of the fixed finger; *est* in finger middle, *et* distinctly closer to fingertip than to *it*; on movable finger, *st* nearer to *sb* than to *t*. **Opisthosoma:** tergal chaetotaxy (I–XI): 10: 12: 13: 14: 16: 16: 14: 19: 19: 15: 12; sternal chaetotaxy (IV–XI): $2 \times 2 + 9$: 11: 12: 12: 10: 14: 10: 9; anal cone with 2 dorsal and 2 ventral setae. Tergite XI with 2 tactile setae. Anterior genital operculum with 73–74 setae and 2 lyrifissures; posterior operculum with 16–17 setae, 7–8 lyrifissures (Fig. 1I). Structure of male genitalia as illustrated (Fig. 1J); eversible sacs large; apodeme of eversible sac and lateral apodeme well developed. **Legs** (Figs 1C–D): Leg I: surface with weak scale-like sculpture, trochanter $1.24\text{--}1.25 \times$, femur $1.76\text{--}1.78 \times$ longer than deep and $0.51\text{--}0.53 \times$ longer than patella; patella $4.21\text{--}4.24 \times$, tibia $5.90\text{--}5.93 \times$, tarsus $5.11\text{--}5.16 \times$ longer than deep, subterminal seta simple, claws modified and asymmetrical, lateral claw shorter than mesal one (Fig. 1C). Leg IV: trochanter $1.94\text{--}1.95 \times$, femoropatella $4.91\text{--}4.95 \times$, tibia $9.20\text{--}9.23 \times$ longer than deep and tarsus $8.00\text{--}8.05 \times$ longer than deep. Arolia on legs I and IV shorter than claws (Fig. 1C, D).

Adult female (Fig. 5B). Mostly the same as the holotype.

Carapace: slightly longer than broad ($1.12\text{--}1.13 \times$), anterior margin with 6 setae, posterior margin with 12–13 setae. Well-developed paramedian impressions behind eyes as in male. **Coxae:** pedipalpal coxa with 14 setae, coxa I 12–15, II 19–21, III

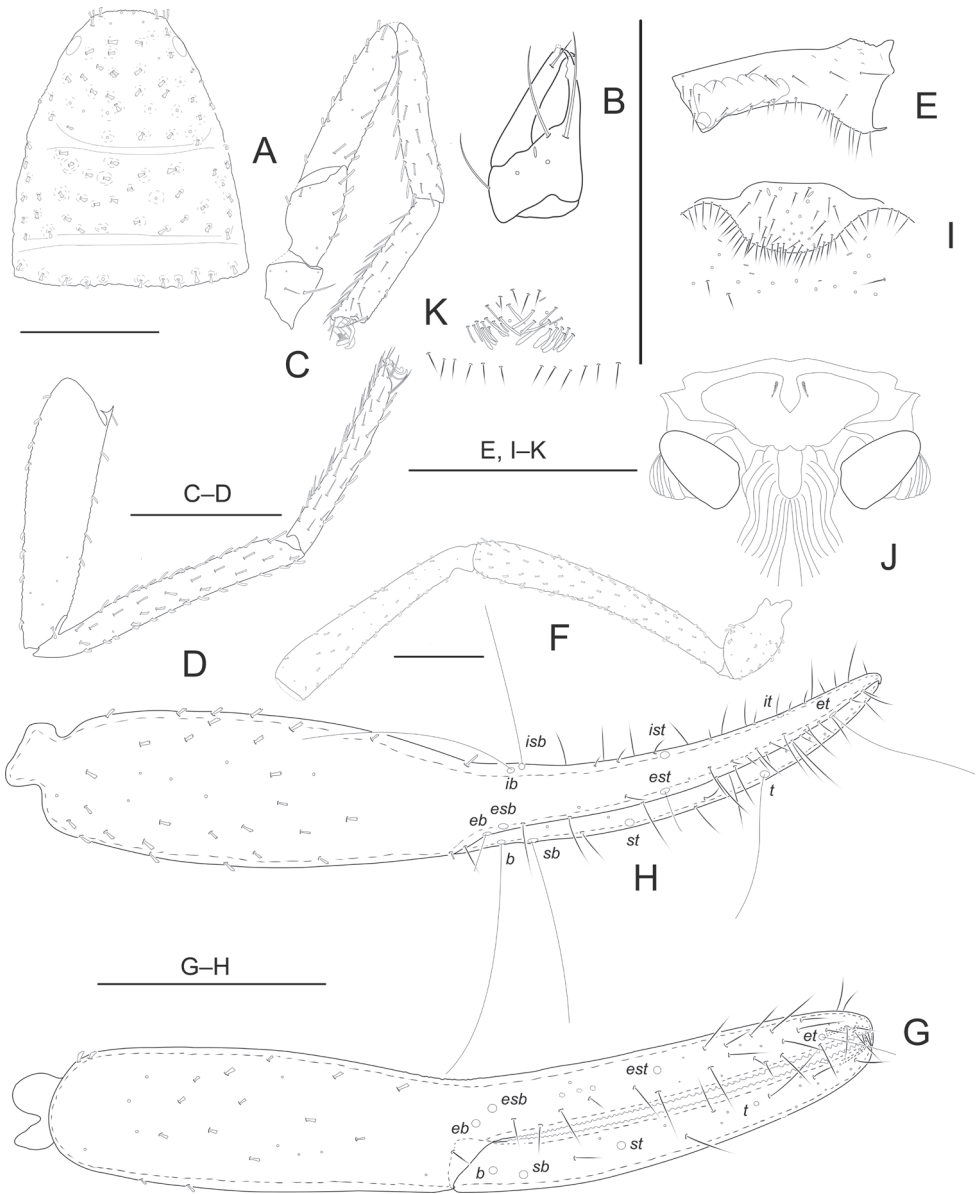


Figure 1. *Metachelifer cheni* sp. nov., holotype male (A–J) and paratype female (K) A carapace B left chelicera C right leg I, lateral view D right leg IV, lateral view E coxa IV, ventral view F palp (minus chela) G chela, retrolateral view H chela, dorsal view I male genital area J male genitalia, dorsal view K female genital area. Scale bars: 0.50 mm.

22–25, IV 33–38. **Chelicera:** 1.98–2.01 × longer than broad, movable finger with 3 teeth. **Pedipalp:** trochanter 2.07–2.09 × longer than broad, femur 6.46–6.48 × longer than broad, patella 5.11–5.15 × longer than broad, femur 1.12–1.13 × longer than patella. Chela with pedicel 5.53–5.56 × longer than broad, hand with pedicel 2.82–2.84

× longer than broad; movable finger 1.02–1.03 × longer than hand with pedicel length.

Opisthosoma: tergal chaetotaxy (I–XI): 11: 14: 13: 14: 16: 18: 18: 18: 16: 9; sternal chaetotaxy (IV–XI): 2 × 1 + 9: 15: 12: 13: 11: 14: 14: 7; anal cone with 2 dorsal and 2 ventral setae. Anterior genital operculum with 31 setae (24 of them tubular) and 2 lyrifissures; posterior operculum with 12 setae, without lyrifissures (Fig. 1K). Sternites with 2 lateral cribriform plates.

Dimensions (length/width or, in the case of the legs, length/depth in mm).

Males (females in parentheses): body length 2.52–2.74 (3.70–3.92). Carapace 0.96–0.98/0.84–0.86 (1.05–1.09/0.94–0.96). Pedipalp: trochanter 0.50–0.52/0.26–0.27 (0.58–0.60/0.28–0.29), femur 1.44–1.46/0.22–0.23 (1.55–1.58/0.24–0.25), patella 1.27–1.29/0.24–0.25 (1.38–1.41/0.27–0.28), hand with pedicel 0.95–0.97/0.31–0.32 (1.07–1.10/0.38–0.39), length of movable chelal finger 0.98–0.99 (1.09–1.11), chela 1.89–1.93/0.31–0.32 (2.10–2.13/0.38–0.39). Chelicera: 0.24–0.26/0.13–0.14 (0.26–0.28/0.14–0.15). Leg I: trochanter 0.21–0.22/0.17–0.18 (0.25–0.26/0.18–0.19), femur 0.30–0.32/0.17–0.18 (0.35–0.37/0.17–0.18), patella 0.59–0.61/0.14–0.15 (0.61–0.65/0.15–0.16), tibia 0.59–0.60/0.10–0.11 (0.65–0.66/0.10–0.11), tarsus 0.46–0.49/0.09–0.10 (0.65–0.67/0.10–0.11). Leg IV: trochanter 0.33–0.34/0.17–0.18 (0.35–0.37/0.23–0.24), femoropatella 1.08–1.10/0.22–0.23 (1.06–1.09/0.25–0.26), tibia 0.92–0.95/0.10–0.11 (0.98–0.99/0.12–0.13), tarsus 0.64–0.65/0.08–0.09 (0.65–0.68/0.09–0.10).

Distribution. Thailand (Nakhon Ratchasima).

***Metachelifer mahnerti* sp. nov.**

<http://zoobank.org/E787CC96-790B-4359-9632-8419F8AA5501>

Figs 2, 5C, D

Type material. *Holotype* male: Thailand, Chiangmai Province, Chom Thong district, Ban Luang Village, Tham Borichinda Cave, 18°29'53.01"N, 98°40'49.97"E, 379 m a.s.l., 15 Oct. 2014, Yun-Chun Li and Zhi-Gang Chen leg., in MCWNU (Ms20141015-01). *Paratypes*: 1 male, 7 females, 1 tritonymph, collected with the holotype in MCWNU (Ms20141015-01); 1 male, 1 female, collected with the holotype, in MNHN.

Diagnosis. Troglobiont habitus. This new species is distinguished from other members of the genus *Metachelifer* by the following combination of characters: anterior margin of carapace with 4 denticuloclavate setae and 91–93 setae; tergite XI without tactile setae; male anterior genital operculum with 68–70 setae (11–16 of them tubular); female anterior genital operculum without tubular setae, posterior operculum with 8 lyrifissures; and female body very large, 4.76–4.85 mm.

Etymology. The new species is named in honour of the late Volker Mahnert (Muséum d'histoire naturelle, Genève, Switzerland).

Description. Adult male (Fig. 5C). Carapace, pedipalps and tergites I–V dark brown, remaining parts yellowish brown (Fig. 5C).

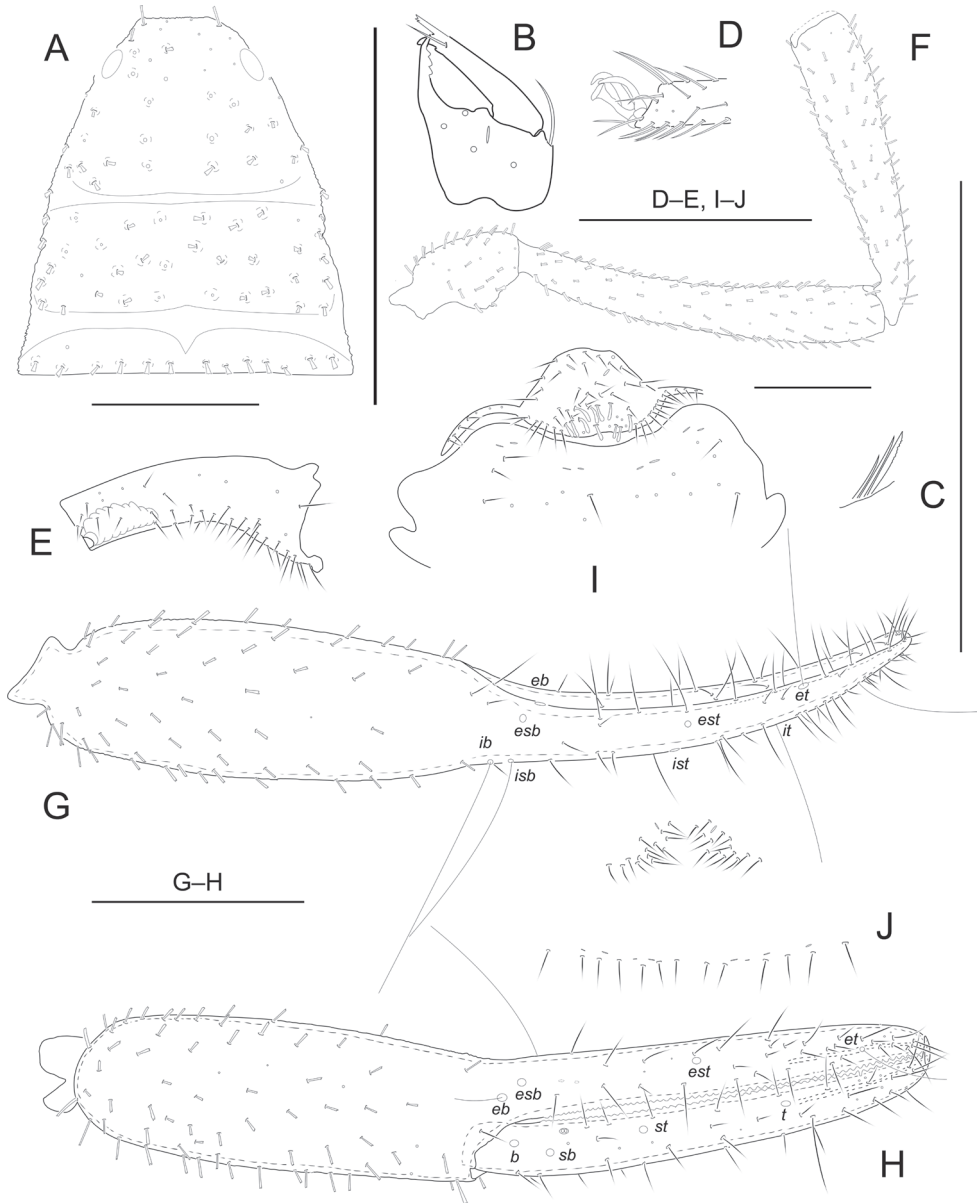


Figure 2. *Metachelifer mahnerti* sp. nov., holotype male (A–I) and paratype female (J) A carapace B left chelicera C rallum of left chelicera D detail on tarsus I, lateral view E coxa IV, ventral view F palp (minus chela) G chela, retrolateral view H chela, dorsal view I male genital area J female genital area. Scale bars: 0.50 mm.

Carapace (Fig. 2A): 1.05–1.06 × longer than broad, with a pair of well-developed eyes, length of eyes 0.10 mm, breadth 0.04 mm, carapace surface evenly and strongly granular. Median and posterior furrows prominent, regularly granular. Dorsal setae of carapace, borne on larger but relatively inconspicuous tubercles. With 91–93 den-

ticuloclavate setae, including 4 on anterior margin and 13–14 on posterior margin. **Coxae:** manducatory process with 4 setae (1 long apical, 2 rather short subapical setae, and 1 suboral seta at base of medial margin). Pedipalpal coxa with 11–12 (non-denticulate) + 4–5 (denticulate) setae, coxa I 20–22, II 19–21, III 21–23, IV with an anterolateral process and 43–47 setae. Coxal sac occupying only 2/5 of coxal length, atrium well developed (Fig. 2E). **Chelicera** (Fig. 2B, C): 1.66–1.69 × longer than broad, hand with 5 setae and 1 lyrifissure dorsally, movable finger with 1 submedial seta and 3 teeth (Fig. 2B). Galea with 3 short branches. Serrula exterior with about 19–20 blades. Rallum with 3 blades, anterior 1 weakly denticulate distally (Fig. 2C). **Pedipalp** (Fig. 2F–H): all segments with well-developed granulations, except for chelal fingers, which are smooth; dorsal setae short and prominently denticuloclavate. Trochanter 1.97–1.99 × longer than broad, femur 6.86–6.90 × longer than broad, patella 4.89–4.91 × longer than broad, femur 1.14–1.15 × longer than patella. Chela with pedicel 6.11–6.14 × longer than broad, hand with pedicel 2.97–2.99 × longer than broad; movable finger 1.06–1.07 × longer than hand with pedicel length. Fixed finger with 58–60 small cusped teeth, movable finger with 57–60 teeth; venom apparatus present in both chelal fingers, very short (Fig. 2H). Fixed chelal finger with 8 trichobothria and movable finger with 4, *eb-esb* (retrolateral view) and *ib-isb* (dorsal view) at the base of the fixed finger; *est* in finger middle, *et* distinctly closer to fingertip than to *it*; on movable finger, *st* nearer to *sb* than to *t*. **Opisthosoma:** tergal chaetotaxy (I–XI): 14: 16: 16: 18: 20: 24: 23: 20: 20: 13: 14; sternal chaetotaxy (IV–XI): 2 × 1 + 10: 12: 14: 12: 14: 13: 15: 13; anal cone with 2 dorsal and 2 ventral setae. Tergite XI without tactile setae. Because only two specimens were available for the study, the structure of the genitalia could not be examined in detail. Anterior genital operculum with 68–70 setae (11–16 of them tubular) and 2 lyrifissures; posterior operculum with 17–19 setae, 8 lyrifissures (Fig. 2I). **Legs:** Leg I: surface with weak scale-like sculpture, trochanter 1.35–1.36 ×, femur 1.84–1.86 × longer than deep and 0.58–0.60 × longer than patella; patella 4.00–4.02 ×, tibia 5.00–5.03 ×, tarsus 6.11–6.14 × longer than deep, subterminal seta simple, claws modified and asymmetrical, lateral claw shorter than mesal one (Fig. 2D). Leg IV: trochanter 1.63–1.64 × longer than deep, femoropatella 3.93–3.96 ×, tibia 7.38–7.40 × longer than deep and tarsus 7.22–7.26 × longer than deep. Arolia on legs I and IV shorter than claws.

Adult female (Fig. 5 D). Mostly the same as the holotype.

Carapace: slightly longer than broad (1.00–1.01 ×), anterior margin with 4 setae, posterior margin with 12–13 setae. Well-developed paramedian impressions behind eyes like in male. **Coxae:** pedipalpal coxa with 9 (non-denticulate) + 4–6 (denticulate) setae, coxa I 20–21, II 18, III 17–19, IV 52–55. **Chelicera:** 1.94–1.97 × longer than broad, movable finger with 2–3 teeth. **Pedipalp:** trochanter 2.03–2.05 × longer than broad, femur 6.18–6.21 × longer than broad, patella 4.81–4.86 × longer than broad, femur 1.16–1.17 × longer than patella. Chela with pedicel 5.10–5.11 × longer than broad, hand with pedicel 2.51–2.53 × longer than broad; movable finger 1.01–1.02 × longer than hand with pedicel length. **Opisthosoma:** tergal chaetotaxy (I–XI): 15: 18: 20: 24: 23: 25: 25: 26: 23: 16: 15; sternal chaetotaxy (IV–XI): 2 × 1 + 11: 15:

15: 15: 13: 14: 13: 10; anal cone with 2 dorsal and 2 ventral setae. Anterior genital operculum with 28 setae (without tubular setae) and 2 lyrifissures; posterior operculum with 13 setae, 8 lyrifissures (Fig. 2J). Sternites with 2 lateral cribriform plates.

Dimensions (length/width or, in the case of the legs, length/depth in mm).

Males (females in parentheses): body length 3.23–3.35 (4.76–4.85). Carapace 1.05–1.06/1.00–1.01 (1.21–1.23/1.21–1.22). Pedipalp: trochanter 0.59–0.61/0.30–0.31 (0.67–0.69/0.33–0.35), femur 1.51–1.53/0.22–0.24 (1.73–1.75/0.28–0.29), patella 1.32–1.34/0.27–0.29 (1.49–1.51/0.31–0.33), hand with pedicel 1.04–1.05/0.35–0.37 (1.23–1.25/0.49–0.51), length of movable chelal finger 1.10–1.11 (1.24–1.26), length of chela 2.14–2.15/0.35–0.37 (2.50–2.53/0.49–0.51). Chelicera: 0.26–0.27/0.14–0.15 (0.28–0.30/0.14–0.15). Leg I: trochanter 0.23–0.25/0.17–0.18 (0.31–0.33/0.22–0.23), femur 0.35–0.37/0.19–0.20 (0.30–0.32/0.21–0.23), patella 0.60–0.61/0.15–0.16 (0.76–0.79/0.16–0.17), tibia 0.60–0.62/0.12–0.13 (0.73–0.75/0.11–0.12), tarsus 0.55–0.56/0.09–0.10 (0.70–0.71/0.10–0.11). Leg IV: trochanter 0.31–0.33/0.19–0.21 (0.39–0.41/0.25–0.26), femoropatella 1.06–1.08/0.27–0.28 (1.18–1.20/0.32–0.33), tibia 0.96–0.97/0.13–0.14 (1.15–1.16/0.14–0.15), tarsus 0.65–0.67/0.09–0.10 (0.78–0.80/0.10–0.11).

Distribution. Thailand (Chiangmai).

***Metachelifer takensis* sp. nov.**

<http://zoobank.org/111C7F85-255E-4A4B-9C29-F9AAAA4AC6ED>

Figs 3, 6A, B

Type material. *Holotype* male: Thailand, Tak Province, Umphang district, Umphang subdistrict, Huai Lao Poo Cave, 15°57.680'N, 098°52.510'E, 534 m a.s.l., 16 Nov 2016, Yun-Chun Li and Zhi-Gang Chen leg, in MCWNU (Ms20161116-01).

Paratypes: 1 male, 1 female, 4 tritonymphs, collected with the holotype, in MCWNU (Ms20161116-01).

Diagnosis. Troglobiont habitus. This new species is distinguished from other members of the genus *Metachelifer* by the following combination of characters: coxa IV with 45–50 setae; movable finger with 2 pseudotactile setae; male anterior genital operculum with 75–80 setae (without tubular setae); female anterior genital operculum with 22 setae (without tubular setae), posterior operculum with 8 lyrifissures.

Etymology. Latinized adjective, derived from the province of Tak, where the type locality is located.

Description. Adult male (Fig. 6A). Carapace, pedipalps and tergites dark brown, remaining parts yellowish brown (Fig. 6 A).

Carapace (Fig. 3A): 1.06–1.08 × longer than broad, with a pair of well-developed eyes, length of eyes 0.11 mm, breadth 0.05 mm, carapace surface evenly and strongly granular. Median and posterior furrows prominent, regularly granular. Dorsal setae of carapace, borne on larger but relatively inconspicuous tubercles. With 95–96 denticulo-lavate setae, including 6 on anterior margin and 11–12 on posterior margin. **Coxae:**

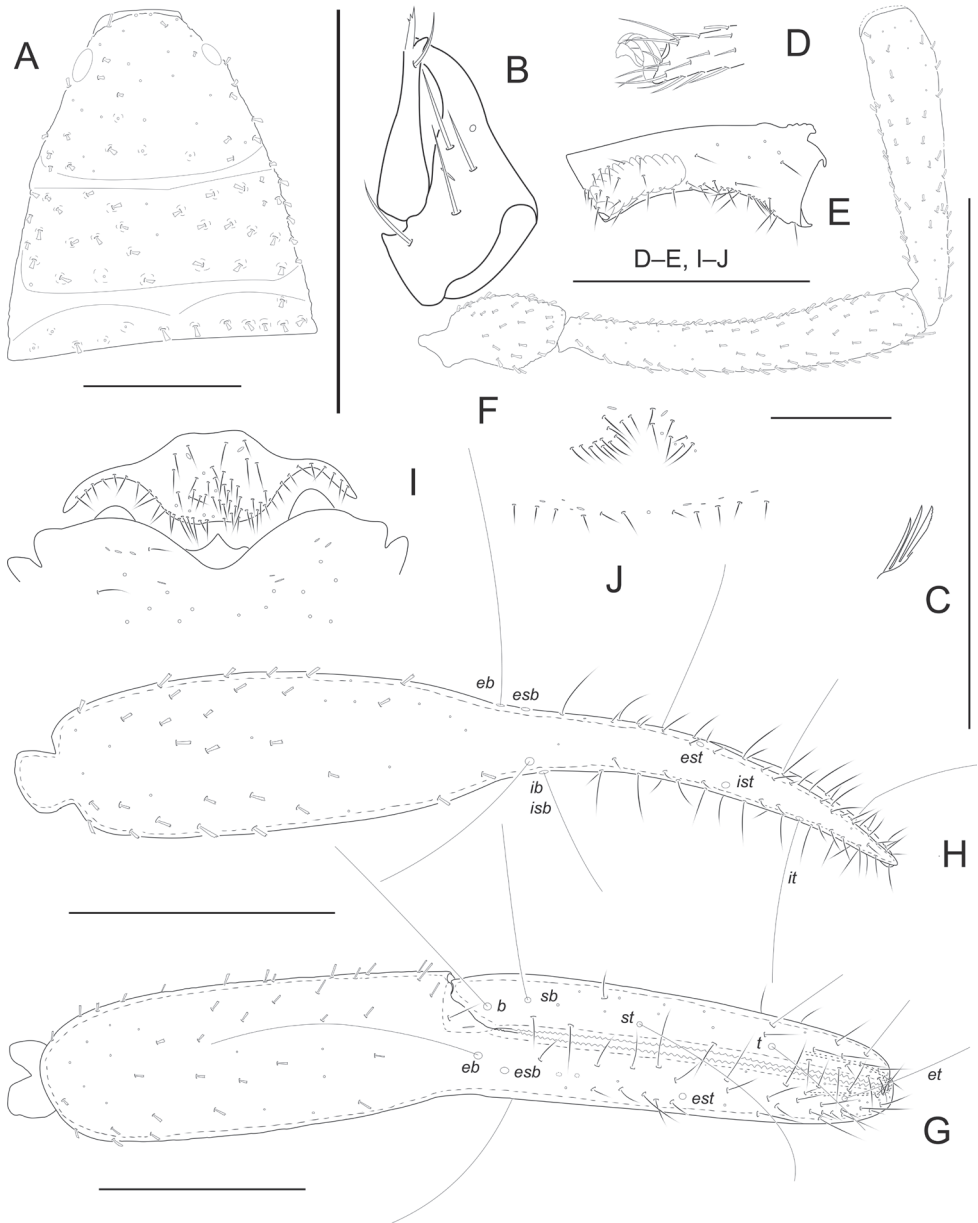


Figure 3. *Metachelifer takensis* sp. nov., holotype male (**A–I**) and paratype female (**J**) **A** carapace **B** left chelicera **C** rallum of left chelicera **D** detail on tarsus I, lateral view **E** coxa IV, ventral view **F** palp (minus chela) **G** chela, retrolateral view **H** chela, dorsal view **I** male genital area **J** female genital area. Scale bars: 0.50 mm.

manducatory process with a total of 4 setae (1 long apical, 1 rather short subapical seta, and 2 suboral setae at base of medial margin). Pedipalpal coxa with 11–12 (non-denticulate) + 6–7 (denticulate) setae, coxa I 13–15, II 15–17, III 15–19, IV with an ante-

rolateral process and 45–50 setae. Coxal sac occupying only 2/5 of coxal length, atrium well developed (Fig. 3E). **Chelicera** (Fig. 3B, C): 1.75–1.80 × longer than broad, hand with 5 setae and 1 lyrifissure dorsally, movable finger with 1 submedial seta and 1–2 teeth (Fig. 3B). Galea with 3 short branches (Fig. 3B). Serrula exterior with about 17–18 blades. Rallum with 3 blades, anterior one weakly denticulate distally (Fig. 3C). **Pedipalp** (Figs 3F–H): all segments with well-developed granulation, except for chelal fingers, which are smooth; dorsal setae short and prominently denticuloclavate. Trochanter 2.00–2.01 × longer than broad, femur 6.04–6.06 × longer than broad, patella 4.64–4.65 × longer than broad, femur 1.16–1.17 × longer than patella. Chela with pedicel 5.94–5.97 × longer than broad, hand with pedicel 2.97–2.99 × longer than broad; movable finger 1.02–1.03 × longer than hand with pedicel length. Fixed finger with 61–62 small cusped teeth, movable finger with 62 teeth; venom apparatus present in both chelal fingers, very short (Fig. 3G). Fixed chelal finger with 8 trichobothria and movable finger with 4, *eb-esb* (retrolateral view) and *ib-isb* (dorsal view) at the base of the fixed finger; *est* in finger middle, *et* distinctly closer to fingertip than to *it*; on movable finger, with two pseudotactile setae, one nearer fingertip, one nearer *t* and on same level, *st* nearer to *sb* than to *t*. **Opisthosoma**: tergal chaetotaxy (I–XI): 12: 15: 13: 14: 13: 21: 16: 18: 15: 14: 13; sternal chaetotaxy (IV–XI): 2 × 1 + 9: 12: 14: 13: 12: 11: 8: 11; anal cone with 2 dorsal and 2 ventral setae. Tergite XI with 2 tactile setae. Because only two specimens were available for the study, the structure of the genitalia could not be examined in detail. It was only possible to see well visible eversible sacs (ramshorn organs). Anterior genital operculum with 75–80 setae (without tubular setae) and 2 lyrifissures; posterior operculum with 16 setae, 8 lyrifissures (Fig. 3I). **Legs**: Leg I: surface with weak scale-like sculpture, trochanter 1.39–1.40 ×, femur 1.53–1.55 × longer than deep and 0.43–0.45 × longer than patella; patella 4.29–4.32 ×, tibia 4.75–4.77 ×, tarsus 5.67–5.70 × longer than deep, subterminal seta simple, claws modified and asymmetrical, lateral claw shorter than mesal one (Fig. 3D). Leg IV: trochanter 1.77–1.79 ×, femoropatella 3.39–3.41 ×, tibia 6.92–6.95 × longer than deep and tarsus 6.56–6.58 × longer than deep. Arolia on legs I and IV shorter than claws (Fig. 3D).

Adult female (Fig. 6B). Mostly the same as the holotype.

Carapace: slightly longer than broad (1.10 ×), anterior margin with 4 setae, posterior margin with 10 setae. Well-developed paramedian impressions behind eyes like in male. **Coxae**: pedipalpal coxa with 14 (non-denticulate) + 4 (denticulate) setae, coxa I 11, II 15, III 23, IV 46. **Chelicera**: 1.79 × longer than broad, movable finger with 2 teeth. **Pedipalp**: trochanter 1.88 × longer than broad, femur 6.04 × longer than broad, patella 4.37 × longer than broad, femur 1.15 × longer than patella. Chela with pedicel 5.31 × longer than broad, hand with pedicel 2.71 × longer than broad; movable finger 1.01 × longer than hand with pedicel length. **Opisthosoma**: tergal chaetotaxy (I–XI): 14: 16: 14: 17: 20: 18: 19: 20: 18: 14: 13; sternal chaetotaxy (IV–XI): 2 × 1 + 11: 13: 14: 14: 13: 12: 10: 10; anal cone with 2 dorsal and 2 ventral setae. Anterior genital operculum with 22 setae (without tubular setae) and 2 lyrifissures; posterior operculum with 12 setae, 8 lyrifissures (Fig. 3J). Sternites with 2 lateral cribriform plates.

Dimensions (length/width or, in the case of the legs, length/depth in mm).

Males (female in parentheses): body length 3.63–3.75 (3.52). Carapace 1.05–

1.06/0.99–1.00 (1.11/1.01). Pedipalp: trochanter 0.60–0.62/0.30–0.31 (0.60/0.32), femur 1.51–1.53/0.25–0.26 (1.51/0.25), patella 1.30–1.32/0.28–0.29 (1.31/0.30), hand with pedicel 1.07–1.09/0.36–0.38 (1.14/0.42), length of movable chelal finger 1.09–1.10 (1.15), length of chela 2.14–2.17/0.36–0.38 (2.23/0.42). Chelicera: 0.32–0.34/0.19–0.20 (0.25/0.14). Leg I: trochanter 0.25–0.26/0.18–0.19 (0.25/0.19), femur 0.26–0.28/0.17–0.18 (0.35/0.18), patella 0.60–0.62/0.14–0.15 (0.62/0.15), tibia 0.57–0.59/0.12–0.13 (0.62/0.15), tarsus 0.51–0.52/0.09–0.10 (0.53/0.08). Leg IV: trochanter 0.39–0.41/0.22–0.23 (0.42/0.21), femoropatella 0.95–0.97/0.28–0.29 (1.05/0.29), tibia 0.90–0.92/0.13–0.14 (0.92/0.13), tarsus 0.59–0.60/0.09–0.10 (0.61/0.09).

Distribution. Thailand (Tak).

***Metachelifer thailandicus* sp. nov.**

<http://zoobank.org/5DD71EBC-2ECC-4EF9-9DF3-AA9D1E9045DD>

Figs 4, 6C, D

Type material. *Holotype* male: Thailand, Tak Province, Phop Phra district, Mae Ku subdistrict, Tham Sua Yai Cave, 16°40.336'N, 98°40.138'E, 466 m a.s.l., 14 Nov 2016, Yun-Chun Li and Zhi-Gang Chen leg., in MCWNU (Ms20161116-01). *Paratypes*: 1 male, 4 females, collected with the holotype in MCWNU (Ms20161116-01).

Diagnosis. Troglobiont habitus. This new species is distinguished from other members of the genus *Metachelifer* by the following combination of characters: anterior margin of carapace with 6 denticuloclavate setae and a total of 86–88 setae; chelicera galea with 2 short branches; male movable chelal finger 0.96–0.98 × and female 0.93–0.95 × longer than hand with pedicel length; male anterior genital operculum without tubular setae; female genital posterior operculum with 6 setae, without lyrifissures.

Etymology. Latinized adjective, derived from the country of Thailand, where the type locality is located.

Description. Adult male (Fig. 6C). Carapace and pedipalps dark brown, remaining parts yellowish brown (Fig. 6C).

Carapace (Fig. 4A): 1.06–1.07 × longer than broad, with a pair of well-developed eyes, length of eyes 0.10 mm, breadth 0.04 mm, carapace surface evenly and strongly granular. Median and posterior furrows prominent, regularly granular. Dorsal setae of carapace, borne on larger but relatively inconspicuous tubercles. With a total of 86–88 denticuloclavate setae, including 6 on anterior margin and 12–13 on posterior margin. **Coxae**: manducatory process with 4 setae (1 long apical, 1 rather short subapical seta, and 2 suboral setae at base of medial margin). Pedipalpal coxa with 11–12 (non-denticulate) + 7–8 (denticulate) setae, coxa I 9–11, II 13–15, III 15–18, IV with an anterolateral process and 39–45 setae. Coxal sac occupying only 2/5 of coxal length, atrium well developed (Fig. 4D). **Chelicera** (Fig. 4B): 1.90–1.91 × longer than broad, hand with 5 setae and 1 lyrifissure dorsally, movable finger with 1 submedial seta and 1–2 teeth (Fig. 4B). Galea with 2 short branches. Serrula exterior with about 18–20 blades. Rallum with 3 blades, anterior one weakly denticulate distally. **Pedipalp** (Figs 4E–G): all

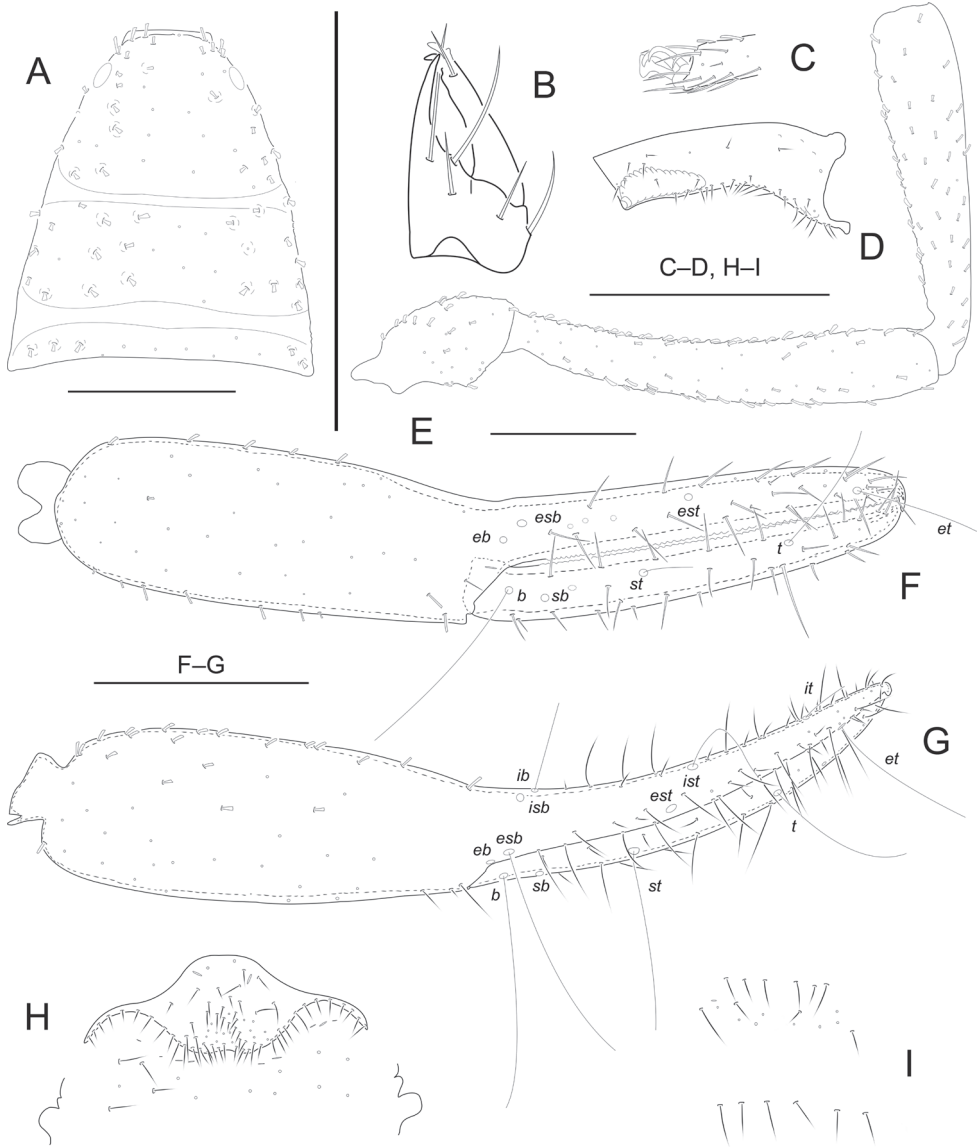


Figure 4. *Metachelifer thailandicus* sp. nov., holotype male (A–H) and paratype female (I) **A** carapace **B** right chelicera **C** detail on tarsus I, lateral view **D** coxa IV, ventral view **E** palp (minus chela) **F** chela, retrolateral view **G** chela, dorsal view **H** male genital area **I** female genital area. Scale bars: 0.50 mm.

segments with well-developed granulations, except for chelal fingers, which are smooth; dorsal setae short and prominently denticuloclavate. Trochanter $2.00\text{--}2.03 \times$ longer than broad, femur $6.13\text{--}6.15 \times$ longer than broad, patella $4.74\text{--}4.77 \times$ longer than broad, femur $1.15\text{--}1.16 \times$ longer than patella. Chela with pedicel $5.50\text{--}5.53 \times$ longer than broad, hand with pedicel $2.84\text{--}2.85 \times$ longer than broad; movable finger $0.96\text{--}0.98 \times$ longer than hand with pedicel length. Fixed finger with 59–61 small cusped

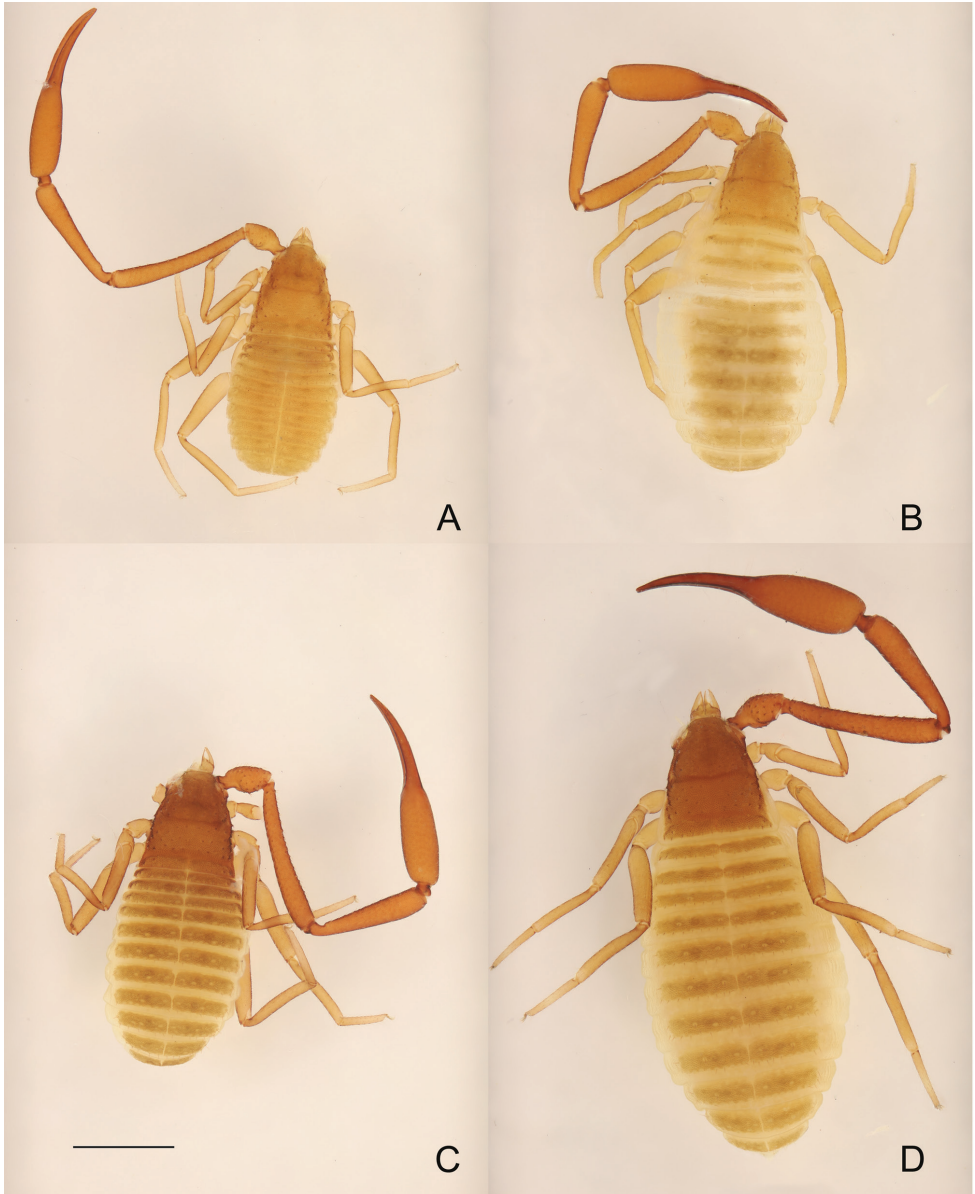


Figure 5. **A, B** *Metachelifer cheni* sp. nov., dorsal views **A** holotype male **B** paratype female **C, D** *M. mahnerti* sp. nov., dorsal views **C** holotype male **D** paratype female. Scale bar: 1.00 mm (**A–D**).

teeth, movable finger with 58–61 teeth; venom apparatus present in both chelal fingers, very short (Fig. 4F). Fixed chelal finger with 8 trichobothria and movable finger with 4, *eb-esb* (retrolateral view) and *ib-isb* (dorsal view) at the base of the fixed finger; *est* in finger middle, *et* distinctly closer to fingertip than to *it*; on movable finger, with one pseudotactile seta, nearer *t*, but the latter distinctly closer to fingertip, *st* nearer to *sb*



Figure 6. **A, B** *Metachelifer takensis* sp. nov., dorsal views **A** holotype male **B** paratype female **C, D** *M. thailandicus* sp. nov., dorsal views **C** holotype male **D** paratype female. Scale bar: 1.00 mm (**A–D**).

than to *t. Opisthosoma*: tergal chaetotaxy (I–XI): 14: 13: 13: 17: 14: 15: 18: 13: 13: 13: 9; sternal chaetotaxy (IV–XI): $2 \times 1 + 11$: 12: 11: 10: 9: 11: 12: 9; anal cone with 2 dorsal and 2 ventral setae. Tergite XI with 2 tactile setae. Because only two specimens were available for the study, the structure of the genitalia could not be examined in detail. Anterior genital operculum with 74–78 setae (without tubular setae) and 2 lyrifissures; posterior operculum with 14–15 setae, 8–9 lyrifissures (Fig. 4H). **Legs:** Leg I: surface weakly scale-like sculptured, trochanter 1.33–1.36 \times , femur 2.06–2.08 \times longer than deep and 0.63–0.64 \times longer than patella; patella 4.00–4.03 \times , tibia 4.67–4.69 \times , tar-

sus 5.00–5.02 × longer than deep, subterminal seta simple, claws modified and asymmetrical, lateral claw shorter than mesal one (Fig. 4C). Leg IV: trochanter 1.94–1.95 ×, femoropatella 3.36–3.39 ×, tibia 7.50–7.53 × longer than deep and tarsus 6.67–6.71 × longer than deep. Arolia on legs I and IV shorter than claws (Fig. 4C).

Adult female (Fig. 6D). Mostly the same as the holotype. **Carapace:** Slightly longer than broad (1.01–1.02 ×), posterior margin with 8–9 setae. Well-developed paramedian impressions behind eyes like in male. **Coxae:** pedipalpal coxa with 11–13 (non-denticulate) + 5–6 (denticulate) setae, coxa I 11, II 15, III 23, IV 46. **Chelicera:** 1.80–1.86 × longer than broad, movable finger with 2 teeth. **Pedipalp:** trochanter 2.04–2.06 × longer than broad, femur 5.94–5.97 × longer than broad, patella 4.29–4.31 × longer than broad, femur 1.19–1.20 × longer than patella. Chela with pedicel 5.47–5.50 × longer than broad, hand with pedicel 2.87–2.89 × longer than broad; movable finger 0.93–0.95 × longer than hand with pedicel length. **Opisthosoma:** tergal chaetotaxy (I–XII): 10: 9: 11: 9: 10: 12: 11: 11: 12: 11: 10; sternal chaetotaxy (IV–XII): 2 × 1 + 9: 12: 13: 14: 13: 12: 11: 10; anal cone with 2 dorsal and 2 ventral setae. Anterior genital operculum with 18–20 setae (without tubular setae) and 1 lyrifissure; posterior operculum with 6 setae, without lyrifissures (Fig. 4I). Sternites with 2 lateral cribriform plates.

Dimensions (length/width or, in the case of the legs, length/depth in mm). **Males** (females in parentheses): body length 3.38–3.42 (2.86–3.32). Carapace 0.99–

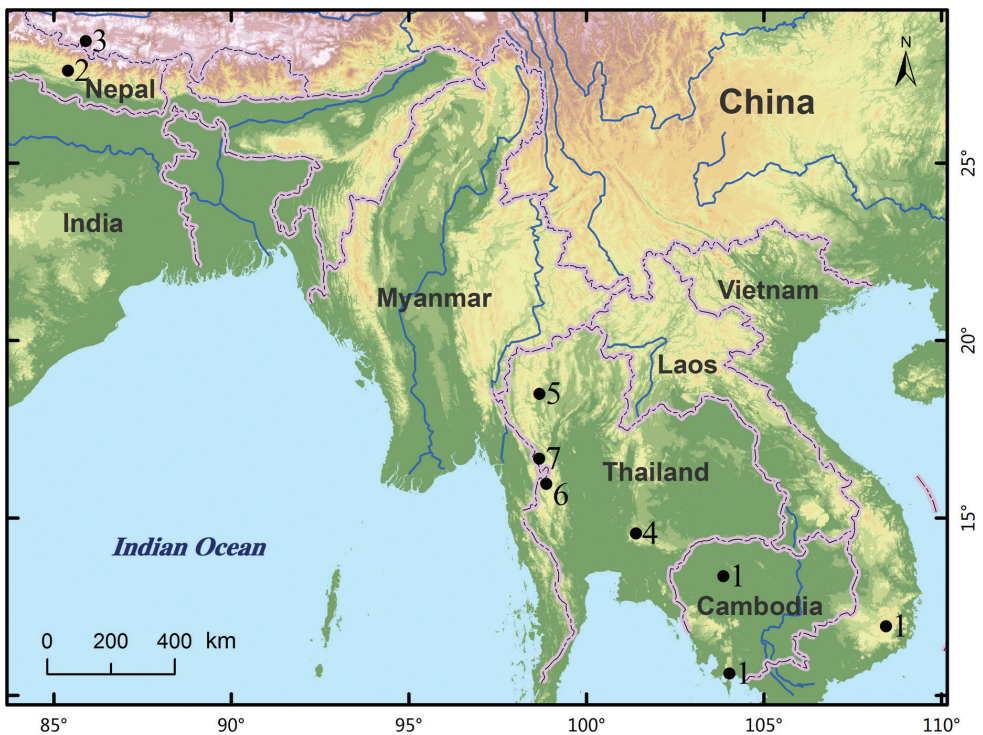


Figure 7. Distribution of known *Metachelifer* species. 1 *M. duboscqui*; 2 *M. macrotuberculatus*; 3 *M. nepalensis*; 4 *M. cheni* sp. nov.; 5 *M. mahnerti* sp. nov.; 6 *M. takensis* sp. nov.; 7 *M. thailandicus* sp. nov.

1.01/0.93–0.94 (0.81–0.82/0.80–0.81). Pedipalp: trochanter 0.60–0.62/0.30–0.31 (0.49–0.51/0.24–0.26), femur 1.47–1.49/0.24–0.25 (1.07–1.09/0.18–0.20), patella 1.28–1.30/0.27–0.28 (0.90–0.92/0.21–0.22), hand with pedicel 1.08–1.10/0.38–0.39 (0.86–0.89/0.30–0.32), length of movable chelal finger 1.04–1.06 (0.80–0.83), length of chela 2.09–2.11/0.38–0.39 (1.64–1.67/0.30–0.32). Chelicera: 0.27–0.28/0.14–0.15 (0.23–0.25/0.13–0.14). Leg I: trochanter 0.24–0.25/0.18–0.19 (0.18–0.20/0.14–0.16), femur 0.35–0.37/0.17–0.19 (0.21–0.23/0.14–0.15), patella 0.56–0.58/0.14–0.15 (0.46–0.49/0.13–0.14), tibia 0.56–0.58/0.12–0.13 (0.40–0.43/0.10–0.11), tarsus 0.50–0.51/0.10–0.11 (0.41–0.42/0.09–0.10). Leg IV: trochanter 0.33–0.34/0.17–0.19 (0.31–0.33/0.17–0.19), femoropatella 0.94–0.97/0.28–0.29 (0.72–0.75/0.22–0.23), tibia 0.90–0.93/0.12–0.13 (0.65–0.68/0.11–0.12), tarsus 0.60–0.61/0.09–0.10 (0.45–0.49/0.08–0.09).

Distribution. Thailand (Tak).

Discussion

Except for *Metachelifer macrotuberculatus* and *M. nepalensis* in Nepal, all other species of *Metachelifer* are distributed in Southeast Asia (Fig. 7). The new species described here all inhabit a low light area about 5–7 m from the entrance of the cave; they were collected from under a mixture of stones and large clods with a slightly drier surface. These species were not found in the environment around the cave entrance. In comparison with species living under tree bark, the length of male pedipalpal patella (tree-dwelling max. 1.20 mm vs cave-dwelling min. 1.27 mm), movable chelal finger (tree-dwelling max. 0.94 mm vs cave-dwelling min. 0.98 mm), pedal tibia I (tree-dwelling max 0.45 mm vs cave-dwelling min 0.56 mm), and pedal tarsus I (tree-dwelling max. 0.45 mm vs. cave-dwelling min. 0.46 mm) are much longer (Redikorzev 1938; Dashdamirov 2006), which suggests that these species are adapt to the cave environment.

Acknowledgements

We are very grateful to Dr Prasit Wongprom (Thai Nature Education Centre) for his collaboration during the fieldwork. We thank Dr Mark Judson (Muséum national d'Histoire naturelle, Paris, France) for help with the identification of specimens from Wat Dewaroop Song Cave 3 and Tham Borichinda Cave. Dr Meng-Lin Wang (College of Life Science, China West Normal University, Nanchong, China) kindly helped to review the original English manuscript. We thank Prof. Mark Harvey (Western Australian Museum, Perth, Australia) and Dr Catalina Romero-Ortiz (Universidad Nacional de Colombia, Bogotá, Colombia) who provided useful comments and suggestions for improvements to the manuscript. This study was supported by the Doctoral Scientific Research Foundation of China West Normal University (18Q043).

References

- Beier M (1974) Pseudoscorpione aus Nepal. *Senckenbergiana Biologica* 55: 261–280.
- Chamberlin JC (1931) The arachnid order Chelonethida. Stanford University Publications, University Series (Biological Sciences) 7(1): 1–284.
- Dashdamirov S (2006) A new species of the falsescorpion family Cheliferidae from Thailand, with remarks on *Ancistrochelifer* and *Metachelifer* (Arachnida Pseudoscorpiones). *Zootaxa* 1325(1): 347–362. <https://doi.org/10.11646/zootaxa.1325.1.23>
- Harvey MS (1992) The phylogeny and classification of the Pseudoscorpionida (Chelicerata: Arachnida). *Invertebrate Taxonomy* 6(6): 1373–1435. <https://doi.org/10.1071/IT9921373>
- Judson MLI (2007) A new and endangered species of the pseudoscorpion genus *Lagynochthonius* from a cave in Vietnam, with notes on chelal morphology and the composition of the Tyrannochthoniini (Arachnida, Chelonethi, Chthoniidae). *Zootaxa* 1627(1): 53–68. <https://doi.org/10.11646/zootaxa.1627.1.4>
- Krumpál M (1987) Ein neuer *Dactylochelifer* aus Nepal Himalaya (Arachnida, Pseudoscorpiones). *Acta Entomologica Bohemoslovaca* 84: 221–226.
- Redikorzev V (1938) Les pseudoscorpions de l'Indochine française recueillis par M. C. Dawydoff. *Mémoires du Muséum National d'Histoire Naturelle* 10: 69–116.
- World Pseudoscorpiones Catalog (2022) World Pseudoscorpiones Catalog. Natural History Museum Bern. <https://wac.nmbe.ch/order/pseudoscorpiones/3> [Accessed on 01.03.2022]

Underestimated cryptic diversity in the *Caryocolum tricolorella* species complex (Lepidoptera, Gelechiidae)

Peter Huemer¹

¹ *Tiroler Landesmuseen Betriebsges.m.b.H., Sammlungs- und Forschungszentrum, Naturwissenschaftliche Sammlungen, Krajnc-Str. 1, A-6060 Hall in Tirol, Innsbruck, Austria*

Corresponding author: Peter Huemer (p.huemer@tiroler-landesmuseen.at)

Academic editor: Mark Metz | Received 17 March 2022 | Accepted 16 May 2022 | Published 3 June 2022

<http://zoobank.org/EE7E5662-E546-4914-B2C5-B375E104F472>

Citation: Huemer P (2022) Underestimated cryptic diversity in the *Caryocolum tricolorella* species complex (Lepidoptera, Gelechiidae). ZooKeys 1103: 189–209. <https://doi.org/10.3897/zookeys.1103.83952>

Abstract

The taxonomy of the *Caryocolum tricolorella* species complex, an informal subsection of the diverse *Caryocolum interalbicella* species group, is revised and four species are separated from DNA barcodes of the mitochondrial COI (cytochrome c oxidase subunit 1) gene and adult morphology: *C. tricolorella* (Haworth, 1812), *C. fibigerium* Huemer, 1988, *C. herwigianstaai* **sp. nov.**, and *C. olekarsholti* **sp. nov.** These species show a vicariant distribution pattern, with *C. tricolorella* widely distributed in Central and Northern Europe, *C. fibigerium* restricted to the Iberian Peninsula and southern France, *C. herwigianstaai* **sp. nov.** to the Italian Peninsula, and *C. olekarsholti* **sp. nov.** to the Balkans. All species are described in detail, and the adults and genitalia of both sexes are illustrated.

Keywords

DNA barcode, Europe, Gelechiinae, morphology, new species, vicariant distribution

Introduction

The European fauna of Lepidoptera is generally considered as well explored, although about 50 species are still described as new to science yearly (www.lepiform.de). However, the species diversity of some families of so-called microlepidoptera seems insufficiently documented. An extraordinarily high portion of potentially overlooked cryptic diversity is found, for example, in the Gracillariidae and Gelechiidae, with an

estimated proportion of up to 10% of undescribed species for both families (Huemer et al. 2020; Lopez-Vaamonde et al. 2021).

With currently about 870 described species, the Gelechiidae are among the most diverse families of Lepidoptera in Europe (Huemer and Karsholt 2020), but despite considerable progress in taxonomic coverage during the last decades [see Huemer and Karsholt (1999, 2010) and bibliography in Huemer and Karsholt (2020)], some diverse genera, for example *Stomopteryx* Heinemann, 1870, *Aproaerema* Durrant, 1897, *Aristotelia* Hübner, 1825, and *Monochroa* Heinemann, 1870, still remain unrevised. In contrast, the genus *Caryocolum* has undergone extensive revisionary work with a constantly growing number of described species, currently 59 (Klimesch 1953–1954; Huemer 1988; Huemer and Karsholt 2010, 2020). However, after implementation of molecular data (DNA barcodes), Huemer et al. (2014) found clear indications of widespread, previously overlooked, cryptic diversity in the genus, documented for example in the recently revised *C. schleichi* species complex (Huemer 2020). In this paper *C. tricolorella* and allied species, a further case of underestimated alpha-diversity, are revised based on morphology and DNA barcodes, and two new species are described.

Material and methods

The generic classification and the definition of species-groups follow Huemer (1988).

Specimens

The study is based on about 140 specimens of the *C. tricolorella* subsection as part of the *C. interalbicella* species-group. Material was pinned and dried and either traditionally set or spread. Genitalia preparations followed standard techniques (Robinson 1976) adapted for the Gelechiidae as described by Pitkin (1986) and Huemer (1987).

Forewing length was measured from wing base to apex (including cilia) with an ocular micrometer, taking into account the smallest and largest specimen of available samples.

DNA Barcodes

DNA barcode sequences are based on a 658 base-pair long segment of the mitochondrial COI gene (cytochrome c oxidase subunit 1). DNA samples (dried legs) were prepared according to the prescribed standards and successfully processed at the Canadian Centre for DNA Barcoding (CCDB, Biodiversity Institute of Ontario, University of Guelph) to obtain DNA barcodes using the standard high-throughput protocol described in deWaard et al. (2008). Altogether 106 successfully sequenced specimens of the *Caryocolum interalbicella* species-group from BOLD (sequence length >600 bp, BIN available) are partially based on external sources (German Barcode of Life, Finnish Barcode of Life, Norwegian Barcode of Life, and others). These sequences cover 17 out of 18 species of the species-group, only leaving *Caryocolum nearcticum* without a DNA barcode. Twenty-seven sequences belong to the *Caryocolum tricolorella* species

complex and details including complete voucher data and images of these specimens can be accessed in the public dataset “Lepidoptera of Europe – *Caryocolum tricolorella* species-group [DS-CARYTRIC]” in the Barcode of Life Data Systems BOLD (Ratnasingham and Hebert 2007). Sequences were finally submitted to GenBank.

Degrees of intra- and interspecific variation of DNA barcode fragments were calculated under the Kimura 2-parameter model of nucleotide substitution using analytical tools of BOLD Systems v. 4.0. (<http://www.boldsystems.org>). A neighbor-joining tree of DNA barcode data of central and south-eastern European taxa was constructed using MEGA6 (Tamura et al. 2013) under the Kimura 2-parameter model for nucleotide substitutions.

Photographic documentation

Photographs of the adults were taken with an Olympus SZX 10 binocular microscope and an Olympus E 3 digital camera and developed using the software Helicon Focus v. 4.3 and Adobe Photoshop CS4 and Lightroom v. 2.3. Genitalia photographs were taken with an Olympus E1 Digital Camera through an Olympus BH2 microscope.

Specimen repositories

LMK	Landesmuseum Kärnten, Klagenfurt, Austria;
NHM	Natural History Museum, London, United Kingdom;
RCJL	Research collection Gerárd Labonne, Montpellier, France;
RCJG	Research Collection Javier Gastón, Getxo, Spain;
RCTM	Research Collection Toni Mayr, Feldkirch, Austria;
TLMF	Tiroler Landesmuseum Ferdinandeum, Innsbruck, Austria;
ZMUC	Zoological Museum, Natural History Museum of Denmark, Copenhagen, Denmark.

Results

Molecular analysis

DNA sequencing resulted in a BIN concordant barcode fragment of >500 bp for 87 specimens and 17 species in the *Caryocolum interalbicella* species group. Sequences of the COI barcode region revealed low intraspecific, but significantly higher interspecific, genetic distances (Table 1, Fig. 1). The normalized mean within-species divergence is 0.60% (SE 0.04). Only three species split in two BINs (Ratnasingham and Hebert 2013): *C. klosi*, *C. junctella*, and *C. herwigvanstaai* sp. nov., but it should be noted that the number of sequences is insufficient to estimate intraspecific variation for several species. A maximum intraspecific distance of 4.28% in *Caryocolum klosi* has to be re-assessed and may be due to unrecognized cryptic diversity. In contrast, minimum interspecific divergence is 1.55% in two BIN-sharing species but considerably higher in the remaining 15 species with a distance to the nearest neighbour ranging from 3.32% to 5.63%.

Table 1. Intraspecific mean K2P (Kimura 2-parameter) divergences, maximum pairwise distances, nearest species, nearest neighbour and distance to nearest neighbour (distances in %) in the *Caryocolum interalbicella* species-group.

Species	Mean IntraSp	Max IntraSp	Nearest Species	Nearest Neighbour	Distance to NN
<i>Caryocolum arenbergeri</i>	N/A	0	<i>Caryocolum blandulella</i>	LEFIL287-10	1.55
<i>Caryocolum blandella</i>	0.12	0.36	<i>Caryocolum blandulella</i>	PHLAI019-12	5.04
<i>Caryocolum blandelloides</i>	0.25	0.98	<i>Caryocolum blandella</i>	GMGMM1305-14	5.29
<i>Caryocolum blandulella</i>	0.21	0.46	<i>Caryocolum arenbergeri</i>	LEASU109-18	1.55
<i>Caryocolum dauphini</i>	0	0	<i>Caryocolum laceratella</i>	PHLAB900-10	5.63
<i>Caryocolum fibigerium</i>	0.89	2.41	<i>Caryocolum olekarsholti</i>	PHLAI014-12	3.37
<i>Caryocolum horoscopa</i>	N/A	0	<i>Caryocolum blandella</i>	GMGMM1305-14	5.08
<i>Caryocolum interalbicella</i>	0.34	0.77	<i>Caryocolum junctella</i>	LEAST920-17	5.27
<i>Caryocolum jaspidella</i>	1.08	1.08	<i>Caryocolum blandulella</i>	PHLAI019-12	4.42
<i>Caryocolum junctella</i>	1.12	2.34	<i>Caryocolum blandulella</i>	PHLAI019-12	4.03
<i>Caryocolum kasyi</i>	N/A	0	<i>Caryocolum junctella</i>	LEAST920-17	4.91
<i>Caryocolum kloisi</i>	2.16	4.28	<i>Caryocolum interalbicella</i>	PHLAD577-11	5.43
<i>Caryocolum laceratella</i>	N/A	0	<i>Caryocolum dauphini</i>	PHLAI447-13	5.63
<i>Caryocolum proxima</i>	0.36	1.08	<i>Caryocolum blandulella</i>	PHLAI019-12	3.8
<i>Caryocolum olekarsholti</i>	0.11	0.16	<i>Caryocolum fibigerium</i>	PHLAI403-13	3.37
<i>Caryocolum herwigvanstaaai</i>	1.46	2.19	<i>Caryocolum olekarsholti</i>	PHLAI015-12	4.12
<i>Caryocolum tricolorella</i>	0.17	0.77	<i>Caryocolum olekarsholti</i>	PHLAI014-12	4.12

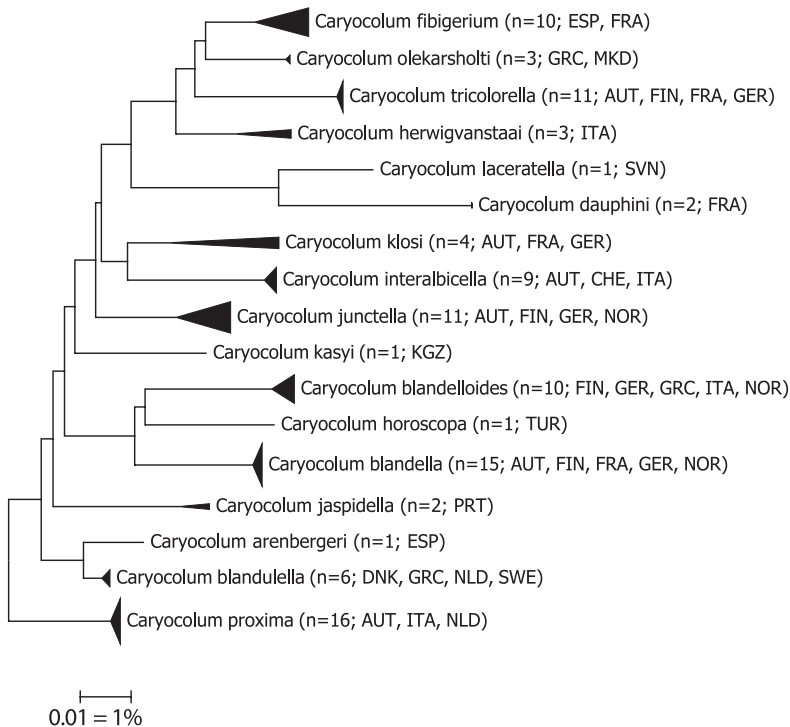


Figure 1. Neighbor-joining tree of species in the *Caryocolum interalbicella* species group (Kimura 2-parameter, built with MEGA 6; Tamura et al. 2013), only sequences (>500 bp) considered. Note: the scale bar only applies to internal branches between species. Width of triangles represent sample size, depth the genetic variation within the cluster. Source: DNA Barcode data from BOLD (Barcode of Life Database; Ratnasingham 2018).

Taxonomy

Caryocolum Gregor & Povolný, 1954

Caryocolum Gregor and Povolný 1954: 8. Type species: *Gelechia leucomelanella* Zeller, 1839: 138.

Caryocolum interalbicella species-group

The *Caryocolum interalbicella* species-group was defined by Huemer (1988) and is characterized in the male genitalia by the following characters: uncus long and narrow; tegumen very broad anteriorly, strongly constricted medially, with large pedunculi; transtilla with spines; valva usually long and slender, subbasally strongly bent, apex frequently bulged, with brush of setae; sacculus knife-shaped; posterior margin of vinculum medially incised to broadly emarginated; saccus slender to moderately broad; phallus without cornuti. Female genitalia are characterized by the following characters: segment VIII with pair of ventral or dorsal processes, ventromedial area sclerotized with or without microtrichia; antrum short ring to long funnel; signum with a semi-oval basal plate and a strong distal hook. The species-group includes 18 species (Huemer 1988; Huemer and Karsholt 2010, 2020).

The informal *Caryocolum tricolorella* subsection is characterized by a long and evenly slender valva without apical bulge in the male genitalia, and a large, broadly funnel-shaped antrum in the female genitalia.

Checklist of *Caryocolum interalbicella* species-group

(species of the *C. tricolorella* species complex are marked with an asterisk; country of the type locality in brackets)

- Caryocolum klosi* (Rebel, 1917) (Austria)
- Caryocolum interalbicella* (Herrich-Schäffer, 1854) (Switzerland)
- Caryocolum laceratella* (Zeller, 1868) (Italy)
- Caryocolum dauphini* Grange & Nel, 2012 (France)
- Caryocolum nearcticum* Huemer, 1988 (USA)
- Caryocolum blandella* (Douglas, 1852) (UK, England)
- Caryocolum blandelloides* Karsholt, 1981 (Denmark)
- Caryocolum horoscopa* (Meyrick, 1926) (India)
- Caryocolum jaspidella* (Chrétien, 1908) (Algeria)
- Caryocolum proxima* (Haworth, 1828) (UK, England)
- Caryocolum blandulella* (Tutt, 1887) (UK, England)
- Caryocolum arenbergeri* Huemer, 1989 (Spain)
- Caryocolum tricolorella* (Haworth, 1812)* (UK, England)
- Caryocolum fibigerium* Huemer, 1988* (Spain)
- Caryocolum herwigvanstaai* sp. nov.* (Italy)

Caryocolum olekarsholti sp. nov.* (Greece)

Caryocolum junctella (Douglas, 1851) (UK, England)

Caryocolum kasyi Huemer, 1988 (Afghanistan)

***Caryocolum tricolorella* (Haworth, 1812)**

Tinea tricolorella Haworth 1812: 338. Syntypes, UK: England (NHM) [not traced].

Recurvaria contigua Haworth 1828: 552. Lectotype ♀, UK: England (NHM).

Designated by Huemer (1988).

Gelechia acernella Herrich-Schäffer 1855: 185, pl. 77, fig. 580. Syntypes, Austria, Germany [not traced].

Other material. [AUSTRIA] • 10 ♂; Burgenland, Jois 1.5 km NE; 200 m; 3 Aug 2021; [DNA barcode ids] TLMF Lep 30932, TLMF Lep 30933; P. Huemer leg.; • 1 ♂; Wien, Haschberg; 28 Jul 1915; all TLMF; [GERMANY] • 2 ♂, 1 ♀; Württemberg, Burgstall/Murr; 9–15 Jun 1973 e.l. (*Stellaria holostea*); L. Süssner leg.; • 2 ♂; Württemberg, Kirchberg/Murr; 24 Jun 1963 e.l. (*Stellaria holostea*); [genitalia slide number] GU 86-032♂, P. Huemer; L. Süssner leg.; • 2 ♂, 3 ♀; Württemberg, Markgröningen; 18–30 May 1961 e.l. (*Stellaria holostea*); L. Süssner leg.; • 1 ♂; Württemberg, Markgröningen; 21 Jun 1963 e.l. (*Stellaria holostea*); L. Süssner leg.; • 2 ♂; Württemberg, Markgröningen; 4–5 Jun 1964 e.l. (*Stellaria holostea*); L. Süssner leg.; 2 ♂; Württemberg, Gronau, Kurzach Tal; 11–16 Jun 1973 e.l. (*Stellaria holostea*); [genitalia slide number] GEL 1092♀, P. Huemer; L. Süssner leg.; 3 ♀; Württemberg, Schwarzwald, Sprollenmühle; 560 m; 18–22 Jun 1968 e.l. (*Stellaria holostea*); [genitalia slide number] GU 86-031♀, P. Huemer; L. Süssner leg.; 1 ♂; Württemberg, Schwarzwald, Sprollenmühle; 550–580 m; 8 Jun 1967 e.l. (*Stellaria holostea*); L. Süssner leg.; 1 ♂; Württemberg, Schwarzwald, Sprollenmühle; 560 m; 22 Jun 1969 e.l. (*Stellaria holostea*); L. Süssner leg.; 5 ♂, 1 ♀; Württemberg, Schwarzwald, Bad Liebenzell; 450 m; 9–11 Jun 1971 e.l. (*Stellaria holostea*); [genitalia slide number] GEL 1288♂, P. Huemer; L. Süssner leg.; all TLMF; [FRANCE] • 1 ♂; Midi-Pyrénées, Soulom; 31 Jul 2002; J. Nel leg.; TLMF; [DENMARK] • 1 ♂, 2 ♀; Bótó; 22 Jul 1967; • 1 ♂; SZ, Vemmetofte; 9 May 1987 (larva) (*Stellaria holostea*); O. Karsholt leg.; all TLMF.

Diagnosis. *Caryocolum tricolorella* differs from other species of the complex by its larger size and the extension of ochreous-orange scales on the dorsum and in the middle of the forewing. The male genitalia are characterized by the particularly long valva and sacculus, and the nearly straight posterior margin of the vinculum with indistinct lateromedial projections. The female genitalia differ from all other species by the distinctly smaller antrum.

Description. Adult (Fig. 2). Forewing length. ♂ 5.4–6.6 mm ($\bar{\sigma} = 5.92$ mm, $n = 5$), ♀ 6.1–6.3 mm ($\bar{\sigma} = 6.20$ mm, $n = 5$). Head with fuscous vertex, frons cream-white; second segment of labial palpus cream-white on inner and upper surface, predominantly grey-brown on outer surface, third segment dark brown with a few white scales

particularly at apex; antenna black, weakly ringed whitish. Thorax and tegula dark brown anteriorly, posterior part intermixed ochreous. Abdomen dorsally grey, ventrally whitish, pale grey at margins. Forewing predominantly ochreous-orange with scattered white scales, costal and terminal area fuscous, distinct subtriangular black patch from fold to costa at about one-third and black dash distad of cell, dorsum ochreous-orange with concolorous extension towards costa at 1/5 and in middle at 3/4, inwardly lined with irregular white suffusion, larger white costal spot and smaller tornal dash separated by ochreous patch or by fuscous scales; cilia light grey with fuscous ciliary line, buff beyond line. Hindwing light grey, cilia greyish buff.

Variation: the wingspan varies from 10.0–14.5 mm [forewing length not stated] (Bland et al. 2002) showing a much greater variation than in the above examined material.

Male genitalia (Fig. 6). Uncus long, suboval, posterior edges rounded; gnathos with large mesial sclerite, culcitula small; posterior third of tegumen slender, anterior part strongly widened towards broadly rounded pedunculi of about twice size of uncus, anterior margin with deep concave emargination; transtilla membranous with few microtrichia; valva basally curved ventrad, long, slender, apical part weakly broadened, apex with group of stiff setae; sacculus long, slightly shorter than valva but about same width, apex knife-shaped; vinculum wide and short, posterior margin moderately sclerotized, nearly straight, with shallow medial incision and hardly developed lateromedial projections, anterior margin with strongly sclerotized concave ridge; saccus slender, basally weakly widened, gradually narrowing towards pointed apex, about length of apex of valva to anterior margin of vinculum; anellus with pair of needle-shaped sclerites; phallus stout, almost straight, coecum weakly inflated, longitudinal ridge from about middle to apex, two small sclerotized hooklets at apex.

Female genitalia (Fig. 10). Apophysis posterior about 4.5 times length of apophysis anterior; segment VIII smoothly sclerotized, with small dorsolateral flaps, posterior and inner edge strongly sclerotized, membranous ventromedial part with numerous microtrichia; apophysis anterior about three-quarters length of segment VIII; antrum comparatively short and small, about 4/5 length and 1/3 width of segment VIII between bases of apophyses anteriores, funnel-shaped; ductus bursae about twice length of apophysis anterior; corpus bursae semi-oval, signum with a large basal plate with long and slender hook.

Molecular data. BIN: BOLD:AAF1506. The intraspecific average distance of the barcode region is 0.17%, the maximum distance 0.77% (*p*-distance) (*n* = 12). The minimum distance to the nearest neighbour, *C. olekarsholti* sp. nov., is 4.12%.

Distribution. *Caryocolum tricolorella* is widely distributed from north-western Europe to Russia, extending to the central parts of the continent in the south, but most probably absent from the Mediterranean. All records from this area require verification and probably refer to other species.

Bionomics. The biology of this species was described in detail by Stainton (1867), supplemented by several other authors (Sorhagen 1886; Schütze 1931; Hering 1935–1937). The young larva produces a gallery-like leaf-mine on *Stellaria holostea* or rarely on other *Stellaria* spp. (Caryophyllaceae), later feeding between spun shoots.

Cerastium arvense requires confirmation as another suspected hostplant. The larva has been observed from September to mid-April (Huemer 1988). Moths are on the wing from June to mid-September. The species prefers thermophilous forests and hedgerows at low elevation. This species is easily attracted to artificial light sources.

Remarks. *Tinea tricolorrella* was described from an unspecified number of specimens from England (Haworth 1812) and is considered undisputed (Huemer 1988). The two junior synonyms are of taxa originating outside the geographic range of sibling species, namely *Recurvaria contigua* from England (Haworth 1828), and *Gelechia acernella* described from Central Europe (Germany, Austria) and figured in detail in the original description (Herrich-Schäffer 1855).

Caryocolum fibigerium Huemer, 1988

Caryocolum fibigerium Huemer 1988: 510, figs 86, 153, 214.

Type material. Holotype. [SPAIN] • ♀; Granada, Sierra Nevada, road to Veleta; 2200 m; 16 Jul 1962; K. Sattler leg; NHM.

Paratypes. [SPAIN] • 2 ♂, 2 ♀; Andalucía, Sierra Nevada, Cam. d. Veleta; 2000 m; 24 Jul 1983; E. Traugott-Olsen leg.; • 9 ♂, 1 ♀; Andalucía, Sierra Nevada, Cam. d. Veleta; 2300 m; 19 Aug 1984; E. Traugott-Olsen leg.; all TLMF.

Other material. [SPAIN] • 2 ♂; Andalucía, Sierra Nevada, Cam. d. Veleta; 2250 m; 1 Aug 1986; E. Traugott-Olsen leg.; • 1 ♂, 1 ♀; Andalucía, Sierra Nevada, Cam. d. Veleta; 2250 m; 3 Aug 1986; E. Traugott-Olsen leg.; • 1 ♂; Andalucía, Sierra Nevada, Cam. d. Veleta; 2250 m; 4 Aug 1986; E. Traugott-Olsen leg.; • 1 ♂; Andalucía, Sierra Nevada, Cam. d. Veleta; 2250 m; 4 Aug 1986; E. Traugott-Olsen leg.; • 2 ♂, 1 ♀; Andalucía, Sierra Nevada, Camino de la Veleta; 2250 m; 21 Jul 1985; [genitalia slide numbers] GEL 1211♂, GEL 1095♀, P. Huemer; G. Baldizzone and E. Traugott-Olsen leg.; • 1 ♂, 2 ♀; Castellon, Penygolosa N-Hang, Banyadera; 1500 m; 31 Aug 2005; [DNA barcode ids] BC TLMF Lep 03257, BC TLMF Lep 03258; P. Huemer leg.; • 4 ♂, 5 ♀; Alicante, Alcoj, Font Roja, W El Menejador, S-Hang; 1300 m; 4 Sep 2005; [DNA barcode ids] BC TLMF Lep 08899, BC TLMF Lep 08899; P. Huemer leg.; all TLMF; • 1 ♂; Almeria, Sierra de Gador; 2020 m; 31 Jul 2019; [genitalia slide number] 6810♂, J. Gastón, [DNA barcode id] TLMF Lep 30599; J. Gastón leg.; • 1 ♂, 1 ♀; Burgos, Castrobarro; 770 m; 13 Sep 2020; [genitalia slide numbers] 8273♂, J. Gastón, 8253♀, J. Gastón [DNA barcode ids] TLMF Lep 30600, TLMF Lep 30601; J. Gastón leg.; all RCJG; [FRANCE] • 1 ♂; Languedoc-Rousillon, Dourbies, Lac de Pises; 1300 m; 13 Sep 2020; [genitalia slide number] Gla 020/1984♂, G. Labonne, [DNA barcode id] TLMF Lep 30991; G. Labonne leg.; 1 ♀; Languedoc-Rousillon, Le Caylar; 740 m; 25 Aug 2016; [genitalia slide number] Gla 016/2825♀, G. Labonne, [DNA barcode id] TLMF Lep 30990; G. Labonne leg.; all RCGL; • 1 ♂; Hautes Pyrénées, Pic du Midi de Bigorre; 2400 m; 7 Aug 2002; [genitalia slide number] 14427♂, J. Nel; [DNA barcode id] BC TLMF Lep 06904; J. Nel leg.; • 1 ♂; Cantal, Lessenat; 700 m; 10 Aug 1995;

[genitalia slide number] 3610♂, J. Nel; J. Nel. leg.; • 1 ♂; Alpes Maritimes, Caussols; 1100 m; 14 Aug 1971; [genitalia slide number] GU 88/136♂, P. Huemer; F. Dujardin leg; 1 ♂; Alpes Maritimes, Col de Vence; 11–12 Jun 1981; 1100 m; F. Hahn leg; • 1 ♂; Basses-Alpes, Montagne de Lure; 1500 m; 20 Jul 1992; J. Nel leg.; • 1 ♂; Basses-Alpes, Montagne de Lure; 1720 m; 8 Jun 1994 e.l. (*Cerastium*); [genitalia slide number] 2035♂, J. Nel; J. Nel leg.; • 1 ♂, 1 ♀; Var, Rougiers, Val. de Pourien; 28 Apr 1994 e.l. (*Cerastium*); [genitalia slide numbers] 1944♂, 1945♀, J. Nel; J. Nel leg.; all TLMF.

Diagnosis. *Caryocolum fibigerium* differs from *C. tricolorella* by its distinctly smaller size on average and the less extensive ochreous markings. It can be distinguished from *C. herwigvanstaaai* and *C. olekarsholti* by the smaller, white costal and tornal spots and the reduced white mottling of the medial and subbasal fasciae. The male genitalia differ from *C. tricolorella* in the shorter valva and sacculus and the additional humps of the posterior margin of the vinculum. *Caryocolum fibigerium* is very similar to *C. herwigvanstaaai* and *C. olekarsholti* in this character, but with a weakly developed lateral hump. Furthermore, the sacculus is wider than in *C. herwigvanstaaai*. The antrum of the female genitalia is much larger than in *C. tricolorella* and also in the latter two species, exceeding the length of the apophysis anterior, furthermore the dorsolateral flaps of segment VIII are larger compared to *C. herwigvanstaaai* and *C. olekarsholti*.

Description. Adult (Fig. 3). Forewing length. ♂ 4.8–6.2 mm ($\bar{\phi}$ = 5.30 mm, n = 5), ♀ 4.6–5.1 mm ($\bar{\phi}$ = 4.90 mm, n = 5). Head with fuscous vertex, frons cream-white; second segment of labial palpus cream-white on inner and upper surface, predominantly grey-brown on outer surface, third segment dark brown with a few white scales particularly at apex; antenna black, weakly ringed whitish. Thorax and tegula dark brown occasionally slightly intermixed ochreous. Abdomen dorsally grey, ventrally whitish, pale grey at margins. Forewing predominantly fuscous in costal and terminal area, dorsum mixed fuscous and ochreous with scattered white scales, extending into middle of wing particularly at 1/5 and at about middle of wing, distinct white costal and tornal spots separated by ochreous or fuscous scales, irregularly shaped black patch from fold to costa at about 1/3 interrupted by ochreous scales, black plical and discal spot; cilia light grey with fuscous ciliary line, buff beyond line. Hindwing light grey, cilia greyish buff.

Variation: the extent of ochreous scales varies considerably and occasionally they are completely absent. Specimens from the Hautes Pyrénées and Alps are larger on average than those from southern Spain with fewer ochreous scales.

Male genitalia (Fig. 7). Uncus long, suboval, posterior edges rounded; gnathos with large mesial sclerite, culcitula small; posterior 1/3 of tegumen slender, anterior part strongly widened towards broadly rounded pedunculi of about twice size of uncus, anterior margin with deep concave emargination; transtilla membranous with few microtrichia; valva basally curved ventrad, moderately short, slender, apical part weakly constricted, oblique apex with group of stiff setae; sacculus long, nearly length and width of valva, apex rounded, with dorsally pointed projection; vinculum wide and short, posterior margin moderately sclerotized, with shallow medial incision and distinctly rounded lateromedial projections, lateral projections shallow, anterior

margin with strongly sclerotized concave ridge; saccus slender, basally weakly widened, gradually narrowing towards pointed apex, slightly exceeding length of apex of valva to anterior margin of vinculum; anellus with pair of needle-shaped sclerites; phallus stout, distal part weakly curved and contorted, coecum weakly inflated, longitudinal ridge from about middle to apex, two small sclerotized hooklets at apex.

Female genitalia (Fig. 11). Apophysis posterior about 4 times length of apophysis anterior; segment VIII with suboval sclerotized dorsolateral zones, with distinct dorso-lateral flaps, posterior and inner edge strongly sclerotized, membranous ventromedial part with numerous microtrichia; apophysis anterior about length of segment VIII; antrum large, funnel-shaped, slightly extending beyond apex of apophysis anterior and basally 2/3 width of segment VIII between bases of apophyses anteriores, posterior edge weakly convex; ductus bursae about twice length of apophysis anterior; corpus bursae semi-oval, signum a crescent-shaped basal plate with moderately long and stout hook.

Molecular data. BIN: BOLD:AAU3076. A genetically variable species, mainly due to a deviating specimen from Spain. The intraspecific average distance of the barcode region is 0.89%, the maximum distance 2.41% (*p*-distance) (*n* = 11) with all sequences clustering in a single BIN. The minimum distance to the nearest neighbour, *C. olekarsholti* sp. nov., is 3.37%.

Distribution. *Caryocolum fibigerium* in its current taxonomic sense is confirmed from the Iberian Peninsula (Spain) and southern parts of France (Huemer and Karsholt 2010), whereas other published records from Morocco (Huemer 1988), Portugal (Corley 2015), and northern Italy (Karsholt and Huemer 1995) require re-examination including DNA barcode analysis.

Bionomics. In Portugal the larva has been found from November to mid-December on *Arenaria montana*, living between two spun leaves, usually at tip of a shoot. Young larvae are suspected as probable leaf-miners (Corley 2002). However, identity of these populations has to be re-assessed. Unpublished breedings from France from *Cerastium* sp. by Jacques Nel show a possibly wider spectrum of host-plants. The adults have been found in from early June to early September at artificial light sources near rock and scree at altitudes of about 700–2400 m.

Remarks. *Caryocolum fibigerium* was described from two disjunct Mediterranean areas, from Morocco to Spain and from Bulgaria to Greece, with the holotype from southern Spain. However, this study indicates that material from Morocco requires verification, populations from the Balkans belong to *C. olekarsholti*, and unpublished records from central Italy are *C. herwigvanstaii*.

***Caryocolum herwigvanstaii* sp. nov.**

<http://zoobank.org/5C8F64C1-7008-4356-8CAC-A775D3F05D12>

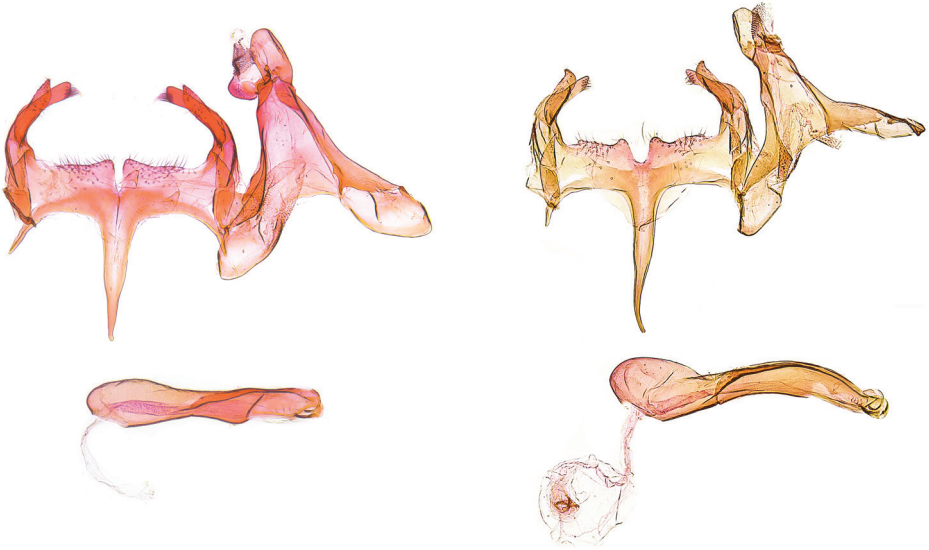
Type material. Holotype. [ITALY] • ♂; L'Aquila, NP Gran Sasso, ex Miniera di Lignite; 1750 m; 14–15 Jul 2010; [genitalia slide number] GEL 1153♂, P. Huemer; P. Huemer leg; TLMF.



Figures 2–5. Adults **2** *Caryocolum tricolorella*, male, Germany **3** *C. fibigerium*, male, paratype, Spain **4** *C. herwigvanstaaai* sp. nov., male, holotype, Italy **5** *C. olekarsholti*, male, holotype, Greece.

Paratypes. [ITALY] • 5 ♂, 5 ♀; same collection data as for holotype; [genitalia slide number] GEL 1155♀, P. Huemer; [1 ♂, 1 ♀ genitalia in glycerin capsule]; [DNA barcode ids] BC TLMF Lep 01600; all TLMF; • 10 ♂, 3 ♀; same collection data as for holotype; 1750 m; 15 Jul 2010; T. Mayr leg.; RCTM; • 1 ♂; same collection data as for holotype; 1750 m; 14 Jul 2010; T. Mayr leg.; RCTM; • 1 ♀; Rieti, Monte Terminillo; 1730–1780 m; 11 Jul 2010; P. Huemer leg.; [DNA barcode ids] BC TLMF Lep 01601; • 6 ♂; Rieti, Monte Terminillo; 1700 m; 17 Jul 2011; T. Mayr leg.; RCTM; • 1 ♀; Chieti, PN della Majella, Taranta Peligna, Pian di Valle; 770 m; 20 Jul 2011; P. Huemer leg.; BC TLMF Lep 05038; all TLMF.

Diagnosis. *Caryocolum herwigvanstaaai* differs from *C. tricolorella* by its distinctly smaller size and the less extensive ochreous-orange markings, and from *C. fibigerium* by the extended white forewing markings which are, however, less pronounced at the inner margin compared to *C. olekarsholti*. The male genitalia differ from *C. tricolorella* by the shorter valva and sacculus and the additional, although moderately low, humps of the posterior margin of the vinculum. From *C. fibigerium* *C. herwigvanstaaai* differs in particular by the more slender sacculus and the distinct lateral humps of the posterior margin of the vinculum, and from *C. olekarsholti* by the apically slightly dilated valva and the slender sacculus. The antrum of the female genitalia is much larger than



6

7

Figures 6, 7. Male genitalia **6** *Caryocolum tricolorella*, Germany, slide GEL 1218 P. Huemer **7** *C. fibigerium*, Spain, slide GEL 1211 P. Huemer.

in *C. tricolorella* but smaller than in *C. fibigerium*, not extending the length of apophysis anterior. The anterior margin of the antrum is concave in *C. herwigvanstaa*i but convex in *C. olekarsholti*.

Description. Adult (Fig. 4). Forewing length. ♂ 4.9–5.5 mm ($\bar{\sigma}$ = 5.25 mm, n = 4), ♀ 5.1–5.7 mm ($\bar{\sigma}$ = 5.40 mm, n = 4). Head with fuscous vertex, frons cream-white; second segment of labial palpus cream-white on inner and upper surface, predominantly grey-brown on outer surface, third segment dark brown with a few white scales particularly at apex; antenna black, weakly ringed whitish. Thorax and tegula dark brown with a few intermixed ochreous scales. Abdomen dorsally grey, ventrally whitish, pale grey at margins. Forewing predominantly fuscous in costal and terminal area, dorsum mixed ochreous-whitish with scattered fuscous scales, extensive white mottling from dorsum to costa at 1/5 and 1/2, large white costal and tornal spots nearly fused, separated by few fuscous scales, irregularly shaped black patch from fold to costa at about 1/3 interrupted by ochreous scales, black plical and discal spot; cilia light grey with fuscous ciliary line, buff-whitish beyond line. Hindwing light grey, cilia greyish buff.

Variation: the extent of ochreous scales, particularly along the dorsum, is slightly variable.

Male genitalia (Fig. 8). Uncus long, suboval, posterior edges rounded; gnathos with large mesial sclerite, culcitula small; posterior 1/3 of tegumen slender, anterior part strongly widened towards broadly rounded pedunculi of about twice size of uncus, anterior margin with deep concave emargination; transtilla membranous with few microtrichia; valva basally curved ventrad, moderately short, slender, apical part slightly

dilated, obliquely pointed apex with group of stiff setae; sacculus moderately long, more slender and shorter than valva, apex rounded, with dorsally pointed projection; vinculum wide and short, posterior margin moderately sclerotized, with shallow medial incision and distinctly rounded lateromedial projections, lateral projections distinct, anterior margin with strongly sclerotized concave ridge; saccus slender, basally weakly widened, gradually narrowing towards pointed apex, slightly exceeding length of apex of valva to anterior margin of vinculum; anellus with pair of needle-shaped sclerites; phallus stout, distal part weakly curved and contorted, coecum weakly inflated, longitudinal ridge from about middle to apex, two small sclerotized hooklets at apex.

Female genitalia (Fig. 12). Apophysis posterior about 4.5 times length of apophysis anterior; segment VIII with suboval sclerotized dorsolateral zones, with small dorsolateral flaps, posterior and inner edge strongly sclerotized, membranous ventromedial part with numerous microtrichia; apophysis anterior about length of segment VIII; antrum moderately large, funnel-shaped, shorter than apophysis anterior and segment VIII, basally about 1/2 width of segment VIII between bases of apophyses anteriores, posterior edge weakly concave; ductus bursae about twice length of apophysis anterior; corpus bursae semi-oval, signum a crescent-shaped basal plate with moderately long and stout hook.

Molecular data. BINs: BOLD:AAO2674, BOLD:ADK9243. A genetically variable species splitting into two BINs which, however, require re-evaluation from additional material. The distance between both BINs is 2.1% ($n = 3$). The minimum distance to the nearest neighbour, *C. olekarsholti*, is 4.12%.

Etymology. The species is dedicated to DDr Herwig van Staa (Innsbruck, Austria), former governor of the province of Tyrol on his 80th birthday on the 10 June 2022, and in recognition of his tremendous support of the Tyrolean Federal State Museums and the Alpenzoo Innsbruck, resulting in a joint Natural History Museum.

Distribution. The species is currently only known from Central Italy but may have a wider distribution on the Italian Peninsula. Mariani (1943) had published a record of *C. tricolorella* from Sicily, which possibly is *C. herwigvanstaa*.

Bionomics. Host-plant and early stages are undescribed but it seems most likely that the species shows a similar behaviour as related taxa with the potential host-plant among *Cerastium* or related genera of Caryophyllaceae. The adults have been found in mid-July at artificial light sources near rock and scree on calcareous soil at altitudes of about 1700–1800 m.

Caryocolum olekarsholti sp. nov.

<http://zoobank.org/52FA17A1-02D7-41BD-8B5B-A6BA384D3E4A>

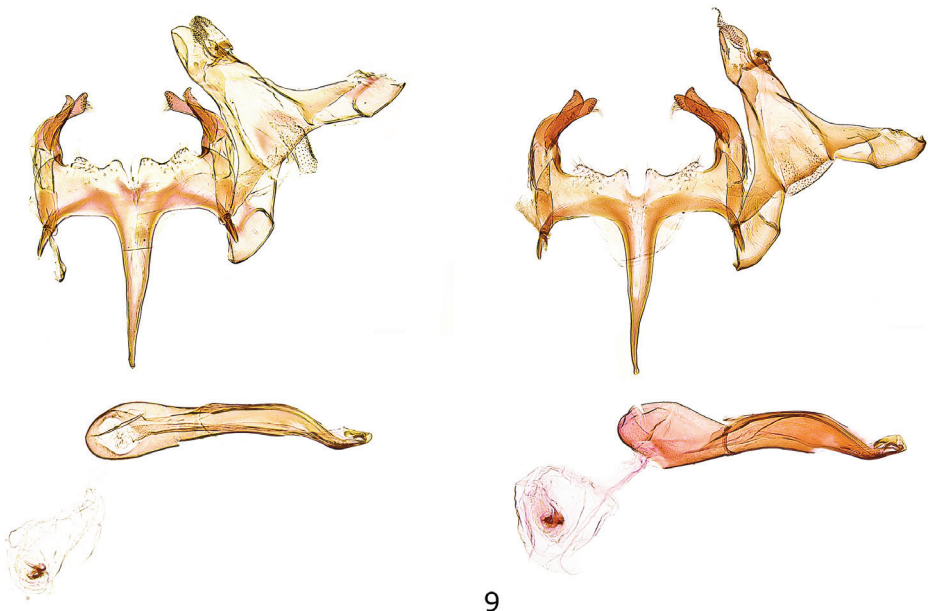
Type material. Holotype. [GREECE] • ♂; Ioannina, Psorovouni NE, Vradheto; 1750 m; 4 Aug 2012; [genitalia slide number] GEL 1209♂, P. Huemer; C. Wieser leg; LMK.

Paratypes. [GREECE] • 18 ♂, 11 ♀; same collection data as for holotype; [genitalia slide numbers] GEL 1213♂, GEL 1233♀, P. Huemer; [DNA barcode ids] KLM Lep 00489, KLM Lep 00490, BC TLMF Lep 05038; all KLM; • 1 ♂; Trikala, Katara pass;

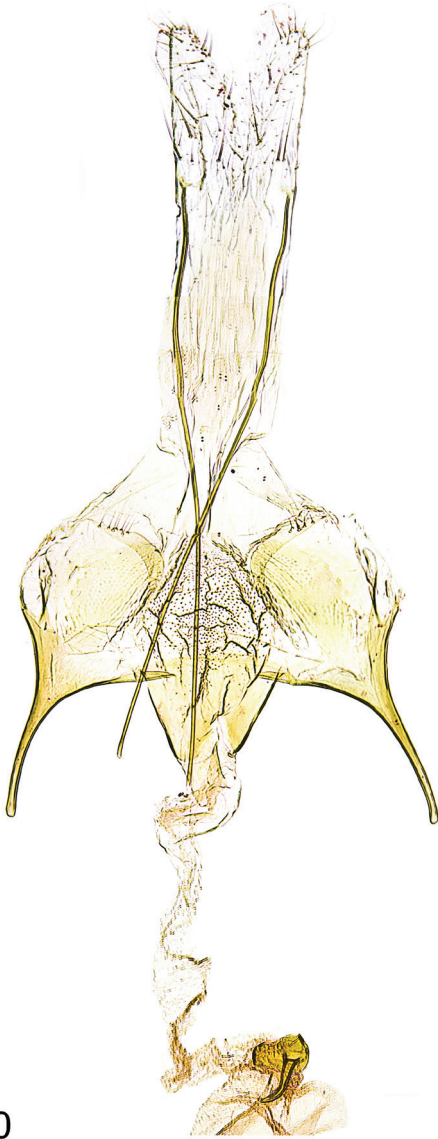
1700 m; 13 Jul 1998; [genitalia in glycerin capsule]; M. Egger leg.; TLMF; 4 ♂; Ioannina, Katar pass; 1600 m; 11 Aug 1985; M. Fibiger leg.; all ZMUC; [NORTH MACEDONIA] • 1 ♂, 2 ♀; Tetovo, Popova Sapka, W Tetovo; 2130 m; 7 Aug 2012; [DNA barcode ids] KLM Lep 00488; C. Wieser leg.; all KLM; [BULGARIA] • 1 ♂; Samokov; 4 Jul 1911; [unknown collector]; NHM.

Diagnosis. *Caryocolum olekarsholti* differs from *C. tricolorella* by its distinctly smaller size and the lack of ochreous-orange markings, and from the other species of the complex by the pronounced white forewing markings with few or completely absent ochreous scales. The male genitalia differ from *C. tricolorella* by the shorter valva and sacculus and the additional humps of the posterior margin of the vinculum. *Caryocolum olekarsholti* is very similar to *C. fibigerium*, with only subtle diagnostic characters such as the more distinct lateral projection of the posterior margin of the vinculum and the distally weakly dilated sacculus. *Caryocolum olekarsholti* differs from *C. herwigvanstaai* in particular by the distinctly broader sacculus and the distally almost parallel-sided valva. The antrum of the female genitalia is much larger in *C. olekarsholti* than in *C. tricolorella* but smaller than in *C. fibigerium*, not extending the length of the apophysis anterior. The anterior margin of the antrum is convex in *C. olekarsholti* but concave in *C. herwigvanstaai*.

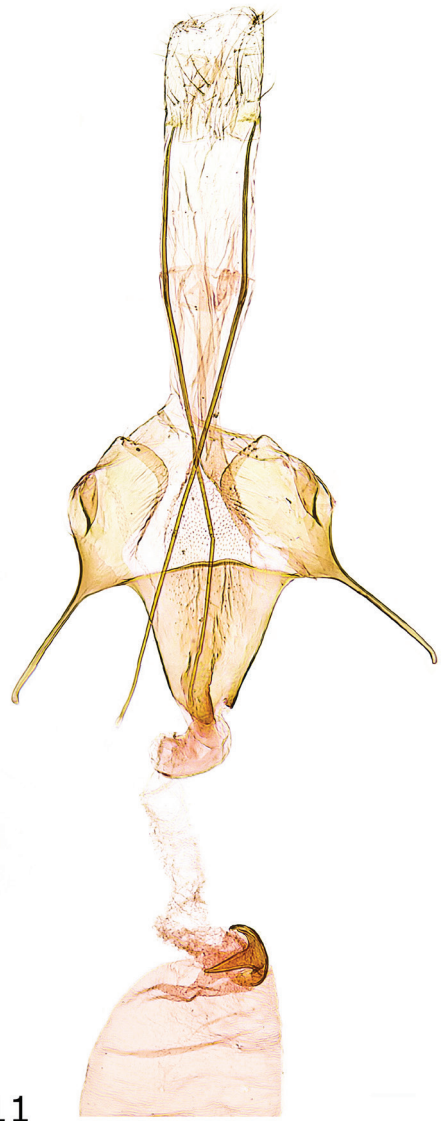
Description. Adult (Fig. 5). Forewing length. ♂ 4.7–4.9 mm ($\bar{\phi}$ = 4.83 mm, n = 4), ♀ 4.7–4.8 mm ($\bar{\phi}$ = 4.73 mm, n = 4). Head with fuscous vertex, frons cream-white; second segment of labial palpus cream-white on inner and upper surface, predominantly grey-brown on outer surface, third segment dark brown with a few white scales particularly at apex; antenna black, weakly ringed whitish. Thorax and tegula dark brown, intermixed with light grey. Abdomen dorsally grey, ventrally whitish, pale



Figures 8, 9. Male genitalia **8** *C. herwigvanstaai* sp. nov., holotype, Italy, slide GEL 1153 P. Huemer
9 *C. olekarsholti*, paratype, Greece, slide GEL 1213 P. Huemer;



10



11

Figures 10, 11. Female genitalia **10** *Caryocolum tricolorella*, Germany, slide GEL 1092 P. Huemer
11 *C. fibigerium*, Spain, slide GEL 1095 P. Huemer.

grey at margins. Forewing predominantly fuscous in costal and terminal area, ochreous scales absent or largely reduced, dorsum whitish with scattered fuscous scales, extensive white mottling from dorsum to costa at 1/5 and 1/2, large white costal and tornal spots nearly fused, separated by a few fuscous scales, irregularly shaped black patch from fold to costa at about 1/3, indistinct black plical and discal spots; cilia light grey with fuscous ciliary line, buff-whitish beyond line. Hindwing light grey, cilia greyish buff.

Variation: the extent of white scales, particularly along dorsum, varies considerably.

Male genitalia (Fig. 9). Uncus long, suboval, posterior edges rounded; gnathos with large mesial sclerite, culcitula small; posterior third of tegumen slender, anterior part strongly widened towards broadly rounded pedunculi of about twice size of uncus, anterior margin with deep concave emargination; transtilla membranous with few microtrichia; valva basally curved ventrad, moderately short, slender, apical part weakly constricted, oblique apex with group of stiff setae; sacculus long, nearly length and width of valva, distally weakly dilated, apex rounded, with dorsally pointed projection; vinculum wide and short, posterior margin moderately sclerotized, with shallow medial incision and distinctly rounded lateromedial and lateral projections, anterior margin with strongly sclerotized concave ridge; saccus slender, basally weakly widened, gradually narrowed towards pointed apex, slightly exceeding length of apex of valva to anterior margin of vinculum; anellus with pair of needle-shaped sclerites; phallus stout, distal part weakly curved and contorted, coecum weakly inflated, longitudinal ridge from about middle to apex, two small sclerotized hooklets at apex.

Female genitalia (Fig. 13). Apophysis posterior about 5 times length of apophysis anterior; segment VIII with suboval sclerotized dorsolateral zones, with distinct dorso-lateral flaps, posterior and inner edge strongly sclerotized, membranous ventromedial part with numerous microtrichia; apophysis anterior about length of segment VIII; antrum moderately large, funnel-shaped, shorter than apophysis anterior and segment VIII, about 1/2 width of segment VIII between bases of apophyses anteriores, posterior edge convex; ductus bursae about twice length of apophysis anterior; corpus bursae semi-oval, signum a crescent-shaped basal plate with moderately long and stout hook.

Molecular data. BIN: BOLD:ACC2659. The intraspecific average distance of the barcode region is 0.11%, the maximum distance 0.16% (*p*-distance) ($n = 3$). The minimum distance to the nearest neighbour, *C. fibigerium*, is 3.37%.

Etymology. The species is named in honour of Ole Karsholt (Copenhagen, Denmark) in recognition of his outstanding contribution to the systematics and taxonomy of European Gelechiidae.

Distribution. The species is currently only known from Bulgaria, Greece, and North Macedonia but is probably more widely distributed on the Balkan Peninsula.

Bionomics. Host-plant and early stages are undescribed, but it seems most likely that the species shows a similar behaviour as related taxa with the potential host-plant among *Cerastium* and/or *Stellaria* spp. The adults have been found from mid-July to early August at artificial light sources in mountainous habitats dominated by rock and scree on calcareous soil.

Discussion

Cryptic diversity has been found in many different families of European Lepidoptera during the last years, progress mainly driven by the implementation of molecular methods and newly collected samples resulting from better access to remote parts of the continent. The majority of cryptic species seems to be hidden among various groups



Figures 12, 13. Female genitalia **12** *C. herwigvanstaai* sp. nov., paratype, Italy, slide GEL 1155 P. Huemer
13 *C. olekarsholti*, paratype, Greece, slide GEL 1231 P. Huemer.

of so-called traditional “micromoths” (Huemer et al. 2020; Lopez-Vaamonde et al. 2021), whereas only a few overlooked species have been detected in the more “spectacular” taxonomic groups such as Papilionoidea (Dincă et al. 2021) or recently in the “macromoths” (Ronkay and Huemer 2018; Šumpich and Jagelka 2021). The majority of newly detected cryptic species seems to occur in allopatry, particularly in mountain

areas of southern Europe, and they often cause ongoing taxonomic problems (Mutanen et al. 2012). In contrast only moderately few sibling species have been found in sympatry (Hernández-Roldán et al. 2016; Mutanen et al. 2020; Berggren et al. 2022).

The likely reasons for increased diversification in the southern part of the continent date back to the Messinian crisis approximately 5.96–5.33 mya and the consequent reflooding of the Mediterranean Sea with the establishment of a Mediterranean climate (Hewitt 2011; Fiz-Palacios and Valcárcel 2013; Carnicero et al. 2017). Furthermore, Pleistocene glaciation processes, which began about 2.5 mya, led to increased isolation of fragmented landscapes with temporary connections and disconnections and thus favouring speciation processes (Médail and Diadema 2009; Morales-Barbero et al. 2018). Vicariant distribution patterns of closely related Lepidoptera in southern Europe may reflect classical Pleistocene macrorefugia for European temperate species in the Iberian, Italian, and Balkan Peninsulas. The current distribution of the *C. tricolorella* species-complex with three species restricted to the three major Mediterranean peninsulas perfectly matches this scenario. However, the taxonomic complexity had not been recognized until now and only two species were formerly separated, with *C. fibigerium* considered as a Holomediterranean and *C. tricolorella* as a Central and Northern European species (Huemer 1988). Unexpectedly, re-assessment of molecular and morphological traits supported the existence of four as opposed to two species. In particular DNA barcodes have been of essential value in resolving the taxonomy of this species complex which is supported by rather subtle morphological characters. Similarly, several cryptic species of *Caryocolum* have been recently detected (Huemer et al. 2014; Huemer 2020). These studies had already indicated that revisionary work was still required on additional species (*C. peregrinella* and *C. klosi*) of this diverse genus with an exceptionally large intraspecific barcode divergence.

Acknowledgements

I am grateful to Paul D.N. Hebert and the entire team at the Canadian Centre for DNA Barcoding (Guelph, Canada), whose sequencing work was enabled through funding from Genome Canada through Ontario Genomics, and to the Ontario Ministry of Research and Innovation and NSERC for their support of the BOLD informatics platform. The study was also supported by the Promotion of Educational Policies, University and Research Department of the Autonomous Province of Bolzano – South Tyrol with funding of the projects “Genetische Artabgrenzung ausgewählter arktalpiner und boreomontaner Tiere Südtirols” and “Erstellung einer DNA-Barcode-Bibliothek der Schmetterlinge des zentralen Alpenraumes (Süd-, Nord- und Osttirol)”. Several colleagues helped with important material and various other support, particularly Christian Wieser (LMK), Javier Gastón (Getxo, Spain), Ole Karsholt (ZMUC), Gérard Labonne (Montpellier, France), Toni Mayr (Feldkirch, Austria), and Jacques Nel (La Ciotat, France). Andreas Eckelt (TLMF) and Stefan Heim (Innsbruck, Austria) are acknowledged for technical assistance. Robert J. Heckford (Plympton, UK) is thanked for his careful language proofreading and valuable comments.

References

- Berggren K, Aarvik L, Huemer P, Lee KM, Mutanen M (2022) Integrative taxonomy reveals overlooked cryptic diversity in the conifer feeding *Batrachedra pinicolella* (Zeller, 1839) (Lepidoptera, Batrachedridae). *ZooKeys* 1085: 165–182. <https://doi.org/10.3897/zookeys.1085.76853>
- Bland KP, Corley MFV, Emmet AM, Heckford RJ, Huemer P, Langmaid JR, Palmer SM, Parsons MS, Pitkin LM, Sattler K, Simpson ANB (2002) Gelechiinae. In: Emmet AM, Langmaid JR (Eds) *The Moths and Butterflies of Great Britain and Ireland, Volume 4, Part 2*. Harley Books, Colchester, 118–204.
- Carnicero P, Sáez L, Garcia-Jacas N, Galbany-Casals M (2017) Different speciation types meet in a Mediterranean genus: The biogeographic history of *Cymbalaria* (Plantaginaceae). *Taxon* 66(2): 393–407. <https://doi.org/10.12705/662.7>
- Corley MFV (2002) The larva of *Caryocolum fibigerium* Huemer, 1988 (Lepidoptera: Gelechiidae). *Entomologist's Gazette* 53: 20.
- Corley MFV (2015) *Lepidoptera of Continental Portugal. A Fully Revised List*. M. Corley, Faringdon, 282 pp.
- deWaard JR, Ivanova NV, Hajibabaei M, Hebert PDN (2008) Assembling DNA Barcodes: Analytical Protocols. In: Martin CC (Ed.) *Methods in Molecular Biology: Environmental Genomics*. Humana Press, Totowa, 275–293. https://doi.org/10.1007/978-1-59745-548-0_15
- Dincă V, Dapporto L, Somervuo P, Vodă R, Cuvelier S, Gascoigne-Pees M, Huemer P, Mutanen M, Hebert PDN, Vila R (2021) High resolution DNA barcode library for European butterflies reveals continental patterns of mitochondrial genetic diversity. *Communications Biology* 4(1): e315. <https://doi.org/10.1038/s42003-021-01834-7>
- Fiz-Palacios O, Valcárcel V (2013) From Messinian crisis to Mediterranean climate: A temporal gap of diversification recovered from multiple plant phylogenies. *Perspectives in Plant Ecology, Evolution and Systematics* 15(2): 130–137. <https://doi.org/10.1016/j.ppees.2013.02.002>
- Gregor F, Povolný D (1954) Systematische und zoogeographische Studie über die Gruppe der Arten *Gnorimoschema* Busck mit Rücksicht auf die richtige Diagnostik des Schädling *Gnorimoschema ocellatellum* Boyd. *Zoologické a Entomologické Listy* 3: 83–97. [pl. 7, map]
- Haworth AH (1812) A brief account of some rare insects announced at various times to the Society, as new to Britain. *The Transactions of the Entomological Society of London* 1: 332–340.
- Haworth AH (1828) *Lepidoptera Britannica* 1828(Part 4): 512–606. [J. Murray, Londini.]
- Hering M (1935–1937) *Die Blatt-Minen Mittel- und Nord-Europas*. G. Feller, Neubrandenburg, 631 pp.
- Hernández-Roldán JL, Dapporto L, Dincă V, Vicente JC, Hornett EA, Šíchová J, Lukhtanov VA, Talavera G, Vila R (2016) Integrative analyses unveil speciation linked to host plant shift in *Spialia* butterflies. *Molecular Ecology* 25(17): 4267–4284. <https://doi.org/10.1111/mec.13756>
- Herrich-Schäffer GAW (1847–1855) *Systematische Bearbeitung der Schmetterlinge von Europa*. 5. Regensburg, 394 pp. [124 + 7 + 1 pls] <https://doi.org/10.5962/bhl.title.67734>
- Hewitt GM (2011) Mediterranean peninsulas: the evolution of hotspots. In: Zachos FE, Habel JC (Eds) *Biodiversity Hotspots*. Springer, Berlin, Heidelberg, 123–147. https://doi.org/10.1007/978-3-642-20992-5_7

- Huemer P (1987) Eine modifizierte Genitalpräparationstechnik für die Gattung *Caryocolum* (Lepidoptera: Gelechiidae). Mitteilungen der Schweizerische Entomologische Gesellschaft 60: 207–211.
- Huemer P (1988) A taxonomic revision of *Caryocolum* (Lepidoptera: Gelechiidae). Bulletin of the British Museum (Natural History). Historical Series 57: 439–571. [Natural History]
- Huemer P (2020) Integrative revision of the *Caryocolum schleichi* species group—A striking example of a temporally changing species concept (Lepidoptera, Gelechiidae). Alpine Entomology 4: 39–63. <https://doi.org/10.3897/alpento.4.50703>
- Huemer P, Karsholt O (1999) Gelechiidae I (Gelechiinae: Teleiodini, Gelechiini). In: Huemer P, Karsholt O, Lyneborg L (Eds) Microlepidoptera of Europe. Vol. 3. Apollo Books, Stenstrup, 356 pp.
- Huemer P, Karsholt O (2010) Gelechiidae II (Gelechiinae: Gnorimoschemini). In: Huemer P, Karsholt O, Nuss M (Eds) Microlepidoptera of Europe. Vol. 6. Apollo Books, Stenstrup, 586 pp. <https://doi.org/10.1163/9789004260986>
- Huemer P, Karsholt O (2020) Commented checklist of European Gelechiidae (Lepidoptera). ZooKeys 921: 65–140. <https://doi.org/10.3897/zookeys.921.49197>
- Huemer P, Karsholt O, Mutanen M (2014) DNA barcoding as a screening tool for cryptic diversity: An example from *Caryocolum*, with description of a new species (Lepidoptera, Gelechiidae). ZooKeys 404: 91–111. <https://doi.org/10.3897/zookeys.404.7234>
- Huemer P, Karsholt O, Aarvik L, Berggren K, Bidzilya O, Junnilainen J, Landry J-F, Mutanen M, Nupponen K, Segerer A, Šumpich J, Wieser C, Wiesmair B, Hebert PDN (2020) DNA barcode library for European Gelechiidae (Lepidoptera) suggests greatly underestimated species diversity. ZooKeys 921: 141–157. <https://doi.org/10.3897/zookeys.921.49199>
- Karsholt O, Huemer P (1995) Additions and corrections to the Gelechiidae fauna of Italy (Lepidoptera). Bolletino di Zoologia Agraria e di Bachicoltura, Serie II 27: 1–17.
- Klimesch J (1953–1954) Die an Caryophyllaceen lebenden europäischen *Gnorimoschema* Busck (= *Phthorimaea* Meyr.)-Arten. Zeitschrift der Wiener Entomologischen Gesellschaft 38(1953): 225–239, 272–282, 311–319; 39(1954): 273–288, 335–341, 357–362.
- Lopez-Vaamonde C, Kirichenko N, Cama A, Doorenweerd C, Godfray HCJ, Guiguet A, Gomboc S, Huemer P, Landry J-F, Laštůvka A, Laštůvka Z, Lee KM, Lees DC, Mutanen M, van Nieukerken EJ, Segerer A, Triberti P, Wieser C, Rougerie R (2021) Evaluating DNA barcoding for species identification and discovery in European gracillariid moths. Frontiers in Ecology and Evolution 9: e626752. <https://doi.org/10.3389/fevo.2021.626752>
- Mariani M (1943) Fauna Lepidopterorum Italiae. Parte I. Catalogo ragionato dei Lepidotteri d'Italia. Giornale di Scienze naturali ed economiche, Palermo, 42 (1940–41). Memoria 3: 1–237.
- Médail F, Diadema K (2009) Glacial refugia influence plant diversity patterns in the Mediterranean Basin. Journal of Biogeography 36(7): 1333–1345. <https://doi.org/10.1111/j.1365-2699.2008.02051.x>
- Morales-Barbero J, Martínez PA, Ferrer-Castán D, Olalla-Tárraga MÁ (2018) Quaternary refugia are associated with higher speciation rates in mammalian faunas of the Western Palearctic. Ecography 41(4): 607–621. <https://doi.org/10.1111/ecog.02647>

- Mutanen M, Hausmann A, Hebert PDN, Landry J-F, de Waard JR, Huemer P (2012) Allopatry as a Gordian knot for taxonomists: Patterns of DNA barcode divergence in Arctic-Alpine Lepidoptera. PLoS ONE 7(10): e47214. <https://doi.org/10.1371/journal.pone.0047214>
- Mutanen M, Huemer P, Autto J, Karsholt O, Kaila L (2020) *Monopis jussii*, a new species (Lepidoptera, Tineidae) inhabiting nests of the boreal owl (*Aegolius funereus*). ZooKeys 992: 157–181. <https://doi.org/10.3897/zookeys.992.53975>
- Pitkin LM (1986) A technique for the preparation of complex male genitalia in microlepidoptera. Entomologist's Gazette 37: 173–179.
- Ratnasingham S (2018) BOLD Barcode of Life Data System, version 4. <http://www.boldsystems.org> [Accessed on: 2022-02-27]
- Ratnasingham S, Hebert PDN (2007) BOLD: The Barcode of Life Data System (<http://www.barcodinglife.org>). Molecular Ecology Notes 7(3): 355–364. <https://doi.org/10.1111/j.1471-8286.2007.01678.x>
- Ratnasingham S, Hebert PDN (2013) A DNA-based registry for all animal species: the Barcode Index Number (BIN) system. PLoS ONE 8: e66213. <https://doi.org/10.1371/journal.pone.0066213>
- Robinson GS (1976) The preparation of slides of Lepidoptera genitalia with special reference to the microlepidoptera. Entomologist's Gazette 27: 127–132.
- Ronkay L, Huemer P (2018) *Agrotis fatidica* (Hübner, 1824) species-group revisited, with description of two new species from the Alps and the Pyrenees (Lepidoptera, Noctuidae). Nota Lepidopterologica 41(1): 145–179. <https://doi.org/10.3897/nl.41.23090>
- Schütze KT (1931) Die Biologie der Kleinschmetterlinge unter besonderer Berücksichtigung ihrer Nährpflanzen und Erscheinungszeiten. Internationaler Entomologischer Vereins e.V, Frankfurt-am-Main, 235 pp.
- Sorhagen L (1886) Die Kleinschmetterlinge der Mark Brandenburg und einiger angrenzenden Landschaften. Mit besonderer Berücksichtigung der Berliner Arten. R. Friedländer, Berlin, [x +] 368 pp. <https://doi.org/10.1002/mmnd.47918860222>
- Stainton HT (1867) The Natural History of the Tineina. Vol. 10. John Van Voorst, London, [ix +] 304 pp.
- Šumpich J, Jagelka M (2021) *Lemonia batavorum* sp. nov. from the Netherlands, an overlooked sibling of *L. dumi* (Lepidoptera: Brahmaeidae). Acta Entomologica Musei Nationalis Praegae 61(2): 483–494. <https://doi.org/10.37520/aemnp.2021.026>
- Tamura K, Stecher G, Peterson D, Filipski A, Kumar S (2013) MEGA6: Molecular Evolutionary Genetics Analysis version 6.0. Molecular Biology and Evolution 30(12): 2725–2729. <https://doi.org/10.1093/molbev/mst197>
- Zeller PC (1839) Versuch einer naturgemäßen Eintheilung der Schaben. Isis von Oken 1839: 167–220.

